OXYLIPINS AS NOVEL SOURCES OF SOYBEAN (*GLYCINE MAX*) TOLERANCE TO *PHYTOPHTHORA SOJAE* INFECTION

(Thesis format: Integrated Article)

By

Oludoyin Adeseun Adigun, M.Sc.

A thesis submitted to the School of Graduate Studies in partial fulfillment of the requirements for the degree of Doctor of Philosophy in Environmental Science (Interdisciplinary)

Department of Environmental Science
Faculty of Science
Memorial university of Newfoundland
St. John's Newfoundland and Labrador

April 2022

Oxylipins as novel sources of soybean (*Glycine max*) tolerance to *Phytophthora sojae* infection

By

Oludoyin Adeseun Adigun

A thesis submitted to the School of Graduate Studies

In partial fulfillment of the requirements of the degree of

Doctor of Philosophy

Environmental Science (Interdisciplinary)

Approved:

Dean of the Graduate School

Supervisor

Date

Committee members:

Dr. Linda Elizabeth Jewell----------

Dr. Mumtaz Akhtar Cheema----------

Abstract

Soybean (*Glycine max*) is an important staple crop currently grown worldwide. The annual global losses of the crop due to root and stem rot infection caused by oomycete *Phytophthora sojae* are currently estimated at approximately $2B USD. The attempt to fight this devastating disease is towards pyramiding tolerant soybean cultivars that could enhance tolerance to *Phytophthora sojae* infection. The initial point of infection is root and could spread to the stem. Lipids are major structural components of cellular membranes, which serve as a component of defense mechanisms used by plants against pathogen infection. I hypothesized that lipid mediated plant immunity including phyto-oxylipin anabolism culminating in unique histochemical and morphological structures appear to be part of the successful mechanisms used by tolerant soybean cultivar to limit colonization and infection by *Phytophthora sojae*. These greater alterations are just a component of successful strategy used by tolerant cultivar to mitigate pathogen infection. To investigate these hypotheses, we employed multi-modal lipidomics, scanning electron microscopy and histochemical techniques to determine, (1) how soybean cultivars remodel their lipid metabolism, (2) to better understand the induction and functions of phyto-oxylipins, and (3) to investigate the mechanism of infection in both soybean cultivars in response to *Phytophthora sojae* infection. Both soybean cultivars demonstrated alterations in lipid metabolism in response to pathogen infection. Relative to non-inoculated controls, induced accumulation of stigmasterol occurred in the susceptible cultivar whereas induced accumulation of phospholipids and glycerolipids was observed in the tolerant cultivar. A comprehensive metabolic map of soybean root and stem lipid metabolism identified unique lipid biomarkers and accumulation of phyto-oxylipins in tolerant cultivar in response to *Phytophthora sojae* infection. Histochemical results revealed differences in morphological changes in both susceptible and tolerant cultivars and seemed to be associated with the successful mechanisms used by tolerant soybeans to limit pathogen infection. Overall, my thesis findings demonstrate the role of lipid metabolisms and phyto-oxylipin induction in

soybeans during pathogen inversion. This information could be useful in pyramiding soybean cultivars with high tolerance to *Phytophthora sojae* infection and may consequently improve sustainable agriculture.

Dedication

This thesis is primarily dedicated to GOD ALMIGHTY, who by His infinite mercy granted me the grace to start and finish this program successfully. Likewise, it is dedicated to the memory of my beloved parents: my dear mom (Late Olufunke Adigun), who died when I was still a little baby and my dad (Late Oguntade Adigun) who also died few days to my PhD comprehensive exams. Very painful, non of them were alive to witness this great achievement in the life of their beloved son! I owe you this, Mum and Dad. May your souls rest in peace (Amen).

Acknowledgments

I give thanks to God Almighty, who by Himself, is the knowledge, wisdom and understanding. I appreciate Him for making me what I am today, glory be to His Holy Name.

First and foremost, I would like to express my deep sense of gratitude to my amazing supervisor, Dr. Raymond Thomas. I am indebted for his excellent and brilliant supervision, constructive criticism, time to time guidance, motivation and encouragement during the studies, the research process, and the writing of this thesis. I am indeed very lucky to have such a great advisor! Likewise, special thanks to my co-supervisor Dr. Linda Jewell from Agriculture Agri-Food Canada (AAFC), her valuable support and deep sense of mentorship is greatly appreciated. I am blessed to meet these amazing advisors in the journey of my academic career.

Besides my supervisor and co-supervisors, I would like to thank my supervisory committee members: Dr Cheema Mumtaz, Dr. Linda Jewell, and Dr. Raymond Thomas for their encouragement and advice throughout the time of this program. I appreciate the School of Graduate Studies, Memorial University of Newfoundland and Labrador, Dean, Faculty of Science, Memorial University of Newfoundland both St. John's Campus and Grenfell Campus for their amazing supports and I also appreciate Natural Science and Engineering Research Council (NSERC), Canada for their financial support. Special thanks are given to Dr. Thu Huong Pham (Alias Nicole), Dr Tao Yuan and Mr Jamie Warren, who gave me access to the BERI Laboratory and Research Facility, Grenfell Campus, MUN. I also acknowledge the support from Pathology Lab, Agriculture Agri-Food Canada, St. John's Research and Development Centre. Without their support, it would be difficult to conduct this research successfully.

I am also indebted to Dr Erika Merschrod, Dr Lakshman Galagedara and Dr Nadeem Muhammed for their guidance and support. And to my lab mates and colleagues: Tiffany, Heather, Amanda, Thilini, Abraham, Albert, Oluwashina, Charles, Melissa, Moganatharsa, and Minh Le Anh for their moral support. I cannot but also appreciate some wonderful friends and brethren, and spiritual leaders in Nigeria, Canada, United State of

America, United Kingdom, and across the globe, they are too numerous to mention. They have been source of inspiration and encouragement to me in words and prayers. Thank you.

To conclude, I would like to appreciate my family members, most especially my wife, Folasade, your prayers, financial and moral supports during this program are acknowledged. My thanks also go to my wonderful children: Favour, Grace and Mercy for their endurance and support in various aspects during my studies. You are indeed a wonderful and great family!

Table of contents

List of tables

List of figures

List of appendices

List of abbreviations

AcHexStE	Acylated hexosyl stigmasterol ester
AcHexSiE	Acylated hexosyl betasitosterol ester
AcHexCmE	Acylated hexosyl campesterol ester
AOS	Allene oxide synthases
avr	Avirulence gene
Avr	Avirulence protein
AZI1	Azelaic insensitive 1
Cer	Ceramide
CmE	Campesterol ester
CRC	Conrad root control
CRI	Conrad root inoculated
Conrad	Tolerant soybean cultivar
CYP450	Cytochrome P450
DES	Divinyl ether synthases
DG	Diacylglycerol
DGDG	Digalactosyldiacylglycerol
9, 10-DiHODE	(12*Z*,15*Z*)-9,10-dihydroxyoctadeca-12,15-dienoic acid

12,13-DiHOME	(*Z*)-12,13-dihydroxyoctadec-9-enoic acid
α-DOX	α-dioxygenase
EH	Epoxide hydrolase
16,17-EpDPE	(4*Z*,7*Z*,10*Z*,13*Z*)-15-[3-[(*Z*)-pent-2-enyl]oxiran-2-yl]pentadeca-4,7,10,13-tetraenoic acid
FA	Fatty acid
GGL	Glycoglycerolipid
GL	Glycerolipid
GPL	Glycerophospholipid
HexCer	Hexosyl ceramide
13-HOTrE	10(E),12(Z), 13S-hydroxy-9(Z),11(E),15(Z)-octadecatrienoic acid
12(S)-HpETE	12S-hydroperoxy-5(Z),8(Z),10(E),14(Z)-eicosatetraenoic acid
9-HpODE	10(E),12(E)-9-hydroperoxyoctadeca-10,12-dienoic acid
HR	Hypersensitivity response
IP_3	Inositol 1,4,5-triphosphate
9-KOTrE	15(Z)-9-oxo-octadecatrienoic acid
13-KODE	(9Z,11E)-13-Oxo-9,11-octadecadienoic acid
LOX	Lipoxygenase
LPA	Lysophosphatidic

LPC	Lysophosphatidylcholine
LPE	Lysophosphatidylethanolamine
MGDG	Monogalactosyldiacylglycerol
12-OPDA	12-oxophytodienoic acid
ORC	OX760-6 root control
ORI	OX760-6 root inoculated
Ox	Oxidized
OX760-6	Susceptible soybean cultivar
P. sojae	*Phytophthora sojae*
PA	Phosphatidic acid
PC	Phosphatidylcholine
PCD	Programmed cell death
PE	Phosphatidylethanolamine
PG	Phosphatidylglycerol
PI	Phosphatidylinositol
PIP_2	Phosphatidylinositol 4,5-biphosphate
PI-PLC	Phosphatidylinositol- phospholipase C
PL-PLC	Phospholipid-Phospholipase C

PLA	Phospholipase A
PLC	Phospholipase C
PLD	Phospholipase D
PO	Peroxygenase
PS	Phosphatidylserine
PST	Phytosterols
PTFE	Polytetrafluoroethylene
PUFA	Polyunsaturated fatty acid
R	Resistance gene
SEM	Scanning electron microscopy
SGL	Sphingolipid
SiE	Sitosterol ester
SM	Sphingomyelin
SPE	Solid phase extraction
StE	Stigmasterol ester
TG	Triacylglycerol

Chapter one

Introduction and overview

Introduction

1.1. Soybean and Phytophthora root and stem rot

Soybean is a versatile legume grown worldwide. Formerly, soybean was cultivated in northern Asia and in recent decades, it is also cultivated in North America, countries of the Southern Cone of Latin America and Sub-Saharan Africa (Cornelius & Goldsmith, 2020; Thomas et al., 2007). Soybean is the most important oil seed crop in the world and a good source of protein for both human and animal nutrition (Bicudo Da Silva, Batistella, Moran, Celidonio, & Millington, 2020; Sharma, Kaur, Goyal, & Gill, 2014). It serves as staple food for most of the world's population because of its high-quality protein and oil content of about 39 % and 17 % respectively (Rizzo & Baroni, 2018; Sharma et al., 2014).

Phytophthora root and stem rot is a devastating disease of soybean caused by the oomycete *Phytophthora sojae* (Dorrance, 2018; Roth et al., 2020; Tada, Kato, Tanaka, & Shiraiwa, 2021; Thomas et al., 2007; Wang et al., 2021). This disease causes approximately $2B USD economic loss yearly (Bandara, Weerasooriya, Bradley, Allen, & Esker, 2020; Wang et al., 2021). This infection occurs at any of the stages of growth in soybean, which may start from seedling to plant maturity (Dorrance, 2018). In the sequence of events that characterize disease progression; zoospores are initially produced from the sporangia and move to soybean roots. Chemotactic movement occurs due to the strong attraction between zoospores and certain components secreted by the root (Zhang et al., 2019). The isoflavones produced by soybean roots trigger zoospore encystment on the surface of the root (Morris, Bone, & Tyler, 1998). Encysted zoospores germinate 2 h post-infection, and germ tubes grow on the root surface and enter the epidermis. They spread from the cortex to vascular cylinder and from there to the entire plant (Mideros, Nita, & Dorrance, 2007; Moy, Qutob, Chapman, Atkinson, & Gijzen, 2004). Early season symptoms of the *P. sojae* infection comprise of pre-emergence seed rot and post-emergence damping off (Dorrance, 2018). The primary symptom of *Phytophthora* stem rot is the appearance of a dark brown lesion at the lower stem that spreads to the soybean taproot (Tyler, 2007). The dark

brown lesion usually extends to some nodes and colonized soybean stems, disallowing flow of water and nutrients, leading to plant death (Dorrance, 2018). The pathogen survives in the soil or on the residue of the plant as oospores. Further germination of oospores occurs in saturated soil at 16 °C to generates zoospores leading to infection at an optimal temperature of 25 °C to 30 °C (Dorrance, 2018; Tyler, 2007). Saturated soil and warm weather provide conducive conditions for disease immediately after planting.

The best method to manage Phytophthora root and stem rot is by cultivating resistant varieties (Burnham, Dorrance, Francis, Fioritto, & St. Martin, 2003). A race is a specific kind of the pathogen that infects certain resistance genes in the soybean. Such a plant, however, may not be effective should the attacking pathogen go through genetic change, and the process is known as race-specific resistance (Keller & Krattinger, 2018). However, there are some soybean varieties, that could exist in a single field with partial resistance that are capable of resisting more than one gene. These could be effective against all pathotypes (MacGregor et al., 2002; Thomas et al., 2007). Therefore, pyramided soybean lines carrying resistance genes with high tolerance against the boom and burst cycle of a single gene is required to ensure tolerance in soybean against *P. sojae* colonization and infection (Dorrance, 2018; Dorrance, McClure, & St. Martin, 2003). Partial resistance limits fungal colonization and infection in all soybean cultivars therefore, it has been inherited as novel quantitative trait locus demonstrated to be effective in managing all races of *P. sojae* (Lee et al., 2013; Schneider et al., 2016; Stasko et al., 2016).

Phytophthora sojae is an oomycete infectious pathogen of soybean, the family of kingdom of *Stramenopiles* (Harper, Waanders, & Keeling, 2005). This class of organisms produces swimming spores (zoospores) which have two flagella and the production of zoospore are mainly triggered by flooding in the laboratory and in the field. The oomycetes are “fungus-like” during their growing stage because they generate mycelium (Harper et al., 2005; Tyler, 2007). One of the most regular media used to culture and aseptically maintain *P. sojae* is V8-Juice agar (Thomas et al., 2007). On this medium, the mycelium grows near to the

surface of the agar and the colour of the hyphae is white, and the optimum temperature for the isolates on any medium to grow is 25 °C to 28 °C (Fig. 1.1). Oospores (thick-walled, sexual spores) form readily, frequently within 24 hrs on V8-juice agar disk. *P. sojae* is self-fertile and reproduce sexually (homothallic). The male structures, antheridia mostly attach to the side of the oogonial stalk, paragynous, but some would be encircling the oogonial stalk, amphigynous. Oospores have smooth walls and the oogonia are 40 µm to 45 µm in diameter (Fig.1.2). The dispersive nature, zoospores move toward the root and encyst the surface of the root and a single germ tube appears and enter the root epidermis and spread from the cortex to vascular cylinder and rest of the plant to give a complete picture of the infection process.

Fig.1.1. The vegetative structure of *P. sojae* Race 2 (P6497) cultured and aseptically maintained in 26 % V8-juice agar disk.

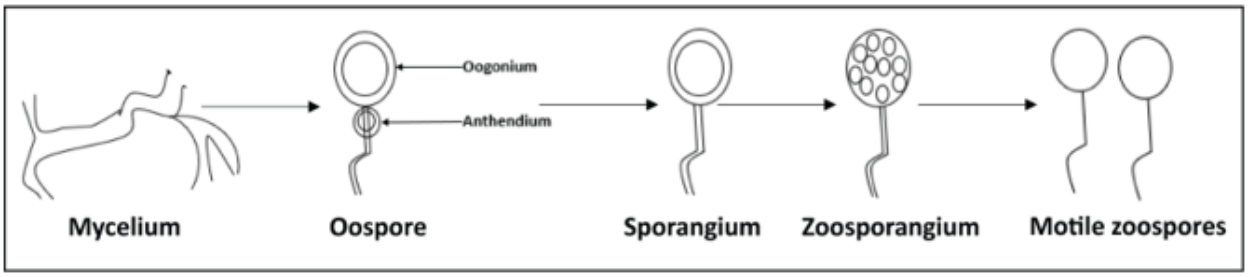

Fig. 1.2. Schematic diagram of zoospore of *P. sojae*.

The level of *P. sojae* infection on soybean starts from germinating seedlings to the maturity stage, depends on the level of tolerance in the plant (Tyler, 2007). *Phytophthora sojae* colonized and infected the cortex and the vascular tissue of soybean cultivars, but the infection rapidly spreads in the vascular tissue of susceptible cultivar (Tyler, 2007). The roots and stem change to dark brown colour, while the leaves turn yellow, and the whole seedlings changes to orange-brown colour. Sometimes, a lesion will only appear on one side of the plant, but it can spread from below the soil line up the plant. The yellowed, wilted leaves remain attached to the plant as it dies (Fig. 1.3a). In highly susceptible soybean cultivars, during the production season, almost all plants in the field may be infected and die (Fig. 1.3a). The taproot of older infected soybean plant would eventually turn dark brown, and the entire root system may become rotted, and the leaves would be chlorotic in between the veins and finally experience wilting and death (Fig. 1.3a). However, soybean cultivars with lower partial resistance may be infected and experience 20 % to 50 % loss (Fig. 1.3b). For soybean cultivars with higher partial resistance, the stem rot stage does not develop but the roots are also colonized and infected by showing light brown coloration, and in some cases the plants may grow stunted (Fig. 1.3b). For soybean cultivars with higher partial resistance, there are generally no visible symptoms were observed (Fig. 1.3b). Meanwhile, oomycete *Phytophthora sojae* is prevalent in many soybeans cultivated regions and countries, and this pathogen infection is mainly managed with varieties of host resistance to *P. sojae* (Thomas et al., 2007).

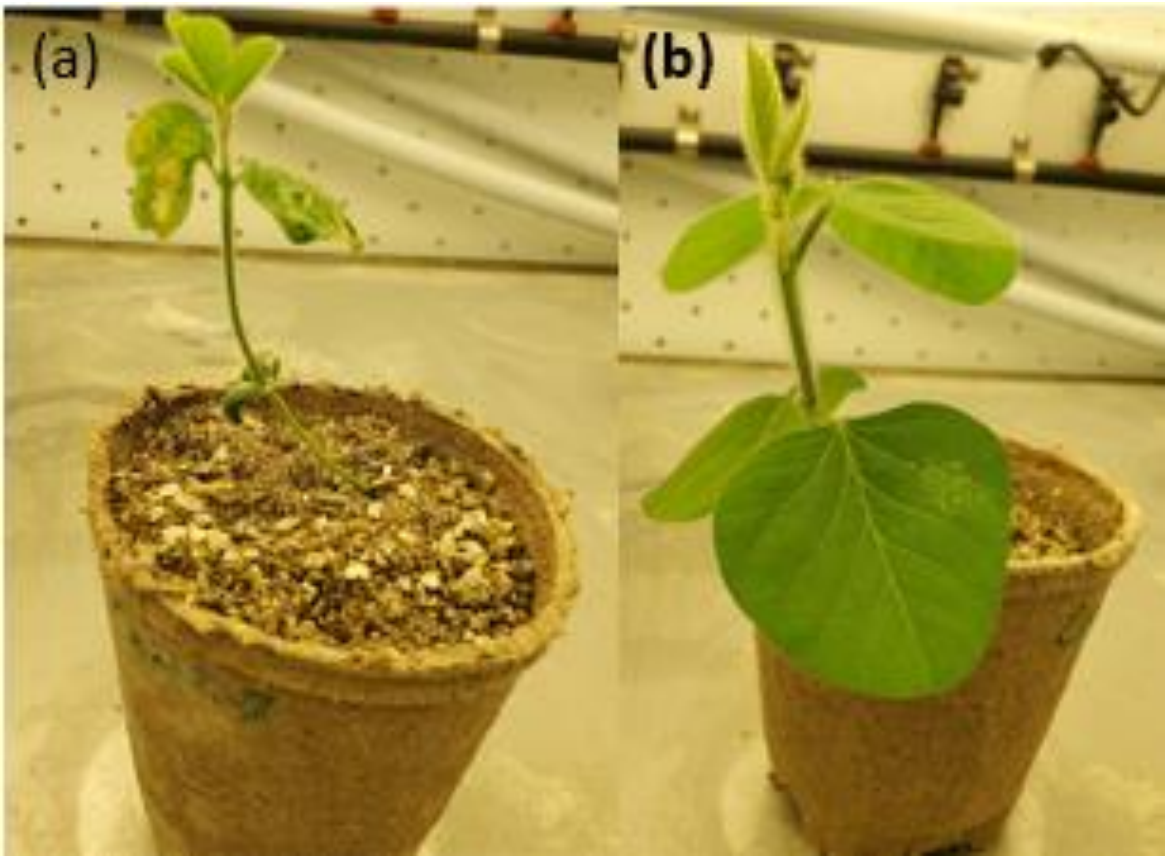

Fig. 1.3. Seedlings of soybean cultivars grown in a growth chamber in a controlled condition of approximately 16 h of alternating light at 25 ^{o}C, and 8 h of dark at 20 ^{o}C under 60 % relative humidity. Plants were watered daily with sterilized water to maintain moist to slightly dry vermiculite. The seedlings were allowed to grow for 10 days (a) Seedling of susceptible soybean cultivar shown disease symptoms of infection, early root and stem rot, stems wilting and yellowing of the leaves following inoculation with *P. sojae*. (b) Seedling of tolerant soybean cultivar following inoculation with *P. sojae*.

1.2. Thesis Rationale

In the 2019 report of World Population Prospects, the United Nations predicts an increase in the world's population to approximately 10 billion by the year 2050, with continued increases to 10.9 billion over the course of the 21st century (DeLong, Burger, & Hamilton, 2013; United Nations, 2019; Vågsholm, Arzoomand,

& Boqvist, 2020). The increase in global population puts a demand on current global food production, the quality and availability of food supplies. This necessitates improvements in food production and sustainable agriculture (Brackin, Atkinson, Sturrock, & Rasmussen, 2017). Improvement in crop production could play an important role in the ability to sustain global food security in the future (Vågsholm et al., 2020). Over the years, advance in agricultural practices have permitted improvement in the yield from crop plants, but it is insufficient to meet the demands of an ever-increasing global population. Most especially during host-pathogen interactions, application of genetically modified crops to improve disease resistance, and increase crop production and yields would likely be required to savage the global population from food insecurity (Qaim & Kouser, 2013). However, there are several biotic constraints such as oomycete *P. sojae* infection that threaten the production of soybean by directly reducing seed quality and yields (Dorrance, 2018; Hartman, West, & Herman, 2011; Thomas et al., 2007). In fact, no single resistance gene gives immunity to all races of *P. sojae* (Sahoo, Abeysekara, Cianzio, Robertson, & Bhattacharyya, 2017). The genetic properties of soybean cultivars differ in their defense responses to isolates of *P. sojae* (Sahoo et al., 2017). This has brought about disease management mechanisms with attention on development and characterization of high level of disease tolerant cultivars expressing quantitative disease resistance or partial resistance, instead of focusing mainly on single resistance genes (Dorrance et al. 2003; Hartman et al. 2015). In this regard, it is essential to understand the innate defense strategies used by plants, and subsequently derive techniques to improve them in cultivars with other desirable agronomic traits. Induced defense responses could be a defense mechanism against pathogens which are typically triggered through gene-for-gene interactions (War et al., 2012). Induced resistance could be utilized for developing crop cultivars, which readily generate the inducible defense response upon pathogen infections and could be a component of integrated disease management for sustainable agriculture (War et al., 2012). Emphasis could be placed on the role of lipid metabolites, oxylipins and related genes in response to pathogen attack (Adigun et al., 2020; Reim et al., 2020). Oxylipins function as intracellular and extracellular signal molecules during pathogen infection in plants and are also antimicrobial (Blée, 2002). One of the major

determinants of disease susceptibility in plants is the ability to respond to pathogen invasion through lipid metabolism and their metabolites, and alterations in gene-expression in response to pathogen attack (Reim et al., 2020; War et al., 2012). Therefore, the study provides a rationale for soybean development based on both qualitative and quantitative levels of the lipid biomarkers and induction of phyto-oxylipins in soybean to develop higher and durable resistance in soybean against *P. sojae* invasion and could possibly has a role in reducing crop loss.

1.3. Objectives of the thesis

Long-term objective: The long-term objective of this study is to understand the mechanism underlying successful disease tolerance in the soybean-*P. sojae* pathosystem.

The following short-term objectives were examined to test the proposed hypotheses:

i. To better understand how tolerant soybean cultivar naturally alter lipid metabolism to successfully limit colonization and infection by *Phytophthora sojae.*
ii. To better understand how oxylipin induction in tolerant soybean cultivar successfully limit colonization and infection by *Phytophthora sojae.*
iii. To better understand how unique morphological and biochemical structures in tolerant soybean root successfully mitigate colonization and infection by *Phytophthora sojae.*

1.4. Hypotheses

Hypothesis 1: Lipid mediated plant immunity appears to be one of the successful mechanisms used by tolerant soybean cultivar to mitigate colonization and infection by *P. sojae.*

Hypothesis 2: Upregulation of phyto-oxylipin anabolism mediated plant immunity appears to be one of the successful strategies used by tolerant soybean cultivar to limit colonization and infection by *P. sojae.*

Hypothesis 3: Unique histochemical and morphological structures is one of the successful mechanisms used by tolerant soybean to mitigate colonization and infection by *P. sojae*.

1.5. Thesis description

This thesis is divided into six chapters, and each chapter starts with relevant literature to the experiments conducted.

Chapter 1: This chapter covers a brief introduction and overview of soybean and Phytophthora root and stem rot, thesis rationale, objectives of the thesis, hypotheses, thesis description, co-authorship statement and selected publications.

Chapter 2: This chapter describes the review of current knowledge of the role of plant membrane lipids and their metabolites in the plant pathology, titled "Chemical, molecular and physiological aspect of lipids derivatives in plant pathology".

Chapter 3: This chapter demonstrates the lipid unique biomarkers of plant lipid metabolism in response to *P. sojae* colonization and infection in susceptible and tolerant soybean (*Glycine max* [L.] Merr) cultivars.

Chapter 4: This chapter describes the plant oxylipins rapid induction in response to *P. sojae* colonization and infection in susceptible and tolerant soybean (*Glycine max* [L.] Merr) cultivars.

Chapter 5: This chapter describes the morphological and biochemical changes in root of susceptible and tolerant soybean cultivars governing tolerance against *P. sojae* colonization and infection.

Chapter 6: This chapter summarized general discussion, conclusion, limitations of the studies, future work, and recommendation.

1.6. References

Adigun, O. A., Nadeem, M., Pham, T. H., Jewell, L. E., Cheema, M., & Thomas, R. (2020). Recent advances in bio-chemical, molecular and physiological aspects of membrane lipid derivatives in plant pathology. *Plant, Cell & Environment, 44*(1), 1-16.

Bandara, A. Y., Weerasooriya, D. K., Bradley, C. A., Allen, T. W., & Esker, P. D. (2020). Dissecting the economic impact of soybean diseases in the United States over two decades. *PLoS One, 15*(4), e0231141-e0231141.

Bicudo Da Silva, R. F., Batistella, M., Moran, E., Celidonio, O. L. D. M., & Millington, J. D. A. (2020). The Soybean Trap: Challenges and risks for Brazilian producers. *Frontiers in Sustainable Food Systems, 4*(12).

Blée, E. (2002). Impact of phyto-oxylipins in plant defense. *Trends Plant Sci, 7*(7), 315-322. doi:10.1016/s1360-1385(02)02290-2.

Brackin, R., Atkinson, B. S., Sturrock, C. J., & Rasmussen, A. (2017). Roots-eye view: Using microdialysis and microCT to non-destructively map root nutrient depletion and accumulation zones. *Plant, Cell & Environment, 40*(12), 3135-3142.

Burnham, K. D., Dorrance, A. E., Francis, D. M., Fioritto, R. J., & St. Martin, S. K. (2003). Rps8, a new locus in soybean for resistance to *Phytophthora sojae*. *Crop Science, 43*(1), 101-105.

Cornelius, M., & Goldsmith, P. (2020). Soybean yield in Africa. *African Journal of Food, Agriculture, Nutrition and Development, 19*, 15169-15172.

DeLong, J. P., Burger, O., & Hamilton, M. J. (2013). The UN medium population projection is an unstable equilibrium. *Frontiers in Ecology and the Environment, 11*(2), 65-66.

Dorrance, A. E. (2018). Management of Phytophthora sojae of soybean: a review and future perspectives. *Canadian Journal of Plant Pathology, 40*(2), 210-219.

Dorrance, A. E., McClure, S. A., & St. Martin, S. K. (2003). Effect of partial resistance on Phytophthora stem rot incidence and yield of soybean in Ohio. *Plant Disease, 87*(3), 308-312.

Harper, J. T., Waanders, E., & Keeling, P. J. (2005). On the monophyly of chromalveolates using a six-protein phylogeny of eukaryotes. *Int J Syst Evol Microbiol, 55*(Pt 1), 487-496.

Hartman, G. L., West, E., & Herman, T. (2011). Crops that feed the World 2. Soybean-worldwide production, use, and constraints caused by pathogens and pests. *Food Security, 3*, 5-17.

Keller, B., & Krattinger, S. G. (2018). A new player in race-specific resistance. *Nature Plants, 4*(4), 197-198.

Lee, S., Mian, M. A. R., McHale, L. K., Wang, H., Wijeratne, A. J., Sneller, C. H., & Dorrance, A. E. (2013). Novel quantitative trait loci for partial resistance to *Phytophthora sojae* in soybean PI 398841. *TAG. Theoretical and applied genetics. Theoretische und angewandte Genetik, 126*(4), 1121-1132.

MacGregor, T., Bhattacharyya, M., Tyler, B., Bhat, R., Schmitthenner, A. F., & Gijzen, M. (2002). Genetic and Physical Mapping of Avr1a in *Phytophthora sojae*. *Genetics, 160*(3), 949-959.

Mideros, S., Nita, M., & Dorrance, A. E. (2007). Characterization of components of partial resistance, Rps2, and root resistance to *Phytophthora sojae* in soybean. *The American Phytopathological Society, 97*(5), 655.

Morris, P., Bone, E., & Tyler, B. (1998). Chemotropic and contact responses of *Phytophthora sojae* hyphae to soybean isoflavonoids and artificial substrates1. *Plant Physiology, 117*.

Moy, P., Qutob, D., Chapman, B. P., Atkinson, I., & Gijzen, M. (2004). Patterns of gene expression upon infection of soybean plants by *Phytophthora sojae*. *Mol Plant Microbe Interact, 17*(10), 1051-1062.

Qaim, M., & Kouser, S. (2013). Genetically modified crops and food security. *PloS one, 8*(6), e64879-e64879.

Reim, S., Rohr, A.-D., Winkelmann, T., Weiß, S., Liu, B., Beerhues, L., . . . Flachowsky, H. (2020). Genes involved in stress response and especially in phytoalexin biosynthesis are upregulated in four malus genotypes in response to apple replant disease. *Frontiers in Plant Science, 10*(1724).

Rizzo, G., & Baroni, L. (2018). Soy, Soy Foods and Their Role in Vegetarian Diets. *Nutrients, 10*(1), 43.

Roth, M. G., Webster, R. W., Mueller, D. S., Chilvers, M. I., Faske, T. R., Mathew, F. M., . . . Smith, D. L. (2020). Integrated management of important soybean pathogens of the United States in changing climate. *Journal of Integrated Pest Management, 11*(1).

Sahoo, D. K., Abeysekara, N. S., Cianzio, S. R., Robertson, A. E., & Bhattacharyya, M. K. (2017). A novel *Phytophthora sojae* resistance Rps12 gene mapped to a genomic region that contains several Rps genes. *PloS one, 12*(1), e0169950-e0169950.

Schneider, R., Rolling, W., Song, Q., Cregan, P., Dorrance, A. E., & McHale, L. K. (2016). Genome-wide association mapping of partial resistance to *Phytophthora sojae* in soybean plant introductions from the Republic of Korea. *BMC Genomics, 17*(1), 607.

Sharma, S., Kaur, M., Goyal, R., & Gill, B. S. (2014). Physical characteristics and nutritional composition of some new soybean (*Glycine max* (L.) Merrill) genotypes. *Journal of food science and technology, 51*(3), 551-557.

Stasko, A. K., Wickramasinghe, D., Nauth, B. J., Acharya, B., Ellis, M. L., Taylor, C. G., . . . Dorrance, A. E. (2016). High-density mapping of resistance QTL toward *Phytophthora sojae*, *Pythium irregulare*, and *Fusarium graminearum* in the same soybean population. *Crop Science, 56*(5), 2476-2492.

Tada, T., Kato, M., Tanaka, C., & Shiraiwa, T. (2021). Effects of *Phytophthora sojae* inoculation under flooded conditions on growth of soybean seedlings. *Plant Production Science, 24*(4), 433-439.

Thomas, R., Fang, X., Ranathunge, K., Anderson, T. R., Peterson, C. A., & Bernards, M. A. (2007). Soybean root suberin: anatomical distribution, chemical composition, and relationship to partial resistance to *Phytophthora sojae*. *Plant Physiology, 144*(1), 299-311.

Tyler, B. M. (2007). *Phytophthora sojae*: root rot pathogen of soybean and model oomycete. *Molecular Plant Pathology, 8*(1), 1-8.

United Nations. (2019). World population prospects (2019). The 2019 revision of world population prospects. New York: United Nations, Department of Economic and Social Affairs. [Press release]

Vågsholm, I., Arzoomand, N. S., & Boqvist, S. (2020). Food security, safety, and sustainability—Getting the trade-offs right. *Frontiers in Sustainable Food Systems, 4*(16).

Wang, W., Chen, L., Fengler, K., Bolar, J., Llaca, V., Wang, X., . . . Ma, J. (2021). A giant NLR gene confers broad-spectrum resistance to *Phytophthora sojae* in soybean. *Nature Communications, 12*(1), 6263.

War, A. R., Paulraj, M. G., Ahmad, T., Buhroo, A. A., Hussain, B., Ignacimuthu, S., & Sharma, H. C. (2012). Mechanisms of plant defense against insect herbivores. *Plant signaling & behavior, 7*(10), 1306-1320.

Zhang, Z., Xu, Y., Song, G., Gao, X., Zhao, Y., Jia, M., . . . Wen, J. (2019). *Phytophthora sojae* zoospores differ in chemotaxis to the root and root exudates of host soybean and nonhost common bean. *Journal of General Plant Pathology, 85*(3), 201-210.

Chapter two

Literature review

Recent advances in bio-chemical, molecular and physiological aspects of membrane lipid derivatives in plant pathology

2.1. Abstract

Plant pathogens pose a significant threat to the food industry and food security accounting for 10-40 % crop losses annually on a global scale. Economic losses from plant diseases are estimated at $300B for major food crops and are associated with reduced food availability and accessibility, and also high food costs. Although strategies exist to reduce the impact of diseases in plants, many of these introduce harmful chemicals to our food chain. Therefore, it is important to understand and utilize plants' immune systems to control plant pathogens to enable more sustainable agriculture. Lipids are core components of cell membranes and as such are a part of the first line of defense against pathogen attack. Recent developments in omics technologies have advanced our understanding of how plant membrane lipid biosynthesis, remodeling, and/or signaling modulate plant responses to infection. Currently, there is limited information available in the scientific literature concerning lipid signaling targets and their biochemical and physiological consequences in response to plant pathogens. This review focuses on the functions of membrane lipid derivatives and their involvement in plant responses to pathogens as biotic stressors. We describe major plant defense systems including systemic acquired resistance, basal resistance, hypersensitivity, and the gene-for-gene concept in this context.

***Keywords*:** Chemical, molecular, lipid, pathogenicity, pathogen, plant pathology

2.2. Introduction

The advancement in global agricultural production, the food industry, and food security necessitates consideration of the impact of infectious pathogens on plants. This is because pathogens are widely recognized as significant obstacles to important and dependable food systems (Savary et al., 2019). Recent reports have demonstrated that plant diseases pose a significant threat to the food industry and to food security accounting for 10 % to 40 % crop losses annually on a global scale. Economic losses from plant diseases are estimated at $300B for major food crops, and diseases are associated with reduced food production, availability and accessibility, and also high food costs (Fletcher et al., 2006; Savary et al., 2019). Plants face different biotic stresses during their life cycle. For instance, a variety of diseases are caused by fungi, bacteria, protozoa, nematodes, viruses, and phytoplasmas. These pathogens change favorable growing environments for plants into unfavorable conditions, particularly during susceptible growth stages. These cause significant yield losses both in greenhouses and under field conditions. Therefore, it is important to understand and utilize plants' innate immune systems to control plant infections to enable more sustainable agriculture (Brackin, Atkinson, Sturrock, & Rasmussen, 2017).

Natural defense mechanisms involve a variety of signaling events and responses, which serve to combat intruding pathogens. The defense mechanism is categorized into constitutive and induced defense mechanisms. As the first line of defense, constitutive mechanisms use pre-formed chemicals and barriers such as cellulose, waxy epidermal cuticles, and suberin to prevent pathogen entry; in contrast, induced defenses are generated in response to pathogen attack (Fig. 2.1). Plants continuously face challenges of multiple biotic stresses in their natural environment. The development of diseases in plants depends on plant-pathogen-environment interactions conceptualized as the disease triangle (Scholthof, 2007). Disease occurs when a pathogen attacks a susceptible plant and environmental conditions favor the disease development (Velásquez, Castroverde, & He, 2018). Plants must cope with various pathogens to survive in their physical environment and have innate immune systems that act as defense mechanisms against potential pathogens. These systems may be effective against all races of a

specific pathogen and can exist in different varieties of a host plant species (Gill, Lee, & Mysore, 2015; Niks & Marcel, 2009). The plant immune systems adopt two layers of defense mechanisms against pathogens. These layers are comprised of pathogen or microbe-associated molecular pattern-triggered immunity accompanied by effector-triggered immunity which recognizes and protects plants from infectious pathogens (Hou, Yang, Wu, & Zhang, 2011). The first layer depends on receptor molecules in the cells and is activated through the specific recognition of pathogen or microbe-associated molecular patterns by plant cell pattern recognition receptors upon perception of microbial general elicitors. This type of plant defense system is called non-host specific resistance. The second layer is effector-triggered immunity, otherwise called host-specific resistance, and occurs when race-specific effector molecules of pathogens are specifically recognized by a plant resistance (R) protein. In the event of non-host specific resistance, a specific plant can be resistant to a given pathogen, while the same pathogen may successfully attack other plants. This process is initiated by the specific recognition of pathogen-associated molecular patterns by pattern recognition receptors. In the first phase of plant innate immunity, pathogen-associated molecular pattern-triggered immunity stops the colonization of plants by pathogens after the pathogen-associated molecular patterns are recognized by pattern recognition receptors in the host (Abdul Malik, Kumar, & Nadarajah, 2020).

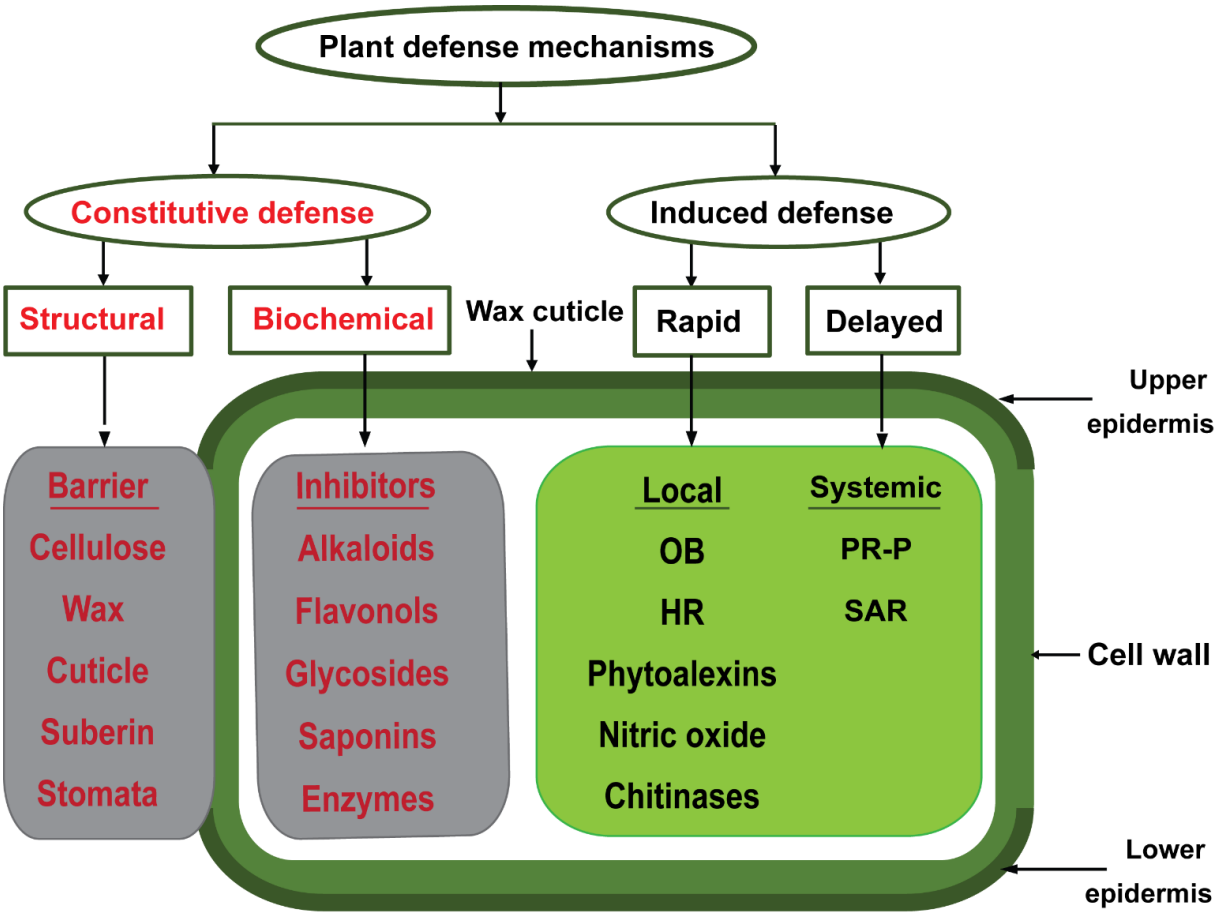

Fig. 2.1. Defense mechanisms used by plants to combat infection. Constitutive (i.e. pre-formed) defenses include the plant's exterior protection and act as the first line of defense against pathogen ingress. Aboveground structural barriers include a waxy cuticle and an epidermis. If pathogens breach the structural barrier, they encounter a variety of constitutive, host-specific secondary metabolites that may be inhibitory or directly toxic. In addition, induced defense mechanisms can be triggered by the presence of pathogens, whereby plants produce additional compounds and/or enzymes as a direct consequence of pathogen detection. Induced defenses may be either localized to the site of pathogenic attack and include enzymes (such as chitinases), processes such as the oxidative burst (OB) or hypersensitive response (HR), or small molecules (such as phytoalexins or nitric oxide); or systemic throughout the plant and involve processes such as the synthesis of pathogenesis-related proteins (PR-P) or the activation of systemic acquired resistance (SAR).

The plant hypersensitive defense reaction is used to protect against pathogenic infection and is an important component of the gene-for-gene resistance mechanism (Balint-Kurti, 2019). The hypersensitive defense reaction occurs in all higher plants and is identified by rapid localized cell death at the infection site associated with defense gene expression (Heath, 2000). The uniqueness of the hypersensitive defense reaction is the isolation of the intruder from cells in the surrounding area thereby causing its starvation and death (Balint-Kurti, 2019; Postel & Kemmerling, 2009). Events that occur concurrently with the localized cell death in the hypersensitive defense reaction response are caused by biochemical changes, and include the production of an oxidative burst, phytoalexins, hydrolytic enzymes, salicylate, pathogenesis-related proteins, proteinase inhibitors, and the deposition of lignin and callose in the compatible and incompatible interactions (Heath, 2000; Hoglund, Larsson, & Wingsle, 2005). Considering the simultaneous nature of these events, it is difficult to determine whether cell death or resistance is a cause or effect of the hypersensitive defense reaction (Aranega-Bou, de la O Leyva, Finiti, García-Agustín, & González-Bosch, 2014; Hoglund et al., 2005). The hypersensitive defense reaction is the result of a biochemical process that eventually kills both host cells and the pathogen (Balint-Kurti, 2019; Chaplin, 2010).

The hypersensitive defense reaction is mainly triggered by the plant after recognition of a pathogen or any other biotic stressor. This often occurs when pathogens secrete avirulence (Avr) gene products that bind to or incidentally interact with R gene products in host plants. This is referred to as gene-for-gene or qualitative resistance. Whenever the R gene from the plant and the matching Avr gene from the pathogen are present, recognition occurs which subsequently results in disease resistance for the host and the avirulence of the pathogen (Fig. 2.2a). However, if either the Avr gene from the pathogen or the R gene in the plant is not present, there is a lack of recognition, which leads to a compatible reaction and disease infection (Fig. 2.2b). The activation of plant defense responses occurs during direct interaction between R and Avr proteins. For example, the tomato (*Solanum lycopersicum*) disease bacterial speck is caused by *Pseudomonas syringae* pv. tomato (Pst), but tomato is a non-

host for other *P. syringae* pathovars. Resistance to strains of Pst containing avr gene *avrPto* is conferred by the *Pto* gene in tomato cultivars (Eckardt, 2004; Mucyn et al., 2006; Veluchamy, Hind, Dunham, Martin, & Panthee, 2014). The interrelationship between these gene products may contribute to resistance to many *P. syringae* pathovars among tomato cultivars (Lin & Martin, 2007). Defense responses are responsible for restricting or preventing pathogen growth. Plants produce various kinds of R gene products that are resistant to pathogens that produce the corresponding Avr gene products. This characteristic property enables R gene products to function as receptors of Avr proteins generated by diverse pathogens (Heath, 2000).

The basal defense system notably overlaps with non-host-specific recognition because it is possible that both host and non-host plants may recognize the same factors to initiate defense responses (Shamrai, 2014). In 2006, Jones and Dangl proposed a famous zig-zag model that highlighted the initiation of plant defense responses and corresponding pathogen attack (Jones & Dangl, 2006). This model explained that there are numerous pattern recognition receptors in plants able to recognize pathogen or microbe-associated molecular patterns and initiate basal defense responses (Jones & Dangl, 2006). Some adapted pathogens secrete effectors to suppress recognition by pattern recognition receptors and promote pathogen colonization and virulence (Thordal-Christensen, Birch, Spanu, & Panstruga, 2018; Toruño, Stergiopoulos, & Coaker, 2016). However, suppression of pathogen-associated molecular pattern-triggered immunity by potential pathogen effectors results in effector-triggered susceptibility. In response to this, plant-triggered R-proteins interact with pathogen effectors directly or indirectly and induce a stronger defense response called effector-triggered immunity.

Reactive oxygen species have been specifically recognized as signals in defense and are significant during the oxidative burst(s). The oxidative burst protects plants against pathogenic infection by generating reactive oxygen species such as hydrogen peroxide, a hydroxide radical, or an anion radical which are extremely reactive and toxic, causing damage to proteins, lipids, carbohydrates, and deoxyribonucleic acid and ultimately resulting in oxidative stress to normal cells and tissues (Nita & Grzybowski, 2016). The oxidative burst occurs in cells

within the vicinity of the infection site due to the activation of nicotinamide adenine dinucleotide phosphate hydrogen oxidase associated with the cellular membrane. This enzyme catalyses the formation of superoxide (O_2^-) anions which readily form other reactive oxygen species products including hydrogen peroxide and perhydroxyl radical ($HOO^{\cdot}$) via non-enzymatic and enzymatic processes (Panday, Sahoo, Osorio, & Batra, 2015). Reactive oxygen species tend to accumulate with low amplitude (moderate concentrations) at the initial phase, but accumulate at a much higher concentration during the sustained phase, correlating with the hypersensitive reaction in gene-for-gene resistance (Balint-Kurti, 2019; Heath, 2000), or during recognition of pathogen- or microbe-associated molecular patterns in basal resistance (Mackey, Holt, Wiig, & Dangl, 2002). They are a class of molecules which limit infections to a localized area and actively participate in the signal transduction system.

Reactive oxygen species mediate signaling by two different modes of oxidative burst. Firstly, the oxidative burst activates Ca^{2+} ion influx across the cellular membrane via cyclic nucleotide-gated channels along with mobilization of Ca^{2+} ions from intracellular resources (Suzuki et al., 2007). Secondly, an alteration in cytoplasmic Ca^{2+} ion concentrations occur by triggering the Ca^{2+} ion-dependent protein kinase along with mitogen-activated protein kinase. It is well established that mitogen-activated protein kinase cascades are functionally active in cell death control, regulation of reactive oxygen species generation, pathogenesis-related gene induction, and initiating induced resistance in plant tissues within and beyond the infection site (Pedley & Martin, 2005).

Another major defense pathway by which plants fight against infectious disease is by remodeling their lipid composition. Lipids and their metabolites have a significant influence on pathogenesis and may be used as a resistance mechanism during plant-microbe interactions (Christensen & Kolomiets, 2011). To attack plants, pathogens secrete toxins that target plant lipid metabolism. These toxins play key functions in host-pathogen interactions (Castro-Moretti, Gentzel, Mackey, & Alonso, 2020). However, plants adopt several defense mechanisms against pathogens using physical barriers, secondary metabolites, and chemical signaling compounds such as lipopolysaccharides, sphingolipids (SGLs), and lipid-binding proteins (Andersen, Ali, Byamukama, Yen,

& Nepal, 2018). Lipids are organic molecules that make up the building blocks of living cells and play a role in a variety of biological functions. They are critical components of membrane structure, and also function as storage molecules and key participants in signaling processes (Ingólfsson et al., 2014; Wältermann & Steinbüchel, 2005). They are fundamental components of prokaryotic and eukaryotic membranes (Coskun & Simons, 2011; van Meer, Voelker, & Feigenson, 2008). Lipids play significant roles in various physiological processes in biological systems (Ayala, Muñoz, & Argüelles, 2014; de Carvalho & Caramujo, 2018; Fernandis & Wenk, 2007; Wenk, 2005). They can be categorised as functional or regulatory molecules.

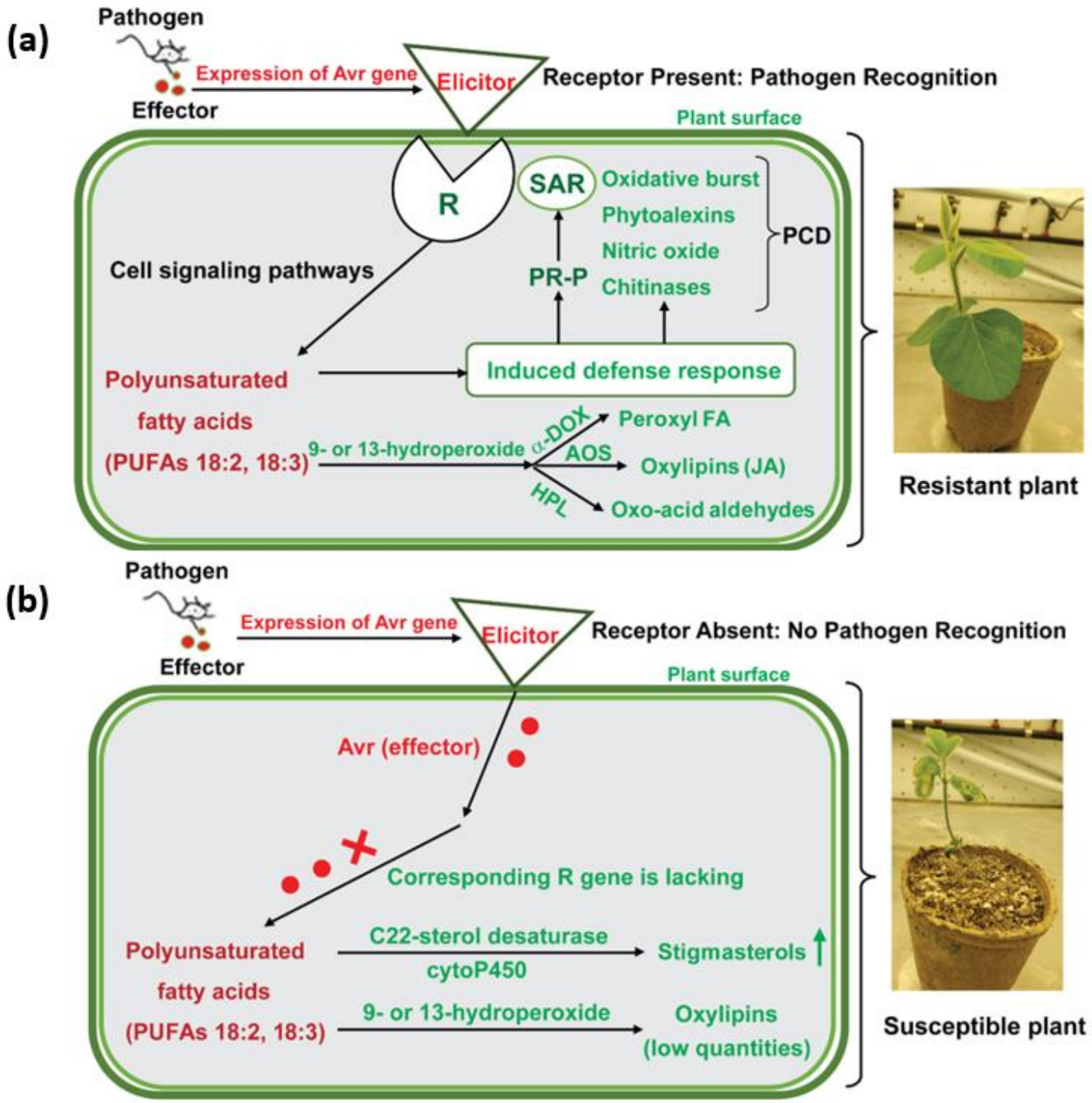

Fig. 2.2. The interaction between plant resistance (R) gene(s) and pathogen avirulence (avr) gene(s) in resistant (a) and susceptible (b) plants. Attachment of pathogen(s) to the plant cell causes avr gene expression. These effectors enter host cells via appropriate receptors or specialized systems. (a) The plant cell expresses R gene

product(s) with the capability of recognizing specific avr gene products from a pathogen. The occurrence of localized cell death in the hypersensitive response (HR) is due to biochemical changes such as production of an oxidative burst, phytoalexins, hydrolytic enzymes, salicylate, and the expression of pathogenesis-related proteins (PR-P). Systemic acquired resistance (SAR) is a complete plant resistance response that occurs following HR. The polyunsaturated fatty acids (PUFAs) 18:2 (linoleic acid) and/or 18:3 (linolenic acid) act as substrates for the enzymes lipoxygenase (LOX), α-dioxygenase (α-DOX), allene oxide synthase (AOS), and hydroperoxide lyase (HPL) and produce compounds that may further stimulate plant defenses. (b) The host cell does not express an R gene and fails to recognize any avr gene products. Induced sterol C22 desaturation by the enzyme CYP450 increases the ratio of stigmasterol to β-sitosterol. Low quantities of oxylipin(s) are produced by inducible LOX in the cell membrane, leading to plant susceptibility.

The functional lipids include FAs, hydroxy FAs, glycolipids, glycerophospholipids (GPLs), SGLs, phytosterols (PSTs), and wax esters (de Carvalho & Caramujo, 2018). These are important constituents of cell membranes that possess multiple yet distinct and essential roles in cellular functions. In plants, lipids and lipid-based derivatives provide diverse biological functions such as storage of carbon energy, cell compartmentalisation, membrane trafficking, exo- and endo-cytosis, photosynthesis, cytoskeletal rearrangements, stress responses, and signal transduction (Qualmann & Kessels, 2002; Shea & Poeta, 2006).

The regulatory lipids are a class of lipids which have been actively demonstrated as mediators of signaling and regulatory cascades, and are capable of functioning effectively at low concentrations (Tholl & Aharoni, 2014). Examples of these classes of bioactive lipids include PUFA derivatives such as oxylipins, eicosanoids, as well as jasmonic acid. The chemical composition of a lipid determines its functionality (Ingólfsson et al., 2014; Wältermann & Steinbüchel, 2005). For example, lipids may differ in FA chain length and the level of unsaturation. Various lipids may help to either eliminate disease-causing organisms or curb their spread in the plant (Wältermann & Steinbüchel, 2005).

Other signaling molecules are phytohormones like salicylic acid and ethylene, which are capable of defending plants against herbivores and necrotrophic pathogens (Tholl & Aharoni, 2014; Yang, Dong, & Hammock, 2011). As essential components of unicellular and multicellular membranes, lipids serve as structural components of plasma membranes. They also play different roles in energy storage, cell signaling and stress defense in plants including modulation of a plant's chemical, molecular and physiological responses to pathogen attack (Christensen & Kolomiets, 2011; Liu & Lam, 2019; Siebers et al., 2016).

From a molecular perspective, Gachomo, Shonukan and Kotchoni (2003) noted that lipids are functionally significant in plant pathology by producing biomolecular compounds, such as lipid-derived metabolites with antibiotic properties and defense regulatory activities. The role of lipids also varies with respect to their molecular

weight (Dowhan, Bogdanov, & Mileykovskaya, 2016). Effector-triggered immunity is an immune response capable of recognizing molecules that are characteristic of microorganisms. Pathogen recognition is key to inherent immune defenses and is triggered by pattern recognition receptors that recognize and distinguish pathogen- or microbe-triggered immunity (Ipcho et al., 2016; Newman, Sundelin, Nielsen, & Erbs, 2013; Noman, Aqeel, & Lou, 2019; Zipfel, 2014). Successful pathogens can overcome pathogen- or microbe-triggered immunity through secreted effectors that suppress pathogen- or microbe-triggered immunity responses, and lead to effector-triggered susceptibility in host plants (Jones & Dangl, 2006).

With regards to physiological impacts, lipids form the basis for metabolism and provide the basic composition of cell membranes. The role of plant lipids is complex due to the numerous ways they combine with other lipid moieties or other compounds leading to a diverse array of complex structures. Thus, there are substantial technical difficulties in differentiating non-pathogenic and pathogenic lipids, which each consist of thousands of isoforms. However, the integration of plant lipidomics with other omics such as genomics, metabolomics or proteomics has created a sophisticated and efficient set of scientific tools. These tools can unravel the chemical, molecular and physiological systems of disease-associated lipids in plants. They are also capable of providing a mechanism to identify biomarkers and cell signaling pathways for plant disease resistance (Hu, Rampitsch, & Bykova, 2015; Plett & Martin, 2018). To this end, this review will elucidate the recent understanding of the chemical, molecular, and physiological aspects of lipids in plant pathology.

2.3. Chemical, molecular and physiological functions of membrane lipids in plant pathology

The chemical properties and the molecular structures of lipids are important in the role they play in plant pathology. Plant lipids are mainly classified as FAs, glycolipids, GPLs, SGLs, PSTs, saccharolipids, prenol lipids, polyketides, and surface lipids such as wax esters and cutin. Plants also contain chemically diverse metabolites of oxygenated FAs called oxylipins which are produced in response to infection. This family of metabolites

includes hydroperoxides, hydroxides, oxoacids, ketoacids, aldehydes and divinyl ethers. They are actively involved in plant defense mechanisms (Blée, 2002; Cheng et al., 2004; Lim, Singhal, Kachroo, & Kachroo, 2017).

The plant oxylipin jasmonic acid interacts with other phytohormone signaling pathways that utilize other chemical signals including abscisic acid, ethylene, and salicylic acid to regulate plant defense against pathogen attack and plant growth (Liechti & Farmer, 2006; Lim et al., 2017). Phytohormones play key roles in plant growth and development and defense responses to stresses; crosstalk between phytohormones controls the balance between these priorities. The major hormones actively involved in plant innate immunity are salicylic acid, jasmonic acid and ethylene. Their production is triggered upon microbe-associated molecular pattern perception (Bigeard, Colcombet, & Hirt, 2015). In general, jasmonic acid and ethylene signaling are primarily responsible for defense against necrotrophs (Bigeard et al., 2015; Zhang, Zhang, Melotto, Yao, & He, 2017). For instance, jasmonic acid-mediated defense responses are raised against fungal pathogens like Botrytis cinerea, bacterial pathogens like *Plectosphaerella cucumerina* and oomycetes like *Pythium spp.* Also, jasmonic acid signaling has been demonstrated to play a role in the defense against some hemibiotrophic pathogens, such as in rice (*Oryzae sativa*) resistance to *Xanthomonas oryzae* (Zhang et al., 2017). In contrast, salicylic acid signaling plays an active role in local and systemic acquired resistance against biotrophic pathogens like *Pseudomonas syringae* (Li, Han, Feng, Yuan, & Huang, 2019). Balance between the competing priorities of growth, reproduction, and defense is achieved through crosstalk between various plant signaling networks. For example, salicylic acid-regulated and ethylene/jasmonic acid-regulated signaling pathways are important in plant immune responses against biotic invaders.

The molecular function of membrane lipids in plant pathology is crucial to the survival of the plant during pathogen invasion. Plant membrane lipids are composed of phospholipids, glycolipids, PSTs and SGLs. According to Christensen and Kolomiets (2011) and Siebers et al. (2016), membrane lipids and their derivatives

play key roles during the process of infection. They are actively involved in the formation of a membrane interface between the host and microbe (Christensen & Kolomiets, 2011; Siebers et al., 2016).

Membrane lipids are a heterogeneous group of molecules from a systemic structural and functional perspective. They have considerable variations in functions with respect to their molecular weight and lipid species (Fahy, Cotter, Sud, & Subramaniam, 2011). Membrane lipids exhibit a huge diversity in structure due to variations in chain length, functional group composition, and unsaturation. This allows for differences in chemical reactivity, ease with which molecular species are remodeled in response to infection by a pathogen, and differences in biosynthetic or metabolic processes that are activated (Fahy et al., 2011). For example, enzymes such as LOXs act as catalysts for the addition of oxygen molecules to PUFAs consisting of (Z,Z)-1,4-pentadienes to form an unsaturated FA hydroperoxide known to possess high anti-pathogenic activity in plants (Porta & Rocha-Sosa, 2002). Moreover, FAs or lipid mediated plant immunity can also play roles in various mechanisms for plant immunity against pathogensinvasion in relation to tolerance or quantitative disease resistance such as in signaling, defense, antimicrobial action, and lipid oxidation to protect plants at all stages of growth and development (Porta & Rocha-Sosa, 2002). Pathogen-derived lipids have also been known to act as pathogen-associated molecular patterns and/or microbe-associated molecular patterns and to trigger immune responses in plants (Ausubel, 2005; Henry, Thonart, & Ongena, 2012).

Plant lipid metabolism is a major aspect in plant pathology and is known to be affected by several factors. Therefore, adequate and accurate physiological adjustment to these factors are of significance with respect to the survival of the plants (Tardieu, 2013). In many plants, substantial evidence exists to reveal that the lipid bilayer is the main site of temperature and environmental sensitivity. At extreme temperatures, the membrane undergoes a change of state from liquid to crystalline (i.e. from its normal state to a gelatin state). This transformational change is followed by elevated permeability and an increase in the activation energy of the membrane-bound enzymes in the plant (Tardieu, 2013). Furthermore, the biochemical basis of temperature-induced change in plants

can be linked to the FA composition of certain membrane lipids in the plant. Usually, these lipids have higher proportions of PUFAs with their unsaturated bonds being distinctly responsive to oxidative damage by free radicals. The physiological process which creates an increase in the saturation of the membrane lipids can change the membrane's structure, and therefore affect membrane lipids' functional roles (Tardieu, 2013). The chemical, molecular and physiological functions of lipids in plant pathology are thus clearly interwoven. Meanwhile, enzymatic actions on phospholipids by phospholipases transform these lipids into secondary messengers or signaling molecules. These signaling molecules play active roles in cell signaling, membrane trafficking, and cell proliferation. Thus, phospholipases are involved in lipid metabolism and disease development.

2.4. Role and regulation of phospholipids in plant defense mechanisms

Phospholipids are important components of cellular membranes. They are actively involved in cellular processes such as cell signaling, cytoskeletal rearrangement, and membrane trafficking. They generally consist of two nonpolar FAs esterified to C1 and C2, and a polar phosphate head-group esterified to C3 of the glycerol (Fig. 2.3). Plant phospholipids are classified as phosphatidyl-chlorine, -ethanolamine, -serine, -inositol, -glycerol and phosphatidic acid (PA).

Phospholipases are enzymes that catalyse the hydrolysis of phospholipids into FAs, lysophospholipids, diacylglycerol (DG), or PA based on their specific activity (Fig. 2.4). Upon microbial infection, phospholipid-hydrolyzing enzymes are activated which are involved in regulatory functions by triggering the synthesis of defense-signaling molecules like phyto-oxylipins, jasmonic acid, and a second messenger PA. These signals activate the physiological responses that ultimately allow the plant to respond to biotic and abiotic stresses. Phospholipases A (PLA), C (PLC) and D (PLD), PA, and lysophospholipids are important constituents of plant membrane lipid signaling routes or pathways. This pathway involves reactions catalyzed by inositol polyphosphate phosphatases, phosphatidylinositol (PI) synthases, PLCs, PI transfer proteins, inositol

polyphosphate multikinase, and putative inositol polyphosphate receptors (Mueller-Roeber & Pical, 2002). Also, PI-specific PLCs are significantly involved in the creatine kinase-induced response (Cowan, 2006; Repp, Mikami, Mittmann, & Hartmann, 2004). Furthermore, auxin-mediated cell elongation is known to be directly related to PLA2 activity (Lee et al., 2003; Scherer, Labusch, & Effendi, 2012). PLA2 also acts as an important enzyme during jasmonic acid biosynthesis (Ryu, Murphy, Mysore, & Kloepper, 2004). Abscisic acid and ethylene-mediated cellular senescence are correlated with modifications in PLD enzymatic activity. In some plant systems, PLD activity upregulates during senescence and stresses (Asad et al., 2019; Finkelstein, Gampala, & Rock, 2002). Moreover, PLD/PA and abscisic acid have been discovered to play significant roles during cellular and physiological processes (Katagiri et al., 2005). Similarly, DG pyrophosphate was observed to act as a secondary messenger in abscisic acid cell signaling channels (Zalejski et al., 2005). In addition, genetic studies in the model species *Arabidopsis thaliana* have shown that modifications in phospholipid homeostasis influence the growth and development of plants (Wang, Cajigas, Peltz, Wilkinson, & Gonzalez, 2006).

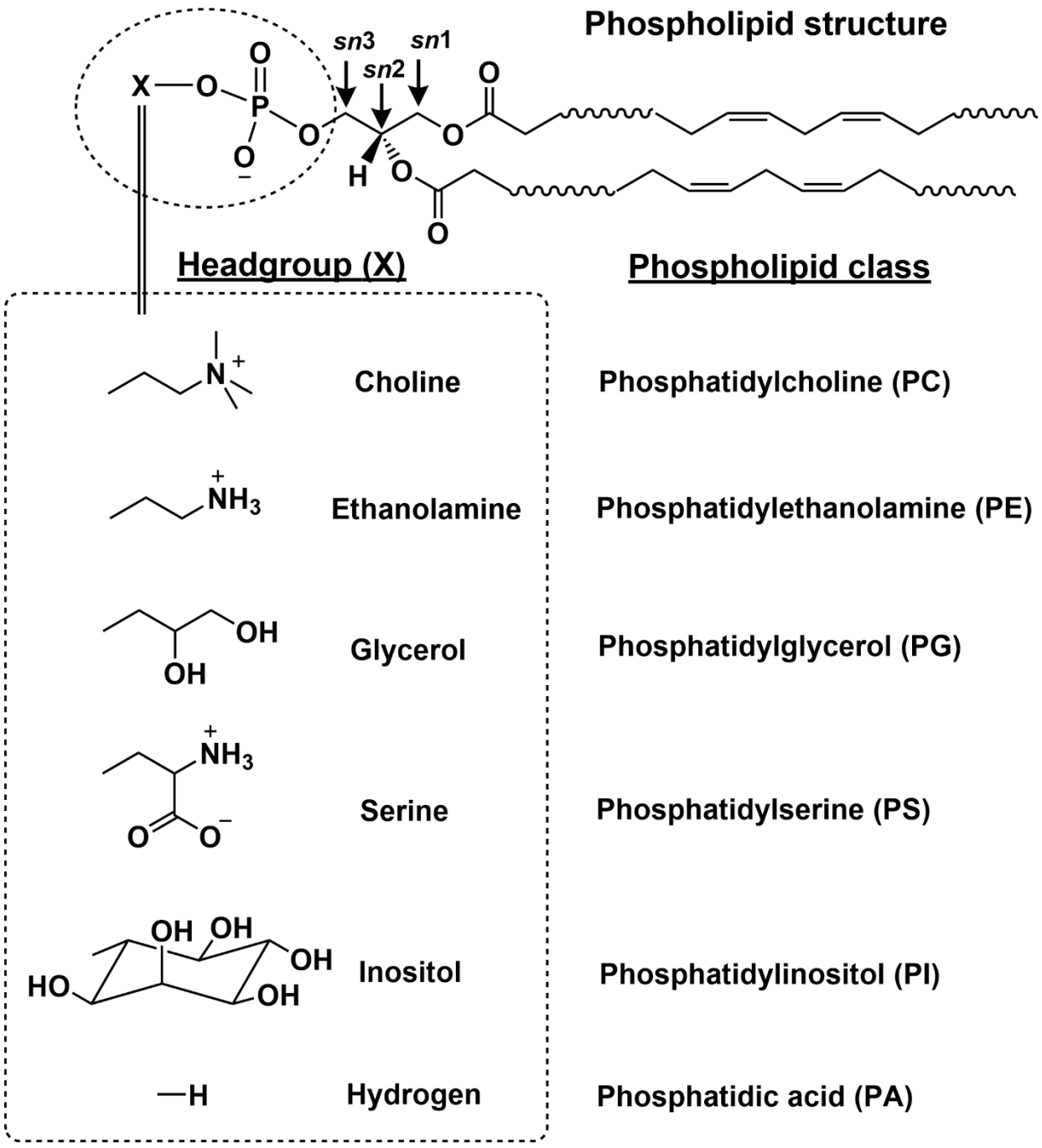

Fig. 2.3. Basic structure of phospholipids (PLs) and common head groups. PLs contain two FAs ester-linked to glycerol at sn_1 and sn_2 and a polar head group attached at the sn_3 position via a phosphodiester bond. The PL's FA can vary in carbon chain length and degree of saturation.

2.4.1. Role of phospholipase D

Phospholipase D (PLD) is a group of heterogeneous enzymes that break the terminal phosphodiester bond of phospholipids leading to the production of PA (Fig. 2.5). The PLD-induced hydrolysis of phospholipids is predominant in plants and its activities are elevated under various biotic stress conditions including pathogen attack (Hong, Dissing-Olesen, & Stevens, 2016). The increase in PA levels is often rapid during environmental stress conditions. Major changes in PLD and PA occur in stress-induced deterioration of membranes, for example during pathogen invasion or injuries. Genetic studies have indicated that PLD and PA participate in regulating the physiological processes in plant-pathogen interactions and other biotic stresses (Bargmann & Munnik, 2006; Wang et al., 2006).

The role of PA as a cellular messenger applies to the regulation of several pathways including G proteins, which are a group of proteins that function as molecular switches within cells. They are implicated in transmitting signals from various stimuli from the cell exterior to its interior. They primarily circulate the information from G-protein-coupled receptors on the cellular membrane to the internal structure of cells for biochemical regulation of cell defense functions. They also function in the modulation of cell physiological and phenotypic outcomes such as disease susceptibility or resistance (Zhao, Chang, Toh, & Arvan, 2007). Phosphatidic acid regulates phosphorylation of proteins, translation and transcription in biosynthesis of glycolipids, proliferation of cells, and growth (Huang & Frohman, 2007; Nadeem et al., 2019; Nadeem et al., 2020). Survival, cell multiplication, and reproduction along with plant-pathogen interactions are linked to the functionality of PA and PLD. Different PLDs seem to possess specific but somewhat overlapping cellular functions (Uraji et al., 2012). The functions of PLDs are usually carried out by their enzymatic product, PA, which is considered to be a general lipid signaling molecule regulating various physiological processes (Pleskot, Li, Zarsky, Potocky, & Staiger, 2013).

The PLD genes are more numerous in plants than in other organisms. In *Arabidopsis thaliana*, there are twelve PLDs classified into six families. Both the PLDα and PLDγ families have three members; PLDβ and PLDζ

have two members; and PLDσ and PLDε have one member each (note that PLDε was originally identified as PLDα4). PLDs can be categorized into two subfamilies according to the structures of the overall protein domain. These subfamilies are the Ca^{2+} and phospholipid-binding domain PLDs (Ca^{2+}-PLDs) and the pleckstrin/phox (PH/PX)-homology PLDs. Among Arabidopsis PLDs, ten PLDs (all members of the α, β, δ, σ, and ε families) belong to the Ca^{2+}-PLD subfamily, whereas the PLDζs belong to the PX/ PH-PLD subfamily. These two PLD subfamilies vary in the main amino acid residues within regulatory motifs of the Ca^{2+} and phospholipid-binding domains, as well as the phosphatidylinositol 4,5-bisphosphate (PIP_2) binding domains. In *Arabidopsis thaliana*, PLDβ1 regulates pathogen-mediated jasmonic acid synthesis and resistance of the plant against the necrotrophic fungal pathogen *Botrytis cinerea.* Accumulation of salicylic and jasmonic acids in response to pathogen attack results in the synthesis of plant defense genes (Spoel et al., 2003) Concurrently, the salicylic acid-dependent signaling pathway was observed to be down-regulated by PLDβ1 in tomato plants tolerant to *Pseudomonas syringae* tomato pv. DC3000, as well as to *Botrytis cinerea* (Spoel et al., 2003). A decrease in bacterial growth after infection of PLDβ1-deficient plants was followed by increased accumulation of reactive oxygen species (Spoel et al., 2003). Furthermore, lysophospholipids specifically lysophosphatidylglycerol (LPG), lysophosphatidylcholine (LPC) and lysophosphatidylethanolamine (LPE) have been reported to accumulate in PLDβ1-deficient mutants (Spoel et al., 2003). Lysophospholipids are currently recognised as active signaling molecules inducing defense responses in plants (Kimberlin et al., 2013). PLD-induced PA usually binds to proteins directly and causes modifications in enzyme activity or localization. PLD-derived PA targets many proteins that are active in various physiological pathways even though their exact functions in plant responses to pathogens are not well understood (Jang, Lee, Hwang, & Ryu, 2012).

Phosphatidic acid regulates various physiological processes such as the activities of phosphatases, phospholipases and/or kinases, membrane trafficking, Ca^{2+} signaling, and the oxidative burst (Sang, Cui, & Wang, 2001; Xue, Chen, & Mei, 2009). Furthermore, PA acts as a precursor for the synthesis of lipid intermediates such

as free FAs, DG, and lysophosphatidic acid which are known to be responsible for plant defense signaling (Sang et al., 2001). Moreover, the levels of PA were observed to increase during infection caused by pathogens or treatment with an elicitor in tomato (*Solanum lycopersicum*) (Van der Luit, 2000), rice (*Oryza sativa*) (Yamaguchi, Minami, Ueki, & Shibuya, 2005), tobacco (*Nicotiana tabacum*) (Suzuki et al., 2007), and *Arabidopsis thaliana* (Dutilleul et al., 2012). Hence, the role of PLDs in plant pathology cannot be overemphasised considering their role in modulating a wide range of physiological processes important in lipid-signal-mediated plant defense.

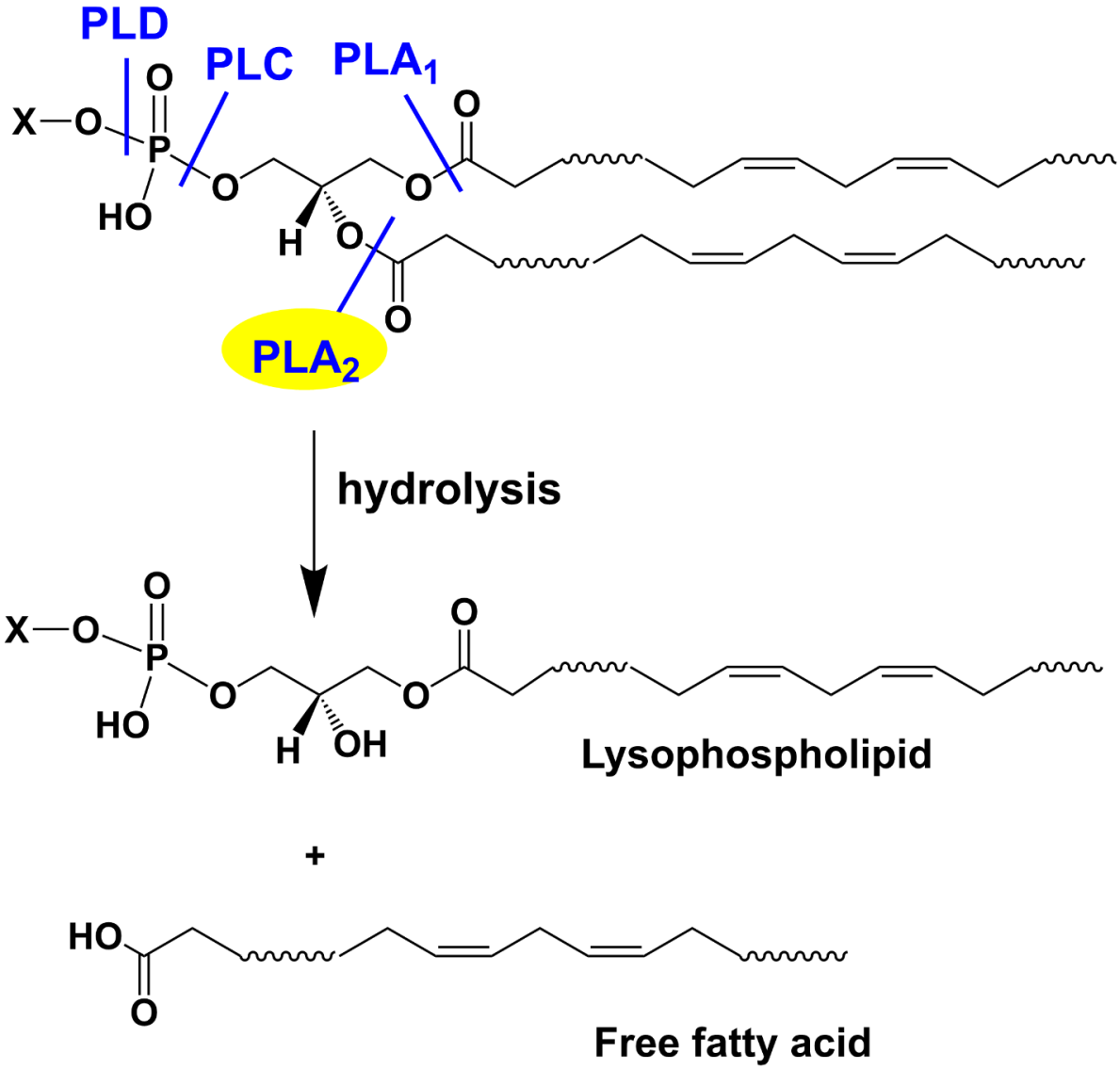

Fig. 2.4. Phospholipid structure (X represents the headgroup) showing different cleavage sites of phospholipases (PLA_1, PLA_2, PLC and PLD). PLA_1 and PLA_2 activities are specific for activating the hydrolysis of the ester bonds at sn_1 and sn_2 respectively. The PLA_2-catalyzed cleavage to form lysophospholipids and FAs is illustrated.

2.4.2. Role of phospholipase C

Phospholipase C (PLC) is classified into three groups based on the specificity of substrate and cell functions. They are: (i) phosphatidylcholine-PLCs, known as non-particular PLCs that hydrolyze phospholipids, especially phosphatidylcholine (PC); (ii) phosphatidylinositol-PLCs (PI-PLCs) which hydrolyse phosphoinositides; and (iii) glycosyl PI-PLCs known to catalyze the hydrolysis of glycosyl PI-linked proteins. In *Arabidopsis*, there are 6 different phospholipid-PLC (PL-PLC) genes, NPC_{1-6}, which have sequences similar to bacterial non-specific PLCs. Under low phosphate conditions, the expression of NPC_4 and NPC_5 is increased, suggesting their involvement in regulating phospholipid levels (Gaude, Nakamura, Scheible, Ohta, & Dormann, 2008; Takáč, Novák, & Šamaj, 2019). PI-PLCs catabolize PIP_2, producing inositol 1,4,5-triphosphate (IP_3) and DG. PI-PLC enzymatic action is up-regulated in host plants following a defense response to pathogen infections where DG and IP_3 act as second messengers (Vossen et al., 2010).

Pathogen-associated molecular pattern identification stimulates the induction of the PLC/ DG kinase route leading to accumulation of PA (Yamaguchi et al., 2005). Further DG phosphorylation via DG kinase by PLC produces PA. In *Arabidopsis*, recognition of avirulence proteins AvrRpm1 or AvrRpt2 from *P. syringae* results in a biphasic PA accumulation, which was initially attributed to the activities of PLC/ DG kinase (Canonne, Froidure-Nicolas, & Rivas, 2011). Furthermore, some pathogen-derived PA is biosynthesized by PLD enzymatic action (Canonne et al., 2011). Additionally, the tomato (*Solanum lycopersicum*) PLC isoform SIPLC4 is important for recognitional specificity of the infectious fungus *Cladosporium fulvum* (Cf), and the corresponding avirulence gene (*Avr4*) expression. Rapid accumulation of PA occurred in cell suspension culture of tomato showing *Cf-4* resistance gene expression following inoculation with the pathogen effector Avr4, and the increase is mediated by the PLC/ DG kinase route (Canonne et al., 2011). However, silencing of SIPLC4 impaired the Avr4/*Cf-4*-mediated hypersensitive defense reaction and consequently resulted in an increase in susceptibility to

C. fulvum (Vossen et al., 2010). Using tomato PLC isoforms, SIPLC6 activity was observed to be important in establishing overall defense responses in plants against various pathogens (Canonne et al., 2011).

PLCs play active roles during the process of elicitor recognition and in downstream disease resistance signaling (Chen, Zhang, Song, & Zheng, 2007). For instance, in rice (*Oryza sativa*), the expression of PLC1 was significantly enhanced by biochemical inducers of the defense signaling pathways in plants, resulting in an increased resistance to infectious disease (Chen et al., 2007). In the *Arabidopsis* genome, nine PI-PLC sequences exist, and the expression of some PI-PLC genes such as AtPLC1, AtPLC4 and AtPLC5 were induced during plant defense responses (Meijer & Munnik, 2003). Similarly, expression of DG kinase is also triggered during the process of microbial elicitation, producing PA as an inducible lipid mediator in plant basal resistance (Bonaventure et al., 2007; Campos, Kang, & Howe, 2014). Many PLC families are implicated in different cellular functions, signaling systems and cell lipid metabolism. They are induced in response to pathogen infection in many plant species. The output from these PLC families suggest they may be novel biochemical sources of enhanced plant resistance or tolerance to a range of pathogens (Singh, Bhatnagar, Pandey, & Pandey, 2015).

2.4.3. Role of phospholipase A

The PLA family is classified into PLA_1 and PLA_2; the two ester bonds of PLs are hydrolysed by PLA_1 and PLA_2 enzymes respectively, generating free FAs and lysophospholipids. PLA_2-induced LPE and LPC participate in systemic defense responses when plants are wounded, including those wounds generated from pathogen incursion (Jang et al., 2012). Lysophospholipids can be further hydrolyzed through lyso-PLA enzymes, generating glycerophosphodiesters.

PLA_1 and PLA_2 actively participate in the regulation of plant defense responses to stresses (Rietz et al., 2010). Additionally, they are strongly correlated with plant immunity through their roles in biosynthesis of jasmonic acid

and oxylipins as well as the activation of downstream defense products. PLAs play a vital role during the oxidative burst by catalyzing the hydrolysis of phospholipids to produce free FAs. These include linolenic and linoleic acids associated with specific biotic elicitors, thus protecting the plant against pathogenic attacks. The correlation between PLAs and the oxidative burst was demonstrated by the application of extracts from the pathogenic fungus *Verticillium dahliae* to soybeans. This triggered PLA activity and reactive oxygen species accumulation in resistant soybean cells (Torres, Jones, & Dangl, 2006). Hence, PLA plays a vital role in plant pathology.

2.5. Role of major components of systemic acquired resistance in plants

Systemic acquired resistance is a global defense response in plants induced at the site of infection, resulting in enhanced, long-lasting disease resistance in distant parts of the plant. Systemic acquired resistance has been identified as a way of controlling plant pathogens due to its stability (Winter et al., 2013), duration through time, and transgenerational effect (Shea & Poeta, 2006). Several mobile molecules were demonstrated as putative systemic acquired resistance signals or important components contributing to movement of systemic acquired resistance signaling elements in *Arabidopsis* and tobacco (Ádám, Nagy, Kátay, Mergenthaler, & Viczián, 2018). The components include azelaic acid, glycerol-3-phosphate, methyl-salicylic acid, pipecolic acid, auxin, nitric acid, reactive oxygen species, diterpenoid dehydroabietinal, galactolipids, cuticle formation factors, and lipid transfer proteins including AZI1 (azelaic insensitive 1) and DIR1 (Detective in Induced Resistance 1). The role of salicylic acid in systemic acquired resistance and its relationship to some of these components has been well-discussed by others (Conrath, 2006). AZI1 and DIR1 mutants lack the ability to activate systemic acquired resistance and are unresponsive to azelaic acid. In such mutants, azelaic acid cannot activate either local (*dir1*) nor systemic (*azi1*) responses (Cecchini, Steffes, Schläppi, Gifford, & Greenberg, 2015).

Signaling from systemic acquired resistance needs the regulation of two related pathways: (i) salicylic acid, and (ii) azelaic acid and glycerol-3-phosphate. Several chemical signals that lead to systemic acquired

resistance have been identified and characterized. For instance, the function of salicylic acid is parallel to azelaic acid and glycerol-3-phosphate, and likewise, azelaic acid and glycerol-3-phosphate-induced signaling function downstream of nitric oxide and reactive oxygen species (Lim, Kachroo, & Kachroo, 2016). During systemic acquired resistance, accumulation of azelaic acid, glycerol-3-phosphate and salicylic acid occurs in the diseased plant leaves, while small quantities of these mobile compounds are transferred to distal unaffected leaves.

In Arabidopsis, azelaic acid accumulated locally and in phloem exudates during the induction of systemic acquired resistance. Salicylic acid accumulation was not promoted during external application of azelaic acid, but induction of local and systemic resistance can occur. Azelaic acid can serve as a priming molecule and generates elevated systemic induction of salicylic acid accumulation following bacterial (*P. syringae* pv. *maculicola*) inoculation of distant leaves, resulting in stronger resistance against the pathogen (Jung, Tschaplinski, Wang, Glazebrook, & Greenberg, 2009). In contrast, phloem-localized azelaic acid and glycerol-3-phosphate are regulated through plasmodesmata gating. The plasmodesmata-localized proteins *pldp1* and *pldp5* regulate systemic acquired resistance along with plasmodesmata gating and subcellular portioning of systemic acquired resistance- associated proteins. The permeability of plasmodesmata in *pdlp1* and *pldp5* mutants was similar or higher, respectively, than in wild-type plants (Lim, Shine, et al., 2016).

The plant immune system can be stimulated by growth-promoting bacteria that mostly originate from the plant rhizosphere, leading to induced or initiated systemic resistance. Like systemic acquired resistance, induced systemic resistance induces resistance or tolerance to a wide range of infections (Pieterse et al., 2014). Systemic acquired resistance and induced systemic resistance also consists of common signaling constituents. However, induced systemic resistance and systemic acquired resistance activities in distant organs are primarily dependent on the characteristic impact of the plant hormones jasmonic acid and salicylic acid respectively (Pieterse et al., 2014). In Arabidopsis, glycerol-3-phosphate takes part in basal defense resistance to the hemibiotrophic fungal

plant pathogen *Colletotrichum higginsianum* and is a significant component in basal resistance and systemic acquired resistance (Chanda et al., 2008).

The PLA by-products (Section 3.3) glycerophosphodiesters, 2-acyl-lysophospholipids, and FAs undergo further hydrolysis by glycerolphosphodiester phosphodiesterases to produce glycerol-3-phosphate. The process of glycerol-3-phosphate accumulation in various organisms is highly conserved (Venugopal, Chanda, Vaillancourt, Kachroo, & Kachroo, 2014). Glycerol-3-phosphate can also be synthesized through the glycerol kinase pathway or through dihydroxyacetone phosphate reduction by glycerol-3-phosphate hydrogenase. The Arabidopsis genome has one glycerol kinase gene and five glycerol-3-phosphate dehydrogenase genes. Glycerol-3-phosphate acts as plant defense signaling regulator and is a significant component of various energy-producing reactions, as well as a precursor for glycolipid synthesis (Chanda et al., 2008; Venugopal et al., 2014). During pathogen infection, free unsaturated FAs are released, which are primarily precursors for azelaic acid. The unsaturated FAs such as linoleic and linolenic acid are oxidized at position C9, leading to azelaic acid (Yu et al., 2013). Azelaic acid is a nine-carbon dicarboxylic acid and, in terms of producing an oxidative signal, very active in systemic acquired resistance (Jung et al., 2009; Zoeller et al., 2012). However, azelaic acid-mediated systemic acquired resistance depends on glycerol-3-phosphate and azelaic acid accumulation, which subsequently induces further glycerol-3-phosphate production (Yu et al., 2013).

2.6. Role of fatty acids in pathogen resistance in plants

Fatty acids are carboxylic acids containing long saturated or unsaturated hydrocarbon chains. They act as reserve energy sources and as vital monomeric components of cellular membrane lipids in plants and microbes. In plants, the metabolic functions of FAs were previously believed to be passive in plant defense, acting only as precursors for biosynthesis of phytohormones such as jasmonic acid. However, recent studies have demonstrated some active roles of FAs and their metabolites, especially in inducing various defense mechanisms in plants (Kachroo &

Kachroo, 2009). For example, C18:0, 18:1, 18:2 and 18:3 are the major FAs involved in modulating plant defense responses to phytopathogens; in soybean, seed colonization by the seed-borne pathogen *Diaporthe phaseolorum* is inhibited by increased levels of C18:0 FAs (Mena, Stewart, Montesano, & Ponce de León, 2020).

Fatty acids are constituents of GPLs and the main structural components of cellular membranes, thylakoid membranes, cutin, and wax esters. Polyunsaturated FAs species such as trienoic FAs, including hexadecatrienoic acid (C16:3) and linolenic acid (C18:3) are commonly found in plant membrane lipids (Upchurch, 2008). They include trienoic FAs perform significant functions in defense responses against avirulent pathogenic bacteria. Avirulent pathogen invasion of plants triggers production of a transient reactive oxygen intermediate, programmed cell death (PCD), and eventually enhanced disease resistance (Yaeno, Matsuda, & Iba, 2004). In addition, the breakdown of FAs is necessary in the metabolism, development, and pathogenicity of some fungi (Hynes, Murray, Duncan, Khew, & Davis, 2006).

The production of FAs *de novo* in plants is confined to the chloroplasts. A major process in the biosynthesis of FAs involves the desaturation of stearic acid to form unsaturated oleic acid, an important cell signaling response to pathogenic stress which functions through nitric oxide (Mandal et al., 2012). In Arabidopsis, stearoyl-acyl-carrier protein desaturase is an enzyme that catalyzes this desaturation process. Changes in oleic acid levels lead to down-regulation of jasmonic acid- and salicylic acid-triggered plant defense responses and consequently causes the activation and repression of the jasmonic acid- and salicylic acid-mediated defense pathways respectively (Ruan et al., 2019).

2.7. Role of phyto-oxylipins as signaling molecules in plant defense

Phyto-oxylipins are a wide range of lipid metabolites synthesized in higher plants through the process of oxidative transformation of PUFAs via a sequence of diverging metabolic pathways. They are induced by environmental stressors such as pathogenic organisms. Oxylipins play significant roles in defense against stressors because they function as protective compounds and/or signal molecules like wound-healing agents and are also antifungal and antibacterial. They are also components of cutin (the substructure of the cuticle) which protects plant aerial parts from their external environment. Biochemical and genetic analyses have confirmed that these oxygenated lipid metabolites are proactively involved in plant defense systems (Blée, 2002). Oxylipins are synthesized during metabolism of PUFAs, predominantly linoleic acid, and linolenic acid via oxidation of one or two molecules of oxygen. The reaction is catalyzed by various enzymes including LOX, CYP450 monooxygenase, and cyclo-oxygenase-like enzymes (Fig. 2.4) (Blée, 2002; Howe & Schilmiller, 2002). The oxidation can also follow non-enzymatic routes via reactive oxygen species, generating a complex array of compounds such as aldehydes and ketones (Lupette et al., 2018). Besides PUFAs, free FAs of galactolipids or acyl groups attached to triacylglycerols (TGs) can be subjected to oxidation in plants. For instance, free FAs and monogalactosyldiglycerides were shown to act as substrates to produce jasmonic acid during the plant defense response (Nakashima et al., 2011).

The first reaction step of oxylipin biosynthesis in plants is the generation of hydroperoxides induced through the action of three major enzymes: LOXs, alpha-dioxygenases, and CYP450 monooxygenases. Many enzyme-induced oxylipins are primarily biosynthesized through LOXs. The LOX pathway initiation starts by attaching oxygen molecule(s) to linoleic and linolenic acids. Different LOXs are categorized based on the specificity of oxygenation, which mainly occurs at either C9 (catalyzed by 9-LOX) or C13 of the carboxylic acid (catalyzed by 13-LOX). The 9-LOXs produce 9-hydroperoxides while 13-LOXs produce 13-hydoperoxides which serve as intermediates or substrates for at least six different biosynthetic routes. They are catalyzed by various enzymes including LOX, allene oxide synthase, peroxygenase, epoxy alcohol synthase, divinyl synthase,

and hydroperoxide lyase. There are up to 150 known phyto-oxylipins collectively formed from these enzymatic reactions to produce metabolites such as oxo- or keto- FAs, hydroxy ethers, green leaf volatile, jasmonic acid, divinyl ethers, and traumatin (Mosblech, Feussner, & Heilmann, 2009). Some studies have shown that the classes of chemical peroxidation products, known as phytoprostanes, are used as powerful signal molecules to regulate plant defense responses to resist pathogenic attack (Mueller, Porter, Hoffman, & Jaehning, 2004).

In the last decade, only a few phyto-oxylipins such as jasmonic acid have been given prominent attention. Minimal information is known about the physiological roles of some other phyto-oxylipins in plant defense. For instance, the roles of many 9-oxylipins biosynthesized via the 9-LOX route are unknown. However, accumulating evidence suggests that derivatives of the 9-LOX pathway possess phytohormone-associated signaling properties required in plant physiological performance, as well as in defenses against biotic stresses including plant pathogens (Xinjiao, Changjiang, Yu, & Xuebiao, 2008). For example, current analysis of the maize mutant LOX3 (deficient in 9-LOX) established genetic proof that the 9-LOX route modulates seed germination, plant growth, and resistance against fungal attack (Xinjiao et al., 2008). Maize susceptibility to fungal attack was demonstrated to be associated with a decreased level of the LOX substrate linolenic acid (Gao, Wu, & Fossett, 2009). Just like jasmonic acid synthesis, formation of green leaf volatile starts with LOX-induced 13-hydroperoxides that are catalyzed enzymatically by hydroperoxide lyase to produce traumatin and green leaf volatile (E)-2-hexenal. The metabolism of (E)-2-hexenal forms (Z)-3-hexen-1-ol through an enzyme called alcohol dehydrogenase, following acylation by acyl transferase and acetyl CoA to form (Z)-3-hexenyl acetate (Blée, 2002; D'Auria, Chen, & Pichersky, 2002; Matsui et al., 2006).

Phyto-oxylipins play crucial roles in plant defenses against pathogens by inducing the production of physical barriers to impede pathogen ingress or acting as antimicrobial or toxic compounds to invading phytopathogens. For example, inducible LOX has been shown to play a significant function in the resistance of tobacco to fungal infection. Furthermore, oxylipins are utilized by plants to signal the initiation of wound-related

pathways, presumably through various recognition systems associated with methyl jasmonate (Wasternack et al., 2006; Yan et al., 2013).

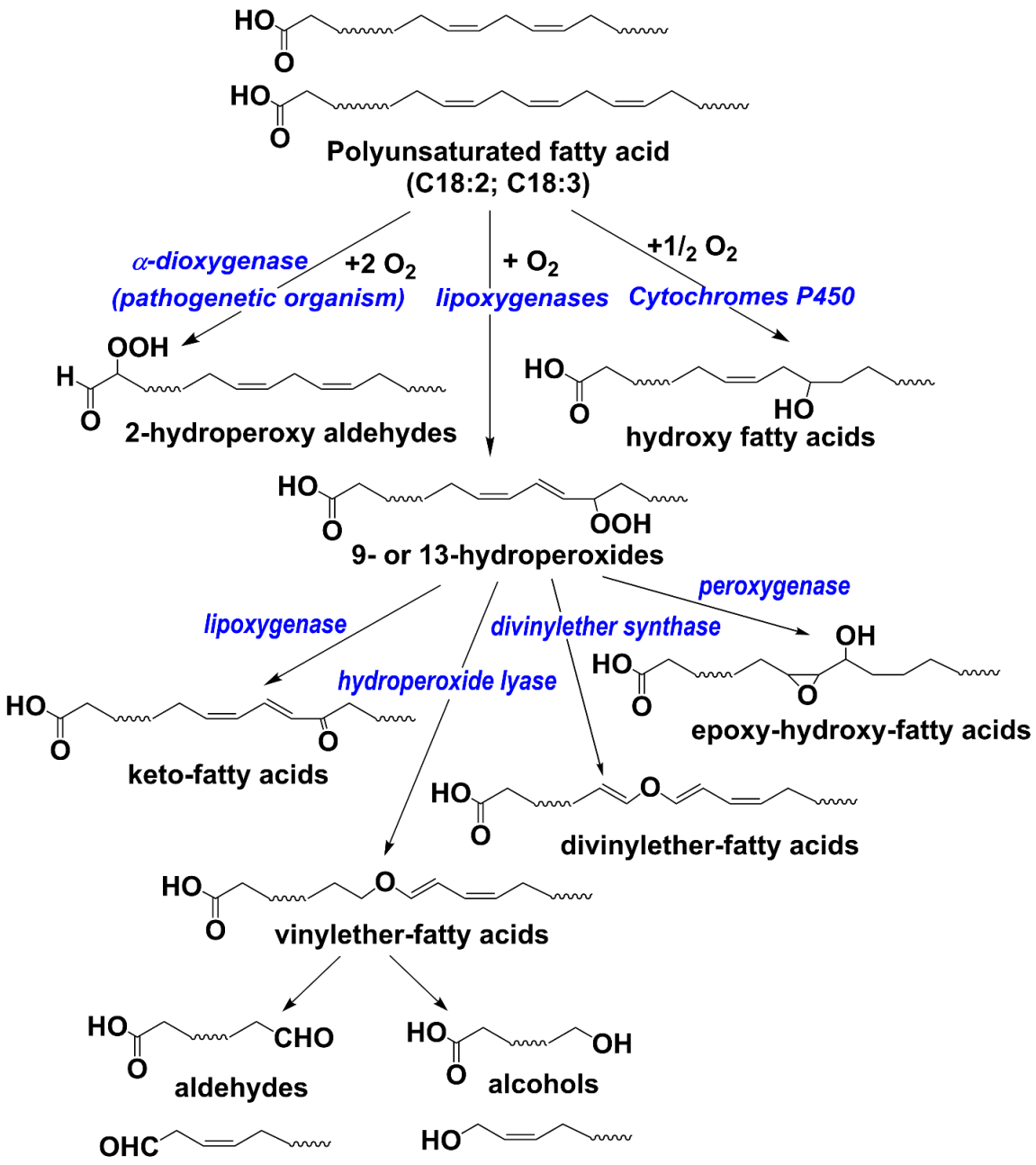

Fig. 2.5. Oxidative metabolism mechanism of FAs in plants, involving oxygenation of FAs by one, two or four atoms of oxygen. Cytochrome P450 and pathogen-induced oxygenases have subsidiary roles. Lipoxygenases catalyse the oxidation of PUFAs to either 9- or 13-hydroperoxides and are metabolized by various enzymes into a series of oxylipins.

2.8. Conclusions and perspectives

Lipids play various functional roles in plant defense especially in host-microbe interactions. To accomplish this, plant lipids are cumulatively utilized according to their chemical structure and molecular functions. They play active roles during recognition of infectious pathogens by cell membranes. For instance, ergosterol and some lipid metabolites or lipid-derived compounds (FAs, oxylipins and glycerol-3-phosphate) are involved in signaling at infection sites, while some (e.g. azelaic acid, glycerol-3-phosphate, and salicylic acid) moderate the transport of disease signals to distant plant organs during systemic acquired resistance.

The study of lipids in plant pathology is essential for understanding this complex internal mechanism of plants in the fight against plant diseases caused by fungi, bacteria, viruses, phytoplasmas, protozoa, and nematodes. Hence, lipid composition, synthesis and metabolism in plants play a significant role in combating disease infection. Plant membrane lipid metabolism is a mechanism of great complexity, with functional outcomes including lipid localization and transport within the intracellular and intercellular components of plants. Additionally, the regulatory roles of lipids during diverse environmental stresses results in the production of further lipid metabolites and signaling molecules via enzymatic processes.

Recent studies into the role of lipids in plant pathology have identified potential novel sources for breeding plant cultivars with strong disease tolerance or resistance. Therefore, further lipidomic studies are required for comprehensive profiling of the broad spectrum of lipid molecular species with respect to cell-to-cell signaling, translational and transcriptional modulation, plant-microbe interactions, and cell-protein interactions in response to pathogen attack and/or disease development to understand the vital role of alterations in membrane lipid metabolism in plant cells. Moreover, the integration of lipid signaling molecules into established stress signaling pathways is essential. This will lead to a detailed and more complete understanding of the functional role of lipids in terms of chemical, molecular and physiological perspectives in plant pathology. The knowledge could then be utilized to produce plants that are adapted to diverse biotic stressors.

2.9. References

Abdul Malik, N. A., Kumar, I. S., & Nadarajah, K. (2020). Elicitor and receptor molecules: Orchestrators of plant pefense and Immunity. *International journal of molecular sciences, 21*(3), 963.

Ádám, A. L., Nagy, Z. Á., Kátay, G., Mergenthaler, E., & Viczián, O. (2018). Signals of systemic immunity in plants: Progress and open questions. *International journal of molecular sciences, 19*(4), 1146.

Andersen, E. J., Ali, S., Byamukama, E., Yen, Y., & Nepal, M. P. (2018). Disease Resistance Mechanisms in Plants. *Genes, 9*(7), 339.

Aranega-Bou, P., de la O Leyva, M., Finiti, I., García-Agustín, P., & González-Bosch, C. (2014). Priming of plant resistance by natural compounds: Hexanoic acid as a model. *Frontiers in Plant Science, 5*(488).

Asad, M. A. U., Zakari, S. A., Zhao, Q., Zhou, L., Ye, Y., & Cheng, F. (2019). Abiotic stresses intervene with ABA signaling to induce destructive metabolic pathways leading to death: Premature leaf senescence in plants. *International Journal of Molecular Sciences, 20*(2), 256.

Ausubel, F. M. (2005). Are innate immune signaling pathways in plants and animals conserved? *Nature Immunology, 6*(10), 973-979. doi:10.1038/ni1253

Ayala, A., Muñoz, M. F., & Argüelles, S. (2014). Lipid peroxidation: Production, metabolism, and signaling mechanisms of malondialdehyde and 4-hydroxy-2-nonenal. *Oxidative medicine and cellular longevity, 2014*, 360438.

Balint-Kurti, P. (2019). The plant hypersensitive response: Concepts, control and consequences. *Molecular Plant Pathology, 20*(8), 1163-1178.

Bargmann, B. O., & Munnik, T. (2006). The role of phospholipase D in plant stress responses. *Current Opinion in Plant Biology, 9*(5), 515-522.

Bigeard, J., Colcombet, J., & Hirt, H. (2015). Signaling mechanisms in pattern-triggered immunity (PTI). *Molecular Plant, 8*(4), 521-539.

Blée, E. (2002). Impact of phyto-oxylipins in plant defense. *Trends in Plant Science, 7*(7), 315-321.

Bonaventure, G., Gfeller, A., Proebsting, W. M., Hörtensteiner, S., Chételat, A., Martinoia, E., & Farmer, E. E. (2007). A gain-of-function allele of TPC1 activates oxylipin biogenesis after leaf wounding in Arabidopsis. *The Plant Journal, 49*(5), 889-898.

Brackin, R., Atkinson, B. S., Sturrock, C. J., & Rasmussen, A. (2017). Roots-eye view: Using microdialysis and microCT to non-destructively map root nutrient depletion and accumulation zones. *Plant, Cell & Environment, 40*(12), 3135-3142.

Campos, M. L., Kang, J.-H., & Howe, G. A. (2014). Jasmonate-triggered plant immunity. *Journal of chemical ecology, 40*(7), 657-675.

Canonne, J., Froidure-Nicolas, S., & Rivas, S. (2011). Phospholipases in action during plant defense signaling. *Plant signaling & behavior, 6*(1), 13-18.

Castro-Moretti, F. R., Gentzel, I. N., Mackey, D., & Alonso, A. P. (2020). Metabolomics as an Emerging Tool for the Study of Plant-Pathogen Interactions. *Metabolites, 10*(2), 52.

Cecchini, N. M., Steffes, K., Schläppi, M. R., Gifford, A. N., & Greenberg, J. T. (2015). Arabidopsis AZI1 family proteins mediate signal mobilization for systemic defence priming. *Nature Communications, 6*(1), 7658.

Chanda, B., Venugopal, S. C., Kulshrestha, S., Navarre, D. A., Downie, B., Vaillancourt, L., . . . Kachroo, P. (2008). Glycerol-3-phosphate levels are associated with basal resistance to the hemibiotrophic fungus Colletotrichum higginsianum in Arabidopsis. *Plant physiology, 147*(4), 2017-2029.

Chaplin, D. D. (2010). Overview of the immune response. *The Journal of allergy and clinical immunology, 125*(2 Suppl 2), S3-S23.

Chen, J., Zhang, W., Song, F., & Zheng, Z. (2007). Phospholipase C/diacylglycerol kinase-mediated signalling is required for benzothiadiazole-induced oxidative burst and hypersensitive cell death in rice suspension-cultured cells. *Protoplasma, 230*(1-2), 13-21.

Cheng, C.-S., Samuel, D., Liu, Y.-J., Shyu, J.-C., Lai, S.-M., Lin, K.-F., & Lyu, P.-C. (2004). Binding mechanism of nonspecific lipid transfer proteins and their role in plant defense. *Biochemistry, 43*(43), 13628-13636.

Christensen, S. A., & Kolomiets, M. V. (2011). The lipid language of plant-fungal interactions. *Fungal Genet Biol, 48*(1), 4-14.

Conrath, U. (2006). Systemic acquired resistance. *Plant Signaling & Behavior, 1*(4), 179-184.

Coskun, Ü., & Simons, K. (2011). Cell Membranes: The lipid perspective. *Structure, 19*(11), 1543-1548.

Cowan, A. (2006). Phospholipids as plant growth regulators. *Plant Growth Regul, 48*, 97-109.

D'Auria, J. C., Chen, F., & Pichersky, E. (2002). Characterization of an Acyltransferase Capable of Synthesizing Benzylbenzoate and Other Volatile Esters in Flowers and Damaged Leaves of Clarkia breweri. *Plant physiology, 130*(1), 466-476.

de Carvalho, C. C. C. R., & Caramujo, M. J. (2018). The various roles of fatty acids. *Molecules, 23*(10), 2583.

Dowhan, W., Bogdanov, M., & Mileykovskaya, E. (2016). Chapter 1 - Functional roles of lipids in membranes. In N. D. Ridgway & R. S. McLeod (Eds.), *Biochemistry of Lipids, Lipoproteins and Membranes (Sixth Edition)* (pp. 1-40). Boston: Elsevier.

Dutilleul, C., Benhassaine-Kesri, G., Demandre, C., Rézé, N., Launay, A., Pelletier, S., . . . Guillas, I. (2012). Phytosphingosine-phosphate is a signal for AtMPK6 activation and Arabidopsis response to chilling. *New Phytologist, 194*(1), 181-191.

Eckardt, N. A. (2004). Mechanism of Pto-mediated disease desistance: Structural analysis provides a new model. *The Plant Cell, 16*(10), 2543-2545.

Fahy, E., Cotter, D., Sud, M., & Subramaniam, S. (2011). Lipid classification, structures and tools. *Biochimica et biophysica acta, 1811*(11), 637-647.

Fernandis, A. Z., & Wenk, M. R. (2007). Membrane lipids as signaling molecules. *Current opinion in lipidology, 18*(2).

Finkelstein, R. R., Gampala, S. S. L., & Rock, C. D. (2002). Abscisic acid signaling in seeds and seedlings. *The Plant cell, 14 Suppl*(Suppl), S15-S45.

Fletcher, J., Bender, C., Budowle, B., Cobb, W. T., Gold, S. E., Ishimaru, C. A., . . . Tolin, S. A. (2006). Plant pathogen forensics: capabilities, needs, and recommendations. *Microbiology and molecular biology reviews : MMBR, 70*(2), 450-471.

Gachomo, E., Shonukan, O., & Kotchoni, S. (2003). The molecular initiation and subsequent acquisition of disease resistance in plants. *African Journal of Biotechnology, 2*. doi:10.5897/AJB2003.000-1005

Gao, H., Wu, X., & Fossett, N. (2009). Upregulation of the Drosophila Friend of GATA gene U-shaped by JAK/STAT signaling maintains lymph gland prohemocyte potency. *Mol Cell Biol, 29*(22), 6086-6096.

Gaude, N., Nakamura, Y., Scheible, W. R., Ohta, H., & Dormann, P. (2008). Phospholipase C5 (NPC5) is involved in galactolipid accumulation during phosphate limitation in leaves of Arabidopsis. *Plant J, 56*(1), 28-39.

Gill, U. S., Lee, S., & Mysore, K. S. (2015). Host versus nonhost resistance: Distinct wars with similar arsenals. *Phytopathology, 105*(5), 580-587.

Heath, M. C. (2000). Hypersensitive response-related death *Programmed Cell Death in Higher Plants* (pp. 77-90). Dordrecht: Springer Netherlands.

Henry, G., Thonart, P., & Ongena, M. (2012). PAMPs, MAMPs, DAMPs and others: An update on the diversity of plant immunity elicitors. *Biotechnology, Agronomy and Society and Environment, 16*, 257-268.

Hoglund, S., Larsson, S., & Wingsle, G. (2005). Both hypersensitive and non-hypersensitive responses are associated with resistance in Salix viminalis against the gall midge Dasineura marginemtorquens. *J Exp Bot, 56*(422), 3215-3222.

Hong, S., Dissing-Olesen, L., & Stevens, B. (2016). New insights on the role of microglia in synaptic pruning in health and disease. *Curr Opin Neurobiol, 36*, 128-134.

Hou, S., Yang, Y., Wu, D., & Zhang, C. (2011). Plant immunity: evolutionary insights from PBS1, Pto, and RIN4. *Plant signaling & behavior, 6*(6), 794-799.

Howe, G. A., & Schilmiller, A. L. (2002). Oxylipin metabolism in response to stress. *Curr Opin Plant Biol, 5*, 230-236.

Hu, J., Rampitsch, C., & Bykova, N. V. (2015). Advances in plant proteomics toward improvement of crop productivity and stress resistance. *Front Plant Sci, 6*, 209.

Huang, P., & Frohman, M. A. (2007). The potential for phospholipase D as a new therapeutic target. *Expert Opinion on Therapeutic Targets, 11*(5), 707-716.

Hynes, M. J., Murray, S. L., Duncan, A., Khew, G. S., & Davis, M. A. (2006). Regulatory genes controlling fatty acid catabolism and peroxisomal functions in the filamentous fungus Aspergillus nidulans. *Eukaryotic cell, 5*(5), 794-805.

Ingólfsson, H. I., Melo, M. N., van Eerden, F. J., Arnarez, C., Lopez, C. A., Wassenaar, T. A., . . . Marrink, S. J. (2014). Lipid organization of the plasma membrane. *Journal of the American Chemical Society, 136*(41), 14554-14559.

Ipcho, S., Sundelin, T., Erbs, G., Kistler, H. C., Newman, M.-A., & Olsson, S. (2016). Fungal innate immunity induced by bacterial microbe-associated molecular patterns (MAMPs). *G3 (Bethesda, Md.), 6*(6), 1585-1595.

Jang, J. H., Lee, C. S., Hwang, D., & Ryu, S. H. (2012). Understanding of the roles of phospholipase D and phosphatidic acid through their binding partners. *Prog Lipid Res, 51*(2), 71-81.

Jones, J. D. G., & Dangl, J. L. (2006). The plant immune system. *Nature, 444*(7117), 323-329.

Jung, H. W., Tschaplinski, T. J., Wang, L., Glazebrook, J., & Greenberg, J. T. (2009). Priming in systemic plant immunity. *Science, 324*(5923), 89-91.

Kachroo, A., & Kachroo, P. (2009). Fatty acid–derived signals in plant defense. *Annu Rev Phytopathol, 47*(1), 153-176.

Katagiri, T., Ishiyama, K., Kato, T., Tabata, S., Kobayashi, M., & Shinozaki, K. (2005). An important role of phosphatidic acid in ABA signaling during germination in Arabidopsis thaliana. *Plant J, 43*, 107-117.

Kimberlin, A. N., Majumder, S., Han, G., Chen, M., Cahoon, R. E., Stone, J. M., . . . Cahoon, E. B. (2013). Arabidopsis 56-amino acid serine palmitoyltransferase-interacting proteins stimulate sphingolipid synthesis, are essential, and affect mycotoxin sensitivity. *Plant Cell, 25*(11), 4627-4639.

Lee, H. Y., Bahn, S. C., Kang, Y.-M., Lee, K. H., Kim, H. J., Noh, E. K., . . . Ryu, S. B. (2003). Secretory low molecular weight phospholipase A2 plays important roles in cell elongation and shoot gravitropism in Arabidopsis. *The Plant cell, 15*(9), 1990-2002.

Li, N., Han, X., Feng, D., Yuan, D., & Huang, L. J. (2019). Signaling crosstalk between salicylic acid and ethylene/jasmonate in plant defense: Do we understand what they are whispering? *International journal of molecular sciences, 20*(3).

Liechti, R., & Farmer, E. E. (2006). Jasmonate Biochemical Pathway. *Science's STKE, 2006*(322), cm3.

Lim, G.-H., Kachroo, A., & Kachroo, P. (2016). Role of plasmodesmata and plasmodesmata localizing proteins in systemic immunity. *Plant signaling & behavior, 11*(9), e1219829-e1219829.

Lim, G.-H., Shine, M. B., de Lorenzo, L., Yu, K., Cui, W., Navarre, D., . . . Kachroo, P. (2016). Plasmodesmata localizing proteins regulate transport and signaling during systemic acquired immunity in plants. *Cell Host & Microbe, 19*(4), 541-549.

Lim, G.-H., Singhal, R., Kachroo, A., & Kachroo, P. (2017). Fatty Acid– and lipid-mediated signaling in plant defense. *Annu Rev Phytopathol, 55*(1), 505-536.

Lin, N.-C., & Martin, G. B. (2007). Pto- and Prf-mediated recognition of AvrPto and AvrPtoB restricts the ability of diverse *Pseudomonas syringae* pathovars to infect tomato. *Molecular plant-microbe interactions : MPMI, 20*(7), 806-815.

Liu, J.-Z., & Lam, H.-M. (2019). Signal transduction pathways in plants for resistance against pathogens. *International journal of molecular sciences, 20*(9), 2335.

Lupette, J., Jaussaud, A., Vigor, C., Oger, C., Galano, J.-M., Réversat, G., . . . Maréchal, E. (2018). Non-Enzymatic Synthesis of Bioactive Isoprostanoids in the Diatom following Oxidative Stress. *Plant physiology, 178*(3), 1344-1357.

Mackey, D., Holt, B. F., Wiig, A., & Dangl, J. L. (2002). RIN4 Interacts with Pseudomonas syringae Type III Effector Molecules and Is Required for RPM1-Mediated Resistance in Arabidopsis. *Cell, 108*(6), 743-754.

Mandal, M. K., Chandra-Shekara, A. C., Jeong, R.-D., Yu, K., Zhu, S., Chanda, B., . . . Kachroo, P. (2012). Oleic acid–dependent modulation of NITRIC OXIDE ASSOCIATED1 protein levels regulates nitric oxide–mediated defense signaling in Arabidopsis. *The Plant Cell, 24*(4), 1654-1674.

Matsui, K., Hirayama, T., Kuroda, K., Shirahige, K., Ashikari, T., & Ueda, M. (2006). Screening for candidate genes involved in tolerance to organic solvents in yeast. *Appl Microbiol Biotechnol, 71*(1), 75-79.

Meijer, H. J., & Munnik, T. (2003). Phospholipid-based signaling in plants. *Annu Rev Plant Biol, 54*, 265-306.

Mena, E., Stewart, S., Montesano, M., & Ponce de León, I. (2020). Soybean stem canker caused by *Diaporthe caulivora*; Pathogen diversity, colonization process, and plant defense activation. *Frontiers in Plant Science, 10*(1733).

Mosblech, A., Feussner, I., & Heilmann, I. (2009). Oxylipins: structurally diverse metabolites from fatty acid oxidation. *Plant Physiol Biochem, 47*(6), 511-517.

Mucyn, T. S., Clemente, A., Andriotis, V. M. E., Balmuth, A. L., Oldroyd, G. E. D., Staskawicz, B. J., & Rathjen, J. P. (2006). The tomato NBARC-LRR protein Prf interacts with Pto kinase in vivo to regulate specific plant immunity. *The Plant Cell, 18*(10), 2792-2806.

Mueller-Roeber, B., & Pical, C. (2002). Inositol phospholipid metabolism in Arabidopsis. Characterized and putative isoforms of inositol phospholipid kinase and phosphoinositide-specific phospholipase C. *Plant Physiol, 130*(1), 22-46.

Mueller, C. L., Porter, S. E., Hoffman, M. G., & Jaehning, J. A. (2004). The Paf1 Complex Has Functions Independentof Actively Transcribing RNA Polymerase II. *Molecular Cell, 14*, 447-456.

Nadeem, M., Pham, T. H., Thomas, R., Galagedara, L., Kavanagh, V., Zhu, X., . . . Cheema, M. (2019). Potential role of root membrane phosphatidic acid in superior agronomic performance of silage-corn cultivated in cool climate cropping systems. *Physiologia Plantarum, 167*(4), 585-596.

Nadeem, M., Thomas, R., Adigun, O., Manful, C., Wu, J., Pham, T. H., . . . Cheema, M. (2020). Root membrane lipids as potential biomarkers to discriminate silage-corn genotypes cultivated on podzolic soils in boreal climate. *Physiologia Plantarum*.

Nakashima, A., Iijima, Y., Aoki, K., Shibata, D., Sugimoto, K., Takabayashi, J., & Matsui, K. (2011). Monogalactosyl diacylglycerol is a substrate for lipoxygenase: its implications for oxylipin formation directly from lipids. *Journal of Plant Interactions, 6*(2-3), 93-97.

Newman, M.-A., Sundelin, T., Nielsen, J., & Erbs, G. (2013). MAMP (microbe-associated molecular pattern) triggered immunity in plants. *Frontiers in Plant Science, 4*(139).

Niks, R. E., & Marcel, T. C. (2009). Nonhost and basal resistance: how to explain specificity? *New Phytologist, 182*(4), 817-828.

Nita, M., & Grzybowski, A. (2016). The role of the reactive oxygen species and oxidative stress in the pathomechanism of the age-related ocular diseases and other pathologies of the anterior and posterior eye segments in adults. *Oxidative medicine and cellular longevity, 2016*, 3164734-3164734.

Noman, A., Aqeel, M., & Lou, Y. (2019). PRRs and NB-LRRs: From signal perception to activation of plant innate immunity. *Int J Mol Sci, 20*(8).

Panday, A., Sahoo, M. K., Osorio, D., & Batra, S. (2015). NADPH oxidases: an overview from structure to innate immunity-associated pathologies. *Cellular & molecular immunology, 12*(1), 5-23.

Pedley, K. F., & Martin, G. B. (2005). Role of mitogen-activated protein kinases in plant immunity. *Curr Opin Plant Biol, 8*(5), 541-547.

Pieterse, C. M., Zamioudis, C., Berendsen, R. L., Weller, D. M., Van Wees, S. C., & Bakker, P. A. (2014). Induced systemic resistance by beneficial microbes. *Annu Rev Phytopathol, 52*, 347-375.

Pleskot, R., Li, J., Zarsky, V., Potocky, M., & Staiger, C. J. (2013). Regulation of cytoskeletal dynamics by phospholipase D and phosphatidic acid. *Trends Plant Sci, 18*(9), 496-504.

Plett, J. M., & Martin, F. M. (2018). Know your enemy, embrace your friend: using omics to understand how plants respond differently to pathogenic and mutualistic microorganisms. *The Plant Journal, 93*(4), 729-746.

Porta, H., & Rocha-Sosa, M. (2002). Plant lipoxygenases. Physiological and molecular features. *Plant physiology, 130*(1), 15.

Postel, S., & Kemmerling, B. (2009). Plant systems for recognition of pathogen-associated molecular patterns. *Seminars in Cell & Developmental Biology, 20*, 1025-1031.

Qualmann, B., & Kessels, M. M. (2002). Endocytosis and the cytoskeleton. *Int Rev Cytol, 220*, 93-144.

Repp, A., Mikami, K., Mittmann, F., & Hartmann, E. (2004). Phosphoinositide-specific phospholipase C is involved in cytokinin and gravity responses in the moss Physcomitrella patens. *The Plant Journal, 40*(2), 250-259.

Rietz, S., Dermendjiev, G., Oppermann, E., Tafesse, F. G., Effendi, Y., Holk, A., . . . Scherer, G. F. (2010). Roles of Arabidopsis patatin-related phospholipases a in root development are related to auxin responses and phosphate deficiency. *Mol Plant, 3*(3), 524-538.

Ruan, J., Zhou, Y., Zhou, M., Yan, J., Khurshid, M., Weng, W., . . . Zhang, K. (2019). Jasmonic acid signaling pathway in plants. *International Journal of Molecular Sciences, 20*(10), 2479.

Ryu, C.-M., Murphy, J. F., Mysore, K. S., & Kloepper, J. W. (2004). Plant growth-promoting rhizobacteria systemically protect Arabidopsis thaliana against Cucumber mosaic virus by a salicylic acid and NPR1-independent and jasmonic acid-dependent signaling pathway. *The Plant Journal, 39*(3), 381-392.

Sang, Y., Cui, D., & Wang, X. (2001). Phospholipase D and phosphatidic acid-mediated generation of superoxide in Arabidopsis. *Plant Physiology, 126*(4), 1449-1458.

Savary, S., Willocquet, L., Pethybridge, S. J., Esker, P., McRoberts, N., & Nelson, A. (2019). The global burden of pathogens and pests on major food crops. *Nat Ecol Evol, 3*(3), 430-439.

Scherer, G. F. E., Labusch, C., & Effendi, Y. (2012). Phospholipases and the network of auxin signal transduction with ABP1 and TIR1 as two receptors: A comprehensive and provocative model. *Frontiers in Plant Science, 3*, 56-56.

Scholthof, K.-B. (2007). The disease triangle: Pathogens, the environment and society. *Nature reviews. Microbiology, 5*, 152-156.

Shamrai, S. N. (2014). Plant immune system: Basal immunity. *Cytology and Genetics, 48*(4), 258-271.

Shea, J. M., & Poeta, M. D. (2006). Lipid signaling in pathogenic fungi. *Curr Opin Microbiol, 9*(4), 352-358.

Siebers, M., Brands, M., Wewer, V., Duan, Y., Hölzl, G., & Dörmann, P. (2016). Lipids in plant–microbe interactions. *Biochimica et Biophysica Acta (BBA) - Molecular and Cell Biology of Lipids, 1861*(9, Part B), 1379-1395.

Singh, A., Bhatnagar, N., Pandey, A., & Pandey, G. K. (2015). Plant phospholipase C family: Regulation and functional role in lipid signaling. *Cell Calcium, 58*(2), 139-146.

Spoel, S. H., Koornneef, A., Claessens, S. M. C., Korzelius, J. P., Van Pelt, J. A., Mueller, M. J., . . . Pieterse, C. M. J. (2003). NPR1 modulates cross-talk between salicylate- and jasmonate-dependent defense pathways through a novel function in the cytosol. *The Plant Cell, 15*(3), 760-770.

Suzuki, K., Yano, A., Nishiuchi, T., Nakano, T., Kodama, H., Yamaguchi, K., & Shinshi, H. (2007). Comprehensive analysis of early response genes to two different microbial elicitors in tobacco cells. *Plant Science, 173*(3), 291-301.

Takáč, T., Novák, D., & Šamaj, J. (2019). Recent advances in the cellular and developmental biology of phospholipases in plants. *Frontiers in Plant Science, 10*(362).

Tardieu, F. (2013). Plant response to environmental conditions: assessing potential production, water demand, and negative effects of water deficit. *Frontiers in physiology, 4*, 17-17.

Tholl, D., & Aharoni, A. (2014). Small molecules: from structural diversity to signalling and regulatory roles. *The Plant Journal, 79*(4), 541-543.

Thordal-Christensen, H., Birch, P. R. J., Spanu, P. D., & Panstruga, R. (2018). Why did filamentous plant pathogens evolve the potential to secrete hundreds of effectors to enable disease? *Molecular plant pathology, 19*(4), 781-785.

Torres, M. A., Jones, J. D., & Dangl, J. L. (2006). Reactive oxygen species signaling in response to pathogens. *Plant physiology, 141*(2), 373-378.

Toruño, T. Y., Stergiopoulos, I., & Coaker, G. (2016). Plant-pathogen effectors: Cellular probes interfering with plant defenses in spatial and temporal manners. *Annual Review of Phytopathology, 54*(1), 419-441.

Upchurch, R. G. (2008). Fatty acid unsaturation, mobilization, and regulation in the response of plants to stress. *Biotechnol Lett, 30*(6), 967-977.

Uraji, M., Katagiri, T., Okuma, E., Ye, W., Hossain, M. A., Masuda, C., . . . Murata, Y. (2012). Cooperative function of PLDδ and PLDα1 in abscisic acid-induced stomatal closure in Arabidopsis. *Plant physiology, 159*(1), 450-460.

Van der Luit, A. H., et al. (2000). Elicitation of Suspension-Cultured Tomato Cells Triggers the Formation of Phosphatidic Acid and Diacylglycerol Pyrophosphate. *Plant physiology, 123*, 1507-1516.

van Meer, G., Voelker, D. R., & Feigenson, G. W. (2008). Membrane lipids: Where they are and how they behave. *Nature Reviews. Molecular Cell Biology, 9*(2), 112-124.

Velásquez, A. C., Castroverde, C. D. M., & He, S. Y. (2018). Plant-pathogen warfare under changing climate conditions. *Current biology : CB, 28*(10), R619-R634.

Veluchamy, S., Hind, S. R., Dunham, D. M., Martin, G. B., & Panthee, D. R. (2014). Natural variation for responsiveness to flg22, flgII-28, and csp22 and *Pseudomonas syringae* pv. tomato in heirloom tomatoes. *PLoS One, 9*(9), e106119.

Venugopal, S. C., Chanda, B., Vaillancourt, L., Kachroo, A., & Kachroo, P. (2014). The common metabolite glycerol-3-phosphate is a novel regulator of plant defense signaling. *Plant signaling & behavior, 4*(8), 746-749. doi:10.4161/psb.4.8.9111

Vossen, J. H., Abd-El-Haliem, A., Fradin, E. F., van den Berg, G. C., Ekengren, S. K., Meijer, H. J., . . . Joosten, M. H. (2010). Identification of tomato phosphatidylinositol-specific phospholipase-C (PI-PLC) family members and the role of PLC4 and PLC6 in HR and disease resistance. *Plant J, 62*(2), 224-239.

Wältermann, M., & Steinbüchel, A. (2005). Neutral Lipid Bodies in Prokaryotes: Recent Insights into Structure, Formation, and Relationship to Eukaryotic Lipid Depots. *Journal of Bacteriology, 187*(11), 3607-3619.

Wang, W., Cajigas, I. J., Peltz, S. W., Wilkinson, M. F., & Gonzalez, C. I. (2006). Role for Upf2p phosphorylation in Saccharomyces cerevisiae nonsense-mediated mRNA decay. *Mol Cell Biol, 26*(9), 3390-3400.

Wasternack, C., Stenzel, I., Hause, B., Hause, G., Kutter, C., Maucher, H., . . . Miersch, O. (2006). The wound response in tomato - Role of jasmonic acid. *Journal of plant physiology, 163*, 297-306.

Wenk, M. R. (2005). The emerging field of lipidomics. *Nat Rev Drug Discov, 4*(7), 594-610.

Winter, S. E., Winter, M. G., Xavier, M. N., Thiennimitr, P., Poon, V., Keestra, A. M., . . . Baumler, A. J. (2013). Host-derived nitrate boosts growth of E. coli in the inflamed gut. *Science, 339*(6120), 708-711.

Xinjiao, G., Changjiang, J., Yu, X., & Xuebiao, Y. (2008). Computational Analyses of TBC Protein Family in Eukaryotes. *Protein & Peptide Letters, 15*(5), 505-509.

Xue, H.-W., Chen, X., & Mei, Y. (2009). Function and regulation of phospholipid signalling in plants. *The Biochemical journal, 421*(2), 145-156.

Yaeno, T., Matsuda, O., & Iba, K. (2004). Role of chloroplast trienoic fatty acids in plant disease defense responses. *Plant J, 40*(6), 931-941.

Yamaguchi, T., Minami, E., Ueki, J., & Shibuya, N. (2005). Elicitor-induced activation of phospholipases plays an important role for the induction of defense responses in suspension-cultured rice cells. *Plant Cell Physiol, 46*(4), 579-587.

Yan, L., Zhai, Q., Wei, J., Li, S., Wang, B., Huang, T., . . . Li, C. (2013). Role of tomato lipoxygenase D in wound-induced jasmonate biosynthesis and plant immunity to insect herbivores. *PLOS Genetics, 9*(12), e1003964.

Yang, J., Dong, H., & Hammock, B. D. (2011). Profiling the regulatory lipids: another systemic way to unveil the biological mystery. *Current opinion in lipidology, 22*(3).

Yu, K., Soares, J. M., Mandal, M. K., Wang, C., Chanda, B., Gifford, A. N., . . . Kachroo, P. (2013). A feedback regulatory loop between G3P and lipid transfer proteins DIR1 and AZI1 mediates azelaic-acid-induced systemic immunity. *Cell Rep, 3*(4), 1266-1278.

Zalejski, C., Zhang, Z., Quettier, A.-L., Maldiney, R., Bonnet, M., Brault, M., . . . Jeannette, E. (2005). Diacylglycerol pyrophosphate is a second messenger of abscisic acid signaling in Arabidopsis thaliana suspension cells. *Plant J, 42*, 145-152.

Zhang, L., Zhang, F., Melotto, M., Yao, J., & He, S. Y. (2017). Jasmonate signaling and manipulation by pathogens and insects. *Journal of Experimental Botany, 68*(6), 1371-1385.

Zhao, X., Chang, A. Y., Toh, E. A., & Arvan, P. (2007). A role for Lte1p (a low temperature essential protein involved in mitosis) in proprotein processing in the yeast secretory pathway. *J Biol Chem, 282*(3), 1670-1678.

Zipfel, C. (2014). Plant pattern-recognition receptors. *Trends in Immunology, 35*(7), 345-351.

Zoeller, M., Stingl, N., Krischke, M., Fekete, A., Waller, F., Berger, S., & Mueller, M. J. (2012). Lipid profiling of the Arabidopsis hypersensitive response reveals specific lipid peroxidation and fragmentation processes: biogenesis of pimelic and azelaic acid. *Plant physiology*, *160*(1), 365-378.

Chapter three

Lipid metabolism in susceptible and tolerant soybean cultivars in response to *Phytophthora sojae* colonization and infection

Plant lipid metabolism in response to *Phytophthora sojae* colonization and infection in susceptible and tolerant soybean (*Glycine max*) cultivars

3.1. Abstract

Soybean (*Glycine max*) is one of the most cultivated crops globally and a staple food for much of the world's population. The annual global crop losses due to infection by the *Phytophthora sojae* are currently estimated at approximately $2B USD. Furthermore, there is limited understanding of the role lipid mediated plant immunity play in the successful adaptative strategies used by tolerant soybean cultivars to limit infection and crop loss in the soybean-*P.sojae* pathosystem. A multi-modal lipidomics approach was employed to investigate how soybean cultivars remodel lipid metabolism to successfully limit infection by *Phytophthora sojae.* Both the tolerant and susceptible soybean cultivars showed alterations in lipid metabolism in response to *Phytophthora sojae* infection. Relative to non-inoculated controls, induced accumulation of stigmasterol was observed in the susceptible cultivar whereas, induced accumulation of phospholipids and glycerolipids occurred in tolerant soybean cultivar. A comprehensive metabolic map of susceptible and tolerant soybean root and stem lipids were generated to identify lipid mediated host immune or tolerance response to *Phytophthora sojae* infection and identified potential pathways and unique lipid biomarkers like TG(18:3/18:2/23:0), TG(10:0/10:0/10:0), TG(10:0/10:0/14:0), DG(18:3/18:3), DG(16:0/18:3) and DG(24:0/18:2) as possible targets for the development of future plant protection solutions.

***Keywords*:** *Glycine max* (soybean), membrane lipids, glycerolipids, lipid metabolism, plant-pathogen interaction, pathogen, *Phytophthora sojae*, root and stem rot, lipid network, lipid metabolism pathway.

3.2. Introduction

The global population is anticipated to increase to almost 9.7 billion by 2050, which will require a 70 % increase in food production (Röös et al., 2017). Food insecurity remains prevalent in many nations despite efforts to improve the production, the quality, and the availability of global food supplies (Matemilola & Elegbede, 2017). Food insecurity is a major challenge that must be addressed to meet the demands of an ever-increasing global population (Mc Carthy et al., 2018). To fulfill global food and feed requirements, innovative agricultural practices must be developed to enhance food production, availability and accessibility, which in turn will require advanced knowledge in plant pathology from seedling to crop harvest (Adigun et al., 2020). For instance, plant diseases are caused by infectious pathogens such as fungi, viruses, bacteria, and nematodes (Adigun et al., 2020). These diseases lead to significant annual economic losses in maize, potato, wheat, rice, and soybean worldwide accounting for a 40% yield reduction (Adigun et al., 2020; Fletcher et al., 2006; Savary et al., 2019). *Phytophthora sojae* is one of the leading-cause of soybean crop loss in North America accounting for approximately 1-2 billion USD in loss revenue on an annual basis (Grau et al., 2004; Tyler, 2007). Soybean root and stem rot are the most devastating threat to seedling and plant survival and productivity, particularly during wet growing seasons (Dorrance, McClure, & St. Martin, 2003; Thomas et al., 2007). During the susceptible crop growth stages, pathogens can alter an otherwise favourable environment for the plant into unfavourable conditions, leading to significant yield losses (Velásquez, Castroverde, & He, 2018). The repeated applications and heavy dependence on synthetic chemicals such as fungicides limit effective long-term control of this disease, as well as pose serious environmental and human health risks (Dangl, Horvath, & Staskawicz, 2013). Reducing the frequency and volume of chemical applications in agricultural crops is one of the primary objectives of plant pathological research. Hence, there is a need to develop innovative disease control systems improving the plant's natural defense mechanisms to build enduring and wide-spectrum disease resistance in crops to improve sustainable

agriculture and food security (Brackin, Atkinson, Sturrock, & Rasmussen, 2017; Sui, Niu, Yue, Yang, & Zhang, 2008).

Plants respond to different biotic and abiotic stress conditions through various defense mechanisms that may be either constitutive or induced (Adigun et al., 2020; Venegas-Molina et al., 2020). The constitutive system utilizes pre-formed inhibitory chemicals such as alkaloids, saponins, and glycosides, and barriers like wax cuticles, cellulose and suberin to reduce pathogen entry (Adigun et al., 2020; Gao et al., 2014; Thomas et al., 2007). Induced defense mechanisms are triggered by pathogen ingress causing plants to synthesize compounds or enzymes as a result of pathogen detection. This may occur at the site of infection by processes like the oxidative burst or the hypersensitive response, or the production of chitinases, nitric oxide or phytoalexins (Adigun et al., 2020). Furthermore, the response can be systemic in nature, producing pathogenesis-related proteins or the induction of systemic acquired resistance. Plants can also adapt to environmental stresses by regulating biochemical, physiological, and molecular properties of their cellular membrane (Adigun et al., 2020). Several studies have demonstrated the roles of lipids in plant pathology as part of a complex internal defense mechanism in the fight against infections caused by various pathogens (Adigun et al., 2020; Bandara, Weerasooriya, Liu, & Little, 2019; Lim, Singhal, Kachroo, & Kachroo, 2017; Raffaele, Leger, & Roby, 2009). Lipid remodeling is a defence mechanism adopted by plants to counteract pathogen attack (Goufo & Cortez, 2020). Depending on the composition, lipid molecular species can regulate membrane fluidity, permeability, stability, and integrity during a plant's response to pathogenic microorganisms. For instance, free FAs such as linoleic acid and oleic acid, which are major components of cellular membranes, play active functions during biosynthesis of the plant cuticular wax, forming the first barrier against pathogens (Lim et al., 2017). Lipid metabolites can also function as intracellular and extracellular signal mediators (Goufo & Cortez, 2020; Lim et al., 2017). Plant lipids include GPLs, PST, SGL, glycoglycerolipids (GGL) and glycerolipids (GL) (Adigun et al., 2020; Nadeem et al., 2019; Nadeem et al., 2020), and their metabolites are actively involved in plant defence responses against pathogen

colonization (Christensen & Kolomiets, 2011; Siebers et al., 2016). They play important roles in the formation of the membrane interface between plant and microbial pathogen (Christensen & Kolomiets, 2011; Siebers et al., 2016).

The GPLs of plant membranes possess two FAs as hydrophobic tails at the *sn1* and *sn2* carbons and a hydrophilic head group esterified to a phosphate group at the *sn3* position of the glycerol moiety. The classes of GPLs include PA, PC, phosphatidylethanolamine (PE), phosphatidylglycerol (PG), PI, and phosphatidylserine (PS). During plant-pathogen interactions, phospholipid-derived molecules rapidly accumulate and participate in plant signaling and membrane trafficking; they can also activate plant immunity (Canonne, Froidure-Nicolas, & Rivas, 2011; Xing, Zhang, Duan, & Lin, 2020). For instance, PA acts as a novel secondary messenger in plants and its biosynthesis has been reported to be triggered in response to pathogen attack (Laxalt & Munnik, 2002; Zhang & Xiao, 2015).

Plant sphingolipids are structural components of eukaryotic cellular membranes and play essential roles in maintaining membrane integrity (Ali, Li, Wang, & Guo, 2018). They have been recently demonstrated to act as signaling molecules playing crucial functions in the regulation of pathophysiological processes (Berkey, Bendigeri, & Xiao, 2012; Hannun & Obeid, 2018; Heung, Luberto, & Del Poeta, 2006). Studies have demonstrated that sphingolipids play important roles during biotic stress in plants by activating defences against bacterial and fungal pathogens. For instance, the fungus *Alternaria alternata f. sp. lycopersici* has been shown to activate cell death through disruption of sphingolipid metabolism (Spassieva, Markham, & Hille, 2002).

Phytosterols are integral components of cellular membranes and the most abundant sterols in plants include campesterol, sitosterol and stigmasterol (Valitova, Sulkarnayeva, & Minibayeva, 2016). Phytosterols are actively involved in regulation of membrane fluidity and integrity, and they influence membrane structural properties and physiological functions of plants. For instance, stigmasterol and beta-sitosterol play a vital role during structural formation and mediate cell membrane functions (Schaller, 2004). They have also been

demonstrated to play essential roles in plant innate immunity against pathogen attack (Wang, Senthil-Kumar, Ryu, Kang, & Mysore, 2012).

Galactolipids, including mono-/di-galactosyldiacylglycerol (MGDG and DGDG) are important membrane components in the chloroplasts of eukaryotic plants (Rocha et al., 2018). They play active roles in cell communication, signal transduction, and response to pathogen invasion (Siebers et al., 2016).

Glycerolipids are actively required during cell growth and cell division (Chapman, Dyer, & Mullen, 2012), serve as energy storage for survival, participate in stress responses, and play an important role in reducing pathogenicity (Murphy, 2012). During environmental stresses in plants, TG levels increase as a function of the sequestration of toxic lipid intermediates (Xu & Shanklin, 2016). Studies have suggested that DGs serve as signaling molecules during plant growth and development, and in response to stimuli during certain environmental stresses (Dong, Lv, Xia, & Wang, 2012; Garay, Boundy-Mills, & German, 2014). In addition, DG and DG kinase are known to activate immunity during plant defence responses to pathogen attack (Laxalt & Munnik, 2002). Although the literature is replete with examples of the plant lipidome mediating plant defence, very little is known concerning how plant lipid metabolism contributes to either successful colonization or tolerance in the soybean-*P. sojae* pathosystem. Previous studies have demonstrated that quantitative trait loci were mapped for partial resistance to *P. sojae* infection in recombinant inbred populations. For instance, 'Conrad' the soybean tolerant cultivar has been known as source of partial resistance to *P. sojae* infection, while 'Sloan' and OX760-6-1 the soybean susceptible cultivars have been identified to be highly susceptible to the same pathogen infection (Ellis et al., 2012; Han et al., 2008; Lee et al., 2013; Stasko et al., 2016; Weng, Yu, Anderson, & Poysa, 2007).

We hypothesized that the relative concentrations of membrane lipids in a *P. sojae*-tolerant soybean cultivar would fluctuate more than those of a *P. sojae*-susceptible cultivar following pathogen infection; we hypothesized that these greater changes are just one component of a successful strategy to limit pathogen

infection. To this end, we assessed the lipidome of soybean root and stem to understand the functions of lipid metabolism in the response of susceptible and tolerant soybean cultivars to pathogen colonization and infection.

3.3. Materials and methods

3.3.1. Plant growth and inoculation method

A virulent strain of *P. sojae* race 2 (strain P6497) obtained from the London Research and Development Center, Agriculture and Agri-Food Canada (AAFC-LRDC; London, ON, Canada) was used as inoculum. The oomycete was cultured and maintained aseptically for 8 days on 26 % V8-juice agar (8400 mg agar, 1600 mg $CaCO_3$, 156 mL V8-juice [Campbell Soup Company, Toronto, ON, Canada], and 440 mL of distilled water). Seeds of soybean cultivars Conrad (*P. sojae*-tolerant) and OX760-6 (*P. sojae*-susceptible) were obtained from AAFC-LRDC (London, ON, Canada). The seeds were surface disinfected for 5 min using 0.5 % sodium hypochlorite (Commercial Javex Bleach; Clorox Co., Brampton, Ontario, Canada) and rinsed with distilled water several times. The seeds were then soaked for 12 h in distilled water before seeding. The bottom of a sterilized empty paper drinking cup was used to cut agar disks consisting of cultures of *P. sojae* P6497 which were then fitted into the bottom of wax-paper cups (Merchants Paper Company, Windsor, ON, Canada) with a top diameter of 8.5 cm and 15.0 cm deep and overlaid with medium-grade vermiculite. Drainage holes were created in the bottom of the cups. The imbibed seeds were planted in the medium-grade vermiculite. Six soybean seedlings from each cultivar were inoculated with *P. sojae* in a cup and another six from each cultivar were mock-inoculated (sterile V8-juice agar disks without a *P. sojae* culture) in a cup as the control and experiment were performed three times. The plants were allowed to grow for 10 days. The plant growth experiment was performed in a growth chamber (Biochambers MB, Canada) at Grenfell Campus, Memorial University of Newfoundland, under controlled growth conditions of 16 h light at 25 °C and 8 h dark at 20 °C, and relative humidity of 60 %. Seedlings were watered daily 4 days after seeding with one-quarter-strength Knop's solution (Thomas et al., 2007). The whole seedlings were collected 10 days after growth and stored at -80 °C until further analysis.

3.3.2. Method of lipid extraction

Soybean seedlings prepared as above were incubated in boiling isopropanol for 10 min. Lipid extraction was conducted by weighing 100 mg each of root and stem from each sample type, and 1 mL MeOH containing 0.01 % butylated hydroxytoluene was added to each sample. Four replications of each combination of treatment (inoculated or control), cultivar (susceptible or tolerant), and tissue (root or stem) combination were performed. The tissues were then homogenized using a probe tissue homogenizer until completely dissolved. Following homogenization, 800 µL water and 1000 µL chloroform were added along with PC14:0/14:0 as internal standard to validate the ion variations detected in the MS spectra according to lipid maps (Jeanne Dit Fouque, Maroto, & Memboeuf, 2018; Rower, Bushman, Hammond, Kadam, & Aquilante, 2010). Each sample was thoroughly vortexed and centrifuged at 3000 rpm for 15 min at room temperature. The organic layers were transferred to pre-weighed 4 mL glass vials with Polytetrafluoroethylene (PTFE)-lined caps (VWR, Mississauga, Canada). The samples were then dried under a gentle stream of nitrogen and the sample vials reweighed to determine the quantity of recovered lipids. The recovered lipids from each sample were re-suspended in 1000 µL solvent (2:1 v/v chloroform: methanol) and stored at -20 °C until lipid analysis using ultra high-performance liquid chromatography coupled to heated electrospray ionization high resolution accurate mass tandem mass spectrometry (UHPLC- C30RP-HESI-HRAM-MS/MS).

3.3.3. Lipid analysis using UHPLC-C30RP-HESI-HRAM-MS/MS

The method of lipid analysis was as described previously (Nadeem et al., 2020). Lipids extracted from the soybean roots and stems were separated using an Accucore C30 reverse phase (C30RP) column (150 × 2 mm I.D., particle size: 2.6 µm, pore diameter: 150 Å; ThermoFisher Scientific, ON, Canada) applying the following solvent system: Solvent A (40: 60 v/v H_2O and acetonitrile), and Solvent B (1:10: 90 v/v/v water: acetonitrile: isopropanol). Both solvents A and B consisting of 0.1 % formic acid and 10 mM ammonium formate. The

conditions for the separation using UHPLC-C30RP were as follows: oven temperature of 30 °C, flow rate of 0.2 mL/min, and 10 µL of the lipid mixture suspended in 1: 2 v/v methanol: chloroform was injected into the instrument. The system gradient used for the separation of lipid classes and molecular species were: 30 % solvent B for 3 min; solvent B increased over 5 min to 43 %, then increased in 1 min to 50 % B and to 90 % B over 9 min; and from 90 % to 99 % B over 8 min; and finally maintained at 99 % B for 4 min. The column was re-equilibrated to 70 % solvent A for 5 min to re-establish the starting conditions before injection of each new sample. Lipid analyses were performed using a Q-Exactive Orbitrap high-resolution accurate mass tandem mass spectrometer (Thermo-Scientific, Berkeley, CA, USA) coupled with an automated Dionex Ulti-Mate 3000 UHPLC system controlled by Chromeleon 6.8 SR13 (Dionex Corporation, Part of Thermo Fisher Scientific) software. Full-scan HESI-MS and MS/MS acquisitions were performed in positive mode of the Q-Exactive Orbitrap mass spectrometer. The following parameters were used for the Orbitrap mass spectrometry techniques: auxiliary gas of 2; sheath gas of 40; capillary temperature of 300 °C; ion spray voltage of 3.2 kV; S-lens RF of 30 V; full-scan mode at a resolution of 70,000 m/z; mass range of 200–2000 m/z; top-20 data dependent MS/MS acquisitions at a resolution of 35,000 m/z; and injection time of 35 min; automatic gain control target of 5e5; isolation window of 1 m/z; collision energy of 35 (arbitrary unit). The external calibration of instrument was performed to 1 ppm using ESI positive and negative calibration solutions (Thermo Scientific, Berkeley CA, USA). Mixtures of lipid standards containing PA 18:1(9Z)/18:1(9Z), diether PC O-18:0/O-18:0, PC 18:0/20:4 (5Z,8Z,11Z,14Z), PG 18:0/20:4(5Z,8Z,11Z,14Z), PE 18:0/20:4(5Z,8Z,11Z,14Z), SQDG 16:0/16:0, MGDG 16:3(7Z,10Z,13Z)/18:3(9Z,12Z,15Z), plasmalogen PE P-18:0/20:4(5Z,8Z,11Z,14Z), plasmalogen PC P-18:0/20:4(5Z,8Z,11Z,14Z), DMPE 16:0/16:0, and MMPE 16:0/16:0, LPC 18:1(9Z), LPA 20:4(5Z,8Z,11Z,14Z), LPE 18:0, plasmalogen LPE P-18:0; PI 18:0/20:4(5Z,8Z,11Z,14Z); SM d18:1/18:0 and DLCL 18:2(9Z,12Z)/18:2(9Z,12Z) were used to optimize tune parameters (Avanti Polar Lipids, Alabaster, AL, USA) in both positive and negative ion modes. Identification and semi-quantification of the classes of lipids and lipid molecular species present in the root and stem of both soybean cultivars (OX760-6 and Conrad) were

performed using LipidSearch version 4.1 (Mitsui Knowledge Industry, Tokyo, Japan) and the parameters adopted for identification in LipidSearch were: target database of Q-Exactive; product tolerance of 5 ppm; precursor tolerance of 5 ppm; Quan m/z tolerance of ±5 ppm; product ion threshold of 5 %; m-score threshold of 2; Quan retention time range of ±1 min; use of all isomer filter; ID quality filters A, B, and C; and $[M+NH_4]^+$ adduct ions for positive ion mode. Following identification, the observed lipid classes and lipid molecular species were merged and aligned according to the parameters established in our previous report (Pham et al., 2019).

3.3.4. Lipid biochemical network mapping

To better understand how soybean cultivars that are tolerant and susceptible to *P. sojae* modulate their membrane lipid metabolism as part of the plant defense response strategy during infection and colonization, lipids that changed significantly between treatments were visualized within lipid structural similarity and implied activity networks. Lipid SMILES identifiers obtained from lipid map were used to calculate PubChem molecular fingerprints describing lipids' sub structures (Guha, 2007). Connections between lipids were defined based on Tanimoto similarity ≥ 0.8 between fingerprints. Significance of fold changes in lipid expression levels were mapped to network node attributes and displayed using Cytoscape (Grapov, Wanichthanarak, & Fiehn, 2015; Shannon et al., 2003). Node size was used to represent fold changes of means between treatments, and colors indicated the direction of change compared to control (orange = increased; blue = decreased; gray = inconclusive) in the lipid network map generated. Node shape was used to indicate lipid structural type (rounded square= membrane lipids; circle = neutral lipids). Lipids displaying significant differences between treatment groups ($p \leq 0.05$) were denoted with black borders.

3.3.5. Statistical analysis

To determine the effects of pathogen infection on lipid composition of the root and stem of susceptible and tolerant cultivars, multivariate analyses including partial least square discriminant analysis (PLS-DA), and heat map were performed to group the treatments based on similarity. Analysis of variance (ANOVA) was next performed to determine whether the groups were significantly different between treatments using XLSTAT (2017 Premium edition, Addinsoft, Paris, France). Where significant differences were observed, the means were compared with Fisher's Least Significant Difference (LSD), α = 0.05. Figures were prepared with SigmaPlot 13.0 (Systat Software Inc., San Jose, CA).

3.4. Results

3.4.1. Lipid composition of the soybean cultivars in response to *P. sojae* infection

We applied a multi-modal lipidomics approach using UHPLC-C30RP-HESI-HRAM-MS/MS to obtain a detailed understanding of how susceptible and tolerant soybean cultivars remodeled their lipid metabolism to successfully limit infection by *P. sojae* using 10-day old seedlings as a model. The results confirmed as hypothesized that there are significant alterations in the root and stem lipidomes within and between susceptible and tolerant soybean cultivars following inoculation with pathogenic *P. sojae* (Tables 3.1, 3.2). Representative chromatograms and mass spectrum demonstrating the separation of the membrane and storage lipids present in the root and stem of the soybean cultivars evaluated (negative and positive ion modes) is shown in Fig. 3.1. The chromatograms of separated membrane lipids in negative ion mode are shown in Fig. 3.1a. The extracted ion chromatogram of *m/z* 671.46, 802.56 and 833.52 precursor ions of the three selected polar lipids are shown in Fig. 3.1b. The MS^2 spectrum of *m/z* 671.46 identified as PA 16:0/18:2 $[M-H]^-$ is depicted in Fig. 3.1c. For example, m/z 152 represent the glycerol moiety (head group) in PA and m/z 255 and 279 represent C16:0 and C18:2 fatty acids present in PA

16:0/18:2 (Fig. 3.1c). The same convention was used in identifying the other lipids present in Fig 3.1. This included *m/z* 802.56 identified as PC 16:0/18:2 $[M+HCOO]^-$ in Fig. 1d, *m/z* 833.52 representing PI 16:0/18:2 $[M-H]^-$ in Fig. 3.1e. Together, these accounted for some of the main membrane lipids identified in the soybean plant tissue. Similarly, a chromatogram demonstrating the separation of GLs from the stem of the soybean cultivar in the positive ion mode is shown in Fig. 3.1f. The extracted ion chromatogram of m/z 630.51, 890.72 and 892.74 representing the precursor ions of the three selected GLs are depicted in Fig. 3.1g. The MS^2 spectrum of *m/z* 630.51 identified as DG 18:3/18:3 $[M+NH_4]^+$ is depicted in Fig. 3.1h, the MS^2 spectrum of *m/z* 802.56 identified as TG 18:3/18:3/18:3 $[M+NH_4]^+$ is depicted in Fig. 3.1i, and the MS^2 spectrum of *m/z* 833.52 representing TG 18:3/18:2/18:3 $[M+NH_4]^+$ is depicted in Fig. 3.1j. These species account for some of the major GLs identified in the plant tissue.

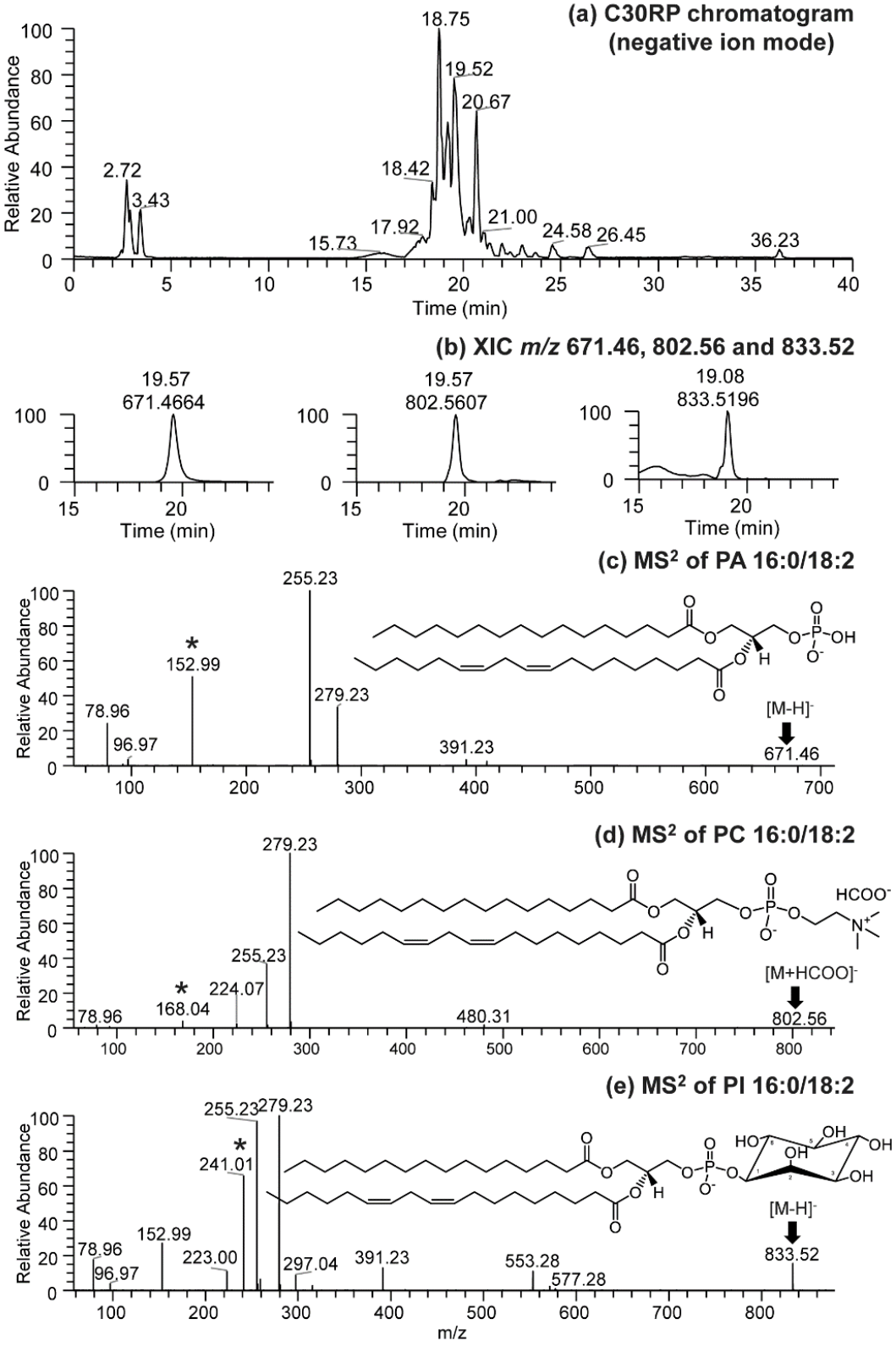
(a) C30RP chromatogram
(negative ion mode)
Relative Abundance
Time (min)
18.75
19.52
20.67
18.42
2.72
3.43
17.92
15.73
21.00
24.58
26.45
36.23
(b) XIC m/z 671.46, 802.56 and 833.52
19.57
671.4664
19.57
802.5607
19.08
833.5196
Time (min)
(c) MS² of PA 16:0/18:2
255.23
152.99
279.23
78.96
96.97
391.23
[M-H]⁻
671.46
(d) MS² of PC 16:0/18:2
279.23
255.23
224.07
168.04
78.96
480.31
HCOO⁻
[M+HCOO]⁻
802.56
(e) MS² of PI 16:0/18:2
255.23
279.23
241.01
152.99
78.96
96.97
223.00
297.04
391.23
553.28
577.28
[M-H]⁻
833.52
m/z

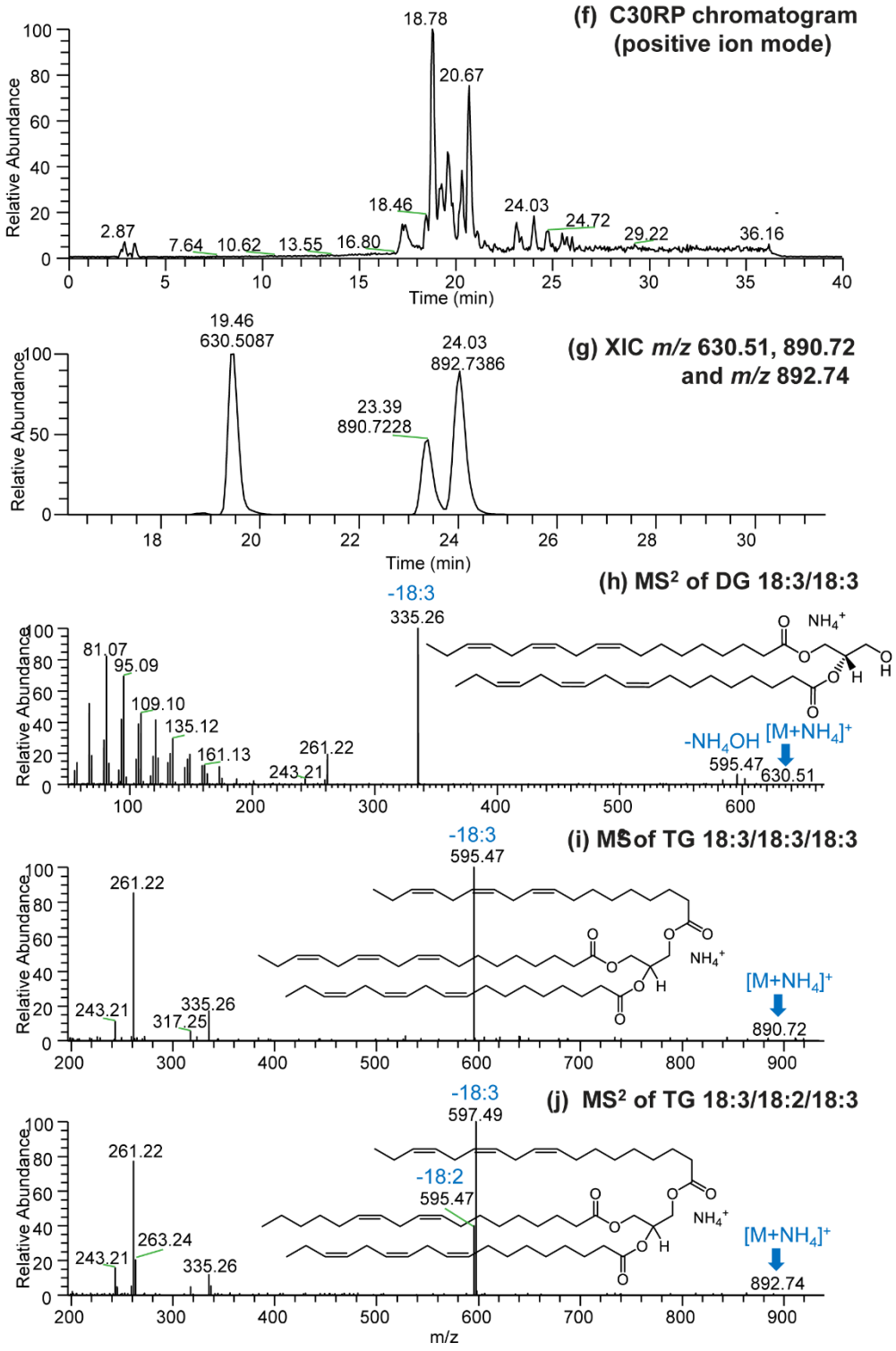
(f) C30RP chromatogram
(positive ion mode)
Relative Abundance
Time (min)
18.78
20.67
18.46
24.03
24.72
29.22
36.16
2.87
7.64
10.62
13.55
16.80
(g) XIC m/z 630.51, 890.72
and m/z 892.74
19.46
630.5087
24.03
892.7386
23.39
890.7228
(h) MS² of DG 18:3/18:3
-18:3
335.26
81.07
95.09
109.10
135.12
161.13
261.22
243.21
-NH4OH
[M+NH4]+
595.47
630.51
(i) MS² of TG 18:3/18:3/18:3
-18:3
595.47
261.22
243.21
317.25
335.26
[M+NH4]+
890.72
(j) MS² of TG 18:3/18:2/18:3
-18:3
597.49
-18:2
595.47
261.22
263.24
243.21
335.26
[M+NH4]+
892.74
m/z

Fig. 3.1. Chromatogram demonstrating the UHPLC-C30RP-HESI-HRAM-MS separation of the membrane lipids and GLs in the root and stem of susceptible and tolerant soybean cultivars. (a) LC-MS chromatogram of separated membrane lipids in negative ion mode, (b) Extracted ion chromatogram of *m/z* 671.46, 802.56 and 833.52 precursor ions of the three selected polar lipids, (c) MS^2 spectrum of *m/z* 671.46 identified as PA 16:0/18:2 $[M-H]^-$, (d) MS^2 spectrum of *m/z* 802.56 identified as PC 16:0/18:2 $[M+HCOO]^-$ and (e) MS^2 spectrum of *m/z* 833.52 representing PI 16:0/18:2 $[M-H]^-$ identified in the negative ion mode; (f) LC-MS chromatogram in positive ion mode of separated GLs (g) Extracted ion chromatogram of *m/z* 630.51, 890.72 and 892.74 precursor ions of the three selected GLs, (h) MS^2 spectrum of *m/z* 630.51 identified as DG 18:3/18:3 $[M+NH_4]^+$, (i) MS^2 spectrum of *m/z* 802.56 identified as TG 18:3/18:3/18:3 $[M+NH_4]^+$ and (j) MS^2 spectrum of *m/z* 833.52 representing TG 18:3/18:2/18:3 $[M+NH_4]^+$ identified in the positive ion mode. PA = phosphatidic acid, PC = phosphatidylcholine, and PI = phosphatidylinositol, DG = diacylglycerol, TG = triacylglycerol, and * represent the head group for each of the lipid class presented.

We observed five lipid classes: GPL, PST, GL, SGL, and GGL in soybean stem and root. Glycerophospholipids accounted for the highest portion of total lipids in both cultivars, irrespective of tissue type or inoculation status, representing 65.37±0.27 nmol% to 76.22±0.25 nmol% of all lipids in root (Table 3.1) and 66.56±1.32 nmol% to 80.67±2.15 nmol% in stem (Table 3.2), followed by GLs which ranged from 21.79±1.03 nmol% to 32.89±2.17 nmol% in the roots and 16.11±1.13 nmol% to 24.90±1.51 nmol% in the stems (Table 3.2). Phytosterols, SGLs, and GGLs were present in lower quantities ranging between 0.02±0.01 nmol% to 2.43±0.02 nmol% for root (Table 3.1) and 0.47±0.07 nmol% to 4.18±0.66 nmol% for stem (Table 3.2). From the five lipid classes investigated, 20 subclasses were analyzed across both root and stem which include eight GPLs, two GLs, six PSTs, three SGLs, and one GGL (Tables 3.1, 3.2). In tolerant root tissue, the percentage of the following lipids increased after inoculation: PC (4.18 %), PE (12.76 %), PA (40.79 %), PI

(133.11 %), PS (433.33 %), hexaceramide (HexCer; 168.63 %), and DG (63.64 %) (Table 3.1). In contrast, the following lipid increases were observed in the susceptible roots: PA (22.73 %), DG (21.74 %) and stigmasterol ester (StE; 730.77 %) (Table 3.1). In the stem of the tolerant cultivar, an increase in lipid levels was observed for PC (13.16 %), PE (5.05 %), PA (59.36 %), PI (8.85 %), HexCer (67.00 %), and DG (69.85 %) whereas in susceptible cultivar's stem, an increase in lipid levels was observed for PA (179.41 %), DG (7.33 %), TG (63.70 %), HexCer (120.22 %) and StE (482.35 %) (Table 3.2). Specifically, we observed significantly higher levels of major GPLs and GLs in the tolerant cultivar, but higher levels of PST in the susceptible cultivar in response to *P. sojae* colonization and infection.

Table 3.1. Effect of *P. sojae* infection on the root lipidome of susceptible (OX760-6) and tolerant (Conrad) soybean cultivars

Lipid classes	Lipid sub-classes	Relative abundance (nmol%) ORC	ORI	CRC	CRI
Glycerophospholipids	PC*	25.67±0.84^{c}	24.47±1.78^{d}	29.87±1.10^{b}	31.12±0.20^{a}
	PE*	25.77±0.25^{a}	24.66±2.47^{b}	20.46±2.39^{d}	23.07±0.52^{c}
	PA*	5.50±0.51^{d}	6.75±0.95^{c}	9.17±1.38^{b}	12.91±0.69^{a}
	PG^{ns}	3.90±0.98	3.62±0.49	3.80±0.54	3.76±0.60
	PI*	7.94±0.49^{a}	7.09±0.59^{a}	1.51±0.45^{c}	3.52±0.33^{b}
	PS*	1.32±0.30^{a}	1.26±0.30^{a}	0.27±0.12^{b}	1.44±0.20^{a}
	LPC^{ns}	0.15±0.01	0.18±0.02	0.25±0.03	0.36±0.04
	LPE^{ns}	0.03±0.00	0.04±0.01	0.04±0.01	0.04±0.00
Glycerolipids	TG*	19.03±0.55^{b}	19.10±0.03^{b}	28.16±3.48^{a}	14.05±1.02^{c}
	DG*	6.90±0.16^{c}	8.40±0.50^{a}	4.73±0.18^{d}	7.74±0.30^{b}
Phytosterols	AcHexSiE*	1.06±0.34^{a}	0.77±0.26^{b}	0.07±0.03^{c}	0.04±0.00^{c}
	SiE^{ns}	0.55±0.09	0.47±0.04	0.07±0.04	0.03±0.02
	AcHexStE^{ns}	0.05±0.10	0.04±0.02	0.05±0.01	0.03±0.01
	AcHexCmE^{ns}	0.09±0.04	0.04±0.02	ND	ND

	CmE^{ns}	0.04±0.01	0.03±0.01	0.01±0.00	ND
	StE*	0.13±0.01^{c}	1.08±0.02^{a}	0.46±0.07^{b}	0.12±0.10^{c}
	HexCer*	1.12±0.08^{a}	1.35±0.16^{a}	0.51±0.42^{b}	1.37±0.25^{a}
Sphingolipids	Cer^{ns}	0.31±0.02	0.29±0.04	0.47±0.03	0.30±0.05
	SM^{ns}	0.01±0.00	0.01±0.00	0.07±0.10	0.08±0.02
Glycoglycerolipid	MGDG^{ns}	0.44±0.14	0.35±0.20	0.03±0.01	0.02±0.01
Total		**100.00**	**100.00**	**100.00**	**100.00**
Glycerophospholipids*		**70.28±0.28^{b}**	**68.07±0.96^{c}**	**65.37±0.27^{b}**	**76.22±0.25^{a}**
Glycerolipids*		**25.93±0.20^{c}**	**27.50±0.55^{b}**	**32.89±2.17^{a}**	**21.79±1.03^{d}**
Phytosterols*		**1.91±0.02^{b}**	**2.43±0.02^{a}**	**0.66±0.02^{c}**	**0.22±0.09^{d}**
Sphingolipids^{ns}		**1.44±0.04^{a}**	**1.65±0.18^{a}**	**1.05±0.02^{a}**	**1.75±0.20^{a}**
Glycoglycerolipid^{ns}		**0.44±0.14**	**0.35±0.20**	**0.03±0.01**	**0.02±0.01**

Values in the table (nmole % by weight composition) denote means ± standard errors for four biological replicates. Means in the same row with different superscript letters (a, b, c, d, and e) are indicated as significantly different (*) or not significantly different (ns) between the treatments, which consisted of susceptible control (ORC) and inoculated (ORI) root tissue; and tolerant control (CRC) and inoculated (CRI) root tissue from 10-day old seedlings, at a significance level of $\alpha < 0.05$. The lipids detected were: phosphatidic acid (PA), phosphatidyl-ethanolamine (PE), choline (PC), glycerol (PG), serine (PS), inositol (PI), triacylglycerol (TG), diacylglycerol (DG), lysophosphatidylcholine (LPC), lysophosphatidylethanolamine (LPE), sphingomyelin (SM), monogalactosyldiacylglycerol (MGDG), beta sitosterol (SiE), stigmasterol ester (StE), hexosyl ceramide

(HexCer), ceramide (Cer), campesterol ester (CmE), acylated hexosyl stigmasterol ester (AcHexStE), acylated hexosyl betasitosterol ester (AcHexSiE), and acylated hexosyl campesterol ester (AcHexCmE). Lipids that were not detected (ND) under the treatment conditions are indicated.

Table 3.2. Effect of *Phytophthora sojae* infection on stem lipidome of susceptible (OX760-6) and tolerant (Conrad) soybean cultivars

Lipid classes	Lipid sub-classes	Relative abundance (nmol%) OSC	OSI	CSC	CSI
Glycerophospholipids	PC*	22.05±2.50^{b}	17.52±0.92^{c}	20.98±0.26^{b}	23.74±0.39^{a}
	PE*	33.89±2.13^{a}	27.45±1.48^{b}	21.18±0.18^{d}	22.25±0.61^{c}
	PA*	2.72±1.27^{d}	7.60±1.52^{c}	8.39±0.20^{b}	13.37±1.88^{a}
	PG*	8.77±1.16^{c}	7.80±0.41^{d}	12.30±0.69^{a}	10.72±1.56^{b}
	PI*	5.16±0.59^{c}	4.54±0.50^{d}	6.67±0.41^{b}	7.26±0.64^{a}
	PS*	2.24±0.66^{b}	1.25±0.63^{c}	5.33±0.76^{a}	2.91±0.40^{b}
	LPC^{ns}	0.42±0.04	0.32±0.03	0.38±0.04	0.36±0.05
	LPE^{ns}	0.09±0.00	0.08±0.02	0.09±0.00	0.06±0.01
Glycerolipids	TG*	10.11±1.25^{d}	16.55±0.02^{b}	17.89±1.50^{a}	11.66±2.00^{c}
	DG*	7.78±1.15^{b}	8.35±0.72^{a}	2.62±0.10^{d}	4.45±0.12^{c}
Phytosterols	AcHexSiE^{ns}	0.55±0.06	0.72±0.14	0.11±0.02	0.60±0.01
	SiE*	1.14±0.25^{a}	0.46±0.20^{b}	0.68±0.11^{a}	0.41±0.05^{b}
	AcHexStE^{ns}	0.75±0.37	0.69±0.21	0.04±0.00	0.05±0.01
	AcHexCmE^{ns}	0.14±0.05	0.20±0.03	0.01±0.00	ND

	CmE^{ns}	0.44±0.12	0.15±0.05	0.01±0.00	0.01±0.01
	StE*	0.34±0.16^{b}	1.98±0.02^{a}	0.33±0.05^{b}	0.40±0.15^{b}
	HexCer*	0.89±0.17^{b}	1.96±0.02^{a}	1.00±0.08^{b}	1.67±0.03^{a}
Sphingolipids	Cer^{ns}	0.27±0.06	0.31±0.02	0.71±0.04	0.21±0.03
	SM^{ns}	ND	ND	0.03±0.01	0.01±0.00
Glyceroglycolipid	MGDG*	2.25±0.08^{a}	2.09±0.06^{a}	1.25±0.18^{b}	0.47±0.07^{c}
Total		**100.00**	**100.00**	**100.00**	**100.00**
Glycerophospholipids*		**75.34±1.20^{b}**	**66.56±1.32^{c}**	**75.32±1.22^{b}**	**80.67±2.15^{a}**
Glycerolipids*		**17.89±0.25^{c}**	**24.90±1.51^{a}**	**20.51±1.60^{b}**	**16.11±1.13^{d}**
Phytosterols*		**3.36±0.12^{b}**	**4.18±0.66^{a}**	**1.18±0.19^{c}**	**0.86±0.06^{d}**
Sphingolipids*		**1.16±0.03^{c}**	**2.27±0.05^{a}**	**1.74±0.12^{b}**	**1.89±0.06^{b}**
Glyceroglycolipid*		**2.25±0.08^{a}**	**2.09±0.06^{a}**	**1.25±0.18^{b}**	**0.47±0.07^{c}**

Values in the table (nmole % by weight composition) denote means ± standard errors for four biological replicates. Means in the same row with different superscript letters (a, b, c, d, and e) are indicated as significantly different (*) or not significantly different (ns) between the treatments, which consisted of susceptible control (OSC) and inoculated (OSI) stem tissue; and tolerant control (CSC) and inoculated (CSI) stem tissue from 10-day old seedlings, at a significance level of $\alpha < 0.05$. The lipids detected were: phosphatidic acid (PA), phosphatidyl-ethanolamine (PE), choline (PC), glycerol (PG), serine (PS), inositol (PI), triacylglycerol (TG), diacylglycerol (DG), lysophosphatidylcholine (LPC), lysophosphatidylethanolamine (LPE), sphingomyelin (SM), monogalactosyldiacylglycerol (MGDG), beta sitosterol (SiE), stigmasterol ester (StE), hexosyl ceramide

(HexCer), ceramide (Cer), campesterol ester (CmE), acylated hexosyl stigmasterol ester (AcHexStE), acylated hexosyl betasitosterol ester (AcHexSiE), and acylated hexosyl campesterol ester (AcHexCmE). Lipids that were not detected (ND) under the treatment conditions are indicated.

3.4.2. Modification of membrane lipids in soybean cultivars in response to *P. sojae* infection

An analysis of membrane lipids in soybean root and stem tissues following infection with *P. sojae* was performed to determine changes and modification of membrane lipids during host-pathogen interaction. Figs. 3.2a-d and 3.3a-d demonstrate the changes that occurred in membrane lipids during host-pathogen interactions. Based upon the membrane lipid molecular species observed, we conducted PLS-DA to determine the most important membrane lipid molecular species with influential loadings (Figs. 3.2a, b and 3.3a, b) segregating the tolerant from the susceptible cultivar based on pathogen challenge. The model quality (Q^2) represents 95 % and 96 % variability in root and stem, respectively (Fig. 3.2a, 3.3a). The result from the PLS-DA observation plot showed the segregation of the susceptible and tolerant soybean cultivars before and after infection into four distinct groups that are in accordance with the root and stem membrane lipid molecular species (Fig. 3.2b, 3.3b). The root membrane lipid molecular species (Fig. 3.2b) separated the treatments into four distinct quadrants (Q). Quadrant 1 contained the lipid molecular species associated with Conrad root control (CRC) treatment, Q-2 contained Conrad root inoculated (CRI) treatment, Q-3 contained OX760-6 root control (ORC) and Q-4 had the OX760-6 root inoculated (ORI) treatment, respectively. Similarly, the changes in soybean stem (Fig. 3.3b), lipid molecular species separated the treatments into 4 distinct quadrants (Q-1, Q-2, Q-3 and Q-4) consisting of Conrad stem control (CSC), Conrad stem inoculated (CSI), OX760-6 stem control (OSC) and OX760-6 stem inoculated (OSI) treatments, respectively.

Based upon Component 3, which demonstrated the highest variation in the data (Figs. 3.2a, 3.3a), 22 membrane lipid molecular species from root tissue and 21 membrane lipid molecular species from stem tissue were selected for further analysis. Heat maps (Figs. 3.2c, 3.3c) were generated for the lipids with influential loadings accounting for the genotype and treatment segregation to further classify the treatments based on the altered membrane lipidome following infection. The cut-off value for variables important in projection (VIP) scores was defined as >1 (Nadeem et al., 2020; Ravipati, Baldwin, Barr, Fogarty, & Barrett, 2015). The 22

important root membrane lipid molecular species and 21 important stem membrane lipid molecular species were selected based on VIP scores greater than 1. The output from the heat map analysis showed four different clusters of the soybean root and stem membrane lipid molecular species following inoculation with *P. sojae* (Figs. 3.2c, 3.3c).

The heat map clusters root membrane lipid species into two main groups (G), G1 and G2, and four sub-groups, G1A, G1B, G2A and G2B. These groupings distinguished the susceptible cultivar (ORC & ORI) from the tolerant cultivar (CRC & CRI) in the root membrane lipid species in response to infection. We observed differences in the root membrane lipid species in G1A, where the relative abundance (nmol%) of PA(16:0/18:2), AcHexSiE(18:2), SiE(18:2), PG(16:0/18:2), PI(16:0/18:3) were significantly elevated in the tolerant cultivar challenged with *P. sojae* relative to the control and the susceptible cultivar (Fig. 3.2c). Lipid molecular species belonging to group G1B {PI(18:0/13:0), PG(16:0/16:0), SiE(22:3), PG(16:0/18:3), and PA(16:0/18:3)} were significantly lower in the tolerant cultivar that was challenged with the pathogen, whereas there was no difference in the susceptible cultivar whether treated or untreated with the pathogen (Fig. 3.2c). Lipid molecular species belonging to group G2A {CmE(20:3), SiE(18:3), AcHexSiE(16:2), AcHexCmE(16:0), AcHexSiE(16:1) and StE(18:3)} were not different in the root of the tolerant cultivar when infected with pathogen, but were significantly reduced in the root of susceptible cultivar when infected with the pathogen (Fig. 3.2c). Finally, in G2B, the relative abundances of StE(19:1), AcHexCmE(18:3), CmE(20:2), AcHexSiE(16:0), and PC(16:0/18:2) were not significantly different in the root of the tolerant cultivar but were significantly higher in the root of the susceptible cultivar infected by the pathogen (Fig. 3.2c). These data are corroborated by Fig. 3.2d, which demonstrates the significant differences in the molecular species in the root of tolerant and susceptible cultivars. In the pathogen challenged roots of the tolerant cultivar, the relative abundances of PA(16:0/18:2), AcHexSiE(18:2), PG(16:0/18:2), PG(16:0/18:3), (StE18:3) and (PC(16:0/18:2) were higher, whereas the relative

abundances of StE (18:2), SiE(22:3), StE (19:1), AcHexCmE(18:3), CmE(20:2), AcHexSiE(16:0), and (PC(16:0/18:2) were lower in the root of susceptible cultivar infected with the pathogen (Fig. 3.2d).

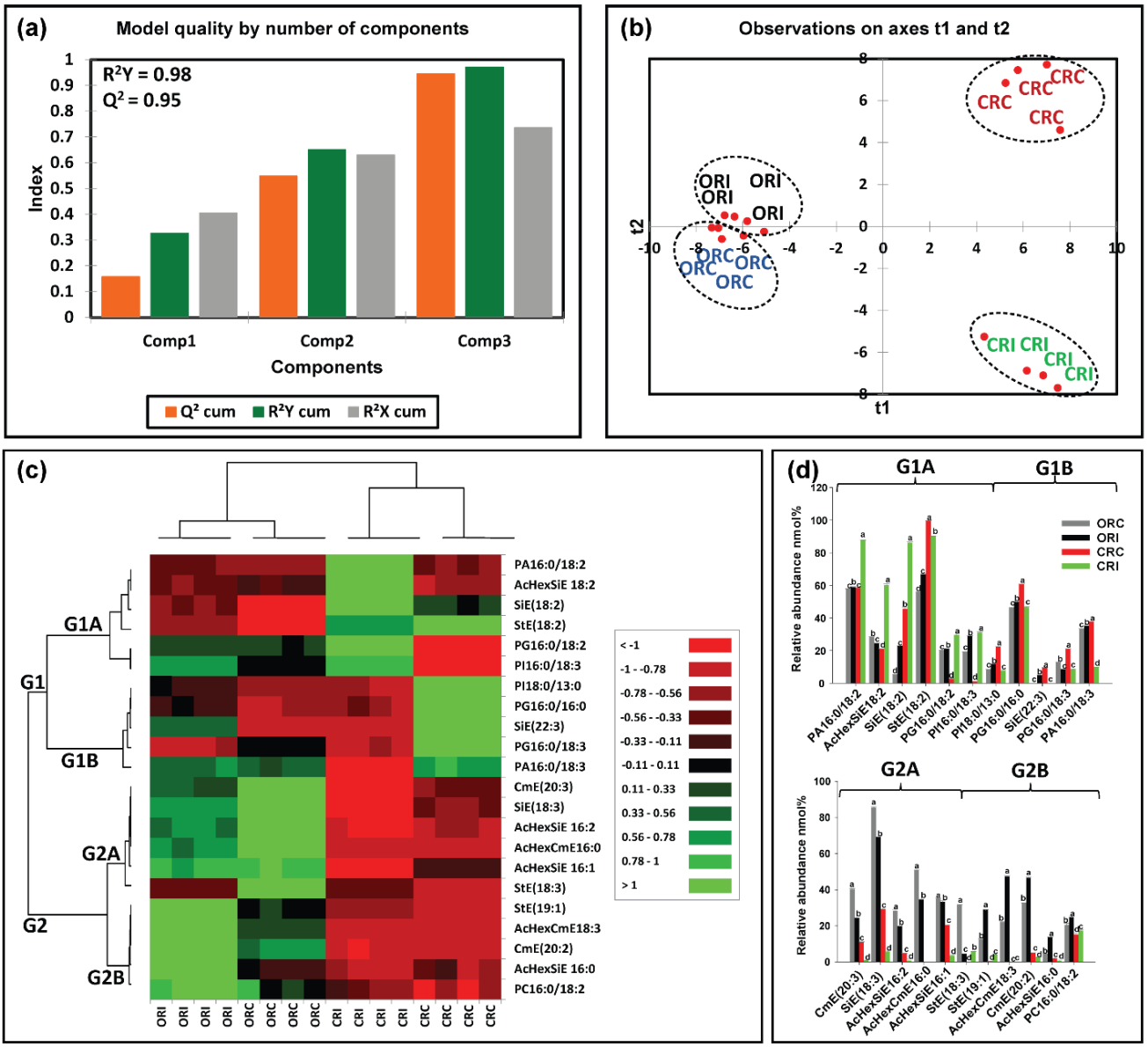

Fig. 3.2. Differences in root membrane lipids in susceptible (OX760-6) and resistant (Conrad) soybean cultivars inoculated with *P. sojae* relative to control plants. (**a**) Model quality for partial least squares-discriminant analysis (PLS-DA); (**b**) Observation plot based upon differences in molecular species in root membrane lipids of OX760-6 and Conrad cultivars; (**c**) Heat map demonstrating clusters of root membrane lipid species in OX760-6 and Conrad cultivars treated or untreated with *P. sojae*. Each cultivar and treatment were grouped separately using ascendant hierarchical cluster analysis based upon Euclidian distance at interquartile range of

0.15. The left columns denote the cluster segregated root membrane lipid species, while the above columns segregated soybean cultivars based upon similarities in abundance. The abundance of root membrane lipid species is denoted using color: red for lower level, black for intermediate level, and green for higher level. Group 1 and 2 (G1 and G2) and subgroups (G1A, G1B, G2A and G2B) are root membrane lipid species that were accountable for the formation of clustered patterns in the heat map that were applied for determination of significant differences between the soybean cultivars (OX760-6 and Conrad) root membrane lipid species in each of the bar chart (Fig. 3.2d) beside the heat map; and (**d**) Bar charts describe the relative abundance of root membrane lipid species as a mean nmol% ± SE (n = 4). Significant differences between root membrane lipid species are indicate using letter a-d on top of the bars as described by Fisher's LSD multiple comparisons test using ANOVA ($\alpha = 0.05$). The G1 and G2, and G1A, G1B, G2A and G2B are root membrane lipid species that were accountable for the formation of clustered patterns in the heat map that were applied for the determination of significant differences between the soybean cultivars (OX760-6 and Conrad) root membrane lipid species as illustrated in the bar charts.

Similarly, the heat map clusters stem membrane lipid molecular species into two major groups (G1and G2) which are further divided into sub-groups G1A, G1B, G2A and G2B. These groupings distinguished the susceptible cultivar (OSC & OSI) from the tolerant cultivar (CSC & CSI) in the stem membrane lipid molecular species. We observed stem membrane lipid molecular species in the tolerant cultivar, corresponding to G1A and consisting of AcHexSiE(18:2), AcHexCmE(18:2), AcHexSiE(18:1), PA(16:0/18:2), and SiE(18:3), were significantly higher in the tolerant cultivar challenged with *P. sojae* but there were no significant differences in the lipids of the susceptible cultivar. On the other hand, PA(16:0/18:2) was higher in the pathogen-infected tissue relative to the control (Fig. 3.3c). Lipid molecular species belonging to G1B {(PI(16:0/18:2), AcHexSiE(16:2), PS(18:0/16:0), AcHexCmE(16:0), PG(16:0/16:1), and PG(16:0/18:2)} were significantly lower in the tolerant cultivar challenged with the pathogen, whereas there was no difference in the susceptible cultivar regardless of infection status (Fig. 3.3c). Lipid molecular species belonging to G2A {AcHexSiE(18:0), CmE(18:3), PS(16:0/18:2), StE(18:3), PA(18:3/18:3), SiE(18:2) and PE(16:1/16:1)} were not significantly different in the stem of the tolerant cultivar but were significantly lower in the stem of susceptible cultivar challenged with the pathogen. Finally, in G2B, the levels of PG(16:0/16:0), PS(16:0/18:1) and CmE(20:2) significantly increased in the stem of the susceptible cultivar challenged with *P. sojae* (Fig. 3.3c). These trends are further corroborated by the output presented in Fig. 3d, which demonstrates the significant differences in the molecular species in the stem of tolerant and susceptible cultivar when challenged with the pathogen. For example, AcHexSiE(18:2), AcHexCmE(18:2), AcHexSiE(18:1), SiE(18:3), PS(16:0/18:2), and PA(18:3/18:3) were significantly higher in the stem of the tolerant cultivar, whereas AcHexSiE(18:1), AcHexSiE(16:2), AcHexCmE(16:0), and CmE(20:2) were significantly higher in the stem of the susceptible cultivar (Fig. 3.3d). These results showed there were significantly higher levels of GPL molecular species in root and stem of tolerant cultivar whereas there were significantly higher relative levels of PST molecular species in the root and stem of the susceptible cultivar in response to infection by the pathogen.

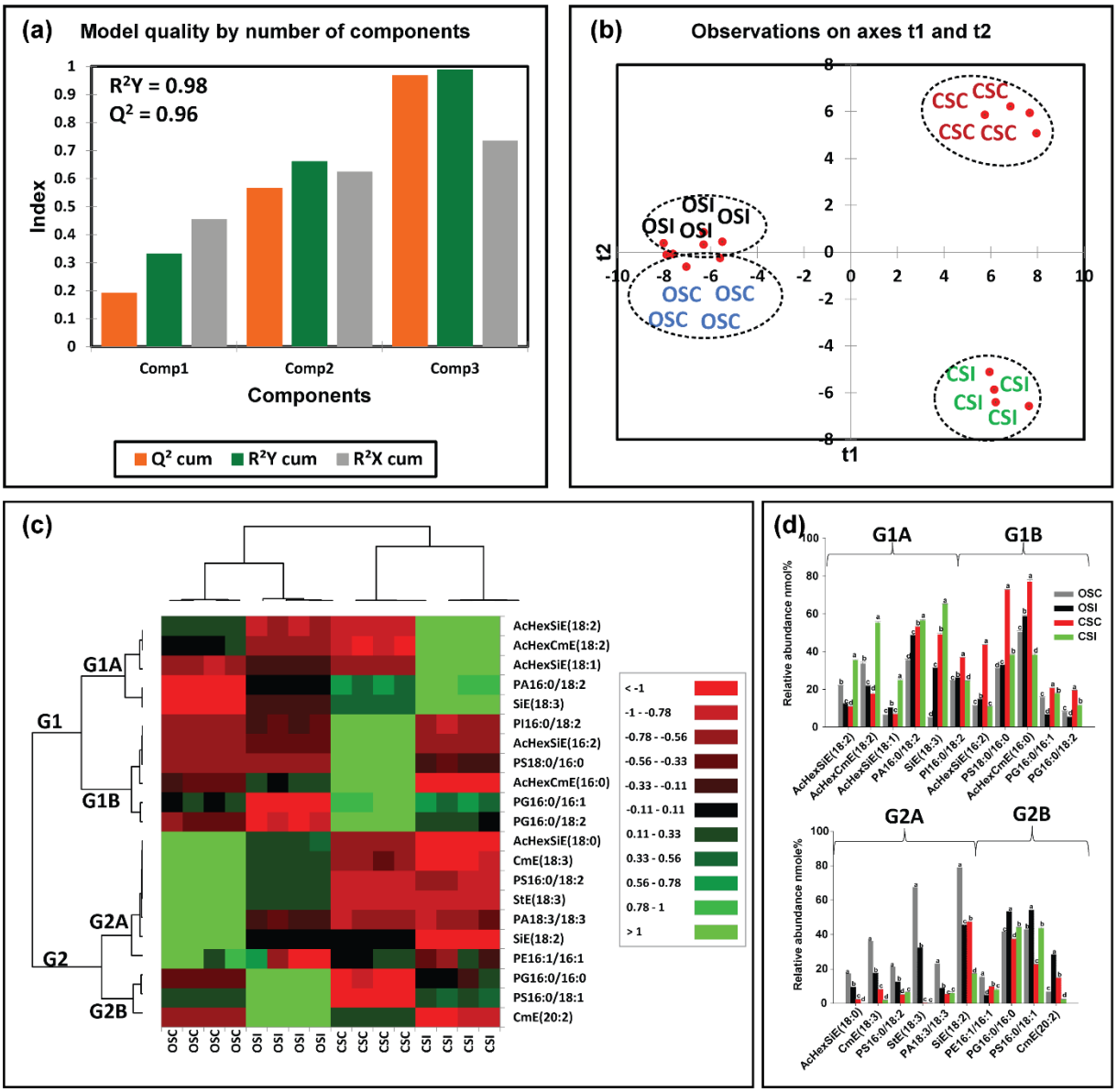

Fig. 3.3. Differences in stem membrane lipids in susceptible (OX760-6) and resistant (Conrad) soybean cultivars inoculated with *P. sojae* relative to control plants. (**a**) Model quality for partial least squares-discriminant analysis (PLS-DA); (**b**) Observation plot based upon differences in molecular species in stem membrane lipids of OX760-6 and Conrad cultivars; (**c**) Heat map demonstrating clusters of stem membrane lipid species in OX760-6 and Conrad cultivars treated or untreated with *P. sojae*. Each cultivar and treatment were grouped separately using ascendant hierarchical cluster analysis based upon Euclidian distance at

interquartile range of 0.15. The left columns denote the cluster segregated stem membrane lipid species, while the above columns segregated soybean cultivars based upon similarities in abundance. The abundance of stem membrane lipid species is denoted using color: red for lower level, black for intermediate level, and green for higher level. Group 1 and 2 (G1 and G2) and subgroups (G1A, G1B, G2A and G2B) are stem membrane lipid species that were accountable for the formation of clustered patterns in the heat map that were applied for determination of significant differences between the soybean cultivars (OX760-6 and Conrad) stem membrane lipid species in each of the bar chart (Fig. 3.3d) beside the heat map; and (**d**) Bar charts describe the relative abundance of stem membrane lipid species as a mean nmol% ± SE (n = 4). Significant differences between stem membrane lipid species are indicate using letter a-d on top of the bars as described by Fisher's LSD multiple comparisons test using ANOVA ($\alpha = 0.05$). The G1 and G2, and G1A, G1B, G2A and G2B are stem membrane lipid species that were accountable for the formation of clustered patterns in the heat map that were applied for the determination of significant differences between the soybean cultivars (OX760-6 and Conrad) stem membrane lipid species as illustrated in the bar charts.

3.4.3. Modification of glycerolipids in soybean cultivars in response to *P. sojae* infection

We also analysed GL in soybean root and stem tissues following infection with *P. sojae* to determine whether their levels and composition were altered during host-pathogen interaction (Figs. 3.4a-d, 3.5a-d). Triacylglycerols and DGs were observed to be the major GLs present regardless of soybean cultivar. We next performed PLS-DA to identify the most important TG and DG species with influential loadings (Figs. 3.4a, 3.4b, 3.5a, 3.5b) segregating the tolerant and susceptible soybean cultivars in their response to *P. sojae* colonization and infection. The model quality (Q^2) represents 80 % and 83 % variability in root and stem, respectively (Fig. 3.4a, 3.5a). The result from the PLS-DA observation plot showed the segregation of the susceptible and tolerant soybean cultivars that were infected or not infected with the pathogen into four distinct quadrants based on the levels of GL molecular species (Figs. 3.4b, 3.5b). The root GL molecular species (Fig. 3.3b) separated the treatments into four distinct quadrants. Quadrants 1-4 were composed of the GL molecular species of CRC, CRI, ORC and ORI treatments, respectively. Similar to the changes in soybean stem (Fig. 3.5b), GL species separated the treatments into 4 distinct quadrants (Q1-Q4) consisting of the GLs from CSC, CSI, OSC and OSI, respectively.

Based upon component 3 which explained the highest level of variation in the data (Figs. 3.4a, 3.5a), 27 GL molecular species from root tissues and 28 GL molecular species from the stem tissue with VIPs greater than 1 were selected for further multivariate analysis. Heat maps (Figs. 3.4c, 3.5c) were next generated for the lipids with influential loadings accounting for the genotype and treatment segregation to further classify the treatments based on the altered GL in the infected tissue. The output from the heat map analysis showed four different clusters of the soybean root and stem membrane lipid molecular species following inoculation with *P. sojae* (Figs. 3.4c, 3.5c). The heat map clustered GL species into two main groups, G1 and G2, and four sub-groups (G1A, G1B, G2A and G2B). These groupings distinguished the GL lipid molecular species in the root of the susceptible cultivar (ORC and ORI) from those of the root of the tolerant cultivar (CRC and CRI), as well as the stem-derived

GL lipid molecular species from both the susceptible (OSC and OSI) and tolerant cultivar (CSC and CSI) (Figs 3.4-3.5).

We observed that root GL molecular species in G1A {TG(22:0/18:2/18:2), TG(18:1/18:2/18:2), TG(18:3/18:2/23:0), TG(20:1/18:1/18:2), TG(16:0/18:2/18:2), TG(18:3/18:2/18:3), DG(18:3/18:2), DG(16:0/18:2), DG(18:3/18:3), and DG(16:0/18:3)} did not differ in the tolerant cultivar challenged with *P. sojae* relative to control, but were significantly higher in the susceptible cultivar challenged with the pathogen (Fig. 3.4c). Lipid molecular species belonging to group G1B {TG(18:1/18:1/18:1), TG(8:0/8:0/8:0), TG(18:0/16:0/18:1), TG(16:0/18:3/18:3), TG(16:0/16:0/18:3), TG(10:0/12:0/14:1), and TG(10:0/10:0/10:0)} also did not differ in the tolerant cultivar regardless of infection status, but were significantly lower in the susceptible cultivar in response to infection (Fig. 3.4c). In contrast, lipid molecular species belonging to group G2A {TG(10:0/10:0/12:0), DG(18:0/18:3), TG(18:4/11:3/12:4), and TG(18:0/18:1/18:1)} were significantly lower in the root of the tolerant cultivar that was challenged with the pathogen, but no differences were observed for the susceptible cultivar regardless of infection status (Fig. 3.4c). Finally, in G2B, the relative abundances of DG(15:0/16:0), TG(15:0/14:0/15:0), TG(16:0/17:0/17:0), DG(16:0/14:0), DG(18:0/16:0) and DG(18:0/18:0) were significantly higher in the tolerant cultivar in response to infection, whereas no differences were observed for the susceptible cultivar regardless of infection status(Fig. 3.4c). These data are corroborated by Fig. 3.4d, which demonstrates the significant differences in the molecular species in the root of tolerant and susceptible cultivars. In response to pathogen challenge, TG(18:0/16:0/18:1), DG(15:0/16:0), TG(15:0/14:0/15:0), TG(16:0/17:0/17:0), DG(16:0/14:0), DG(18:0/16:0) and DG(18:0/18:0) were significantly higher in the root of the tolerant cultivar while TG(18:1/18:2/18:2), TG(20:1/18:1/18:2), TG(16:0/18:2/18:2), TG(18:3/18:2/18:3), DG(18:3/18:2), DG(16:0/18:2), DG(18:0/18:3) were significantly higher in the root of the susceptible cultivar after infection (Fig. 3.4d).

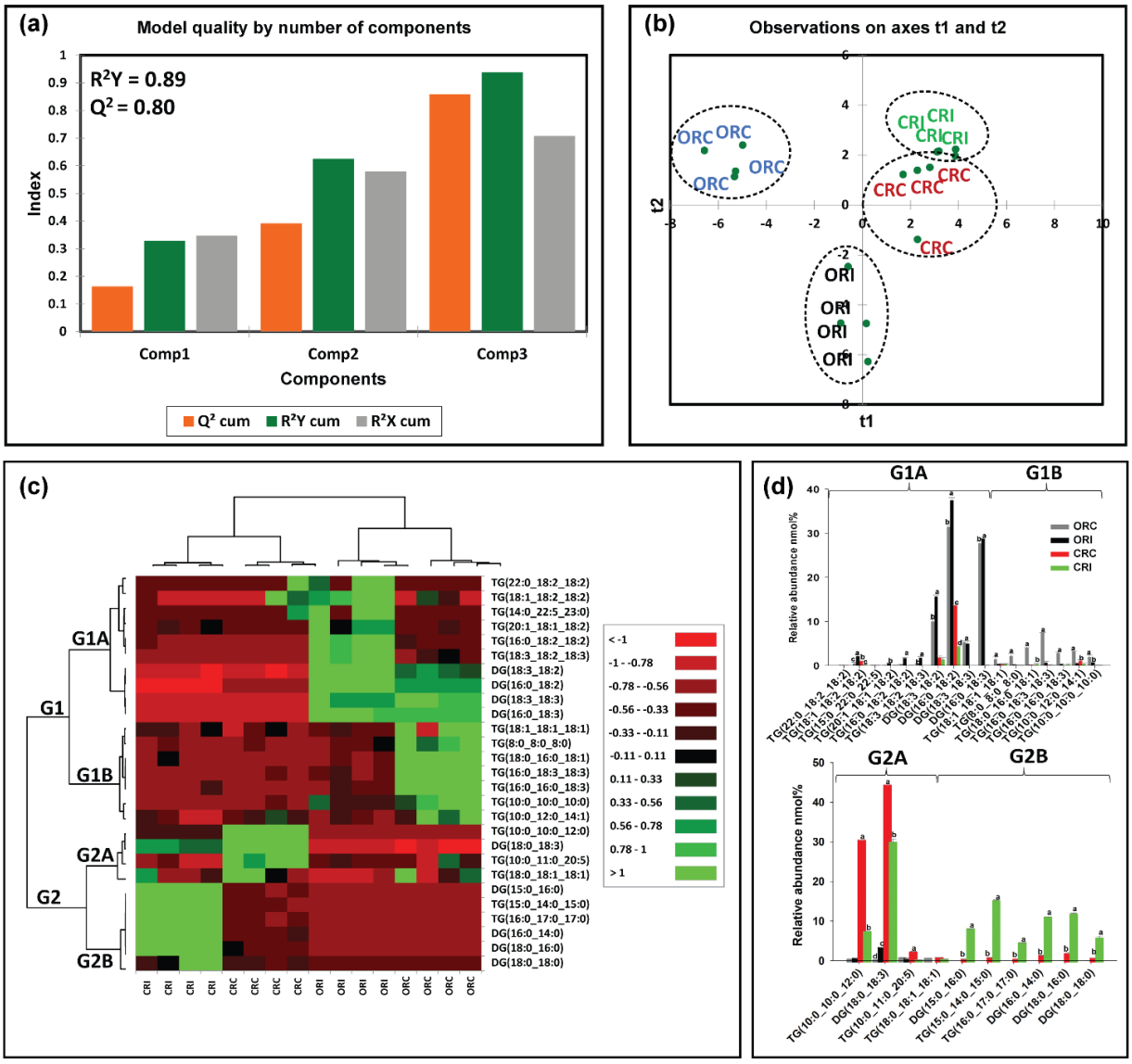

Fig. 3.4. Differences in root GL species in susceptible (OX760-6) and resistant (Conrad) soybean cultivars inoculated with *P. sojae* relative to control plants. (**a**) Model quality for partial least squares-discriminant analysis (PLS-DA); (**b**) Observation plot based upon differences in molecular species in root GL species of OX760-6 and Conrad cultivars; (**c**) Heat map demonstrating clusters of root GL species in OX760-6 and Conrad cultivars treated or untreated with *P. sojae*. Each cultivar and treatment were grouped separately using ascendant hierarchical cluster analysis based upon Euclidian distance at interquartile range of 0.15. The left columns denote the cluster segregated root GL species, while the above columns segregated soybean cultivars

based upon similarities in abundance. The abundance of root GL species is denoted using color: red for lower level, black for intermediate level, and green for higher level. Group 1 and 2 (G1 and G2) and subgroups (G1A, G1B, G2A and G2B) are root GL species that were accountable for the formation of clustered patterns in the heat map that were applied for determination of significant differences between the soybean cultivars (OX760-6 and Conrad) root GL species in each of the bar chart (Fig. 3.4d) beside the heat map; and (**d**) Bar charts describe the relative abundance of root GL species as a mean nmol% ± SE (n = 4). Significant differences between root GL species are indicate using letter a-d on top of the bars as described by Fisher's LSD multiple comparisons test using ANOVA ($\alpha = 0.05$). The G1 and G2, and G1A, G1B, G2A and G2B are root GL species that were accountable for the formation of clustered patterns in the heat map that were applied for the determination of significant differences between the soybean cultivars (OX760-6 and Conrad) root GL species as illustrated in the bar charts.

Likewise, the heat map clusters stem GL lipid molecular species into G1and G2, and sub-groups G1A, G1B, G2A and G2B. These groupings distinguished the susceptible cultivar from the tolerant cultivar in the stem GL molecular species. We observed stem GL lipid molecular species that belonged to G1A {TG(12:0/12:0/12:0), TG(10:0/10:0/14:0), TG(10:0/10:0/14:1), TG(18:3/18:3/18:3), TG(16:0/18:2/18:3), TG(18:2/18:2/18:3), DG(24:0/18:2), DG(22:0/18:2), DG(20:2/20:3), DG(16:0/18:3) TG(18:3/18:2/18:3), and DG(18:3/18:3)} did not change in the tolerant cultivar challenged with *P. sojae* relative to the control, but were significantly lower in the susceptible cultivar that had been infected (Fig. 3.5c). Lipid molecular species belonging to group G1B {TG(16:0/16:0/18:3), TG(16:0/18:3/18:3), TG(10:0/10:0/10:0), TG(8:0/8:0/8:0), TG(18:1/18:1/18:1), TG(18:1/18:1/18:2)} also did not differ among the tolerant cultivar, but were significantly higher in the susceptible cultivar that had been treated with the pathogen (Fig. 3.5c). In contrast, lipid molecular species belonging to group G2A {TG(16:0/18:2/18:2), TG(16:0/18:1/18:2), TG(10:0/10:0/12:0), TG(18:2/18:2/18:2), TG(15:0/18:2/18:3), TG(18:1/18:2/18:2), DG(16:0/18:1), and TG(16:0/16:0/18:2)} were significantly higher in the stem of the tolerant cultivar that had been challenged with the pathogen, but no significant differences were observed in the stem of susceptible cultivar (Fig. 3.5c). Finally, in G2B, the relative abundances of DG(20:0/22:0) and TG(10:0/10:0/14:1) were significantly lower in the stem of the tolerant cultivar when challenged with *P. sojae* but did not differ among the susceptible cultivar (Fig. 3.5c). These data are corroborated by Fig. 3.5d, which demonstrates the significant differences in the GL molecular species in the stem of tolerant and susceptible cultivars. In response to pathogen challenge, TG(12:0/12:0/12:0), TG(10:0/10:0/14:1), TG(16:0/18:2/18:3), TG(18:2/18:2/18:3), TG(16:0/18:2/18:2), TG(16:0/18:1/18:2), TG(10:0/10:0/12:0), TG(18:2/18:2/18:2), TG(15:0/18:2/18:3), TG(18:1/18:2/18:2), DG(16:0/18:1), and TG(16:0/16:0/18:2) were significantly higher in the stem of the tolerant cultivar while TG(10:0/10:0/14:0), DG(18:3/18:3), TG(16:0/16:0/18:3), TG(16:0/18:3/18:3), TG(18:3/18:2/18:3), TG(10:0/10:0/10:0), TG(8:0/8:0/8:0), TG(18:1/18:1/18:1), TG(18:1/18:1/18:2) and TG(16:0/16:0/18:2) were significantly higher in the stem of the susceptible cultivar in response to infection (Fig. 3.5d). These results showed that there were significantly higher levels of TG and DG

molecular species in root and stem of tolerant cultivar challenged with the pathogen compared to the stem of the susceptible cultivar following infection.

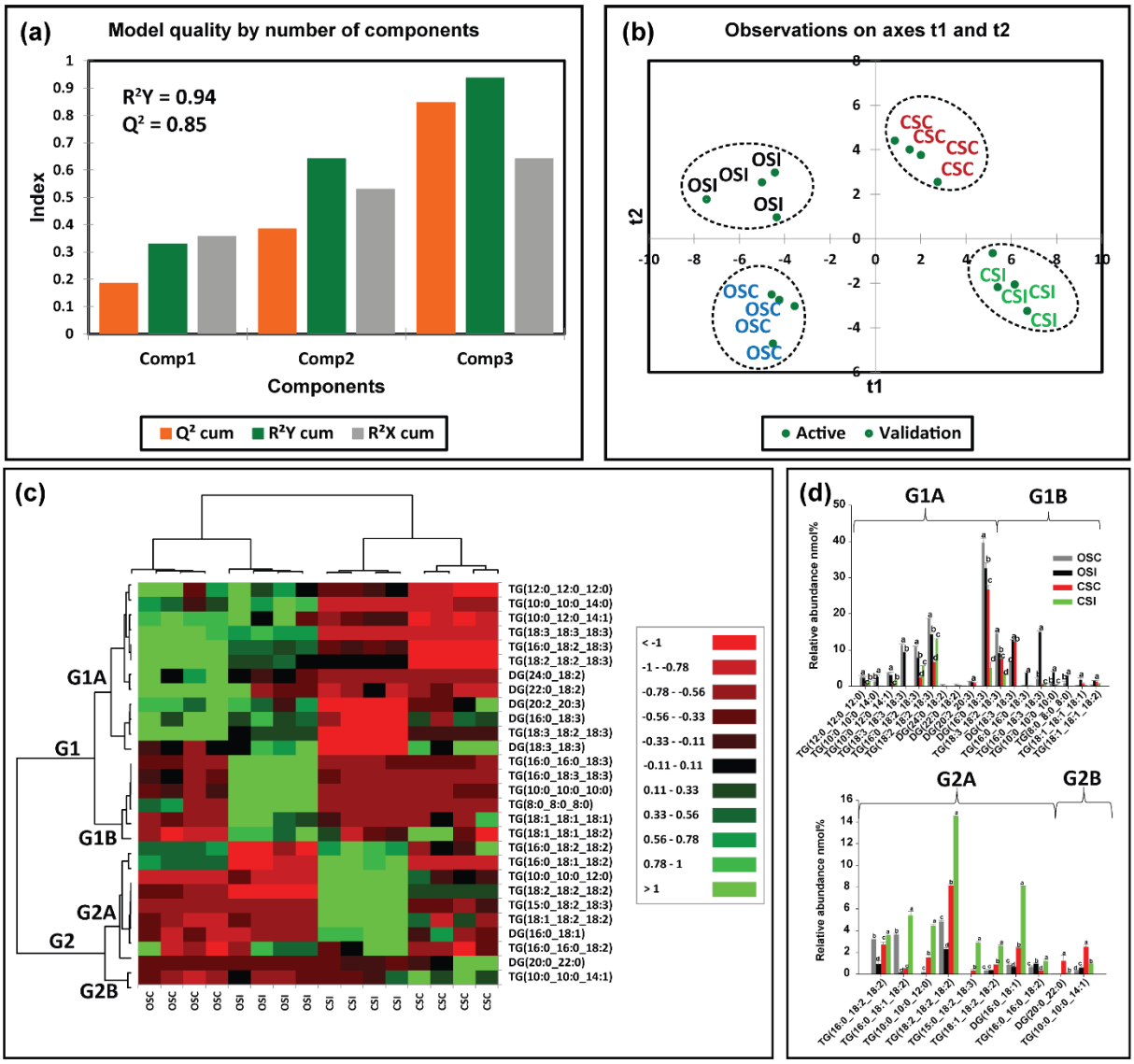

Fig. 3.5. Differences in stem GL species in susceptible (OX760-6) and resistant (Conrad) soybean cultivars inoculated with *P. sojae* relative to control plants. (**a**) Model quality for partial least squares-discriminant analysis (PLS-DA); (**b**) Observation plot based upon differences in molecular species in stem GL species of OX760-6 and Conrad cultivars; (**c**) Heat map demonstrating clusters of stem GL species in OX760-6 and Conrad cultivars treated or untreated with *P. sojae*. Each cultivar and treatment were grouped separately using ascendant hierarchical cluster analysis based upon Euclidian distance at interquartile range of 0.15. The left

columns denote the cluster segregated stem GL species, while the above columns segregated soybean cultivars based upon similarities in abundance. The abundance of stem GL species is denoted using color: red for lower level, black for intermediate level, and green for higher level. Group 1 and 2 (G1 and G2) and subgroups (G1A, G1B, G2A and G2B) are stem GL species that were accountable for the formation of clustered patterns in the heat map that were applied for determination of significant differences between the soybean cultivars (OX760-6 and Conrad) stem GL species in each of the bar chart (Fig. 3.5d) beside the heat map; and (**d**) Bar charts describe the relative abundance of stem GL species as a mean nmol% ± SE (n = 4). Significant differences between stem GL species are indicate using letter a-d on top of the bars as described by Fisher's LSD multiple comparisons test using ANOVA ($\alpha = 0.05$). The G1 and G2, and G1A, G1B, G2A and G2B are stem GL species that were accountable for the formation of clustered patterns in the heat map that were applied for the determination of significant differences between the soybean cultivars (OX760-6 and Conrad) stem GL species as illustrated in the bar charts.

3.4.4. Lipid biochemical network demonstrating from a system biology perspective how the tolerant and susceptible soybean cultivars respond to *P. sojae* infection

Lipid structural similarity networks were used to visualize changes in soybean root and stem lipids. For instance, the networks display three major clusters including top left (PSTs), top right (DGs and TGs containing saturated FAs), and bottom (a mixture of GPLs, DGs and TGs containing unsaturated FAs. CME 20:3 is the precursor for the biosynthesis of all the PSTs in the pathway presented, the level was significantly decrease resulting in downstream decrease in all unsaturated acylated hexocyl sitosterols. StE 18:3 had the biggest decrease in the ORC vs. ORI network of PST. In contrast, StE 18:3 increased several folds in CRC vs. CRI network, and it had the biggest increase. Generally, almost all the PSTs were decreased in the tolerant cultivar in response to infection. In the ORC vs ORI network, TG8:0/8:0/8:0, TG18:0/16:0/18:1, TG16:0/18:3/18:3, TG16:0/18:3/18:3 and TG16:0/16:0/18:3 are unique biomarkers differentiating the ORC vs. ORI while TG18:4/11:3/12:4 and DG18:0/18:0 were unique biomarkers differentiating CRC vs. CRI (Fig. 3.6). In OSC vs. OSI, StE 18:3 is a precursor for biosynthesis of all the PSTs, the level was significantly reduced leading upstream increase in all unsaturated acylated hexocyl sitosterols. AcHexSiE18:2 and AcHexSiE18:1 was increased several folds in CRC vs. CRI network. Similar to the root, almost all the PSTs in stem were reduced in the tolerant cultivar compared to the susceptible cultivar. In OSC vs. OSI, DG22:0/18:2 was the only unique biomarker differentiating OSC vs. OSI while in the CSC vs. CSI, TG12:0/12:0/12:0, TG16:0/16:0/18:2, TG10:0/10:0/14:1 and DG20:0/22:0 were unique biomarkers differentiating CSC vs. CSI (Fig. 3.7). In the ORI vs. CRI, TG10:0/10:0/10:0, TG(18:3/18:2/23:0), DG 18:3/18:3 and DG16:0/18:3 were unique biomarkers differentiating ORI vs. CRI and TG10:0/10:0/14:0 and DG24:0/18:2 were unique biomarkers differentiating OSI vs. CSI (Fig. 3.8). Lipid species that changed only within one of these comparisons when considering all other comparisons (root and stem combined) are denoted with hashed outlines and may identify unique markers representative of the biological changes between these groups (Supplemental Table 3.1).

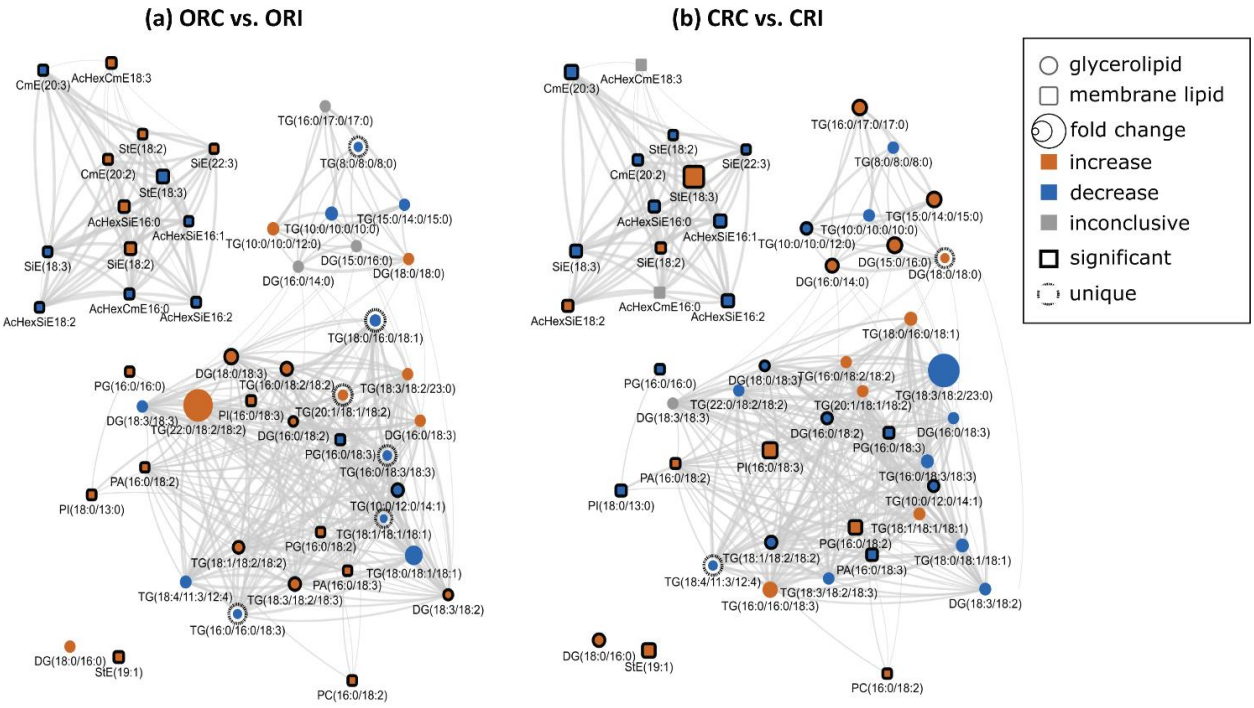

Fig. 3.6. Lipid biochemical network displaying differences in membrane lipids and GLs in the root of susceptible and resistant soybean cultivars inoculated with *P. sojae* relative to control plants. (**a**) Control susceptible soybean cultivar (ORC) versus inoculated (ORI); (**b**) control tolerant soybean cultivar (CRC) versus inoculated (CRI). The lipid biochemical network demonstrates fold differences in 22 root membrane lipid molecular species and 27 GL molecular species following inoculation with *P. sojae*. Lipid SMILES identifiers were used to calculate PubChem molecular fingerprints and structural similarities. Mapped networks, displaying significance of fold differences in lipids were calculated for all comparisons. Network visualizations display lipids connected based on structural Tanimoto similarity ≥ 0.8 (edge width: 0.8 to 1.0). Node size displays fold differences of means between comparisons and color shows the direction of change compared to control (orange: increased; blue: decreased; gray: inconclusive). Node shape displays lipid structural type (rounded square: membrane lipids; circle: GLs). Lipids displaying significant differences between treatment groups ($p \leq 0.05$) are denoted with black borders.

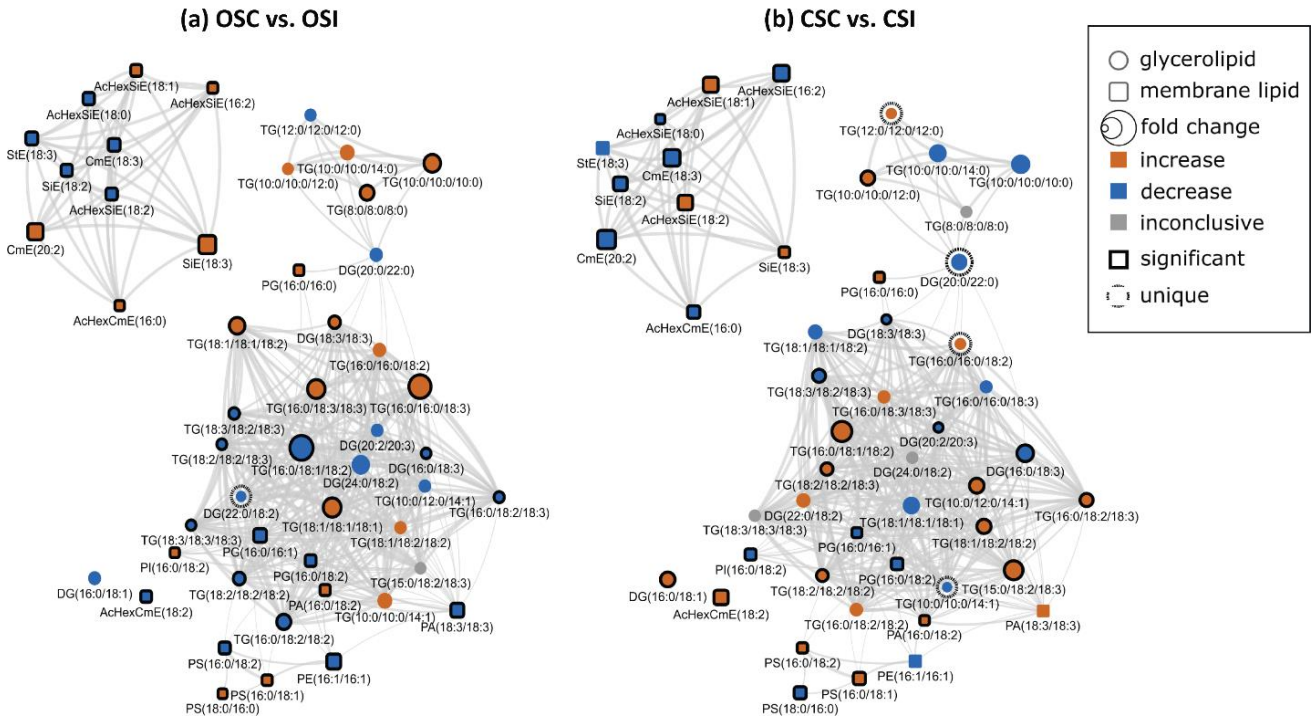

Fig. 3.7. Lipid structural similarity network displaying differences in stem membrane lipids and GLs in susceptible and resistant soybean cultivars inoculated with *P. sojae* relative to control plants. (**a**) Control susceptible soybean cultivar (OSC) versus inoculated (OSI); (**b**) control tolerant soybean cultivar (CSC) versus inoculated (CSI). The biochemical lipid network demonstrates fold differences in 21 stem membrane lipid molecular species and 28 GL molecular species following inoculation with *P. sojae*. Lipid SMILES identifiers were used to calculate PubChem molecular fingerprints and structural similarities. Mapped networks, displaying significance of fold differences in lipids were calculated for all comparisons. Network visualizations display lipids connected based on structural Tanimoto similarity ≥ 0.8 (edge width: 0.8 to 1.0). Node size displays fold differences of means between comparisons and color shows the direction of change compared to control (orange: increased; blue: decreased; gray: inconclusive). Node shape displays lipid structural type (rounded square: membrane lipids; circle: GLs). Lipids displaying significant differences between treatment groups ($p \leq 0.05$) are denoted with black borders.

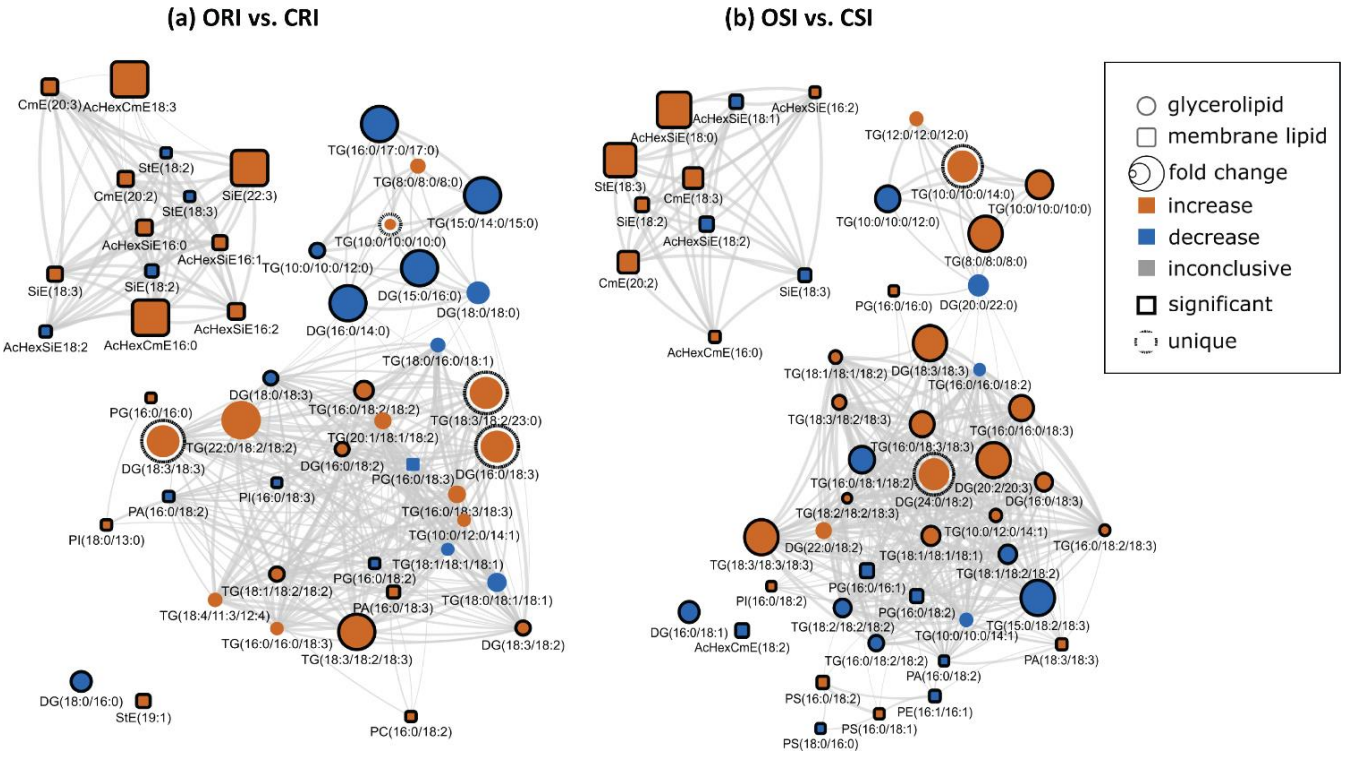

Fig. 3.8. Lipid structural similarity network displaying differences in root and stem membrane lipids and GLs in susceptible and resistant soybean cultivars inoculated with *P. sojae*. (**a**) Lipids from inoculated root tissue of susceptible (ORI) versus tolerant (CRI) soybean cultivars inoculated with *P. sojae*; and (**b**) Lipids from inoculated stem tissue of susceptible (OSI) versus tolerant (CSI) soybean cultivars inoculated with *P. sojae*. The biochemical lipid network demonstrates fold changes in 22 root membrane lipid molecular species and 27 GL molecular species, and 21 stem membrane lipid molecular species and 28 GL molecular species following inoculation with *P. sojae*. Lipid SMILES identifiers were used to calculate PubChem molecular fingerprints and structural similarities. Mapped networks, displaying significance of fold differences in lipids were calculated for all comparisons. Network visualizations display lipids connected based on structural Tanimoto similarity ≥ 0.8

(edge width: 0.8 to 1.0). Node size displays fold differences of means between comparisons and color shows the direction of change compared to control (orange: increased; blue: decreased; gray: inconclusive). Node shape displays lipid structural type (rounded square: membrane lipids; circle: GLs). Lipids displaying significant differences between treatment groups ($p \leq 0.05$) are denoted with black borders.

3.5. Discussion

As essential components of cellular membranes, lipids are involved in various physiological roles including as structural components of cellular membranes, cell signaling, storage of energy, and membrane trafficking. In plants, alterations in lipid composition have been reported in response to pathogenic stress conditions (Nurul Islam, Chambers, & Ng, 2012). Biotic stress have been reported to profoundly alter the lipidome in plants (D. Kim, Jeannotte, Welti, & Bockus, 2013). Additionally, Ferrer et al. (2017) demonstrated that alterations in the relative composition of PSTs in cellular membranes affect their biophysical properties and hence their physiological functions. The results describe here indicate how lipid mediated plant immunity in both a resistant and a susceptible soybean cultivar in response to *P. sojae* infection. Specifically, in the pathogen-infected soybeans, we observed significantly higher levels of major GPLs and GLs (DGs and TGs) in the tolerant cultivar, whereas PSTs (StEs and CmEs) were found to be higher in quantity in the susceptible cultivar. More interestingly, these classes of lipids varied in a similar manner in the root and stem of each cultivar in response to pathogen infection, which is in line with eggplants in the literature (D. Kim et al., 2013; Naguib, 2019; Shah, 2005). For example, similar trends were observed for the lipidome of eggplants (*Solanum melongena*) resistant to Fusarium wilt infection (Naguib, 2019), demonstrating the significant difference in the levels of lipid metabolites and response of the susceptible and tolerant eggplants to Fusarium disease. This further illustrate the importance of lipid mediated plant immune response as an important component of the successful strategy used to fight infection in this pathosystem (Naguib, 2019).

The biosynthesis and lipid composition of cellular membranes play an essential role in the physiological functioning of plants (Reszczyńska & Hanaka, 2020). During growth, plants adapt to adverse stress conditions through the remodelling of lipid membranes resulting from alterations in the fatty acid content and, consequently, the biosynthesis of lipids (Reszczyńska & Hanaka, 2020). Several studies have demonstrated that high levels of

lipid remodeling in plant membrane lipids under different adverse conditions result in resistance to environmental stressors (Reszczyńska & Hanaka, 2020).

Our results clearly show that there are differences in both membrane and storage lipid metabolism in resistant and susceptible soybean cultivars in response to *P. sojae* infection. For instance, we observed higher levels of 18:2 and 18:3 fatty acyl-enriched phospholipid and sterol molecular species in the membrane lipids of the root and stem from the tolerant cultivar when challenged with the pathogen, in contrast to lower C18:2 and C18:3-enriched molecular species in tissues from the susceptible cultivar (Fig. 3.2, 3.3). Fatty acids like C18:2, C18:3 and C18:1 are major and important constituents of cellular membranes that provide structural integrity, energy for different metabolic processes, and also associate with defense signaling during host pathogen interaction (Lim et al., 2017). For instance, increased levels of certain FAs like C18:2 and C18:3 appeared to play a role in enhance plant immunity and higher resistance in soybean tolerance to *P. sojae* and improved quantitative resistance or plant protection in this soybean-*P. sojae* pathosystem. In contrast, the StEs were significantly higher in the root and stem from the susceptible cultivar challenged with *P. sojae* infection but were significantly lower in the susceptible control plants and in the tolerant \cultivar under both treatment conditions (Table 3.1, 3.2; Fig. 3.2, 3.3). This is in agreement with a recent study which demonstrated the role of sterols in disease resistance (Kopischke et al., 2013). In addition, studies have shown that oomycete *P. sojae* is lacking sterols and therefore obtain the exogenous sterols for the normal life cycle from the colonized host plants (Gamir et al., 2017). Stigmasterol ester was identified as a factor of susceptibility in *Arabidopsis*, as inhibition of its biosynthesis resulted in increased resistance to *Pseudomonas syringae* (Griebel & Zeier, 2010; Kopischke et al., 2013). Another report indicated that C22 desaturation of the main phytosterol, β-sitosterol, in *Arabidopsis* through the enzyme CYP710A1, and the associated stigmasterol accumulation, are important metabolic activities in *P. syringae*-inoculated leaves of *Arabidopsis* that can increase susceptibility (Griebel & Zeier, 2010). The formation of stigmasterol in leaves is induced by recognition of bacterial pathogen-associated molecular patterns and

synthesis of reactive oxygen species, but is independent of the jasmonic acid, salicylic acid or ethylene-associated signalling pathways (Griebel & Zeier, 2010). Through analysis of mutants and application of exogenous sterol, it was demonstrated that an increase in the ratio of stigmasterol to β-sterol in leaves reduces specific defence responses in *Arabidopsis*, and consequently makes the plants more susceptible to *P. syringae* (Adigun et al., 2020; Wang et al., 2012). These were in line with the results obtained in this study, and these modes of action may account for the higher resistance of the tolerant cultivar to pathogen infection.

Pathogenic fungi can secrete various extracellular enzymes that are involved in pathogenicity (Subramoni, Suárez-Moreno, & Venturi, 2010). For example, secreted lipases from fungal pathogens are involved in the penetration of plant barriers such as the wax cuticle. Likewise, internal fungal lipases are capable of degrading storage lipids and/or signaling via the release of secondary messengers. The significant decrease in the TG molecular species in the soybean susceptible cultivar could be as a result of increased lipase activity during infection. Lipases hydrolyze carboxyl esters in TGs and liberate FAs and glycerol (Watt & Steinberg, 2008). This is in agreement with the fact that lipases appear to function as virulence factors in plant pathogens. Interestingly, in this study, the tolerant cultivar demonstrated significantly higher DG levels in response to pathogen infection, but there was no observed difference in TG levels. This is in agreement with the fact that DGs are primarily derived either from TGs through TG lipases or PAs by phospholipase activity (Bates & Browse, 2012). However, it has also been reported that DG levels in a tolerant eggplant cultivar can be generated by the activity of phospholipase on PAs, and not only the activity of TG lipases (Naguib, 2019).

The lipid biochemical network demonstrated significant alterations in lipid metabolism in both cultivars in response to *P. sojae* infection. The head group and FA composition of complex lipids are a useful proxy for localization and biological function (Casares, Escribá, & Rosselló, 2019). Networks display increased density in connectivity between biochemically related groups of lipids and the lipid biosynthesis metabolism pathway in the tolerant soybean cultivar as defense response to pathogen inversion. Generally, there is dearth of

information on the role of lipid metabolism in determining either incompatible or compatible interactions in the soybean-*P sojae* pathosystem during host-pathogen interaction. The unique biomarkers between the susceptible and tolerant cultivars including the production of DG molecular species, which was well pronounced in tolerant cultivar than susceptible (Figs. 3.6, 3.7 and 3.8). Studies have demonstrated that signaling enzymes, DG kinases (DGKs) play important roles in response to biotic stress by phosphorylating DG to synthesis PA (Fig. 3.9) and both PA and DG are lipid mediators during physiological process (Yuan, Kim, Deng, Hong, & Wang, 2019). Our findings from this study demonstrate that lipid metabolism and signalling possibly involving DG could play a significant role in pathogen resistance in the tolerant soybean cultivar. Also, DG signally related to TG hydrolysis which was differentially demonstrated between susceptible and tolerant soybean cultivars when challenged with pathogen (Figs 3.6, 3.7 and 3.8). Study has demonstrated that TG is accumulated in plant tissues due to TG turnover, as a result of disruption of SUGAR-DEPENDENT1, a cytosolic lipase accountable for TG hydrolysis in lipid droplets into free FAs and DG and consequently enhance TG accumulation in plant tissues (Kelly et al., 2013). Fan et al (2017) demonstrated that TG accumulation plays important role, thus buffering homeostasis of lipid and protecting plant cells against lipotoxic death during plant immune response to pathogen invasion.

Phytosterols also known to play important role in plant innate immunity against pathogen attack (Wang et al., 2012). However, the odd chain FAs that appear in the soybean lipid profile are usually and maybe fungal origin and they are mainly unique to the soybean challenged with *P. sojae* (Řezanka, Kolouchová, & Sigler, 2015). The extracted ion chromatograms of the odd chain FAs are shown in Fig. S3.1 and MS^2 spectrum of *m/z* 856.73 identified as TG 15:0/18:2/18:3 $[M+NH_4]^+$ is depicted in Fig. S3.2. The membrane and neutral lipids identified in mycelium of *P. sojae* are shown in Fig. S3.3.

Lipid biosynthesis in soybean cultivars follow common routes where FAs are generated from plastid, transported to the endoplasmic reticulum (ED) (H. U. Kim, 2020), which starts with the addition of fatty acyl-

CoA leading to biosynthesis of lysophosphatidic acid (LPA) and the reaction is catalyzed by glycerol phosphate acyltransferase (GPAT) and is a rate limiting-step for PA biosynthesis. In ED, PA biosynthesis occurs by addition of fatty acyl-CoA to LPA via lysophosphatidic acid acyltransferase (LPAAT) to form central precursor PA by which several GPLs are synthesized (Fig. 3.9). The first step in GPLs biosynthesis involves the hydrolysis of the phosphate group from PA to generate DG by phosphatidic acid phosphatase (PAP). The resulting DG is later phosphorylated by DGKs to PA, which is subsequently reused in biosynthesis of GPLs. Also, DG acts as a precursor for biosynthesis of primary form of storage energy, TG. The isopentenyl diphosphate (IPP) and dimethylallyl pyrophosphate (DMAPP) generated via cytosolic mevalonate (MVA) pathway are primarily used for the biosynthesis of PSTs (Lohr, Schwender, & Polle, 2012; Vriese, Pollier, Goossens, Beeckman, & Vanneste, 2019). Our results demonstrate novel information about pathogen-stress responses in the root and stem of both soybean cultivars, which can be put within the broad context of plant lipid metabolism. The metabolic pathway of relative abundance of GPL, PST and GL biosynthesized in the root and stem of the susceptible and tolerant soybean cultivars when challenged with *P. sojae* are demonstrated in Fig. 3.9. These lipid classes could be used as biomarkers for disease resistance or susceptibility by soybean cultivars. Based on our understanding, this is the first report of lipid alteration in soybean root and stem in response to *P. sojae* infection.

(a) Proposed lipid mediated plant immunity in soybean roots

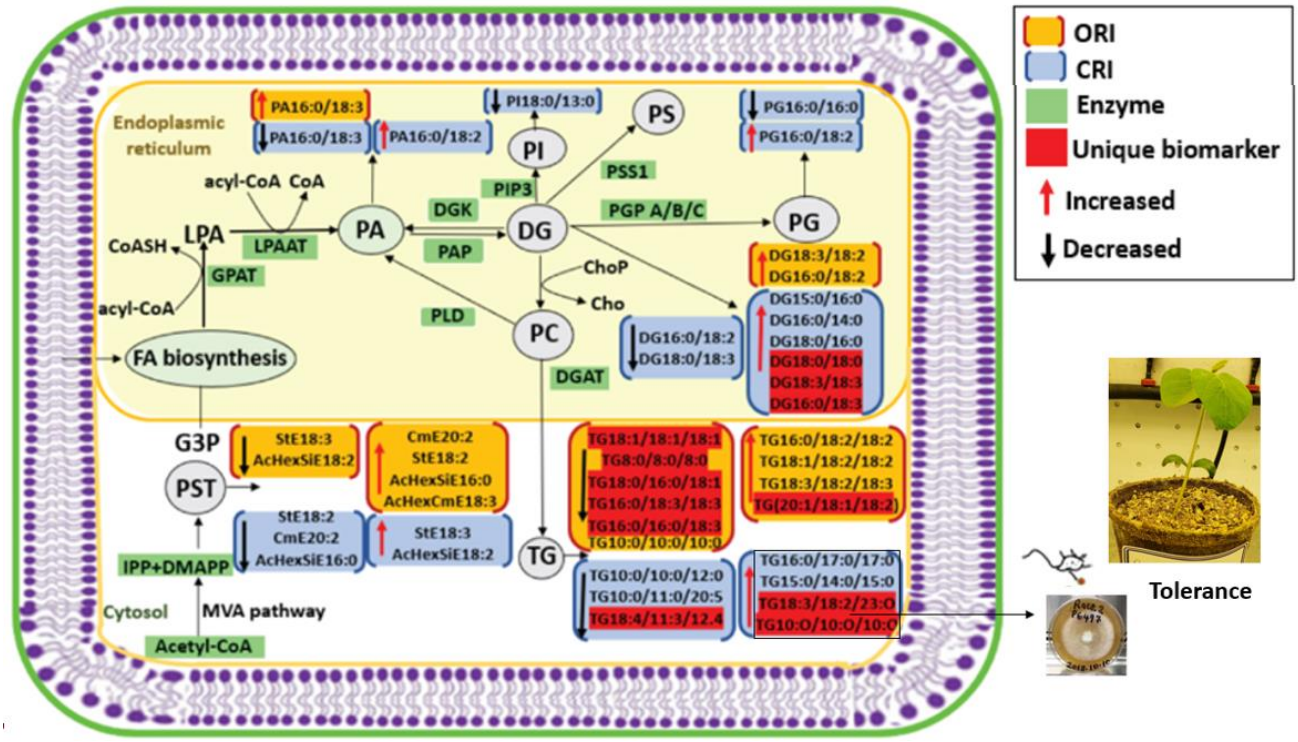

(b) Proposed lipid mediated plant immunity in soybean stems

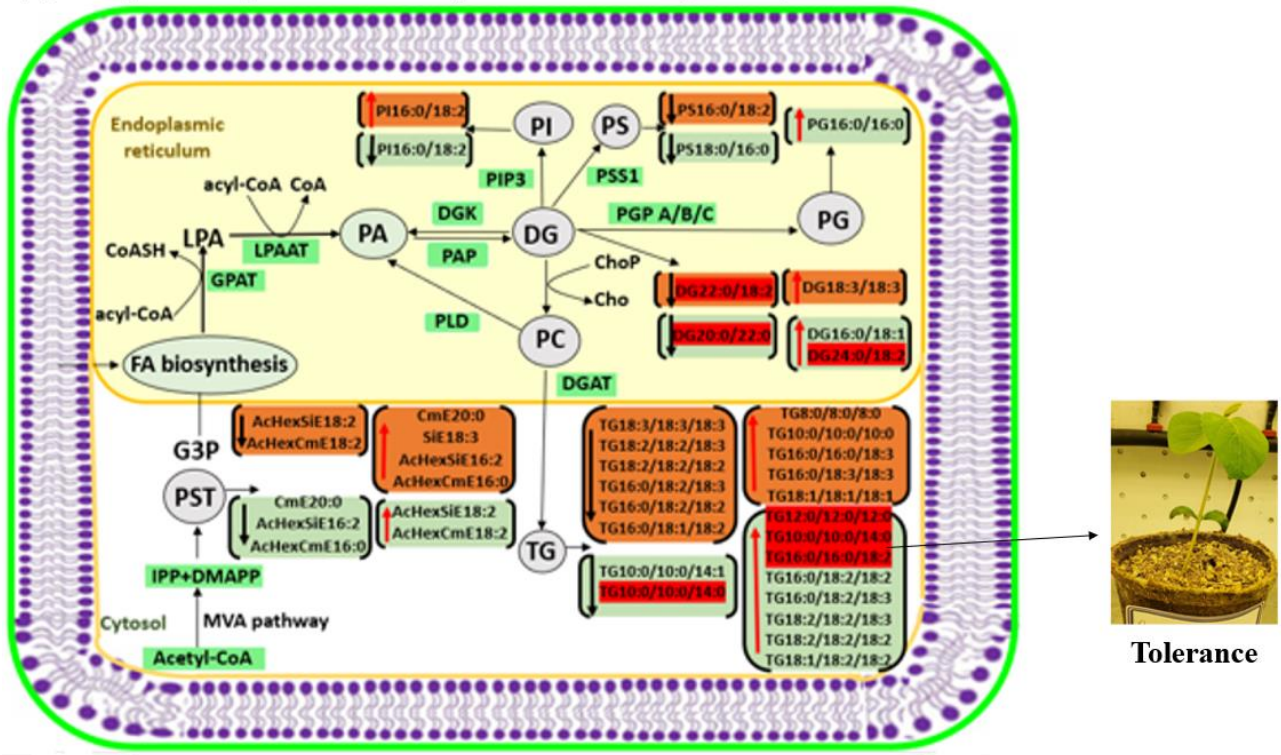

Fig. 3.9. Proposed lipid metabolism pathways suggesting the mechanism that maybe associated with the altered lipidome and disease tolerance or susceptibility in soybean cultivars (OX760-6 and Conrad) following inoculation with *P. sojae*. (a) The most significantly altered root lipids in soybean cultivars (OX760 and Conrad) in response to colonization and infection with *P.sojae*: and (b) The most significantly altered stem lipids in soybean cultivars (OX760 and Conrad) in response to *P. sojae* colonization and infection. In the Kennedy pathway fatty acyl-CoA and coenzyme A begins with the sequential acylation of GPATs and LPAATs utilizing fatty acyl-CoA to biosynthesis the central precursor PA through which other downstream GPLs are produced. GLPs are produced through hydrolysis of the phosphate group in PA, and this PA then dephosphorylated through PAP to generate DG. The DG acts as a precursor for biosynthesis of TG via DGAT or PDAT transferring the sn-2 fatty acyl group from GPLs to DG, producing TG. Biosynthesis of IPP and DMAPP through mevalonate (MVA) pathway, and they act as precursors for phytosterol synthesis. The altered lipidome observed in this study suggest DG and PA mediated lipid signalling impacting phytosterol anabolism appears to be the strategy used by tolerant soybean cultivars to successfully limit infection and colonization by *P.sojae*. The following molecular species are suggested as unique lipid biomarkers in the ORI vs CRI and CSI vs OSI networks that could potentially discriminate tolerance interations in the soybean-P.sojae pathosystem: TG(18:3/18:2/23:0), TG(10:0/10:0/10:0), TG(10:0/10:0/14:0), DG(18:3/18:3), DG(16:0/18:3) and DG(24:0/18:2). PLD = phospholipase D, DGK = diacylglycerol kinase, LPAAT = lysophosphatidic acid acylteransferase, PAP = phosphatic acid phosphatase, G3P = glycerol-3-phosphate, DGAT = diacylglycerol acyltranferase, GPAT = Glycerol-3-phosphate acyltransferase, PDAT = phospholipid:diacylglycerol acyltransferases, PSS1 = phosphatidylserine synthase-1, PGP = glycerol-3-phosphate phosphatase, PAP = phosphatidic acid phosphatase, IPP = isopentenyl pyrophosphate, DMAPP = dimethylallyl pyrophosphate, MVA = mevalonic acid, PIP3 =1-phosphatidylinositol-4-phosphate 5-kinase, CoASH = coenzyme A, Chop = cholinephosphotransferase and cho = choline. ORI = root of susceptible inoculated, CRI = root of tolerant inoculated, OSI = stem of susceptible inoculated, CSI = stem of tolerant inoculated, GPLs =

glycerophospholipids, GLs = glycerolipids, LPA = lysophosphatidic, PA = phosphatidic acid, PC = phosphatidylcholine, PG = phosphatidyl glycerol, PI = phosphatidylinositol, PS = phosphatidylserine, DG = diacylglycerol, TG = triacylglycerol and PST = phytosterols.

3.6. Conclusion

The results demonstrate a novel mechanism to engineer soybean cultivars for wide spectrum disease susceptibility or resistance due to FAs metabolism or lipid mediated plant immunity that plays a vital role in defense response against pathogens inversion. Both soybean cultivars altered lipid biosynthesis upon infection by *P. sojae*. Induced accumulation of phytosterol such as CmE20:2, StE18:2, AcHexSiE16:0, AcHexCmE18:3 in the susceptible soybean cultivar was associated with higher levels of pathogens and then improved disease susceptibility whereas induced accumulation and overall increase in GPLs and GLs such as PA16:0/18:2, PG16:0/18:2) and glycerolipids (DG18:0/18:0, DG18:3/18:3, DG16:0/18:3, DG16:0/14:0, DG18:0/16:0, DG15:0/16:0, TG10:0/10:0/10:0, TG16:0/18:2/18:3, TG18:1/18:2/18:2, TG18:3/18:2/18:3, TG20:1/18:1/18:2 and TG18:3/18:2/23:0) in tolerant soybean cultivar enhance plant immunity against pathogen. Glycerophospholipids strengthen the cellular membrane and protect plant cells from various infections while DGs mainly act as signalling molecules during response to various environmental stresses. The altered lipidome observed in this study suggest DG and PA mediated lipid signalling impacting PST anabolism appears to be the strategy used by tolerant soybean cultivar to successfully limit infection and colonization by *P.sojae*. The following molecular species are suggested as unique lipid biomarkers in the networks that could potentially discriminate tolerance interactions in the soybean-*P.sojae* pathosystem: ORC vs ORI {TG(20:1/18:1/18:2), TG(18:1/18:1/18:1), TG(8:0/8:0/8:0), TG(18:0/16:0/18:1), TG(16:0/18:3/18:3), TG(16:0/16:0/18:3)}; CRC vs CRI {TG(18:4/11:3/12:4), DG18:0/18:0}; OSC vs OSI {DG22:0/18:2}; CSC vs CSI {TG(12:0/12:0/12:0), TG(16:0/16:0/18:2), TG(10:0/10:0/14:0), DG20:0/22:0}; ORI vs CRI {TG(18:3/18:2/23:0, TG(10:0/10:0/10:0),

DG(18:3/18:3), DG(16:0/18:3)} and CSI vs OSI {TG(10:0/10:0/14:0), DG(24:0/18:2)}. To understand the exact roles of these plant lipids in membrane permeability and as signaling molecules warrant further studies.

3.7. References

Adigun, O. A., Nadeem, M., Pham, T. H., Jewell, L. E., Cheema, M., & Thomas, R. (2020). Recent advances in bio-chemical, molecular and physiological aspects of membrane lipid derivatives in plant pathology. *Plant, Cell & Environment, 44*(1), 1-16.

Ali, U., Li, H., Wang, X., & Guo, L. (2018). Emerging Roles of Sphingolipid Signaling in Plant Response to Biotic and Abiotic Stresses. *Mol Plant, 11*(11), 1328-1343.

Bandara, A. Y., Weerasooriya, D. K., Liu, S., & Little, C. R. (2019). Host lipid alterations after *Macrophomina phaseolina* infection contribute to charcoal rot disease susceptibility in grain sorghum: Evidence from transcriptomic and lipidomic data. *bioRxiv*, 854067.

Bates, P. D., & Browse, J. (2012). The significance of different diacylgycerol synthesis pathways on plant oil composition and bioengineering. *Front Plant Sci, 3*, 147.

Berkey, R., Bendigeri, D., & Xiao, S. (2012). Sphingolipids and plant defense/disease: the "death" connection and beyond. *Frontiers in Plant Science, 3*, 68-68.

Brackin, R., Atkinson, B. S., Sturrock, C. J., & Rasmussen, A. (2017). Roots-eye view: Using microdialysis and microCT to non-destructively map root nutrient depletion and accumulation zones. *Plant, Cell & Environment, 40*(12), 3135-3142.

Canonne, J., Froidure-Nicolas, S., & Rivas, S. (2011). Phospholipases in action during plant defense signaling. *Plant Signaling & Behavior, 6*(1), 13-18.

Casares, D., Escribá, P. V., & Rosselló, C. A. (2019). Membrane lipid composition: Effect on membrane and organelle structure, function and compartmentalization and therapeutic avenues. *International Journal of Molecular Sciences, 20*(9), 2167.

Chapman, K. D., Dyer, J. M., & Mullen, R. T. (2012). Biogenesis and functions of lipid droplets in plants: Thematic Review Series: Lipid Droplet Synthesis and Metabolism: from Yeast to Man. *Journal of lipid research, 53*(2), 215-226.

Christensen, S. A., & Kolomiets, M. V. (2011). The lipid language of plant-fungal interactions. *Fungal Genet Biol, 48*(1), 4-14.

Dangl, J. L., Horvath, D. M., & Staskawicz, B. J. (2013). Pivoting the plant immune system from dissection to deployment. *Science, 341*(6147), 746-751.

Dong, W., Lv, H., Xia, G., & Wang, M. (2012). Does diacylglycerol serve as a signaling molecule in plants? *Plant signaling & behavior, 7*(4), 472-475.

Dorrance, A. E., McClure, S. A., & St. Martin, S. K. (2003). Effect of partial resistance on Phytophthora stem rot incidence and yield of soybean in Ohio. *Plant Disease, 87*(3), 308-312.

Ellis, M. L., Wang, H., Paul, P. A., St. Martin, S. K., McHale, L. K., & Dorrance, A. E. (2012). Identification of soybean genotypes resistant to Fusarium graminearum and genetic mapping of resistance quantitative trait loci in the cultivar Conrad. *Crop Science, 52*(5), 2224-2233.

Fan, J., Yu, L., & Xu, C. (2017). A Central Role for Triacylglycerol in Membrane Lipid Breakdown, Fatty Acid β-Oxidation, and Plant Survival under Extended Darkness *Plant physiology, 174*(3), 1517-1530.

Ferrer, A., Altabella, T., Arró, M., & Boronat, A. (2017). Emerging roles for conjugated sterols in plants. *Prog Lipid Res, 67*, 27-37.

Fletcher, J., Bender, C., Budowle, B., Cobb, W. T., Gold, S. E., Ishimaru, C. A., . . . Tolin, S. A. (2006). Plant pathogen forensics: Capabilities, needs, and recommendations. *Microbiology and Molecular Biology Reviews, 70*(2), 450-471.

Gamir, J., Darwiche, R., Van't Hof, P., Choudhary, V., Stumpe, M., Schneiter, R., & Mauch, F. (2017). The sterol-binding activity of pathogenesis-related protein1 reveals the mode of action of an antimicrobial protein. *The Plant Journal, 89*(3), 502-509.

Gao, Q. M., Yu, K., Xia, Y., Shine, M. B., Wang, C., Navarre, D., . . . Kachroo, P. (2014). Mono- and digalactosyldiacylglycerol lipids function nonredundantly to regulate systemic acquired resistance in plants. *Cell Rep, 9*(5), 1681-1691. doi:10.1016/j.celrep.2014.10.069

Garay, L. A., Boundy-Mills, K. L., & German, J. B. (2014). Accumulation of High-Value Lipids in Single-Cell Microorganisms: A Mechanistic Approach and Future Perspectives. *Journal of Agricultural and Food Chemistry, 62*(13), 2709-2727.

Goufo, P., & Cortez, I. (2020). A Lipidomic analysis of leaves of esca-affected grapevine suggests a role for galactolipids in the defense response and appearance of foliar symptoms. *Biology, 9*(9), 268.

Grapov, D., Wanichthanarak, K., & Fiehn, O. (2015). MetaMapR: pathway independent metabolomic network analysis incorporating unknowns. *Bioinformatics (Oxford, England), 31*(16), 2757-2760.

Grau, C., Dorrance, A., Bond, J., Russin, J., Boerma, H., & Specht, J. (2004). Soybeans: improvement, production, and uses: American Society of Agronomy, Crop Science Society of America, Soil Science ….

Griebel, T., & Zeier, J. (2010). A role for β-sitosterol to stigmasterol conversion in plant–pathogen interactions. *The Plant Journal, 63*(2), 254-268.

Guha, R. (2007). Chemical Informatics Functionality in R. *Journal of Statistical Software, 18*(5), 1-16.

Han, Y., Teng, W., Yu, K., Poysa, V., Anderson, T., Qiu, L., . . . Li, W. (2008). Mapping QTL tolerance to Phytophthora root rot in soybean using microsatellite and RAPD/SCAR derived markers. *Euphytica, 162*(2), 231-239.

Hannun, Y. A., & Obeid, L. M. (2018). Sphingolipids and their metabolism in physiology and disease. *Nature reviews. Molecular cell biology, 19*(3), 175-191.

Heung, L. J., Luberto, C., & Del Poeta, M. (2006). Role of sphingolipids in microbial pathogenesis. *Infection and immunity, 74*(1), 28-39.

Jeanne Dit Fouque, D., Maroto, A., & Memboeuf, A. (2018). Internal standard quantification using tandem mass spectrometry of a tryptic peptide in the presence of an isobaric interference. *Analytical Chemistry, 90*(24), 14126-14130.

Kelly, A. A., van Erp, H., Quettier, A.-L., Shaw, E., Menard, G., Kurup, S., & Eastmond, P. J. (2013). The SUGAR-DEPENDENT1 Lipase Limits Triacylglycerol Accumulation in Vegetative Tissues of Arabidopsis *Plant physiology, 162*(3), 1282-1289.

Kim, D., Jeannotte, R., Welti, R., & Bockus, W. W. (2013). Lipid profiles in wheat cultivars resistant and susceptible to tan spot and the effect of disease on the profiles. *Phytopathology, 103*(1), 74-80.

Kim, H. U. (2020). Lipid Metabolism in Plants. *Plants (Basel, Switzerland), 9*(7), 871.

Kopischke, M., Westphal, L., Schneeberger, K., Clark, R., Ossowski, S., Wewer, V., . . . Rosahl, S. (2013). Impaired sterol ester synthesis alters the response of *Arabidopsis thaliana* to *Phytophthora infestans*. *The Plant Journal, 73*(3), 456-468.

Laxalt, A. M., & Munnik, T. (2002). Phospholipid signalling in plant defence. *Curr Opin Plant Biol, 5*(4), 332-338.

Lee, S., Mian, M. A. R., McHale, L. K., Wang, H., Wijeratne, A. J., Sneller, C. H., & Dorrance, A. E. (2013). Novel quantitative trait loci for partial resistance to *Phytophthora sojae* in soybean PI 398841. *TAG. Theoretical and applied genetics. Theoretische und angewandte Genetik, 126*(4), 1121-1132.

Lim, G.-H., Singhal, R., Kachroo, A., & Kachroo, P. (2017). Fatty Acid– and lipid-mediated signaling in plant defense. *Annual Review of Phytopathology, 55*(1), 505-536.

Lohr, M., Schwender, J., & Polle, J. E. W. (2012). Isoprenoid biosynthesis in eukaryotic phototrophs: A spotlight on algae. *Plant Science, 185-186*, 9-22.

Matemilola, S., & Elegbede, I. (2017). The challenges of food security in Nigeria. *Open Access Library Journal, Vol.04No.12*, 22.

Mc Carthy, U., Uysal, I., Badia-Melis, R., Mercier, S., O'Donnell, C., & Ktenioudaki, A. (2018). Global food security – Issues, challenges and technological solutions. *Trends in Food Science & Technology, 77*, 11-20.

Murphy, D. J. (2012). The dynamic roles of intracellular lipid droplets: from archaea to mammals. *Protoplasma, 249*(3), 541-585.

Nadeem, M., Pham, T. H., Nieuwenhuis, A., Ali, W., Zaeem, M., Ashiq, W., . . . Thomas, R. (2019). Adaptation strategies of forage soybeans cultivated on acidic soils under cool climate to produce high quality forage. *Plant Science, 283*, 278-289.

Nadeem, M., Thomas, R., Adigun, O., Manful, C., Wu, J., Pham, T. H., . . . Cheema, M. (2020). Root membrane lipids as potential biomarkers to discriminate silage-corn genotypes cultivated on podzolic soils in boreal climate. *Physiologia Plantarum, 170*(3), 440-450.

Naguib, D. M. (2019). Comparative lipid profiling for studying resistance mechanism against *Fusarium wilt*. *Physiological and Molecular Plant Pathology, 108*, 101421.

Nurul Islam, M., Chambers, J. P., & Ng, C. K. Y. (2012). Lipid profiling of the model temperate grass, *Brachypodium distachyon*. *Metabolomics, 8*(4), 598-613.

Pham, T. H., Zaeem, M., Fillier, T. A., Nadeem, M., Vidal, N. P., Manful, C., . . . Thomas, R. H. (2019). Targeting Modified Lipids during Routine Lipidomics Analysis using HILIC and C30 Reverse Phase Liquid Chromatography coupled to Mass Spectrometry. *Scientific Reports, 9*(1), 5048.

Raffaele, S., Leger, A., & Roby, D. (2009). Very long chain fatty acid and lipid signaling in the response of plants to pathogens. *Plant signaling & behavior, 4*(2), 94-99.

Ravipati, S., Baldwin, D. R., Barr, H. L., Fogarty, A. W., & Barrett, D. A. (2015). Plasma lipid biomarker signatures in squamous carcinoma and adenocarcinoma lung cancer patients. *Metabolomics, 11*(6), 1600-1611.

Reszczyńska, E., & Hanaka, A. (2020). Lipids composition in plant membranes. *Cell Biochemistry and Biophysics, 78*(4), 401-414.

Řezanka, T., Kolouchová, I., & Sigler, K. (2015). Precursor directed biosynthesis of odd-numbered fatty acids by different yeasts. *Folia Microbiologica, 60*(5), 457-464.

Rocha, J., Nitenberg, M., Girard-Egrot, A., Jouhet, J., Maréchal, E., Block, M. A., & Breton, C. (2018). Do galactolipid synthases play a key role in the biogenesis of chloroplast membranes of higher plants? *Frontiers in Plant Science, 9*(126).

Röös, E., Bajželj, B., Smith, P., Patel, M., Little, D., & Garnett, T. (2017). Greedy or needy? Land use and climate impacts of food in 2050 under different livestock futures. *Global Environmental Change, 47*, 1-12.

Rower, J. E., Bushman, L. R., Hammond, K. P., Kadam, R. S., & Aquilante, C. L. (2010). Validation of an LC/MS method for the determination of gemfibrozil in human plasma and its application to a pharmacokinetic study. *Biomedical chromatography : BMC, 24*(12), 1300-1308.

Savary, S., Willocquet, L., Pethybridge, S. J., Esker, P., McRoberts, N., & Nelson, A. (2019). The global burden of pathogens and pests on major food crops. *Nat Ecol Evol, 3*(3), 430-439.

Schaller, H. (2004). New aspects of sterol biosynthesis in growth and development of higher plants. *Plant Physiol Biochem, 42*(6), 465-476.

Shah, J. (2005). Lipids, lipases, and lipid-modifying enzymes in plant disease resistance. *Annu Rev Phytopathol, 43*, 229-260.

Shannon, P., Markiel, A., Ozier, O., Baliga, N. S., Wang, J. T., Ramage, D., . . . Ideker, T. (2003). Cytoscape: a software environment for integrated models of biomolecular interaction networks. *Genome Res, 13*(11), 2498-2504.

Siebers, M., Brands, M., Wewer, V., Duan, Y., Hölzl, G., & Dörmann, P. (2016). Lipids in plant–microbe interactions. *Biochimica et Biophysica Acta (BBA) - Molecular and Cell Biology of Lipids, 1861*(9, Part B), 1379-1395.

Spassieva, S. D., Markham, J. E., & Hille, J. (2002). The plant disease resistance gene *Asc-1* prevents disruption of sphingolipid metabolism during AAL-toxin-induced programmed cell death. *Plant J, 32*(4), 561-572.

Stasko, A. K., Wickramasinghe, D., Nauth, B. J., Acharya, B., Ellis, M. L., Taylor, C. G., . . . Dorrance, A. E. (2016). High-density mapping of resistance QTL toward *Phytophthora sojae*, *Pythium irregulare*, and *Fusarium graminearum* in the same soybean population. *Crop Science, 56*(5), 2476-2492.

Subramoni, S., Suárez-Moreno, Z. R., & Venturi, V. (2010). Lipases as pathogenicity factors of plant pathogens. In K. N. Timmis (Ed.), *Handbook of Hydrocarbon and Lipid Microbiology* (pp. 3269-3277). Berlin, Heidelberg: Springer Berlin Heidelberg.

Sui, Z., Niu, L., Yue, G., Yang, A., & Zhang, J. (2008). Cloning and expression analysis of some genes involved in the phosphoinositide and phospholipid signaling pathways from maize (*Zea mays L.*). *Gene, 426*(1-2), 47-56.

Thomas, R., Fang, X., Ranathunge, K., Anderson, T. R., Peterson, C. A., & Bernards, M. A. (2007). Soybean root suberin: anatomical distribution, chemical composition, and relationship to partial resistance to *Phytophthora sojae*. *Plant Physiology, 144*(1), 299-311.

Tyler, B. M. (2007). Phytophthora sojae: root rot pathogen of soybean and model oomycete. *Molecular Plant Pathology, 8*(1), 1-8.

Valitova, J. N., Sulkarnayeva, A. G., & Minibayeva, F. V. (2016). Plant sterols: Diversity, biosynthesis, and physiological functions. *Biochemistry (Moscow), 81*(8), 819-834.

Velásquez, A. C., Castroverde, C. D. M., & He, S. Y. (2018). Plant-Pathogen Warfare under Changing Climate Conditions. *Current biology : CB, 28*(10), R619-R634.

Venegas-Molina, J., Proietti, S., Pollier, J., Orozco-Freire, W., Ramirez-Villacis, D., & Leon-Reyes, A. (2020). Induced tolerance to abiotic and biotic stresses of broccoli and *Arabidopsis* after treatment with elicitor molecules. *Scientific Reports, 10*(1), 10319.

Vriese, K. D., Pollier, J., Goossens, A., Beeckman, T., & Vanneste, S. (2019). The use of mutants and inhibitors to study sterol biosynthesis in plants. *bioRxiv*, 784272.

Wang, K., Senthil-Kumar, M., Ryu, C.-M., Kang, L., & Mysore, K. S. (2012). Phytosterols play a key role in plant innate immunity against bacterial pathogens by regulating nutrient efflux into the apoplast. *Plant physiology, 158*(4), 1789-1802.

Watt, Matthew J., & Steinberg, Gregory R. (2008). Regulation and function of triacylglycerol lipases in cellular metabolism. *Biochemical Journal, 414*(3), 313-325.

Weng, C., Yu, K., Anderson, T. R., & Poysa, V. (2007). A quantitative trait locus influencing tolerance to Phytophthora root rot in the soybean cultivar 'Conrad'. *Euphytica, 158*(1), 81-86.

Xing, J., Zhang, L., Duan, Z., & Lin, J. (2020). Coordination of Phospholipid-Based Signaling and Membrane Trafficking in Plant Immunity. *Trends in Plant Science*.

Xu, C., & Shanklin, J. (2016). Triacylglycerol metabolism, function, and accumulation in plant vegetative tissues. *Annual Review of Plant Biology, 67*(1), 179-206.

Yuan, S., Kim, S.-C., Deng, X., Hong, Y., & Wang, X. (2019). Diacylglycerol kinase and associated lipid mediators modulate rice root architecture. *New Phytologist, 223*(1), 261-276.

Zhang, Q., & Xiao, S. (2015). Lipids in salicylic acid-mediated defense in plants: focusing on the roles of phosphatidic acid and phosphatidylinositol 4-phosphate. *Frontiers in Plant Science, 6*, 387-387.

Chapter four

Plant oxylipin induction in soybean (*Glycine max*) cultivars in response to *Phytophthora sojae* colonization and infection

Plant oxylipins induction in soybean (*Glycine max*) cultivars in response to *Phytophthora sojae* colonization and infection

4.1. Abstract

Food security is a major challenge to sustainably supply food to meet the demands of the ever-growing global population. Crop loss due to pathogens is a major concern to overcoming this global food security challenge. Soybean root and stem rot caused by *Phytophthora sojae* results in over 1B $US in crop loss annually. Phyto-oxylipins are significant sources of natural disease resistance in plant pathosystems, but very little is known of their role in the successful strategies used by tolerant soybean cultivars to limit *Phytophthora sojae* colonization and disease infection. A targeted lipidomics approached was undertaken using high resolution accurate mass tandem mass spectrometry and high-resolution ethylene bridge and C30 reverse phase liquid chromatography to assess phyto-oxylipin metabolism during successful soybean response to *Phytophthora sojae* infection. Two soybean cultivars, one susceptible and one tolerant to *Phytophthora sojae* were inoculated with either zoospores or agar plugs containing mycelia from *Phytophthora sojae*. In a tolerant cultivar, accumulation of the oxylipins

10(E),12(Z), 13S-hydroxy-9(Z),11(E),15(Z)-octadecatrienoic acid, (*Z*)-12,13-dihydroxyoctadec-9-enoic acid, (9Z,11E)-13-Oxo-9,11-octadecadienoic acid, 15(Z)-9-oxo-octadecatrienoic acid, 10(E*)*,12(E)-9-hydroperoxyoctadeca-10,12-dienoic acid, 12-oxophytodienoic acid and (12*Z*,15*Z*)-9,10-dihydroxyoctadeca-12,15-dienoic acid were significantly increased but decreased in susceptible cultivar, while (4*Z*,7*Z*,10*Z*,13*Z*)-15-[3-[(*Z*)-pent-2-enyl]oxiran-2-yl]pentadeca-4,7,10,13-tetraenoic acid and 12S-hydroperoxy-5(Z),8(Z),10(E),14(Z)-eicosatetraenoic acid were significantly increased in susceptible cultivar but decreased in tolerant cultivar relative to non-inoculated controls after 48 h, 72 h and 96 h of infection by *Phytophthora sojae.* The altered oxylipins were highly correlated with the induction of oxidized intact phospholipids and triacylglycerol. Visualization of the phyto-oxylipins using structural network reveals alterations in oxylipins in soybean cultivars. This study demonstrated novel evidence for the metabolism of phyto-oxylipins in soybean

cultivars tolerant or susceptible *Phytophthora sojae*. This work provides potential applications of the altered oxylipins as possible biomarkers that may be useful in further elucidation of oxylipin anabolism mediated plant immunity in soybean tolerance to *Phytophthora sojae* colonization.

***Keywords*:** Phyto-oxylipin, soybean root and stem rot, lipoxygenase, allene oxide synthase, cytochrome P450, oomycete *Phytophthora sojae*, sustainable agriculture.

4.2. Introduction

The Food and Agriculture Organization has predicted that the world's population will be approximately 10B by 2050 and there may need to be an increase of approximately 70 % in food production (DeLong, Burger, & Hamilton, 2013; Diaz-Ambrona & Maletta, 2014). Therefore, securing a food supply that is sustainable with current population growth patterns and ever-changing food desires are the major challenges of agricultural and food industries (Diaz-Ambrona & Maletta, 2014). Plants are vital components of every food chain, therefore, to fulfil this requirement globally, there is a need to develop sustainable agricultural practices that could mitigate biotic and abiotic stresses in agricultural production systems. Pathogen attack is one of the most devastating biotic stresses preventing the growth, development, and productivity of agricultural crops worldwide (McDonald & Stukenbrock, 2016). Pathogens cause huge losses in terms of crop yield and quality, and consequently lead to reduction of food security and availability at global levels (Savary et al., 2019). In the past four decades, disease management has contributed massively to improved plant health and food production (Nelson, 2020), but global harvests are still reduced by 10-16 % due to plant diseases caused by infectious microorganisms like bacteria, viruses, nematodes and fungi (Chakraborty & Newton, 2011; Wei et al., 2019). Today, sustainable agriculture is capable of reducing the economic effects of infectious pathogens by developing disease-resistant crops using

selective cross-breeding and genetic engineering to improve long-term food production and availability to meet the ever-increasing world population food security needs (Zhao, Luo, Deng, & Yan, 2008).

Phytophthora root and stem-rot is one of the major destructive soybean diseases and the causal agent is oomycete *Phytophthora sojae* resulting in global annual crop losses of approximately $2B USD (Tyler, 2007). Dependence and over-application of synthetic chemicals such as fertilizers, fungicides, herbicides that can lead to potential non-target microorganisms, human, animal and total environment health issues (Borrego & Kolomiets, 2016; McDonald & Stukenbrock, 2016). Thus, considering these impacts, health-conscious, environmentally cognisant farmers have started moving towards eco-friendly farming practices (Pretty, 2008). Environmentally sustainable agricultural practices are now embraced to prevent phytopathogen attack in plants and to enhance plant health. Higher plants possess sophisticated strategies by which to defend against stresses from infectious pathogens. Generally, plants have two kinds of disease resistance, the host resistance and nonhost resistance. Host resistance is mainly cultivar-specific and non-durable (Mysore & Ryu, 2004) while nonhost can defend against all races of a specific pathogens and can exist in all cultivars of host plant species (Heath, 2000). Therefore, nonhost resistance is more durable and is the usual form defense mechanism displayed by plants towards a wide spectrum of potential pathogens (Heath, 2000; Mysore & Ryu, 2004; Senthil-Kumar & Mysore, 2013). Other defense mechanism used by higher plants include remodulation of membrane lipidome (Adigun et al., 2021) and production of bioactive compounds has been shown to be effective response strategies to limit pathogen infection (Adigun et al., 2020; Thomas et al., 2007). For instance, biosynthesis of oxygenated PUFAs generally called oxylipins, is one of the early mechanisms of plant's defense responses against pathogenic bacterial and fungal infection (Blée, 2002; Howe & Schilmiller, 2002).

Phyto-oxylipins constitute a broad class of oxygenated bioactive metabolites or lipid anabolism mediated immunity, believed to be involved in signaling and defense responses against pathogen attack in higher plants (Adigun et al., 2020; Stumpe & Feussner, 2006). Plant oxylipins are produced from oxidation and conversion of

PUFAs, mainly linolenic and linoleic (C18:3 and C18:2) acids, and they have been demonstrated to function in the signaling pathways that control the expression of defense-related genes such as *9-LOX*-, *13-LOX*-, and α-*DOX-1* (García-Marcos, Pacheco, Manzano, Aguilar, & Tenllado, 2013; Howe & Schilmiller, 2002; Wu & Baldwin, 2010). Biosynthesis of phyto-oxylipins from PUFAs via enzymatic processes is primarily initiated by LOXs and *α*-DOXs (Blée, 2002; Howe & Schilmiller, 2002). These lipids can also be subjected to nonenzymatic decarboxylation to form one-carbon-shortened FAs and aldehydes (Granér, Hamberg, & Meijer, 2003). Hydroperoxides produced via the enzymatic action of 9-/13-LOXs can be metabolized by six major enzymatic paths: (1) to generate 9- or 13-HOD and 9- or 13-HOT through reduction via peroxygenase (PO) (Blée, 2002) or peroxidase activity (Brodhun et al., 2013); (2) conversion of trihydroxylated FAs into epoxy alcohols, through enzymatic action of a PO, and subsequently by an epoxide hydrolase (EH) (Blée, 2002) or through an epoxy-alcohol synthase (Brodhun et al., 2013); (3) into FA ketotrienes or ketodienes via dehydration through LOXs (Vollenweider, Weber, Stolz, Chételat, & Farmer, 2000) or through dehydrogenation of FA hydroxides by characterized enzyme (Vincenti et al., 2019); (4) into reactive hemiacetals through the activity of 9- or 13-hydroperoxide lyases (Grechkin, Brühlmann, Mukhtarova, Gogolev, & Hamberg, 2006; Stumpe & Feussner, 2006); (5) into divinyl ether FAs through the activity of divinyl ether synthases (DESs) (Stumpe & Feussner, 2006); and (6) into reactive allene oxides produced via allene oxide synthases (AOSs) (Tijet & Brash, 2002). Unstable allene oxides can undergo nonenzymatic hydrolysis producing *α*- or *γ*-ketols, or generation of cyclic compounds like cyclopentenones via enzymatic cyclization by allene oxide cyclases. C18 cyclopentenones, such as 12-oxo-10,15(*Z*)-phytodienoic acid undergo reduction to form cyclopentanones and are β-oxidized into short-chain compounds like jasmonic acid (JA) (Mukhtarova, Lantsova, Khairutdinov, & Grechkin, 2020). Other oxylipins like dihydroxy FAs can be produced from C18 PUFAs through the action of the PO or EH pathways (Blée, 2002). Free FAs can also serve as substrates to produce phyto-oxylipins.

Production of oxylipins occurs constitutively in plants and as a response to various environmental stresses (Scala et al., 2018). Over 200 phyto-oxylipins have been observed so far in plants (Prost et al., 2005). Phyto-oxylipins are mainly induced during plant-pathogen interactions (Adigun et al., 2020; Blée, 2002). In fact, some phyto-oxylipins generated in defense responses against pathogen infections are antimicrobial in nature (Prost et al., 2005). Some phytooxylipins were described as antioomycete or antifungal compounds capable to inhibit spore germination and mycelial growth of eukaryotic microbes in host-pathosystem such as 13(*S*)-Hydroperoxy-9(*Z*),11(*E*),15(*Z*)-octadecatrienoic acid, 13(*S*)-Hydroxy-9(*Z*),11(*E*),15(*Z*)-octadecatrienoic acid (Granér et al., 2003), epoxy-FAs or polyhydroxylated FAs (Blée, 2002), and colnelenic acid and colneleic acid (Göbel, Feussner, Hamberg, & Rosahl, 2002).

In addition, the growth of *Pseudomonas* spp. in vitro could be strongly inhibited by trans-2-hexenal and cis-3-hexenol (Prost et al., 2005). They are mainly understood as agents that promote resistance to pathogen attack (Christensen & Kolomiets, 2011).

Genetic studies have demonstrated the functions of α-DOX-1 and 9-LOX in the defense response of Arabidopsis and tobacco to infectious pathogen attack, likely by controlling oxidative stress and PCD (De León, Sanz, Hamberg, & Castresana, 2002; Rancé, Fournier, & Esquerré-Tugayé, 1998). More importantly, several phyto-oxylipins generated from the activity of 9-/13-LOX were capable of initiating PCD and hypersensitivity response (HR) in some pathosystems (Cacas et al., 2005). Additionally, JA has been involved in the signaling cascade resulting in elicitation of LOX. Methyl jasmonate (MeJA) was demonstrated to trigger LOX activities and the expression of the synthesis-related genes such as *PtLOX1, PtLOX2* and *PtLOX3* (Chen et al., 2015; Marmey et al., 2007). Several pieces of evidence indicate that phyto-oxylipins play critical functions in the development of HR and disease resistance (Gullner, Künstler, Király, Pogány, & Tóbiás, 2010; Kovač et al., 2009). However, there is a paucity of information about the function of phyto-oxylipins during oomycete-plant interactions. Detailed knowledge of the molecular signaling that occurs during plant–pathogen interactions can

pave the way for mechanisms of disease resistance in plants. As demonstrated in our previous studies, understanding the plant lipidome and metabolism during pathogen attack or infections is critical to elucidate their roles in susceptible or tolerant host-pathogen interactions, lipid metabolism mediated signaling, and defense responses during pathogenicity. We hypothesized that a tolerant soybean cultivar would upregulate oxylipin synthesis compared to a susceptible cultivar following *P. sojae* infection as a component of its successful mechanism used to mitigate infection by pathogens. Hence, we analyzed phyto-oxylipin compounds in the root and stem tissues of both a resistant and a tolerant soybean cultivar to better understand the roles and induction of phyto-oxylipins in defense response during colonization and infection by *P. sojae*.

4.3. Materials and methods

4.3.1. Planting and inoculation of soybean cultivars

Seeds of OX760-6 and Conrad cultivars were surface sterilized using dilute sodium hypochlorite (0.5 %) for 5 min (Commercial Javex Bleach; Clorox Co., Brampton, Ontario, Canada), and washed several times with distilled water (dH_2O). Seeds were submerged for 12 h in dH_2O and then seeded in plastic pots (195 mm diameter and 195 mm depth) containing vermiculite (#2A, Thermo-O-Rock East Inc., New Eagle, Pennsylvania) as a medium, which was then saturated with dH_2O and the seeds were allowed to germinate. Seedlings were maintained under controlled conditions with 16 h of alternating light at 25 °C and 8 h of dark at 20 °C with relative humidity of 60 % inside a growth chamber (Biochambers MB, Canada). Sterilized dH_2O was applied every day to maintain the vermiculite water content from moist to slightly dry to provide optimum nutrients and moisture to seedlings. *Phytophthora sojae* virulent strain race 2 (strain P6497) was obtained from Agriculture and Agri-Food Canada (AAFC), London, Ontario, Canada. The culture of *P. sojae* was cultured and aseptically grown on 26 % V8-juice agar (8.4 g agar, 1.6 g $CaCO_3$, 156 mL V8-juice [Campbell Soup Company, Toronto, ON, Canada], and 440 mL dH_2O) for 8 days. To monitor the successive events in the process of infection in roots and stems of both soybean

cultivars, 8-day-old cultures of *P. sojae* were flooded with dH_2O to produce zoospores, and then incubated overnight at 22 °C. When zoospores could be observed microscopically, the concentration of zoospores was determined by adding of one drop of 0.1 % wt/vol of aniline blue in lactophenol (1:1:1 85 % lactic acid, phenol, and water) to 1 mL zoospore suspension; a 10 µL aliquot of this zoospore suspension was loaded onto a hemocytometer using a micropipette. The concentration of zoospores was calculated and adjusted to 1×10^{-4} zoospores/mL by adding deionized water. The seedlings were allowed to grow for 10 days and then carefully removed from vermiculite and washed with water to remove any remaining vermiculite from the roots. Whole seedlings from each sample were placed into 15 mL centrifuge tube containing 10 mL dH_2O and inoculated with 1000/ mL *P. sojae* zoospore suspension, and another set of samples were mock inoculated as control without *P. sojae* zoospore suspension. There were four replications per treatment and the experiment were performed three times. The 10 days old seedlings were then incubated at room temperature for periods of 48 h, 72 h and 96 h.

For determination of oxidized GLs in both soybean cultivars, the seeds and fungal cultures were prepared as described above. Agar disks containing cultures of *P. sojae* strain P6497 were cut and fitted into the bottom of wax-paper cups (top diameter 8.5 cm by 15 cm deep: Merchants Paper Company, Windsor, ON, Canada). These cups were then filled up with medium-grade vermiculite, drainage holes were created in the bottom of the cups, and six seeds were planted in each of four replications cups containing vermiculite. For non-inoculated controls, agar disks without *P. sojae* were used. Seedlings were maintained in the growth chamber at the same conditions as described above for 10 days. Six seedlings from each soybean cultivar were inoculated with *P. sojae* in a cup and another six from each soybean cultivar were mock-inoculated using only sterile V8-juice agar disks to serve as a control. Beginning four days after seeding, seedlings were watered daily using one-quarter-strength Knop's solution (Thomas et al., 2007). The entire plants were harvested 10 days after germination and kept at -80 °C until analysis. The plant samples were divided into three groups. The first group were used for membrane and storage

lipid analysis, the second group were used for oxidized GL analysis, and the third group were used for histochemical analysis.

4.3.2. Extraction of oxidized glycerolipids from root and stem of soybean cultivars

Soybean seedlings prepared as above were incubated in boiling isopropanol for 10 min. Lipid extraction was conducted by weighing 100 mg each of root and stem from each sample type, and 1 mL MeOH containing 0.01 % butylated hydroxytoluene was added to each sample. Four replications of each combination of treatment (inoculated or control), cultivar (susceptible or tolerant), and tissue (root or stem) combination were performed. The tissues were then homogenized using a probe tissue homogenizer until completely dissolved. Following homogenization, 800 µL water and 1000 µL chloroform were added along with PC 14:0/14:0 as internal standard. Each sample was thoroughly vortexed and centrifuged at 3000 rpm for 15 min at room temperature. The organic layers were transferred to pre-weighed 4 mL glass vials with PTFE-lined caps (VWR, Mississauga, Canada). The samples were then dried under a gentle stream of nitrogen and the sample vials reweighed to determine the quantity of recovered lipids. The recovered lipids from each sample were re-suspended in 1000 µL solvent (2:1 v/v chloroform: methanol) and stored at -20 °C until lipid analysis using ultra high-performance liquid chromatography coupled to heated electrospray ionization high resolution accurate mass tandem mass spectrometry (UHPLC- C30RP-HESI-HRAM-MS/MS).

4.3.3. Extraction of primary oxylipins from root and stem of soybean cultivars

Soybean seedlings (root and stem), non-inoculated control and inoculated were weighed into 100 mg samples and used for analysis. The samples were placed into 2 mL glass centrifuge tubes containing 300 µL of 10 % glycerol in water and treated immediately with 5 µL of 10 mg/mL butylated hydroxyl toluene (BHT) dissolved in ethanol.

Then, they were spiked with 20 µL of a suitable deuterium-labeled internal standard with a concentration of 500 ng/mL in ethanol. The sample volume was made up to 3 mL with 25 % aqueous acetonitrile in a centrifuge tube before the tube was placed in ice and homogenized using a probe tissue homogenizer. The extracted solvent mixtures were centrifuged for 10 mins at 5500 rpm and 4 °C to obtain the supernatants. The extraction of plant samples was performed using solid phase extraction (SPE) with water using an OASIS MAX SPE column (3 cc, Vac Cartridge, 30 µM particle size, part number 186000367) used for concentrating phyto-oxylipins. The column was initially conditioned with 3 mL acetonitrile, and subsequently with 3 mL of 25 % aqueous acetonitrile. Then, the entire supernatant from the centrifuged sample was loaded onto the SPE column and the SPE column was gently washed with 3 mL of 25 % aqueous acetonitrile, followed by 3 mL acetonitrile. Oxylipins were eluted from the column into a glass vial containing 200 µL of 10 % glycerol in methanol with 1.3 mL of 1 % formic acid in acetonitrile (1: 99 v/v). The eluent was dried under nitrogen at 40 °C until only the glycerol remained. The dried eluates were then reconstituted in 60 µL of a methanol:acetonitrile (1:1 v/v) solution and vortexed thoroughly. Afterwards, the eluates were filtered using 0.1 µM Amicon Ultrafree-MC Durapore PVDF filter (pore-size 0.1 µM; Millipore, Bedford, MA). Finally, 3 µL of each sample were injected and oxylipins resolved using ultra high-performance liquid chromatography containing a C18 bridge ethylene hybrid column coupled to heated electrospray ionization high resolution accurate mass tandem mass spectrometry (UHPLC-C18-BEH-HESI-HRAM-MS/MS; Q-Exactive, ThermoFisher Scientific, ON, Canada). Four replications per sample were performed.

4.3.4. Analysis of oxidized glycerolipids using UHPLC-C30RP-HESI-HRAM-MS/MS

The method of lipid analysis was as described previously (Nadeem et al., 2020). Lipids extracted from the soybean roots and stems were separated using an Accucore C30 reverse phase (C30RP) column (150 × 2 mm I.D., particle size: 2.6 µm, pore diameter: 150 Å; ThermoFisher Scientific, ON, Canada) applying the following solvent system:

Solvent A (40: 60 v/v H_2O and acetonitrile), and Solvent B (1:10: 90 v/v/v water: acetonitrile: isopropanol). Both solvents A and B consisting of 0.1 % formic acid and 10 mM ammonium formate. The conditions for the separation using UHPLC-C30RP were as follows: oven temperature of 30 °C, flow rate of 0.2 mL/min, and 10 µL of the lipid mixture suspended in 1: 2 v/v methanol: chloroform was injected into the instrument. The system gradient used for the separation of lipid classes and molecular species were: 30 % solvent B for 3 min; solvent B increased over 5 min to 43 %, then increased in 1 min to 50 % B and to 90 % B over 9 min; and from 90 % to 99 % B over 8 min; and finally maintained at 99 % B for 4 min. The column was re-equilibrated to 70 % solvent A for 5 min to re-establish the starting conditions before injection of each new sample. Lipid analyses were performed using a Q-Exactive Orbitrap high-resolution accurate mass tandem mass spectrometer (Thermo-Scientific, Berkeley, CA, USA) coupled with an automated Dionex Ulti-Mate 3000 UHPLC system controlled by Chromeleon 6.8 SR13 (Dionex Corporation, Part of Thermo Fisher Scientific) software. Full-scan HESI-MS and MS/MS acquisitions were performed in positive mode of the Q-Exactive Orbitrap mass spectrometer. The following parameters were used for the Orbitrap mass spectrometry techniques: auxiliary gas of 2; sheath gas of 40; capillary temperature of 300 °C; ion spray voltage of 3.2 kV; S-lens RF of 30 V; full-scan mode at a resolution of 70,000 m/z; mass range of 200–2000 m/z; top-20 data dependent MS/MS acquisitions at a resolution of 35,000 m/z; and injection time of 35 min; automatic gain control target of 5e5; isolation window of 1 m/z; collision energy of 35 (arbitrary unit). The external calibration of instrument was performed to 1 ppm using ESI positive and negative calibration solutions (Thermo Scientific, Berkeley CA, USA). Mixtures of lipid standards were used to optimize tune parameters (Avanti Polar Lipids, Alabaster, AL, USA) in both positive and negative ion modes. Identification and semi-quantification of the classes of lipids and lipid molecular species present in the root and stem of both soybean cultivars (OX760-6 and Conrad) were performed using LipidSearch version 4.1 (Mitsui Knowledge Industry, Tokyo, Japan) and the parameters adopted for identification in LipidSearch were: target database of Q-Exactive; product tolerance of 5 ppm; precursor tolerance of 5 ppm; Quan m/z tolerance of ±5 ppm; product ion threshold of 5 %; m-score threshold of 2; Quan retention time range of ±1 min; use of all isomer

filter; ID quality filters A, B, and C; and $[M+NH_4]^+$ adduct ions for positive ion mode. Following identification, the observed lipid classes and lipid molecular species were merged and aligned according to the parameters established in our previous report (Adigun et al., 2021; Nadeem et al., 2020; Pham et al., 2019).

4.3.5. Analysis of primary oxylipins from susceptible and tolerant soybean cultivars

100 µL extracts from the soybean roots and stems were introduced into automated Dionex UltiMate 3000 UHPLC system and the auto sampler was cooled to a temperature of 10 °C. Chromatographic separation was performed on an Acquity UHPLC-BEH, 1.7 µM, 2.1 x 100 mm C18 column using a flow rate of 0.2 mL/min at 30 °C during a 26 min gradient (0–3.5 min from 15 % B to 33 % B, 3.5–5.5 min to 38 % B, 5–7 min to 42 % B, 7–9 min to 48 % B, 9–15 min to 65 % B, 15–17 min to 75 % B, 17–18.5 min to 85 % B, 18.5–19.5 min to 95 % B, from 19.5 to 21 min to 15 % B, and from 21–26 min 15 % B). Mobile phase A consisted of aqueous 0.1 % acetic acid, and mobile phase B was 90:10 v/v acetonitrile/isopropyl alcohol. A Q-Exactive orbitrap mass spectrometer was used and the data acquired in the negative mode at temperature 100 °C, capillary spray voltage 3.0 kV, capillary temperature 300 °C, S-lens RF level 30 V, sheath gas temperature 350 °C, auxiliary gas setting 2, energy: 32.5 (stepped collision energy 30 and 35, arbitrary unit). The full scan mode at 70,000 m/z resolution, top-10 data dependent MS/MS at 35,000 m/z resolution, 1 m/z isolation window and 1e6 automatic gain control target was utilized. The equipment was calibrated externally to 1 ppm using tuning solution (Pierce™ LTQ Velos ESI Positive Ion Calibration Solution and Pierce™ Negative Ion Calibration Solution) purchased from Thermo Scientific (Waltham, MA, USA).

4.3.6. Oxylipin network mapping from susceptible and tolerant soybean cultivars

To obtain comprehensive knowledge from a systems biology perspective of how susceptible and tolerant soybean cultivars biosynthesize phyto-oxylipins as part of defense strategy against pathogen invasion, phyto-oxylipins that exhibited significant changes in relative concentrations as a result of the treatment were visualized within oxylipin structural similarity networks. Regularized oxylipin correlation networks were calculated and visualized to obtain insights into alterations between soybean cultivars. Networks were separately calculated for root and stem tissue at 48 h, 72 h and 96 h of inoculation inoculation. Correlations between oxylipins were calculated using high-dimensional undirected graph estimation method (Jiang et al., 2019). Relationships between lipids were estimated based on Meinshausen-Buhlmann graph estimation and the stability approach to regularization selection to identify conditionally independent oxylipin-oxylipin connections (Meinshausen & Bühlmann, 2006). The relationships were created between both soybean cultivars and experimental groups inoculated at 48 h, 72 h and 96 h time points. The regularization lambda for root and stem network at time points 48 h, 72 h and 96 h were specified at 0.46, 0.28 and 0.34 for root and 0.46, 0.17 and 0.13 for stem networks respectively. Mapped networks were created to visualize changes in relationships between oxylipins and experimental differences. Linear models were built to identify significant interactions between changes in oxylipins between cultivars and inoculation status at each individual time point of 48 h, 72 h and 96 h (R-Core-Team, 2019). Significant interactions were identified based on false discovery adjusted p-values (pFDR) < 0.05. Significant changes in oxylipin abundances between pairwise comparisons of cultivar and inoculation groups were evaluated based on Tukey's Honestly Significant Difference (HSD) method. Significant changes between groups were identified based on HSD-adjusted $p < 0.05$. Magnitude and direction (positive or negative) of the relationships were determined based on the Spearman correlations (pFDF < 0.05). Significant interactions between cultivar and inoculation were identified based on linear model pFDR < 0.05 and HSD p-values < 0.05. Cytoscape was used render oxylipin-oxylipin interactions (Shannon et al., 2003) and show all pairwise differences between cultivar and inoculation

groups. Network node colors was used to show magnitude (size) and direction (color) of fold changes and will be reported as means for all experimental groups compared to the following references: tissue type (root or stem), cultivar (susceptible or resistant), and treatment type (inoculated or control).

4.3.7. Statistical method of data analysis

To determine the effects of plant-pathogen interaction on phyto-oxylipin induction in the root and stem of susceptible (OX760-6) and tolerant (Conrad) soybean cultivars, PLS-DA, and heatmap analysis were conducted with XLSTAT (Premium 2017, Version 19.5, Addinsoft). Results are presented as average ± standard error unless noted otherwise. The means with significant differences were compared using Fisher's Least Significant Difference (LSD), $\alpha = 0.05$. SigmaPlot 13.0 software (Systat Software Inc., San Jose, CA) was used for figure preparation. Linear models were built to identify significant interactions between changes in oxylipins due to tissue, cultivar and treatment at each individual inoculation time point. Significant interactions were identified based on false discovery adjusted p-values (pFDR) < 0.05. Pairwise changes between all groups (tissue × cultivar × treatment) were evaluated based on Tukey's LSD method. Significant changes between groups were identified based on HSD-adjusted $p < 0.05$. Note that all analyses were done separately for each time point due to observed non-linear trends in lipids changes over time.

4.4. Results

4.4.1. Phyto-oxylipin profiling in susceptible and tolerant soybean cultivars in response to *P. sojae* infection

In order to elucidate the relationship between soybean-*P. sojae* interaction and accumulation of oxylipins, we applied lipidomic techniques to analyze the oxidized GLs and primary oxylipin profiles in the root and stem tissues of susceptible and tolerant soybean cultivars after inoculation with *P. sojae* for 48 h, 72 h and 96 h to

assess alterations in phyto-oxylipins accompanying pathogen infection. We selected 48 h as the earliest time point for this study because no detectable response was observed at 24 h of inoculation (data not shown). A comprehensive lipidomic technique was done using UHPLC-C18-BEH-HESI-HRAM-MS/MS and UHPLC-C30RP-HESI-HRAM-MS/MS to determine the primary oxylipins and oxidized GLs, respectively in the roots and stems of tolerant and susceptible soybean cultivars following infection with *P. sojae*.

Approximately 30 oxylipins from both soybean cultivars irrespective of the treatment were identified. Primary oxylipins and oxidized GLs with the highest influential loading were determined using PLSDA. Nine primary oxylipins were identified from the root and stem of both soybean cultivars and they were classified according to their pathway of origin (either LOX, AOS, or CYP450). Detected oxylipins originating from LOX were: 10(E),12(E)-9-hydroperoxyoctadeca-10,12-dienoic acid (9-HpODE), 10(E),12(Z), 13S-hydroxy-9(Z),11(E),15(Z)-octadecatrienoic acid (13-HOTrE), and 12S-hydroperoxy 5(Z),8(Z),10(E),14(Z)-eicosatetraenoic acid (12(S)-HpETE), 9-oxo-10E,12Z,15Z-octadecatrienoic acid (9-KOTrE) and (9Z,11E)-13-Oxo-9,11-octadecadienoic acid (13-KODE). Those identified from the AOS pathway were: 12-oxophytodienoic acid (12-OPDA); and while the following were from the CYP450 pathway: (*12Z,15Z*)-9,10-dihydroxyoctadeca-12,15-dienoic acid (9, 10-DiHODE), (*Z*)-12,13-dihydroxyoctadec-9-enoic acid (12,13-DiHOME), and (4*Z*,7*Z*,10*Z*,13*Z*)-15-(3-((*Z*)-pent-2-enyl)oxiran-2-yl)pentadeca-4,7,10,13-tetraenoic acid (16,17-EpDPE) (Tables 4.1 and 4.2). A chromatogram showing the separation of primary oxylipins from inoculated root of both soybean cultivars is presented in Fig. 4.1a. The extracted ion chromatogram (XIC) of m/z 293.21, 313.24 and 335.22 precursor ions of the selected primary oxylipins is shown in Fig. 4.1b. The MS^2 spectrum of *m/z* 293.21 recognized as 13-KODE is presented in Fig. 4.1c, the MS^2 spectrum of *m/z* 313.22 recognized as 12,13-DiHOME is presented in Fig. 4.1d, and the MS^2 spectrum of *m/z* 335.22 recognized as 12(S)-HpETE is presented in Fig. 4.1e; these account for some of the major primary oxylipins identified in the tissues of both soybean cultivars. From our previous lipid metabolism studies of soybean cultivars challenged with *P. sojae*, we have generated a list of

oxidized GLs that could serve as substrates for biosynthesis of primary oxylipins. The 12 oxidized GLs observed in the root of both soybean cultivars included PC36:6+2O, PC36:5+2O, PE38:6+O, PE38:6+2O, PA34:3+O, PI28:3+2O, TG50:3+O, TG52:6+O, TG54:2+O, TG54:8+2O, TG54:8+3O and TG54:6+Ox (Table 4.3), and the 13 oxidized GLs in the stem of both cultivars included (PC36:6+2O, PC36:5+2O, PE38:6+O, PE38:6+2O, PA34:3+O, TG54:8+2O, TG54:8+3O, TG52:6+O, TG54:9+O, TG60:9+5O, TG60:8+5O, TG60:10+6O and TG54:2+Ox (Table 4.4). The chromatogram showing GLs in the inoculated stem of both soybean cultivars is presented in Fig. 4.1f. The XIC of precursor ions *m/z* 685.44, 669.45 in negative ion mode and *m/z* 884.73 and 868.74 in the positive ion mode show the oxidized and unoxidized GLs observed in soybean roots (Fig. 4.1g), the MS^2 spectra of *m/z* 685.44 and 669.45 $(M-H)^-$ precursor ions showing the presence of Ox-PA (PA16:0/18:3+O) in addition to the unoxidized PA 16:0/18:3 are presented in Figs. 4.1h and 4.1i, and the MS^2 spectra of *m/z* 884.73 and 868.74 $(M+NH4)^+$ precursor ions showing the presence of Ox-TG (TG 16:0/18:3/18:3+O) in addition to the unoxidized TG 16:0/18:3/18:3 are presented in Figs. 4.1j and 4.1k.

Across all time points, as well as infected and non-infected plants, the relative abundance of the primary oxylipins in the root ranged between 0.00 to 58,117.16 nmol for the susceptible cultivar and 0.00 to 98,027.91 nmol for the tolerant cultivar (Table 4.1) while the relative abundance of the primary oxylipins in the stem ranged between 0.00 to 152,625.22 nmol for the susceptible cultivar and 0.00 to 147,879.60 nmol for the tolerant cultivar (Table 4.2). Similarly, the relative abundance of the oxidized GLs in the root ranged between 0.38±0.20 to 25.23±0.45 nmol for the susceptible cultivar and 0.00±00 to 51.45±0.29 nmol for the tolerant cultivar (Table 4.3), and the relative abundance of the oxidized GLs in the stem ranged between 0.00±00 to 67.13±4.46 nmol for the susceptible cultivar and 0.00±00 to 24.22±0.47 nmol for the tolerant cultivar (Table 4.4). Notably, the levels of all primary oxylipins in the root and stem were significantly increased in the tolerant cultivar relative to the non-inoculated controls, but significantly reduced in susceptible cultivar in response to *P. sojae* infection and colonization.

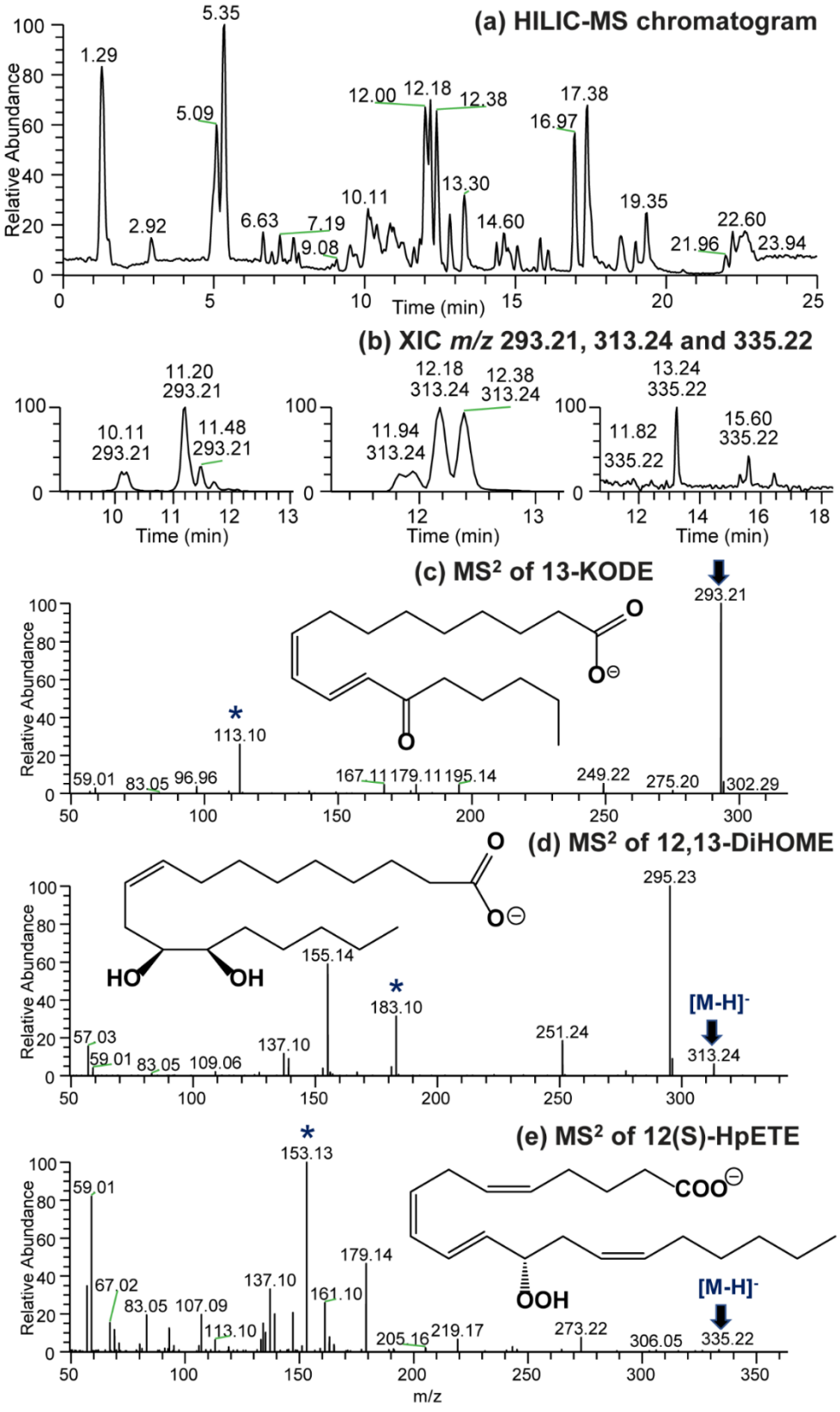
(a) HILIC-MS chromatogram
Relative Abundance
Time (min)
1.29
5.35
5.09
2.92
6.63
7.19
9.08
10.11
12.00
12.18
12.38
13.30
14.60
16.97
17.38
19.35
21.96
22.60
23.94
(b) XIC m/z 293.21, 313.24 and 335.22
11.20
293.21
10.11
293.21
11.48
293.21
12.18
313.24
12.38
313.24
11.94
313.24
13.24
335.22
11.82
335.22
15.60
335.22
Time (min)
(c) MS² of 13-KODE
293.21
113.10
59.01
83.05
96.96
167.11
179.11
195.14
249.22
275.20
302.29
(d) MS² of 12,13-DiHOME
295.23
155.14
183.10
[M-H]-
313.24
57.03
59.01
83.05
109.06
137.10
251.24
HO
OH
(e) MS² of 12(S)-HpETE
153.13
59.01
67.02
83.05
107.09
113.10
137.10
161.10
179.14
205.16
219.17
273.22
306.05
335.22
[M-H]-
COO
OOH
m/z

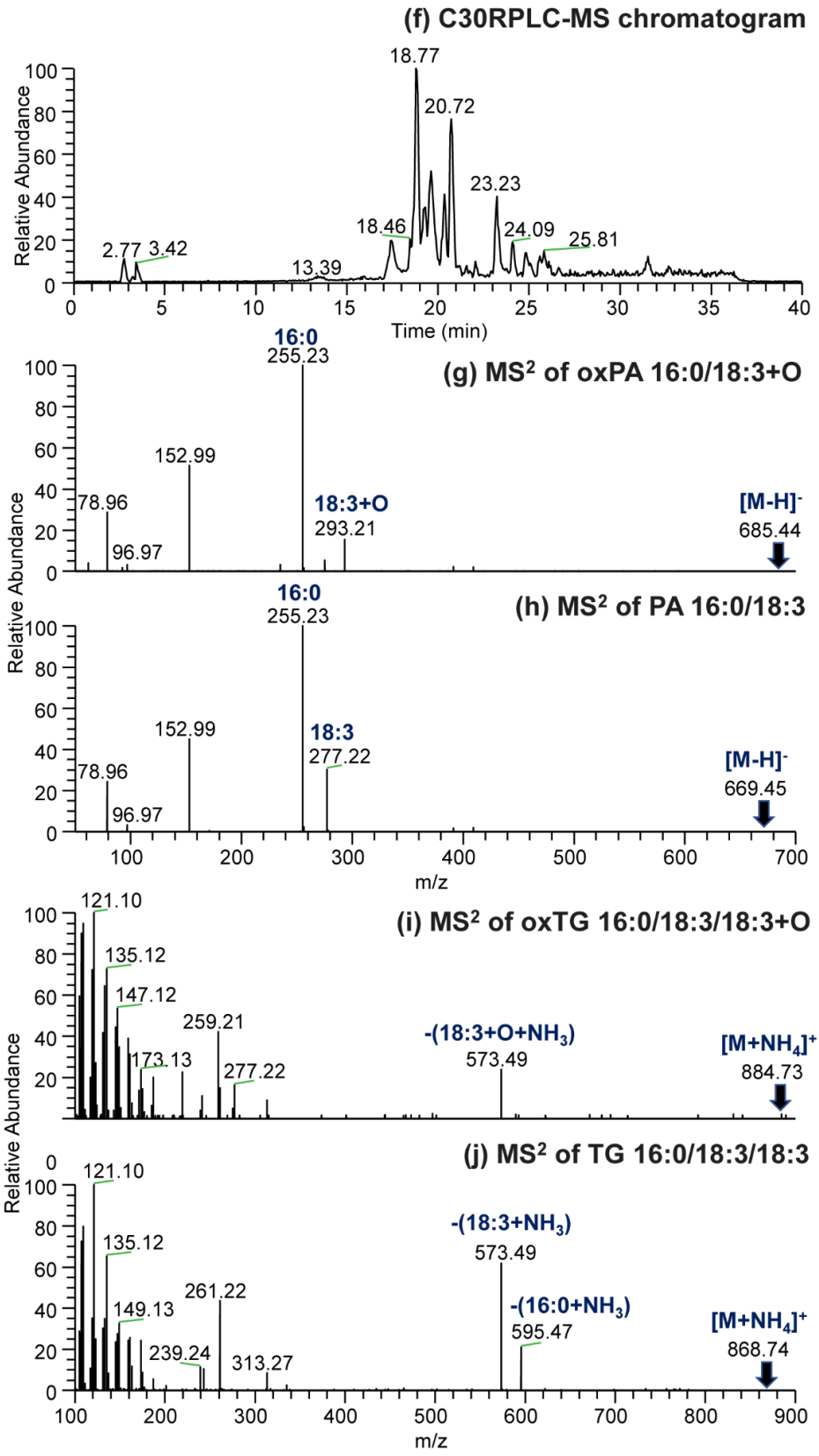
(f) C30RPLC-MS chromatogram
Relative Abundance
Time (min)
18.77
20.72
23.23
18.46
24.09
25.81
2.77
3.42
13.39
(g) MS² of oxPA 16:0/18:3+O
16:0
255.23
152.99
78.96
96.97
18:3+O
293.21
[M-H]⁻
685.44
(h) MS² of PA 16:0/18:3
16:0
255.23
152.99
78.96
96.97
18:3
277.22
[M-H]⁻
669.45
m/z
(i) MS² of oxTG 16:0/18:3/18:3+O
121.10
135.12
147.12
259.21
173.13
277.22
-(18:3+O+NH3)
573.49
[M+NH4]⁺
884.73
(j) MS² of TG 16:0/18:3/18:3
121.10
135.12
149.13
261.22
239.24
313.27
-(18:3+NH3)
573.49
-(16:0+NH3)
595.47
[M+NH4]⁺
868.74
m/z

Fig. 4.1. Chromatogram and mass spectrum of oxylipins observed in tolerant and susceptible soybean roots and stems in response to *P. sojae* infection. (a) Chromatogram demonstrating the C18-BEH-UHPLC-HRAM-MS/MS separation of primary oxylipins in the roots of both susceptible (OX760-6) and tolerant (Conrad) soybean cultivars infected with *P. sojae*; (b) Extracted ion chromatogram of *m/z* 293.21, 313.24 and 335.22 precursor ions of the selected oxylipin compounds present in the inoculated root of both soybean cultivars in response to infection with *P. sojae*; (c) MS^2 spectrum of *m/z* 293.21 identified as 13-KODE; (d) MS^2 spectrum of *m/z* 313.24 identified as 12,13-DiHOME and (e) MS^2 spectrum of *m/z* 335.22 identified as 12(S)-HpETE. The characteristic ions for identifying the different classes of oxylipins are marked with (*) and observed at *m/z* 113.10, 183.10 and 153.13 in (c-e), respectively; (f) UHPLC-C30RP-HESI-MS chromatogram showing oxidized intact GLs in soybean roots following infection with *P. sojae*; (g) Extracted ion chromatogram of precursor ions *m/z* 685.44, 669.45 in negative ion mode and *m/z* 884.73 and 868.74 in the positive ion mode of the selected oxidized /unoxidized) GLs; (h, i) MS^2 spectra of *m/z* 685.44 and 669.45 $[M-H]^-$ precursor ions showing the presence of Ox-PA (PA16:0/18:3+O) in addition to the unoxidized PA 16:0/18:3 compound; and (j, k) MS^2 spectra of *m/z* 884.73 and 868.74 $[M+NH4]^+$ precursor ions showing the presence of Ox-TG (TG 16:0/18:3/18:3+O) in addition to the unoxidized version (TG 16:0/18:3/18:3). 13-KODE = (9Z,11E)-13-Oxo-9,11-octadecadienoic acid, 12,13-DiHOME = (*Z*)-12,13-dihydroxyoctadec-9-enoic acid, and 12(S)-HpETE = 12S-hydroperoxy-5(Z),8(Z),10(E),14(Z)-eicosatetraenoic acid, Ox-PA = oxidized phosphatidic acid, Ox-TG = oxidized triacylglycerol.

Table 4.1. Primary oxylipins (nmol) induced in the root of soybean cultivars following inoculation with *P. sojae*

Oxylipin pathway	Oxylipin	Relative abundance (nmol)											
		48- h				**72-h**				**96-h**			
		ORC	**ORI**	**CRC**	**CRI**	**ORC**	**ORI**	**CRC**	**CRI**	**ORC**	**ORI**	**CRC**	**CRI**
Lipoxygenase	9-HpODE*	45401.96^{b}	19235.13^{c}	3232.84^{d}	60002.61^{a}	44827.97^{b}	0.00^{d}	3308.41^{d}	0.00^{d}	44697.89^{b}	2.67^{d}	3168.44^{d}	0.00^{d}
	13-HOTrE*	740.27^{b}	779.18^{b}	84.27^{c}	1615.88^{a}	753.39^{b}	123.22^{c}	85.52^{c}	530.84^{b}	746.61^{b}	160.55^{c}	81.30^{c}	1807.62^{a}
	12(S)-HpETE*	0.27^{b}	254.80^{a}	0.35^{b}	0.37^{b}	0.52^{b}	264.63^{a}	0.58^{b}	0.37^{b}	0.50^{b}	251.89^{a}	0.11^{b}	0.31^{b}
	9-KOTrE*	17879.31^{a}	14914.77^{b}	764.41^{e}	12639.78^{b}	18380.18^{a}	3527.42^{d}	758.20^{e}	7829.71^{c}	18377.79^{a}	2315.78^{e}	761.83^{e}	15073.73^{b}
	13-KODE*	10103.22^{b}	7810.54^{c}	1321.30^{d}	16099.55^{a}	10042.41^{b}	2122.81^{d}	1330.11^{d}	5622.89^{c}	10042.41^{b}	2379.03^{d}	1318.21^{d}	16051.70^{a}
Allene oxide synthase	12-OPDA*	1050.02^{c}	2351.15^{b}	214.08^{c}	1984.07^{b}	1072.48^{c}	306.58^{c}	219.00^{c}	1358.62^{c}	1066.01^{c}	265.42^{c}	212.16^{c}	6824.43^{a}
Cytochrome P450	9,10-DiHODE*	54929.60^{b}	58177.16^{b}	6063.29^{e}	65571.54^{b}	55481.44^{b}	7123.79^{e}	6122.00^{e}	30229.56^{c}	55539.04^{b}	12852.18^{d}	6054.92^{e}	98027.91^{a}
	12,13-DiHOME*	2218.28^{b}	2755.52^{b}	326.19^{e}	2395.72^{b}	2032.80^{b}	431.09^{e}	323.49^{e}	1289.37^{c}	2024.81^{b}	759.33^{d}	328.39^{e}	3918.76^{a}
	16,17-EpDPE*	0.02^{d}	5161.15^{c}	0.52^{d}	0.34^{d}	0.45^{d}	6357.31^{b}	0.18^{d}	0.53^{d}	0.25^{d}	7519.81^{a}	0.72^{d}	0.30^{d}

Summary of primary oxylipin (nmol) in the roots of both soybean cultivars. Data presented are means ± standard errors for four sample replicates. Means in the same row accompanied by different superscripts represent significance differences (*) between the treatments, consisting of susceptible root control (ORC) and susceptible root inoculated (ORI); and tolerant root control (CRC) and tolerant root inoculated (CRI) from 10-day old

plants following a of inoculation period of 48 h, 72 h or 96 h. Means in the same row with different superscript letters (a, b, c, d, and e) are indicated as significantly different (*) between the treatments, which consisted of ORC and ORI root tissue; CRC and CRI root tissue, significance level assessed at $\alpha < 0.05$. The oxylipins detected were 10(E),12(E)-9-hydroperoxyoctadeca-10,12-dienoic acid (9-HpODE), 10(E),12(Z), 13S-hydroxy-9(Z),11(E),15(Z)-octadecatrienoic acid (13-HOTrE), and 12S-hydroperoxy-5(Z),8(Z),10(E),14(Z)-eicosatetraenoic acid (12(S)-HpETE), 15(Z)-9-oxo-octadecatrienoic acid (9-KOTrE) and (9Z,11E)-13-Oxo-9,11-octadecadienoic acid (13-KODE), 12-oxophytodienoic acid (12-OPDA), (12*Z*,15*Z*)-9,10-dihydroxyoctadeca-12,15-dienoic acid (9, 10-DiHODE), (*Z*)-12,13-dihydroxyoctadec-9-enoic acid (12,13-DiHOME), and (4*Z*,7*Z*,10*Z*,13*Z*)-15-[3-[(*Z*)-pent-2-enyl]oxiran-2-yl]pentadeca-4,7,10,13-tetraenoic acid (16,17-EpDPE).

Table 4.2. Primary oxylipins (nmol) induced in the stem of soybean cultivars following inoculation with *P. sojae*

Oxylipin pathway	Oxylipin	Relative abundance (nmol)											
		48- h				**72-h**				**96-h**			
		OSC	**OSI**	**CSC**	**CSI**	**OSC**	**OSI**	**CSC**	**CSI**	**OSC**	**OSI**	**CSC**	**CSI**
Lipoxygenase	9-HpODE*	104843.20^{a}	52336.91^{b}	6.88^{c}	0.00^{c}	105792.80^{a}	0.00^{c}	8.47^{c}	0.00^{c}	104642.24^{a}	9.67^{c}	6.67^{c}	52456.14^{b}
	13-HOTrE*	2624.07^{a}	2337.83^{a}	8.35^{c}	1417.53^{b}	2671.72^{a}	744.03^{b}	7.56^{c}	964.44^{b}	2527.26^{a}	4.36^{c}	8.44^{c}	2085.09^{a}
	12(S)-HpETE*	0.39^{d}	32238.70^{c}	0.69^{d}	0.37^{d}	0.64^{d}	48119.54^{b}	0.71^{d}	0.31^{d}	0.59^{d}	87843.49^{a}	0.29^{d}	0.88^{d}
	9-KOTrE*	54403.13^{a}	56014.66^{a}	17.52^{d}	10710.23^{c}	53573.05^{a}	26098.06^{b}	16.95^{d}	8448.08^{c}	55636.58^{a}	0.00^{d}	19.41^{d}	29448.44^{b}
	13-KODE*	39289.67^{a}	34647.07^{a}	34.84^{c}	18152.65^{b}	40906.82^{a}	15947.95^{b}	33.13^{c}	13203.10^{b}	38933.45^{a}	9.80^{c}	35.42^{c}	30887.31^{a}
Allene oxide synthase	12-OPDA*	5209.15^{c}	4683.41^{c}	17.43^{e}	8482.57^{b}	5158.26^{c}	1751.61^{d}	16.12^{e}	4358.54^{c}	5250.67^{c}	0.00^{e}	20.83^{e}	13173.55^{a}
Cytochrome P450	9,10-DiHODE*	135559.71^{a}	152625.22^{a}	64.04^{c}	51317.76^{b}	135578.00^{a}	31076.93^{b}	61.22^{c}	38868.45^{b}	134435.30^{a}	6.48^{c}	64.53^{c}	147879.60^{a}
	12,13-DiHOME*	6514.48^{a}	7361.51^{a}	10.21^{d}	4128.60^{b}	6011.53^{a}	2179.51^{c}	8.04^{d}	4379.30^{b}	7502.90^{a}	6.24^{d}	10.14^{d}	7845.75^{a}
	16,17-EpDPE*	0.59^{d}	19069.21^{b}	0.22^{d}	0.99^{d}	0.60^{d}	16544.95^{c}	0.58^{d}	0.76^{d}	0.46^{d}	72849.52^{a}	0.27^{d}	0.42^{d}

Summary of primary oxylipin (nmol) in the roots of both soybean cultivars. Data represented are means ± standard errors for four sample replicates. Means in the same row accompanied by different superscripts represent significance differences (*) between the treatments, consisting of susceptible stem control (OSC) and susceptible stem inoculated (OSI); and tolerant stem control (CSC) and tolerant stem inoculated (CSI)

from 10-day old plants following of inoculation period of 48 h, 72 h or 96 h. Means in the same row with different superscript letters (a, b, c, d, and e) are indicated as significantly different (*) between the treatments, which consisted of OSC and OSI root tissue; CSC and CSI root tissue, significance level assessed at $\alpha < 0.05$. The oxylipins detected were 10(E*)*,12(E)-9-hydroperoxyoctadeca-10,12-dienoic acid (9-HpODE), 10(E),12(Z), 13S-hydroxy-9(Z),11(E),15(Z)-octadecatrienoic acid (13-HOTrE), and 12S-hydroperoxy-5(Z),8(Z),10(E),14(Z)-eicosatetraenoic acid (12(S)-HpETE), 15(Z)-9-oxo-octadecatrienoic acid (9-KOTrE) and (9Z,11E)-13-Oxo-9,11-octadecadienoic acid (13-KODE), 12-oxophytodienoic acid (12-OPDA), (12*Z*,15*Z*)-9,10-dihydroxyoctadeca-12,15-dienoic acid (9, 10-DiHODE), (*Z*)-12,13-dihydroxyoctadec-9-enoic acid (12,13-DiHOME), and (4*Z*,7*Z*,10*Z*,13*Z*)-15-[3-[(*Z*)-pent-2-enyl]oxiran-2-yl]pentadeca-4,7,10,13-tetraenoic acid (16,17-EpDPE).

Table 4.3. Oxidized glycerolipids (nmol) present in the root of soybean cultivars following inoculation with *P. sojae*

Lipid class	Oxidized glycerolipids	Relative abundance (nmol)			
		ORC	**ORI**	**CRC**	**CRI**
Phosphatidylcholine	PC36:6+2O*	9.65±0.88^{c}	12.47±0.61^{b}	0.00±00^{d}	18.02±0.10^{a}
	PC36:5+2O*	20.10±0.78^{b}	16.58±0.46^{c}	0.00±00^{d}	23.34±0.21^{a}
Phosphatidylethanolamine	PE38:6+O*	15.39±0.28^{b}	25.23±0.45^{a}	0.00±00^{d}	8.58±0.18^{c}
	PE38:6+2O*	9.65±0.88^{b}	11.97±0.39^{a}	0.00±00^{d}	8.79±0.40^{c}
Phosphatidic acid	PA34:3+O*	10.67±0.25^{a}	6.48±0.38^{b}	0.00±00^{c}	10.85±0.26^{a}
Phosphatidylinositol	PI28:3+2O*	3.60±0.21^{a}	3.06±0.13^{a}	0.00±00^{b}	0.36±0.02^{b}
Triacylglycerol	TG50:3+O*	7.63±0.17^{b}	12.81±0.57^{a}	0.38±0.16^{d}	6.49±0.23^{c}
	TG52:6+O*	5.33±0.16^{a}	3.97±0.32^{b}	0.00±00^{d}	0.75±0.05^{c}
	TG54:2+O*	2.52±0.20^{b}	1.63±0.60^{c}	0.12±0.01^{d}	3.51±0.20^{a}
	TG54:8+2O*	1.34±0.53^{d}	5.05±0.25^{c}	37.92±0.23^{a}	19.63±0.15^{b}
	TG54:8+3O*	1.55±0.41^{b}	2.03±0.50^{a}	0.31±0.01^{c}	2.12±0.04^{a}
	TG54:6+Ox*	0.38±0.20^{d}	3.02±0.13^{c}	51.45±0.29^{a}	24.56±0.41^{b}

Summary of oxidized GLs (nmol) in the roots of both soybean cultivars. Data represented are means ± standard errors for four sample replicates. Means in the same row accompanied by different superscripts represent significance differences (*) between the treatments, consisting of susceptible root control (ORC) and susceptible root inoculated (ORI); and tolerant root control (CRC) and tolerant root inoculated (CRI) from 10-day old plants. Means in the same row with

different superscript letters (a, b, c, d, and e) are indicated as significantly different (*) between the treatments, which consisted of ORC and ORI root tissue; CRC and CRI root tissue, significance level assessed at $\alpha < 0.05$. The oxylipins detected were oxidized phosphatidylcholine (Ox-PC), oxidized phosphatidylethanolamine (Ox-PE), oxidized phosphatidic acid (Ox-PA), oxidized phosphatidylinositol (Ox-PI), and oxidized triacylglycerol (Ox-TG), O = monoxide, 2O = dioxide, 3O = trioxide and Ox = oxidized.

Table 4.4. Oxidized glycerolipids (nmol) in the stem of soybean cultivars following inoculation with *P. sojae*

Lipid class	Oxidized glycerolipid	Relative abundance (nmol)			
		OSC	**OSI**	**CSC**	**CSI**
Phosphatidylcholine	PC36:6+2O*	1.85±0.07^{b}	0.19±0.07^{c}	0.35±0.20^{c}	3.75±0.20^{a}
	PC36:5+2O*	17.41±0.40^{b}	20.18±0.58^{a}	17.62±0.66^{b}	19.75±0.16^{a}
Phosphatidylethanolamine	PE38:6+O*	22.45±0.31^{b}	24.17±0.60^{a}	21.81±0.35^{b}	20.96±0.36^{c}
	PE38:6+2O*	18.07±0.63^{b}	20.18±0.58^{a}	17.63±0.60^{b}	19.53±0.46^{a}
Phosphatidic acid	PA34:3+O*	0.04±0.00^{c}	0.05±0.02^{c}	16.27±0.21^{a}	6.40±0.17^{b}
Triacylglycerol	TG54:8+2O*	1.76±0.32^{c}	0.69±0.23^{d}	9.79±2.00^{a}	6.20±0.30^{c}
	TG54:8+3O*	0.93±0.02^{c}	1.20±0.90^{b}	1.30±0.30^{b}	2.03±0.90^{a}
	TG52:6+O*	0.62±0.13^{c}	0.33±0.21^{c}	1.81±0.20^{b}	2.87±0.85^{a}
	TG54:9+O*	4.29±1.55^{a}	3.10±0.72^{b}	0.09±0.05^{d}	0.49±0.14^{c}
	TG60:9+5O*	4.24±1.00^{d}	6.37±0.82^{c}	22.46±6.00^{b}	24.22±0.47^{a}
	TG60:8+5O*	0.47±0.20^{d}	2.35±1.16^{c}	17.90±5.00^{b}	24.19±0.62^{a}
	TG60:10+6O*	47.05±0.31^{b}	67.13±4.64^{a}	0.17±0.10^{c}	0.00±0.00^{c}
	TG54:2+Ox*	0.00±0.00^{c}	0.00±0.00^{c}	5.26±2.00^{b}	7.34±0.47^{a}

Summary of oxidized GLs (nmol) in the stems of both soybean cultivars. Data represented are means ± standard errors for four sample replicates. Means in the same row accompanied by different superscripts represent significance differences (*) between the treatments, consisting of susceptible stem control (OSC) and susceptible stem inoculated (OSI); and tolerant stem control

(CSC) and tolerant stem inoculated (CSI) from 10-day old plants. Means in the same row with different superscript letters (a, b, c, d, and e) are indicated as significantly different (*) between the treatments, which consisted of OSC and OSI root tissue; CSC and CSI root tissue, significance level assessed at $\alpha < 0.05$. The oxylipins detected were oxidized phosphatidylcholine (Ox-PC), oxidized phosphatidylethanolamine (Ox-PE), oxidized phosphatidic acid (Ox-PA), and oxidized triacylglycerol (Ox-TG), O = monoxide, 2O = dioxide, 3O = trioxide, 4O = tetroxide, 5O = pentoxide, 6O = hexoxide and Ox = oxidized.

4.4.2. Phyto-oxylipin induction in susceptible and tolerant soybean cultivars in response to *P. sojae* infection

Analysis of primary oxylipins demonstrated significant changes in the root and stem phyto-oxylipins between the two soybean cultivars prior to and during interaction with the oomycete *P. sojae.* Figs. 4.2a-c and 4.3a-c show the levels of oxylipin alterations that occurred during soybean-*P. sojae* interactions. The model quality (Q^2) generated from PLS-DA explains 65 % variability in the root and 60 % variability in the stem. Heat maps (Figs. 4.2a, 4.3a) were prepared for both oxidized GLs and primary oxylipins with important loadings representing the cultivar and treatment separation to further categorize the treatments based on the alterations observed in response to *P. sojae* infection. Meanwhile, no significant differences were observed between the time points for the control treated plants, therefore, averaged results were used in the heat map. The cut-off score for variables important in projection (VIP) results was defined as >1 (Nadeem et al., 2020; Ravipati, Baldwin, Barr, Fogarty, & Barrett, 2015). The 21 phyto-oxylipins in the root (12 oxidized GLs and nine primary oxylipins) and 22 phyto-oxylipins in the stem (13 oxidized GLs and nine primary oxylipins) were selected based on VIP results. The outcome from the heatmap demonstrated four distinct clusters of the soybean root and stem oxylipins following inoculation with *P. sojae* (Figs. 4.2a, 4.3a).

The heatmap ordinate root and stem phyto-oxylipins into two major groups (G), G1 and G2 (Figs. 4.2a, 4.3a). The susceptible and tolerant cultivars could be distinguished at each time point and by inoculation status (Fig. 4.2a). Differences were observed in phyto-oxylipins in both soybean cultivars, corresponding to G1, where the relative abundance of five GLs, PA34:3+O, PC36:5+2O, PC36:6+2O, TG(54:2+O) and TG(54:8+3O) and seven primary oxylipins, 9-HpODE, 12,13-DiHOME, 9,10-DiHODE, 13-HOTrE, 12-OPDA, 13-KODE, 9-KOTrE were

significantly increased in the tolerant cultivar but significantly decreased in the susceptible cultivar when challenged with *P. sojae* for 48 h, 72 h and 96 h time points, except 9-HpODE that reduced in the tolerant cultivar at 72 h and 96 h time points (Fig. 4.2a). In G2, the relative abundance of seven GLs {TG(50:3+O), PE38:6+O, PE38:6+2O, TG(52:6+O), PI28:3+2O, TG(54:8+2O) and TG(54:6+Ox)} and two primary oxylipins, 12(S)-HpETE and 16,17-EpDPE were significantly increased in the susceptible cultivar at 48 h, 72 h and 96 h after infection with the pathogen, but contrarily, these oxylipins were not observed in the non-infected control of both cultivars and infected tolerant cultivar (Fig. 4.2a). These results were supported by the relative abundance of the oxidized GLs (Fig. 4.2b) and the concentration of primary oxylipins (Fig. 4.2c) in the root of both soybean cultivars. In a similar manner, the heat map groupings differentiated the stem oxylipins in the susceptible cultivar from the tolerant cultivar based on time of inoculation (Fig. 4.3a). Differences were observed in phyto-oxylipins in both soybean cultivars, corresponding to G1, where the relative abundance of five oxidized GLs {PE38:6+2O, PC36:5+2O, TG(54:9+O), TG(60:10+6O) and PE38:6+O} and eight primary oxylipins, 16,17-EpDPE, 12(S)-HpETE, were significantly increased in infected susceptible cultivar but not observed both non-infected control of both cultivars and infected tolerant cultivar, while 9-KOTrE, 9-HpODE, 12,13-DiHOME, 9,10-DiHODE, 13-HOTrE and 13-KODE were significantly increased in infected tolerant cultivar but reduced in infected susceptible cultivar at 48 h, 72 h and 96 h (Fig. 4.3a). Oxylipins belonging to G2 consisted of eight oxidized GLs {PC36:6+2O, TG(52:6+O), TG(54:8+3O), TG(54:8+2O), PA34:3+O, TG(54:2+Ox), TG(60:9+5O), TG(60:8+5O)} and one primary oxylipins, 12-OPDA which was increased in the tolerant cultivar but reduced in the susceptible cultivar at 48 h, 72 h and 96 h after infection with *P. sojae*. We observed significant increases in seven primary oxylipins at all time points in the tolerant cultivar relative to the non-inoculated control while only two

primary oxylipins were increased in the susceptible cultivar at all three time points relative to the control in response to the pathogen infection (Fig. 4.3a). These results were supported by the relative abundance of the oxidized GLs (Fig. 4.3b) and the concentration of primary oxylipins (Fig. 4.3c) in the stem of both soybean cultivars. Generally, these results demonstrated that the total numbers of primary oxylipins in root and stem significantly increased in the tolerant soybean cultivar than that of the susceptible cultivar following inoculation with *P. sojae*.

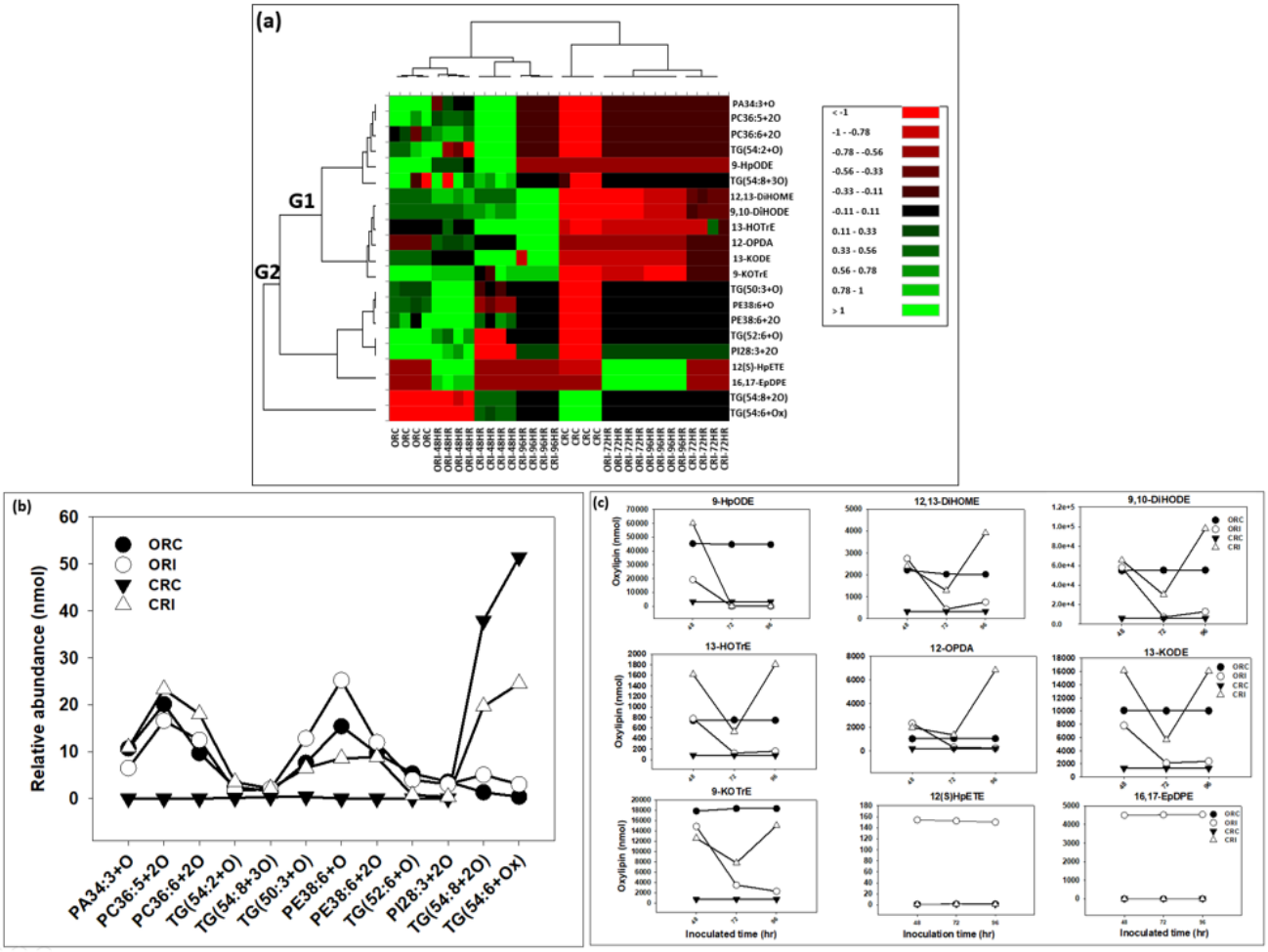

Fig. 4.2. Changes in phyto-oxylipins biosynthesized in root of both soybean cultivars infected with *P. sojae* relative to non-infected plants. (a) Heat map showing clusters of oxylipins in susceptible (OX760-6) and tolerant (Conrad) inoculated or non-inoculated with *P. sojae*. Each soybean cultivar and treatment were clustered independently using ascendant order clustering established on Euclidian distance at 0.15 interquartile range. The left columns represent the cluster-separated root phyto-oxylipins, whereas the top columns separated the cultivars

established on similarities in abundance of phyto-oxylipins. Red, black, and green colors denote lower, intermediate, and higher abundance of root phyto-oxylipins. Group 1 and 2 (G1 and G2) are induced phyto-oxylipins that were responsible cluster patterns in the heat map used to determine differences between susceptible and tolerant cultivars; (b) Line graphs showing significant changes in oxidized GLs in the root of both cultivars following inoculation over 96 h and (c) Line graphs showing significant changes in primary oxylipins in the root of both cultivars following inoculation for over 96 h. The phyto-oxylipins observed to be significantly different in each group (G1 and G2) of the heat map are displayed in the line graphs. Values represents mean nanomole percent with n = 4 per time point. No detectable response was observed at 24 h of inoculation (data not shown).

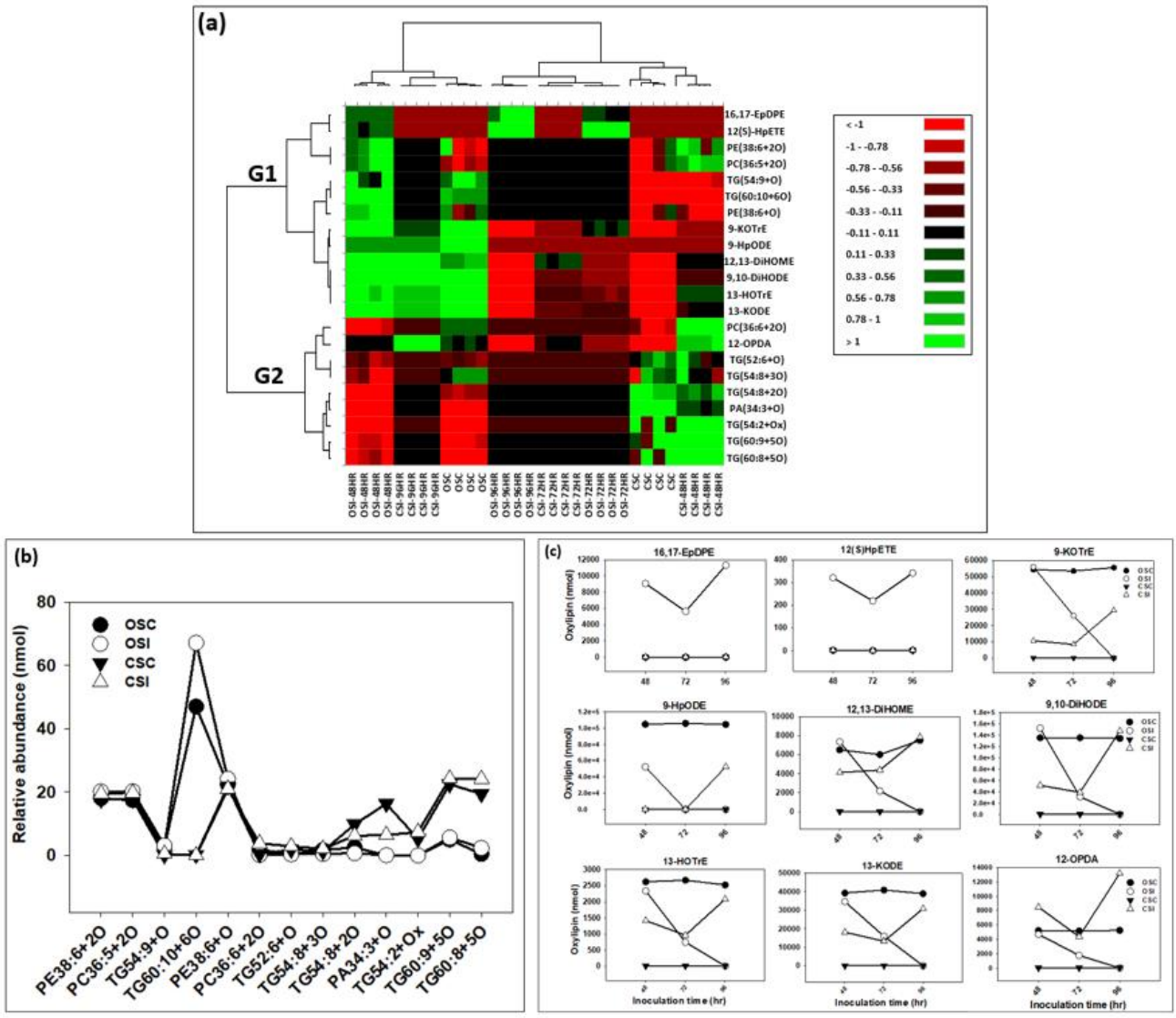

Fig. 4.3. Changes in phyto-oxylipins biosynthesized in stem of both soybean cultivars infected with *P. sojae* relative to non-infected plants. (a) Heat map showing clusters of oxylipins in susceptible (OX760-6) and tolerant (Conrad) inoculated or non-inoculated with *P. sojae*. Each soybean cultivar and treatment were clustered independently using ascendant order clustering established on Euclidian distance at 0.15 interquartile range. The left columns represent the cluster separated stem phyto-oxylipins, whereas the top columns separated the cultivars established on similarities in abundance of phyto-oxylipins. Red, black, and green colors denote

lower, intermediate, and higher abundance of stem phyto-oxylipins. Group 1 and 2 (G1 and G2) are induced oxylipins that were responsible cluster patterns in the heat map used to determine differences between susceptible and tolerant cultivars; (b) Line graphs showing significant changes in oxidized GLs in the stem of both cultivars following inoculation over 96 h and (c) Line graphs showing significant changes in primary oxylipins in the stem of both cultivars following inoculation for over 96 h. The phyto-oxylipins observed to be significantly different in each group (G1 and G2) of the heat map are displayed in the line graphs. Values represents mean nanomole percent with n = 4 per time point. No detectable response was observed at 24 h of inoculation (data not shown).

4.4.3. Spearman's correlation between oxidized glycerolipids and primary oxylipins in soybean cultivars in response to *P. sojae* infection

Spearman's correlation coefficients of 12 oxidized GLs and nine primary oxylipins are shown in Fig. 4.4a. The correlation coefficient (r) was strongly positive for the relationships between 16,17-EpDPE, 13-HOTrE, 12,13-DiHOME, 9,10-DiHODE, 12-OPDA, 13-KODE, 9-KOTrE, 12(S)-HpETE, 9-HpODE and PA30:4+2O, PC36:5+2O, PC36:6+2O TG(54:2+O), TG(54:8+3O), TG(50:3+O), PE38:6+3O, PE38:6+2O, TG(52:2+O) and PI28:3+2O but strongly negative for TG(54:6+Ox) and TG(54:8+2O). The strongest significant positive correlation ranged between 0.455 to >1.000 for these relationships. Generally, strong positive correlations were observed between oxidized GLs and primary oxylipins in the root of both soybean cultivars following inoculation with *P. sojae* infection (Fig. 4.4a). Similarly, in the stems of both cultivars, strongly positive and negative correlations were observed in response to infection (Fig. 4.4b). As demonstrated in Fig. 4.4b, 12-OPDA was strongly positively correlated with oxidized GLs with correlation ranging between 0.445 to > 0.818. The other primary oxylipins, 12,13-DiHOME, 9,10-DiHODE, 12(S)-HpETE, 9-KOTrE, 16,17-EpDPE, 13-KODE, 13-HOTrE, and 9-HpODE, exhibited significant positive correlation ranging between 0.273 to > 0.455 as well as significant inverse (negative) correlation ranging between -0.455 to > -0.273 with TG(60:8+5O), TG(60:9+5O) and TG(54:2+Ox).

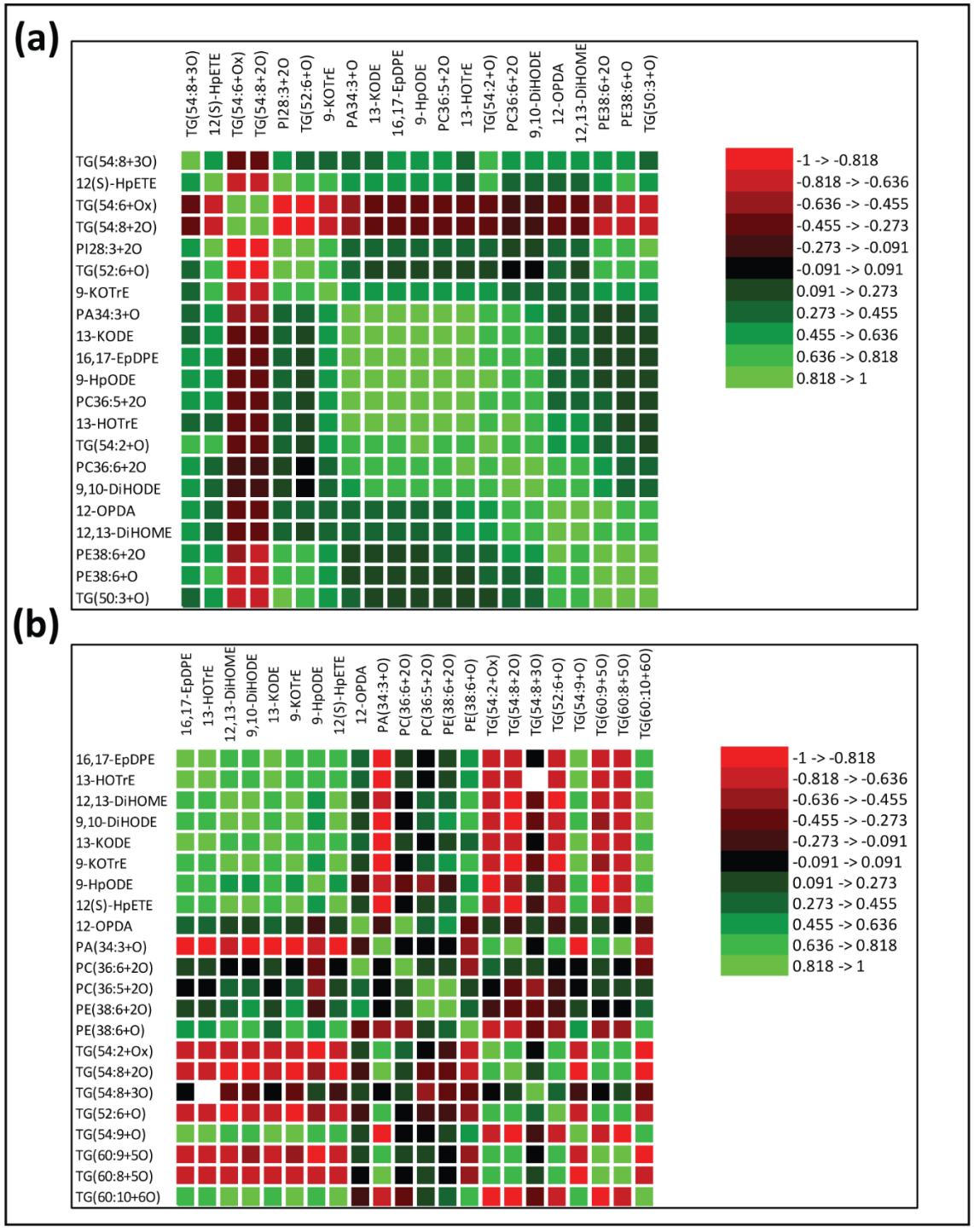

Fig. 4.4. Spearman's rank correlation coefficients heatmap between relative abundance of oxidized GLs and primary oxylipins in the susceptible (OX760-6) and tolerant (Conrad) soybean cultivars. (a) Correlation between oxidized GLs and primary oxylipins in the root of susceptible

and tolerant soybean cultivars infected with pathogen relative to non-infected plants; (b) Correlation between oxidized GLs and primary oxylipins in the stem of susceptible and tolerant soybean cultivars infected with pathogen relative to non-infected plants. Colours indicate the Spearman correlations' ρ values, that's the level of correlation between oxidized GLs and primary oxylipins. The ρ values between <-0.5 and > 0.5 have a significant value of $P < 0.05$. To generate the heatmap, cluster analyses were carried out using the group average method to cluster oxidized GLs and primary oxylipins that have similar Spearman rank coefficients. 16,17-EpDPE = (4*Z*,7*Z*,10*Z*,13*Z*)-15-[3-[(*Z*)-pent-2-enyl] oxiran-2-yl] pentadeca-4,7,10,13-tetraenoic acid, 13-HOTrE = 10(E),12(Z),13S-hydroxy-9(Z),11(E),15(Z)-octadecatrienoic acid, 12,13-DiHOME = (*Z*)-12,13-dihydroxyoctadec-9-enoic acid, 9, 10-DiHODE = (12*Z*,15*Z*)-9,10-dihydroxyoctadeca-12,15-dienoic acid, 12-OPDA = 12-oxophytodienoic acid, 13-KODE = (9Z,11E)-13-Oxo-9,11-octadecadienoic acid, 9-KOTrE = 15(Z)-9-oxo-octadecatrienoic acid, 12(S)-HpETE = 12S-hydroperoxy-5(Z),8(Z),10(E),14(Z)-eicosatetraenoic acid, and 9-HpODE = 10(E*)*,12(E)-9-hydroperoxyoctadeca-10,12-dienoic acid, oxidized phosphatidylcholine (Ox-PC), oxidized phosphatidylethanolamine (Ox-PE), oxidized phosphatidic acid (Ox-PA), oxidized phosphatidylinositol (Ox-PI), and oxidized triacylglycerol (Ox-TG), O = monoxide, 2O = dioxide, 3O = trioxide and Ox = oxidized.

4.4.4. Phyto-oxylipin network analysis showing from a systems biology perspective how root and stem lipidome of both soybean cultivars respond to *P. sojae* infection

A phyto-oxylipin biochemical network was used to visualize the alterations in soybean root and stem oxylipin induction when challenged with *P. sojae* infection. It was demonstrated that phyto-oxylipin anabolism mediated plant immunity significantly increases among the primary oxylipins at all time points in the tolerant cultivar relative to the non-inoculated control, while the same FA mediated plant immunity were reduced in the susceptible cultivar at all three time points relative to the control in response to the pathogen infection. Selected root and stem oxylipins among the inoculated susceptible cultivar showed significant decreases compared to the reference group at 96 h (Figs. 4.5, 4.6). Generally, only two primary oxylipins in the root, including 16,17-EpDPE, and 12(S)-HpETE were significantly increased in the susceptible cultivar at 48 h, 72 h and 96 h following inoculation with *P. sojae* relative to the non-inoculated control, except 12-OPDA which was increased after 48 h inoculated and later decreased at 72 h and 96 h. Contrary to susceptible cultivar, six primary oxylipins in the root of the tolerant cultivar, which included 13-HOTrE, 12,13-DiHOME, 13-KODE, 9-KOTrE, 12-OPDA and 9, 10-DiHODE, were significantly increased at all time points following inoculation relative to the non-inoculated control; the one exception was 9-HpODE, which significantly increased only 48 h after inoculation (Fig. 4.5). Similarly, only primary oxylipins in stem, including 16,17-EpDPE and 12(S)-HpETE were significantly increased in the susceptible soybean cultivar at all time points following inoculation relative to the non-inoculated control. Contrary to the susceptible cultivar, seven primary oxylipins in stem, which included 13-HOTrE, 12,13-DiHOME, 13-KODE**,** 9-KOTrE, 12-OPDA, 9-HpODE, and 9, 10-DiHODE were significantly increased in the tolerant cultivar at all time points following inoculation relative to the non-inoculated control. Notably, there were fold increase in 9-HpODE,

13HOTrE, 13-KODE, 9,10-DiHODE, 9-KOTrE, 12-OPDA and 12,13-DiHOME in the root and stem control but decreased in the infected root and stem of susceptible cultivar at 48 h, 72 h and 96 h time points. In contrast, fold increase of seven oxylipins were observed in the infected root and stem of tolerant cultivars and two oxylipins in the infected root and stem of susceptible cultivar but decreased in control root and stem of both cultivars at 48 h, 72 h and 96 h time points (Fig. 4.5, 4.6).

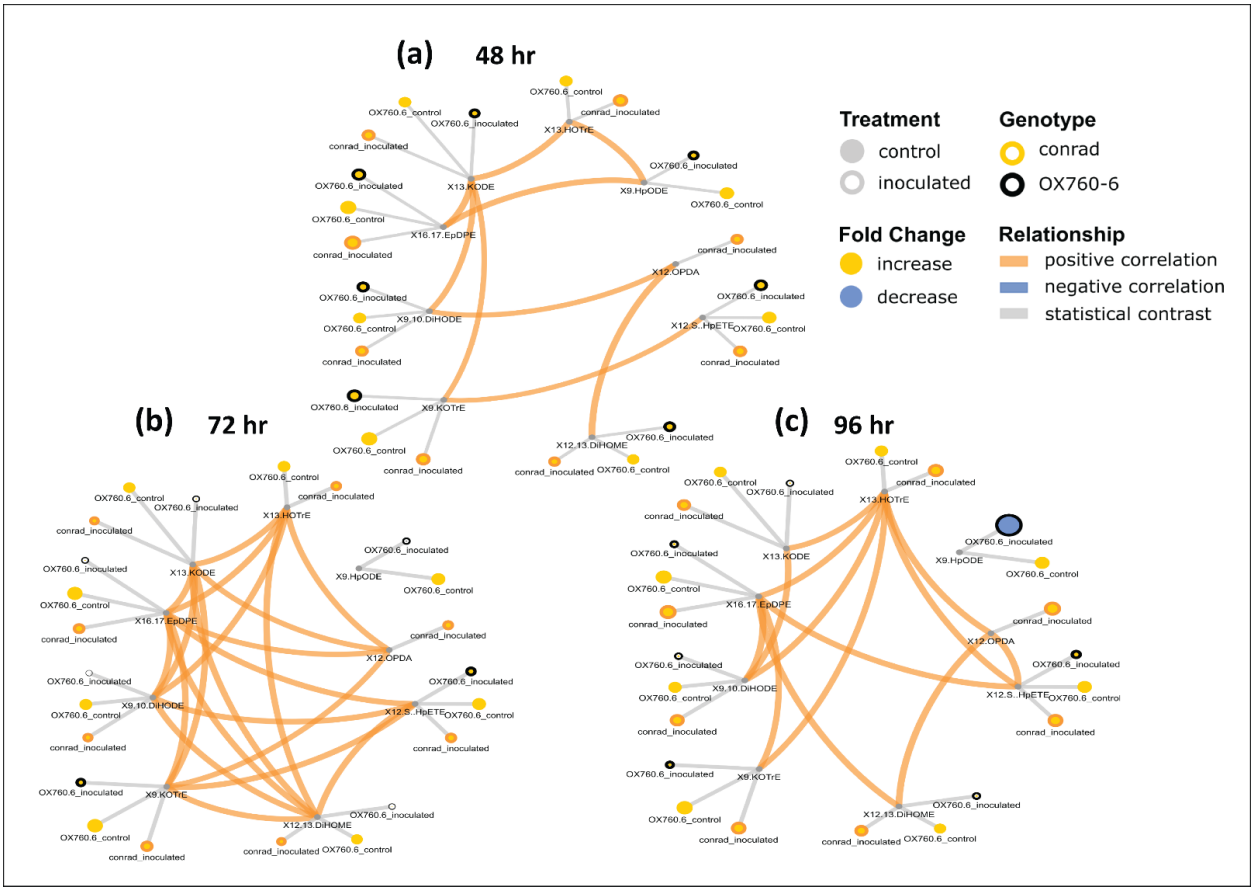

Fig. 4.5. Oxylipin network displaying differences in root phyto-oxylipins in susceptible and resistant soybean cultivars following *P. sojae* inoculation relative to non-inoculated plants. (a) Control and inoculated susceptible soybean root (ORC and ORI), and control and inoculated tolerant soybean root (CRC and CRI) at 48 h time point, (b) control and inoculated susceptible soybean root (ORC and ORI), and control and inoculated tolerant soybean root (CRC and CRI) at 72 h time point, (c) control and inoculated susceptible soybean root (ORC and ORI), and control and inoculated tolerant soybean root (CRC and CRI) at 96 h time point. The network of phyto-oxylipins demonstrate fold changes in nine root primary oxylipins following infection with *P. sojae*. Lipid SMILES identifiers were applied to determine PubChem molecular

fingerprints and phyto-oxylipin similarity structure. Mapped structural networks showing significance of fold changes in phyto-oxylipins were calculated for all comparisons. The network visualizes the phyto-oxylipins with connections established on structural Tanimoto similarity ≥ 0.8 (edge width: 0.8-1.0). Node size shows fold changes of means between comparisons and color demonstrates the direction of alteration compared to control (yellow: increased; blue: decreased; gray: statistical contrast). Node shape shows phyto-oxylipin structural type (gray circle: control, rounded gray: inoculated; rounded yellow: Conrad (tolerant soybean cultivar) and rounded black: OX760-6 (susceptible soybean cultivar), brown = positive correlation and blue = negative correlation. Oxylipins displaying significant differences between treatment groups (*p-value* ≤ 0.05) are denoted with rounded yellow.

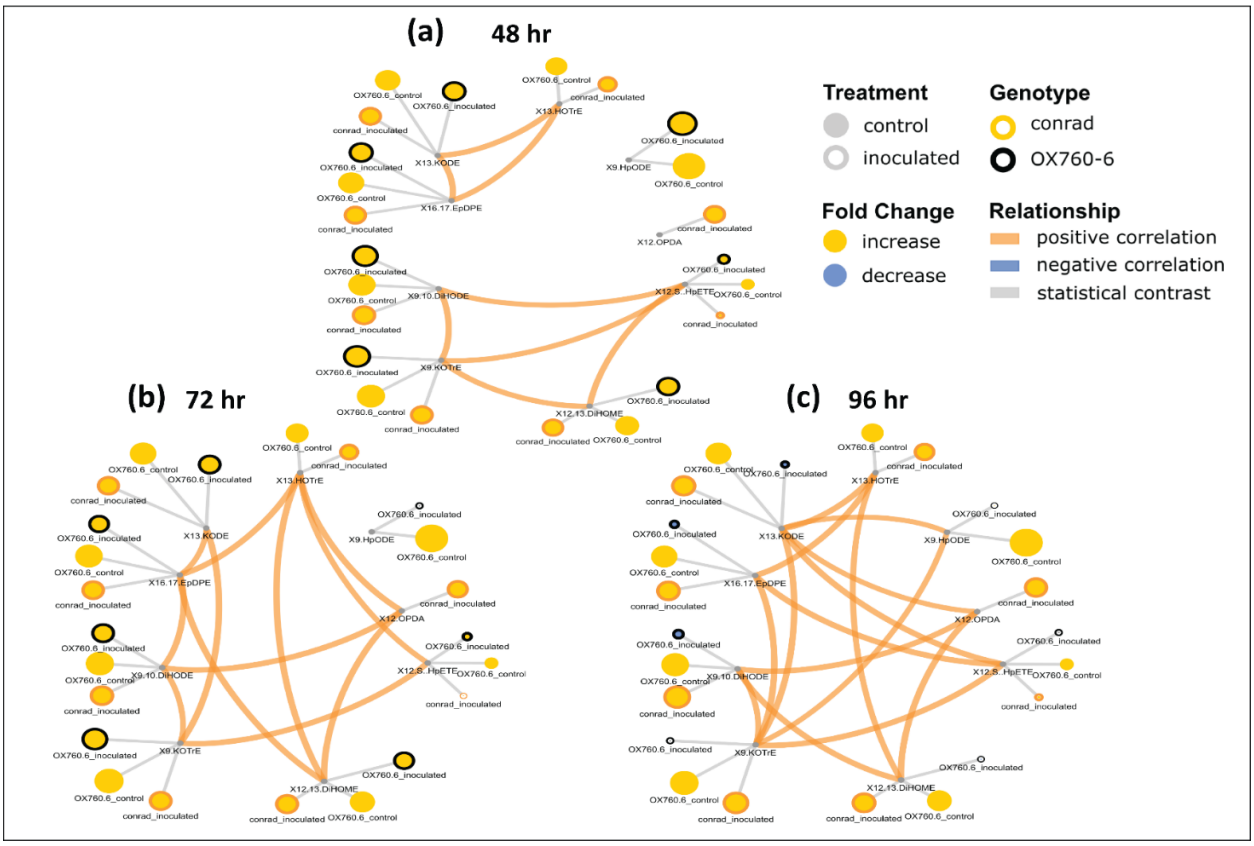

Fig. 4.6. Oxylipin network displaying differences in stem phyto-oxylipins in susceptible and resistant soybean cultivars following *P. sojae* inoculation relative to non-inoculated plants. (a) Control and inoculated susceptible soybean stem (OSC and OSI), and control and inoculated tolerant soybean stem (CSC and CSI) at 48 h time point, (b) control and inoculated susceptible soybean stem (OSC and OSI), and control and inoculated tolerant soybean stem (CSC and CSI) at 72 h time point, and (c) control and inoculated susceptible soybean stem (OSC and OSI) and control and inoculated tolerant soybean stem (CSC and CSI) at 96 h time point. The network of phyto-oxylipins demonstrates fold changes in nine root primary oxylipins following infection with *P. sojae*. Lipid SMILES identifiers were applied to determine PubChem molecular fingerprints and phyto-oxylipin similarity structure. Mapped structural networks, showing

significance of fold changes in phyto-oxylipins were calculated for all comparisons. The network visualizes the phyto-oxylipins with connections established on structural Tanimoto similarity ≥ 0.8 (edge width: 0.8-1.0). Node size shows fold changes of means between comparisons and color demonstrates the direction of alteration compared to control (yellow: increased; blue: decreased; gray: statistical contrast). Node shape shows phyto-oxylipin structural type (gray circle: control, rounded gray: inoculated; rounded yellow: Conrad (tolerant soybean cultivar) and rounded black: OX760-6 (susceptible soybean cultivar), brown = positive correlation and blue = negative correlation. Oxylipins displaying significant differences between treatment groups (*p-value* ≤ 0.05) are denoted with rounded yellow.

4.5. Discussion

Based on the limited understanding of the biochemical and physiological properties of oxylipins, a comprehensive study of oxylipins was generated from the root and stem of tolerant and susceptible soybean cultivars challenged with *P. sojae* to examine the alterations in oxylipin levels across three time points. All identified primary oxylipins generated from both soybean cultivars demonstrated significant alterations in response to infection, and oxidized GLs generated from membrane lipids following oxidation of PUFAs. These PUFAs are predicted to serve as substrates for the biosynthesis of primary oxylipins following *P. sojae* colonization and infection. At 48 h, 72 h and 96 h of infection by *P. sojae*, compared to controls, we observed that oxylipins significantly decreased in the root and stem of susceptible soybean while they significantly increased in the root and stem of tolerant soybean. The results obtained from our studies are in agreement with the responses observed for different classes of oxylipins studies reported in literature (Gao et al., 2008). For instance, studies have shown that application of synthetic JA to tomato foliage triggers a systemic effect that allows the plant to resist root-knot nematode invasion (Gao, Stumpe, Feussner, & Kolomiets, 2008). This was accompanied by the production of JA to enclose the nematode invasion at the initial area of infection, and then inhibit nematode colonization and infection (Jingwei et al., 2014). Also, other studies have demonstrated the effects of JA-induced defense responses on pathogenic organisms and the use of exogenous MeJA was observed to induce resistance in the root of oats and spinach against pathogenic nematodes (Soriano, Asenstorfer, Schmidt, & Riley, 2004). It has been well established that jasmonates play active roles during foliar and root defense responses to infection (Smith, De Moraes, & Mescher, 2009).

Similarly, several studies have implicated LOXs and their derivatives in the plant defense response against diverse pathogens (Kolomiets, Hannapel, Chen, Tymeson, & Gladon, 2001). For instance, a novel cyclopentenone, 10-oxo-11-phytodienoic acid synthesized through 9-LOX activities, and which is an isomer of 12-OPDA, the precursor of jasmonate, was isolated from young tubers and stolons of potato (*Solanum tuberosum*). It is possible that 9-LOX may play a role during jasmonate biosynthesis to control tuber growth and also function in the defense response against pathogenic attack (Kolomiets et al., 2001). Moreover, the application of some hydroperoxide derivatives of oxylipins have been demonstrated to inhibit conidial germination and elongation of germ-tube of the rice blast pathogen *Pyricularia oryzae* (Naor et al., 2018), and C18:2 hydroperoxides have demonstrated toxic effects on *Saccharomyces cerevisiae* (Naor et al., 2018). Furthermore, it was demonstrated that following pathogenic attack of the moss *Physcomitrella patens* by various microbial pathogens including *Pectobacterium carotovorum, Pectobacterium wasabiae* and *Botrytis cinerea*, the host induces a defense response by elevating the levels of endogenous FFAs and activating gene transcription encoding various LOXs, AOS, and OPDA acid reductase (Inés Ponce de León et al., 2007; I. Ponce De León et al., 2012). In these pathosystems, the 13-/ 12-LOX pathways were suggested to be activated after pathogen attack. The transcript levels of PpLOX1 and PpLOX6 were increased following infection by *Pythium cinerea* and *Botrytis cinerea* respectively, and the concentrations of OPDA increased in response to both pathogens (Oliver et al., 2009; I. Ponce De León et al., 2012). In the present study, we found that primary oxylipins 9-HpODE, 12,13-DiHOME, 9,10-DiHODE, 12-OPDA, 9-KOTrE, 13-HOTrE and 13-KODE were significantly decreased in the susceptible soybean cultivar in contrast to the significant increase observed in the tolerant soybean cultivar. These subclasses of oxylipins mediated tolerance to *P. sojae* infection in tolerant soybean as a function of time.

Contrarily, 16,17-EpDPE and 12(S)-HpETE were observed to be significantly increased in the root and stem of the susceptible soybean cultivar, and they were known to be microbial-derived oxylipins associated with pathogenesis in susceptible soybean cultivar (Niu & Keller, 2019). Taken together, these results demonstrate that oxylipins participate in early defenses in soybean response to *P. sojae* infection.

The oxidized GLs network analysis presents a significant challenge due to a lack of well-defined biochemical interaction databases and general lipid enzyme substrate promiscuity among FFA, membrane and neutral lipids. When lipid structures are known, estimates of similarities among lipid activities can be inferred based on structural similarities or mass spectra. Regularized correlations between lipid measurements were used to calculate primary oxylipin interaction networks for each of the three inoculation time points. All observed conditionally independent correlations between lipids were positive which can occur in cases where lipids are in homeostasis or share storage and sources of release (DeMarsay, 2005). Lipid statistical contrasts between groups can be compared between time points to identify patterns of change. The network demonstrates the connectivity between the changes in phyto-oxylipins induction and the oxylipin biosynthesis pathway in the tolerant cultivar as defense response to *P. sojae* invasion. Generally, there is scarcity of information on the function of oxylipin induction to determine either compatible or incompatible interactions governing tolerance or susceptibility in the soybean-*P.sojae* pathosystem. The unique level of alterations in oxylipin induction between susceptible and tolerant cultivars showed that primary oxylipins 9-HpODE, 12,13-DiHOME, 9,10-DiHODE, 12-OPDA, 9-KOTrE, 13-HOTrE, and 13-KODE were significantly decreased in the root and stem of the susceptible soybean cultivar in contrast to the significant increase observed in the root and stem of the tolerant soybean cultivar (Figs 4.5, 4.6). Studies have demonstrated that these oxylipins play

active roles during plant disease resistance, or are involved in plant defense strategies against pathogen invasion (Blée, 2002).

Biosynthesis of oxylipins has been characterized in other systems (Genva et al., 2019). Polyunsaturated FAs such as C18:3 and C18:2 may be hydrolyzed by one, two or four oxygen atoms through PLA and undergo further enzymatic reactions to generate oxidized GLs (Blée, 2002; Liu et al., 2019). Acyltransferases biosynthesize oxidized phospholipids (Domingues, Reis, & Domingues, 2008; Liu et al., 2019), and diacylglycerol acyltransferases biosynthesize oxidized TG (Irshad, Dimitri, Christian, & Zammit, 2017). These oxidized lipids were associated with primary oxylipins that were further generated through enzymatic activities (Figs 4.7, 4.8). In the root samples of both cultivars, TG(54:8+3O) correlated with 12(S)-HpETE, 16,17-EpDPE, 9-HpODE, 9,10-DiHODE, 12-OPDA and 12,13-DiHOME; TG(52:6+O) correlated with 12(S)-HpETE, 9-KOTrE and 12,13-DiHOME, TG(54:2+O) correlated with 12(S)-HpETE, 13-KODE, 16,17-EpDPE, 9-HpODE, 13-HOTrE and 9,10-DiHODE; TG50:3+O correlated with 12(S)-HpETE, 9-KOTrE, 12-OPDA and 12,13-DiHOME; PI28:3+2O correlated with 12(S)-HpETE and 9-KOTrE; PA34:3+O correlated with 12(S)-HpETE, 9-KOTrE, 13-KODE, 16,17-EpDPE, 9-HpODE, 13-HOTrE and 9,10-DiHODE; PC36:5+2O correlated with 12(S)-HpETE, 9-KOTrE, 13-KODE, 16,17-EpDPE, 9-HpODE, 13-HOTrE and 9,10-DiHODE; PC36:6+2O correlated with 9-KOTrE, 13-KODE, 16,17-EpDPE, 9-HpODE, 13-HOTrE, 9,10-DiHODE, 12-OPDA and 12,13-DiHOME; PE38:6+2O correlated with 9-KOTrE, 9,10-DiHODE, 12-OPDA and 12,13-DiHOME; and PE38:6+O correlated with 12-(S)HpETE, 9-KOTrE, 9,10-DiHODE, 12-OPDA and 12,13-DiHOME (Fig 4.7). Seven of these primary oxylipins produced in the root of tolerant cultivar were generally increased across the time points (48 h, 72 h and 96 h) but reduced in the root of susceptible cultivar, and it seems that it was signally pathway activated that may appear to be the

route tolerance or protection achieved in tolerant cultivar (Fig. 4.7). In the stems of both cultivars, TG54:2+Ox correlated with 12-OPDA; TG(54:8+3O) correlated with 9-HpODE and 12-OPDA; TG(54:9+O) correlated with 16,17-EpDPE, 13-HOTrE, 12,13-DiHOME, 9,10-DiHODE; 13-KODE, 9-KOTrE, 9-HpODE, 12-(S)HpETE and 12-OPDA; TG(60:9+5O) correlated with 12-OPDA; TG(60:10+6O) correlated with 9-HpODE and 12-OPDA; TG(54:9+O) correlated with 16,17-EpDPE, 13-HOTrE, 12,13-DiHOME, 9,10-DiHODE; 13-KODE, 9-KOTrE, 9-HpODE and 12(S)-HpETE; PC(36:6+2O) correlated with 16,17-EpDPE, 13-HOTrE, 13-KODE and 12-OPDA; PC(36:5+2O) correlated with 12,13-DiHOME, 9,10-DiHODE, 9-KOTrE, 12(S)-HpETE and 12-OPDA; PE(38:6+2O) correlated with 16,17-EpDPE, 13-HOTrE, 12,13-DiHOME, 9,10-DiHODE, 13-KODE, 9-KOTrE, 12(S)-HpETE and 12-OPDA, and PE(38:6+O) correlated with 16,17-EpDPE, 13-HOTrE, 12,13-DiHOME, 9,10-DiHODE, 13-KODE, 9-KOTrE, 9-HpODE and 12(S)-HpETE (Fig 4.8).

Similarly, these oxidized GLs are highly associated with primary oxylipins and seven of these primary oxylipins produced in the stem of tolerant cultivar were generally increased across the time points (48 h, 72 h and 96 h) but reduced in the stem of susceptible cultivar, and it seems that it was signally pathway activated that may appear to be the route tolerance or protection achieved in tolerant cultivar (Fig. 4.8). The hydroperoxides were further metabolized through enzymatic activities to produce various array of oxylipins. Various groups of enzymes have been shown to participate in oxylipin formation, and radical pathways are also important (Blée, 2002). These enzymes, including LOX and α-DOX, insert atoms of oxygen into FA chains and initiate pathways involving specialised CYP450 monooxygenases that may be responsible for their downstream regulation (Blée, 2002; Griffiths, 2015). Furthermore, enzymes like AOS leading to JA signaling which may be responsible for synthesizing pathogen defensive volatiles, as well as

POs and DESs that involved in producing antimicrobials may form part of the biochemical mediated response mounted by tolerant or resistant plants to limit pathogen infection (Griffiths, 2015; Prost et al., 2005). These oxylipin species could serve as biomarkers for disease susceptibility or tolerance by soybean cultivars when infected by pathogens (Figs. 4.7, 4.8). Based on our knowledge, the study of phyto-oxylipins and their rapid induction in the root and stem of susceptible and tolerant soybean cultivars in response to *P. sojae* colonization and infection, has not been previously reported in the literature. However, further study needs to be done to assess the gene expression levels associated with the pathway activated to further validate the proposed mechanism.

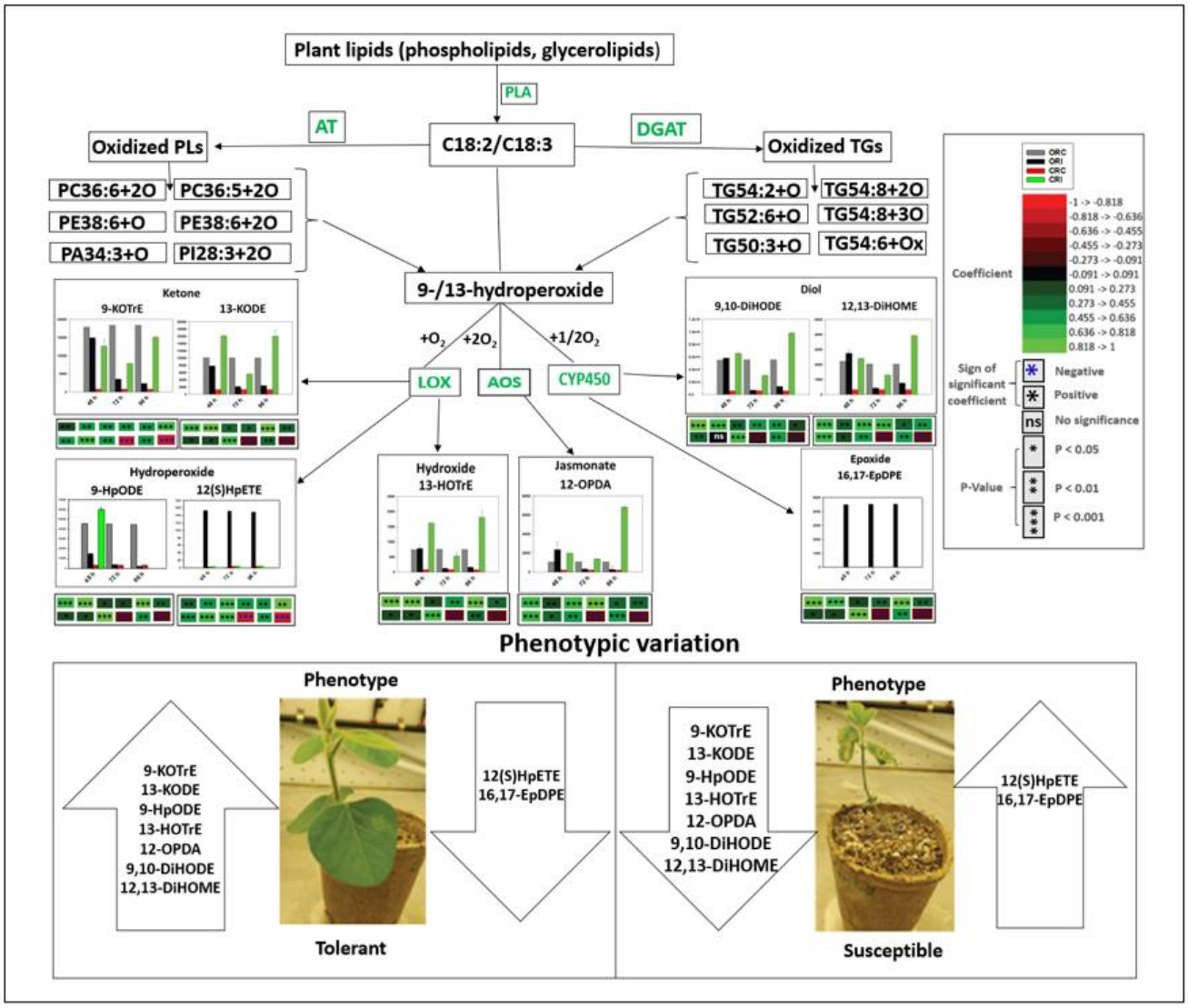

Fig. 4.7. Proposed pathways demonstrating the mechanisms that may be connected with oxidized GL and primary oxylipin biosynthesis, and disease susceptibility or tolerance in both tolerant (OX760-6) and resistant (Conrad) soybean cultivars at 48 h, 72 h and 96 h after challenge with *P. sojae*. The most significantly altered phyto-oxylipins biosynthesized in root of susceptible and

tolerant soybean cultivars following inoculation with *P. sojae* are presented in this diagram. We propose that following infection with *P. sojae*, PUFAs (C18:3 and C18:2) from membrane complex lipids were hydrolyzed by PLA followed by oxidation involving one, two or four oxygen atoms to synthesize oxidized GLs. Acyltransferases biosynthesize oxidized phospholipids, and DG acyltransferases biosynthesize oxidized TG. These oxidized lipids appear to serve as potential precursor for the primary oxylipins forming the hydroperoxides based on the strong correlations between these oxidized GLs and primary oxylipins. These hydroperoxides are further metabolized through enzymatic activities to produce various array of oxylipins catalyzed by LOX, CYP450 and AOS. The strongest correlations were observed between the following oxidized GLs: PC36:6+2O, PC36:5+2O, PE38:6+O, PE38:6+2O, PA34:3+O, PI28:3+2O, TG50:3+O, TG52:6+O, TG54:2+O and TG54:8+3O and primary oxylipins, 9HpODE, 12,13-DiHOME, 9,10-DiHODE, 12(S)-HpETE, 12-OPDA, 9-KOTrE, 13-HOTrE, 16,17-EpDPE and 13-KODE. The tolerant cultivar appears to produce several folds higher level of select oxylipins (jasmonates, diols, epoxides, hydroperoxides, ketones and hydroxides) in response to infection beginning at 48 h after inoculation over a 96 h time point. In contrast, these oxylipins are induced at lower levels in the susceptible soybean cultivars. The levels of primary oxylipins produced in the root of tolerant cultivar were generally increased across the time points (48 h, 72 h and 96 h) but reduced in the root of susceptible cultivar and may be associated with the successful strategy used by tolerant soybean cultivar to limit *P. sojae* infection. AOS = allene oxide synthase, and CYP450 =cytochrome P450. 9-KOTrE = 15(Z)-9-oxo-octadecatrienoic acid, 13-KODE = (9Z,11E)-13-Oxo-9,11-octadecadienoic acid, 9-HpODE = 10(E*)*,12(E)-9-hydroperoxyoctadeca-10,12-dienoic acid, 12(S)-HpETE = 12S-hydroperoxy-5(Z),8(Z),10(E),14(Z)-eicosatetraenoic acid, 13-HOTrE = 10(E),12(Z),13S-hydroxy-

9(Z),11(E),15(Z)-octadecatrienoic acid, 12-OPDA = 12-oxophytodienoic acid**,** (9Z,11E)-13-Oxo-9,11-octadecadienoic acid (13-KODE), 16,17-EpDPE = (4*Z*,7*Z*,10*Z*,13*Z*)-15-[3-[(*Z*)-pent-2-enyl] oxiran-2-yl] pentadeca-4,7,10,13-tetraenoic acid, 9, 10-DiHODE = (12*Z*,15*Z*)-9,10-dihydroxyoctadeca-12,15-dienoic acid, and 12,13-DiHOME = (*Z*)-12,13-dihydroxyoctadec-9-enoic acid. Control susceptible soybean root (ORC), inoculated susceptible soybean root (ORI), control tolerant soybean root (CRC), inoculated tolerant soybean root (CRI).

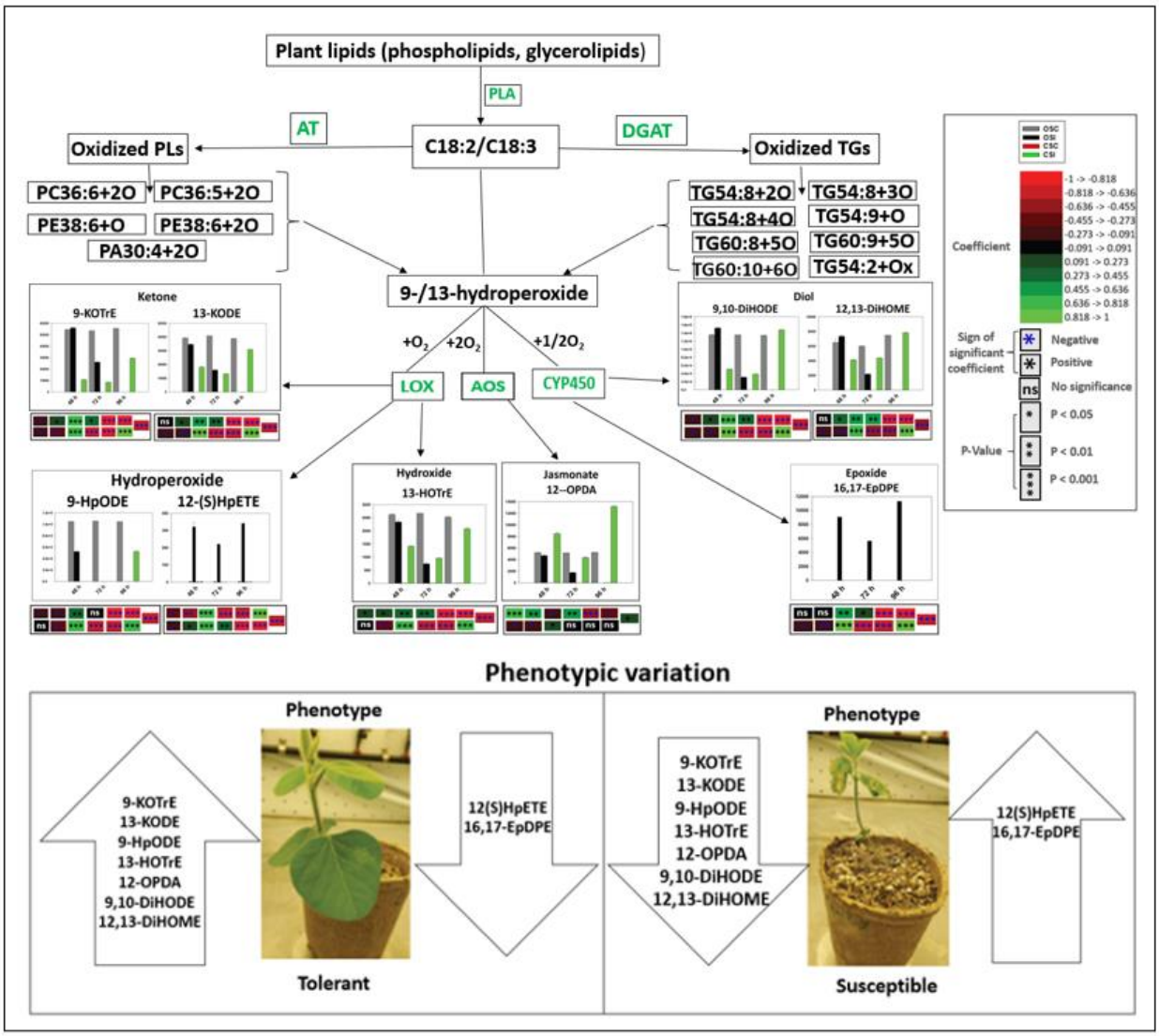

Fig. 4.8. Proposed pathways demonstrating the mechanisms that may be connected with oxidized GL and primary oxylipin biosynthesis, and disease susceptibility or tolerance in both tolerant (OX760-6) and resistant (Conrad) soybean cultivars at 48 h, 72 h and 96 h after challenge with *P. sojae*. The most significantly altered phyto-oxylipins biosynthesized in stem of susceptible and tolerant soybean cultivars following inoculation with *P. sojae* are presented in this diagram. We propose that following infection with *P. sojae*, PUFAs (C18:3 and C18:2) from membrane complex lipids were hydrolyzed by PLA followed by oxidation involving one, two or four

oxygen atoms to synthesize oxidized GLs. Acyltransferases biosynthesize oxidized phospholipids, and DG acyltransferases biosynthesize oxidized TG. These oxidized lipids appear to serve as potential precursor for the primary oxylipins forming the hydroperoxides based on the strong correlations between these oxidized GLs and primary oxylipins. These hydroperoxides are further metabolized through enzymatic activities to produce various array of oxylipins catalyzed by LOX, CYP450 and AOS. The strongest correlations were observed between the following oxidized GLs: PC36:6+2O, PC36:5+2O, PE38:6+O, PE38:6+2O, TG54:8+3O, TG54:9+O, TG60:9+5O, TG60:10+6O and TG54:2+Ox and primary oxylipins, 9HpODE, 12,13-DiHOME, 9,10-DiHODE, 12(S)-HpETE, 12-OPDA, 9-KOTrE, 13-HOTrE, 16,17-EpDPE and 13-KODE. The tolerant cultivar appears to produce several folds higher level of select oxylipins (jasmonates, diols, epoxides, hydroperoxides, ketones and hydroxides) in response to infection beginning at 48 h after inoculation to 96 h time point. In contrast, these oxylipins are induced at lower levels in the susceptible soybean cultivars. The levels of primary oxylipins produced in the stem of tolerant cultivar were generally increased across the time points (48 h, 72 h and 96 h) but reduced in the stem of susceptible cultivar and may be associated with the successful strategy used by tolerant soybean cultivar to limit *P. sojae* infection. AOS = allene oxide synthase, and CYP450 =cytochrome P450. 9-KOTrE = 15(Z)-9-oxo-octadecatrienoic acid, 13-KODE = (9Z,11E)-13-Oxo-9,11-octadecadienoic acid, **9**-HpODE = 10(E*)*,12(E)-9-hydroperoxyoctadeca-10,12-dienoic acid, 12(S)-HpETE = 12S-hydroperoxy-5(Z),8(Z),10(E),14(Z)-eicosatetraenoic acid, 13-HOTrE = 10(E),12(Z),13S-hydroxy-9(Z),11(E),15(Z)-octadecatrienoic acid, 12-OPDA = 12-oxophytodienoic acid**,** (9Z,11E)-13-Oxo-9,11-octadecadienoic acid (13-KODE), 16,17-EpDPE = (4*Z*,7*Z*,10*Z*,13*Z*)-15-[3-[(*Z*)-pent-2-enyl] oxiran-2-yl] pentadeca-4,7,10,13-tetraenoic acid, 9, 10-DiHODE = (12*Z*,15*Z*)-9,10-dihydroxyoctadeca-12,15-dienoic acid, and 12,13-

DiHOME = (*Z*)-12,13-dihydroxyoctadec-9-enoic acid. Control susceptible soybean stem (OSC), inoculated susceptible soybean stem (OSI), control tolerant soybean stem (CSC), inoculated tolerant soybean stem (CSI).

4.6. Conclusion

In conclusion, the results we present in this study demonstrate phyto-oxylipin induction increased in tolerant but decreased in susceptible soybean cultivars in the response against *P. sojae* infection and colonization. Knowledge of oxylipins has recently intensified interest in the functional roles of the phyto-oxylipin pathway in plant defense responses against various infectious pathogens. Based on this, the assumed functional roles of phyto-oxylipins include activation of defense gene expression in plants, participation in plant defense by functioning as signaling molecules to trigger defense responses, directly serving as antimicrobial compounds, and regulating PCD. Thus, this study may support advancements in the study of plant oxylipins as signalling molecules. The exact contribution of these phyto-oxylipins in soybean defense against pathogen infection remains unknown. However, this study has shown unequivocally that most oxylipins significantly increased after inoculation in tolerant soybean cultivars, suggesting that these FA mediated plant immunity may be a critical component of the defense strategies used against *P. sojae* colonization and infection. Therefore, this analysis is evidence suggesting that oxylipins could serve as signalling molecules that are capable of limiting pathogen infection in plants, particularly in respect to disease tolerance. Meanwhile, it requires further study to investigate whether the properties of these phyto-oxylipins could present an indication of pathogen tolerance level in soybean. Phyto-oxylipin anabolism mediated immunity in the root and stem of soybean cultivars challenged with *P. sojae* infection suggests that oxylipins appears to be produced mainly from PUFAs via enzymatic processes, which initially produced oxidized GLs, and these oxidized GLs could act as potential precursors of primary oxylipins by further conversions of hydroperoxides through the activities of LOX, AOS and CYP450 to produce phyto-oxylipins in soybean tissues (Figs 7, 8). This is evidenced based on the results obtained in this study and of the literature

regarding the PUFAs involved in oxylipins biosynthesis. To summarize, this study has revealed new evidence of phyto-oxylipin anabolism mediated plant immunity in soybean could be part of a successful strategy used by a tolerant soybean cultivar to mitigate infection by *P. sojae*. This evidence of the direct role of phyto-oxylipins identifies chemical biomarkers and potential enzymatic pathways that may be leveraged to improve environmentally sustainable agricultural practices, food production and security.

4.7. References

Adigun, O. A., Nadeem, M., Pham, T. H., Jewell, L. E., Cheema, M., & Thomas, R. (2020). Recent advances in bio-chemical, molecular and physiological aspects of membrane lipid derivatives in plant pathology. *Plant, Cell & Environment, 44*(1), 1-16.

Adigun, O. A., Pham, T. H., Dmitry, G., Nadeem, M., Jewell, L. E., Cheema, M., . . . Thomas, R. (2021). Plant lipid metabolism in susceptible and tolerant soybean (*Glycine max*) cultivars in response to *Phytophthora sojae* colonization and infection. *Research square*, 1-44.

Blée, E. (2002). Impact of phyto-oxylipins in plant defense. *TRENDS in Plant Science, 7*(7), 315-321.

Borrego, J. E., & Kolomiets, V. M. (2016). Synthesis and functions of jasmonates in maize. *Plants, 5*(4). doi:10.3390/plants5040041

Brodhun, F., Cristobal-Sarramian, A., Zabel, S., Newie, J., Hamberg, M., & Feussner, I. (2013). An iron 13S-lipoxygenase with an α-linolenic acid specific hydroperoxidase activity from Fusarium oxysporum. *PloS one, 8*(5), e64919-e64919.

Cacas, J.-L., Vailleau, F., Davoine, C., Ennar, N., Agnel, J.-P., Tronchet, M., . . . Montillet, J.-L. (2005). The combined action of 9 lipoxygenase and galactolipase is sufficient to bring about programmed cell death during tobacco hypersensitive response. *Plant, Cell & Environment, 28*(11), 1367-1378.

Chakraborty, S., & Newton, A. C. (2011). Climate change, plant diseases and food security: an overview. *Plant Pathology, 60*(1), 2-14.

Chen, Z., Chen, X., Yan, H., Li, W., Li, Y., Cai, R., & Xiang, Y. (2015). The lipoxygenase gene family in poplar: identification, classification, and expression in response to MeJA treatment. *PLOS ONE, 10*(4), e0125526.

Christensen, S. A., & Kolomiets, M. V. (2011). The lipid language of plant-fungal interactions. *Fungal Genet Biol, 48*(1), 4-14.

De León, I. P., Sanz, A., Hamberg, M., & Castresana, C. (2002). Involvement of the Arabidopsisα-DOX1 fatty acid dioxygenase in protection against oxidative stress and cell death. *The Plant Journal, 29*(1), 61-72.

DeLong, J. P., Burger, O., & Hamilton, M. J. (2013). The UN medium population projection is an unstable equilibrium. *Frontiers in Ecology and the Environment, 11*(2), 65-66.

DeMarsay, A. (2005). *Anthracnose Fuit Rot of Highbush Blueberry: Biology and Epidemiology.* (PhD), Rutgers, New Brunswick, New Jersey, USA.

Diaz-Ambrona, C. G. H., & Maletta, E. (2014). Achieving global food security through sustainable development of agriculture and food systems with regard to nutrients, soil, land, and waste management. *Current Sustainable/Renewable Energy Reports, 1*(2), 57-65.

Domingues, M. R. M., Reis, A., & Domingues, P. (2008). Mass spectrometry analysis of oxidized phospholipids. *Chemistry and Physics of Lipids, 156*(1), 1-12.

Gao, Starr, J., Göbel, C., Engelberth, J., Feussner, I., Tumlinson, J., & Kolomiets, M. (2008). Maize 9-lipoxygenase ZmLOX3 controls development, root-specific expression of defense genes, and resistance to root-knot nematodes. *Molecular Plant-Microbe Interactions®, 21*(1), 98-109.

Gao, X., Stumpe, M., Feussner, I., & Kolomiets, M. (2008). A novel plastidial lipoxygenase of maize (*Zea mays*) *ZmLOX6* encodes for a fatty acid hydroperoxide lyase and is uniquely regulated by phytohormones and pathogen infection. *Planta, 227*(2), 491-503.

García-Marcos, A., Pacheco, R., Manzano, A., Aguilar, E., & Tenllado, F. (2013). Oxylipin biosynthesis genes positively regulate programmed cell death during compatible infections with the synergistic pair potato virus X-potato virus Y and Tomato spotted wilt virus. *Journal of virology, 87*(10), 5769-5783.

Genva, M., Obounou Akong, F., Andersson, M. X., Deleu, M., Lins, L., & Fauconnier, M.-L. (2019). New insights into the biosynthesis of esterified oxylipins and their involvement in plant defense and developmental mechanisms. *Phytochemistry Reviews, 18*(1), 343-358.

Göbel, C., Feussner, I., Hamberg, M., & Rosahl, S. (2002). Oxylipin profiling in pathogen-infected potato leaves. *Biochimica et Biophysica Acta (BBA) - Molecular and Cell Biology of Lipids, 1584*(1), 55-64.

Granér, G., Hamberg, M., & Meijer, J. (2003). Screening of oxylipins for control of oilseed rape (Brassica napus) fungal pathogens. *Phytochemistry, 63*(1), 89-95.

Grechkin, A. N., Brühlmann, F., Mukhtarova, L. S., Gogolev, Y. V., & Hamberg, M. (2006). Hydroperoxide lyases (CYP74C and CYP74B) catalyze the homolytic isomerization of fatty acid hydroperoxides into hemiacetals. *Biochimica et Biophysica Acta (BBA) - Molecular and Cell Biology of Lipids, 1761*(12), 1419-1428.

Griffiths, G. (2015). Biosynthesis and analysis of plant oxylipins. *Free Radic Res, 49*(5), 565-582.

Gullner, G., Künstler, A., Király, L., Pogány, M., & Tóbiás, I. (2010). Up-regulated expression of lipoxygenase and divinyl ether synthase genes in pepper leaves inoculated with Tobamoviruses. *Physiological and Molecular Plant Pathology, 74*(5), 387-393.

Heath, M. C. (2000). Nonhost resistance and nonspecific plant defenses. *Current Opinion in Plant Biology, 3*(4), 315-319.

Howe, G. A., & Schilmiller, A. L. (2002). Oxylipin metabolism in response to stress. *Current Opinion in Plant Biology, 5*, 230-236.

https://www.ncbi.nlm.nih.gov/pmc/articles/PMC4528626/.

Irshad, Z., Dimitri, F., Christian, M., & Zammit, V. A. (2017). Diacylglycerol acyltransferase 2 links glucose utilization to fatty acid oxidation in the brown adipocytes. *Journal of Lipid Research, 58*(1), 15-30.

Jiang, H., Fei, X., Liu, H., Roeder, K., Lafferty, J., Wasserman, L., . . . Zhao, T. (2019). High-Dimensional Undirected Graph Estimation *Huge, R package version 1.3.4.* .

Jingwei, F., Hu, C., Zhang, L., Li, Z., Zhao, F., & Wang, S. (2014). Jasmonic acid mediates tomato's response to root knot nematodes. *Journal of Plant Growth Regulation, 34*, 196-205.

Kolomiets, M. V., Hannapel, D. J., Chen, H., Tymeson, M., & Gladon, R. J. (2001). Lipoxygenase is involved in the control of potato tuber development. *The Plant Cell, 13*(3), 613. doi:10.1105/tpc.13.3.613

Kovač, M., Müller, A., Milovanovič Jarh, D., Milavec, M., Düchting, P., & Ravnikar, M. (2009). Multiple hormone analysis indicates involvement of jasmonate signalling in the early defence of potato to potato virus YNTN. *Biologia Plantarum, 53*(1), 195-199.

Liu, G.-Y., Moon, S. H., Jenkins, C. M., Sims, H. F., Guan, S., & Gross, R. W. (2019). Synthesis of oxidized phospholipids by sn-1 acyltransferase using 2-15-HETE lysophospholipids. *Journal of Biological Chemistry, 294*(26), 10146-10159.

Marmey, P., Jalloul, A., Alhamdia, M., Assigbetse, K., Cacas, J.-L., Voloudakis, A. E., . . . Nicole, M. (2007). The 9-lipoxygenase GhLOX1 gene is associated with the hypersensitive reaction of cotton Gossypium hirsutum to Xanthomonas campestris pv malvacearum. *Plant Physiology and Biochemistry, 45*(8), 596-606.

McDonald, B. A., & Stukenbrock, E. H. (2016). Rapid emergence of pathogens in agro-ecosystems: global threats to agricultural sustainability and food security. *Philosophical transactions of the Royal Society of London. Series B, Biological sciences, 371*(1709), 20160026.

Meinshausen, N., & Bühlmann, P. (2006). High-dimensional graphs and variable selection with the Lasso. *The Annals of Statistics, 34*(3), 1436-1462, 1427.

Mukhtarova, L. S., Lantsova, N. V., Khairutdinov, B. I., & Grechkin, A. N. (2020). Lipoxygenase pathway in model bryophytes: 12-oxo-9(13),15-phytodienoic acid is a predominant oxylipin in Physcomitrella patens. *Phytochemistry, 180,* 112533.

Mysore, K. S., & Ryu, C. M. (2004). Nonhost resistance: how much do we know? *Trends Plant Sci, 9*(2), 97-104.

Nadeem, M., Thomas, R., Adigun, O., Manful, C., Wu, J., Pham, T. H., . . . Cheema, M. (2020). Root membrane lipids as potential biomarkers to discriminate silage-corn genotypes cultivated on podzolic soils in boreal climate. *Physiologia Plantarum, 170*(3), 440-450.

Naor, N., Gurung, F. B., Ozalvo, R., Bucki, P., Sanadhya, P., & Miyara, S. B. (2018). Tight regulation of allene oxide synthase (AOS) and allene oxide cyclase-3 (AOC3) promote

Arabidopsis susceptibility to the root-knot nematode *Meloidogyne javanica*. *European Journal of Plant Pathology, 150*(1), 149-165.

Nelson, R. (2020). International plant pathology: Past and future contributions to global food security. *Phytopathology®, 110*(2), 245-253.

Niu, M., & Keller, N. P. (2019). Co-opting oxylipin signals in microbial disease. *Cellular Microbiology, 21*(6), e13025-e13025.

Oliver, J. P., Castro, A., Gaggero, C., Cascón, T., Schmelz, E. A., Castresana, C., & Ponce de León, I. (2009). Pythium infection activates conserved plant defense responses in mosses. *Planta, 230*(3), 569-579.

Pham, T. H., Zaeem, M., Fillier, T. A., Nadeem, M., Vidal, N. P., Manful, C., . . . Thomas, R. H. (2019). Targeting Modified Lipids during Routine Lipidomics Analysis using HILIC and C30 Reverse Phase Liquid Chromatography coupled to Mass Spectrometry. *Scientific Reports, 9*(1), 5048.

Ponce de León, I., Oliver, J. P., Castro, A., Gaggero, C., Bentancor, M., & Vidal, S. (2007). *Erwinia carotovora* elicitors and *Botrytis cinerea* activate defense responses in *Physcomitrella patens. BMC Plant Biology, 7*(1), 52.

Ponce De León, I., Schmelz, E. A., Gaggero, C., Castro, A., Álvarez, A., & Montesano, M. (2012). *Physcomitrella patens* activates reinforcement of the cell wall, programmed cell death and accumulation of evolutionary conserved defence signals, such as salicylic acid and 12-oxo-phytodienoic acid, but not jasmonic acid, upon *Botrytis cinerea* infection. *Mol Plant Pathol, 13*(8), 960-974.

Pretty, J. (2008). Agricultural sustainability: concepts, principles and evidence. *Philosophical transactions of the Royal Society of London. Series B, Biological sciences, 363*(1491), 447-465.

Prost, I., Dhondt, S., Rothe, G., Vicente, J., Rodriguez, M. J., Kift, N., . . . Fournier, J. (2005). Evaluation of the antimicrobial activities of plant oxylipins supports their involvement in defense against pathogens. *Plant physiology, 139*(4), 1902-1913.

R-Core-Team. (2019). R: A language and environment for statistical computing. . *Foundation for Statistical Computing, Vienna, Austria.*

Rancé, I., Fournier, J., & Esquerré-Tugayé, M.-T. (1998). The incompatible interaction between Phytophthora parasitica var. nicotianae race 0 and tobacco is suppressed in transgenic plants expressing antisense lipoxygenase sequences. *Proceedings of the National Academy of Sciences, 95*(11), 6554-6559. doi:10.1073/pnas.95.11.6554

Ravipati, S., Baldwin, D. R., Barr, H. L., Fogarty, A. W., & Barrett, D. A. (2015). Plasma lipid biomarker signatures in squamous carcinoma and adenocarcinoma lung cancer patients. *Metabolomics, 11*(6), 1600-1611.

Savary, S., Willocquet, L., Pethybridge, S. J., Esker, P., McRoberts, N., & Nelson, A. (2019). The global burden of pathogens and pests on major food crops. *Nat Ecol Evol, 3*(3), 430-439.

Scala, V., Reverberi, M., Salustri, M., Pucci, N., Modesti, V., Lucchesi, S., & Loreti, S. (2018). Lipid profile of Xylella fastidiosa Subsp. pauca associated with the olive quick decline syndrome. *Frontiers in Microbiology, 9*(1839).

Senthil-Kumar, M., & Mysore, K. S. (2013). Nonhost Resistance Against Bacterial Pathogens: Retrospectives and Prospects. *Annual Review of Phytopathology, 51*(1), 407-427.

Shannon, P., Markiel, A., Ozier, O., Baliga, N. S., Wang, J. T., Ramage, D., . . . Ideker, T. (2003). Cytoscape: a software environment for integrated models of biomolecular interaction networks. *Genome Res, 13*(11), 2498-2504.

Smith, J. L., De Moraes, C. M., & Mescher, M. C. (2009). Jasmonate- and salicylate-mediated plant defense responses to insect herbivores, pathogens and parasitic plants. *Pest Manag Sci, 65*(5), 497-503.

Soriano, I. R., Asenstorfer, R. E., Schmidt, O., & Riley, I. T. (2004). Inducible flavone in oats (*Avena sativa*) is a novel defense against plant-parasitic nematodes. *Phytopathology, 94*(11), 1207-1214.

Stumpe, M., & Feussner, I. (2006). Formation of oxylipins by CYP74 enzymes. *Phytochemistry Reviews, 5*(2), 347-357.

Thomas, R., Fang, X., Ranathunge, K., Anderson, T. R., Peterson, C. A., & Bernards, M. A. (2007). Soybean root suberin: anatomical distribution, chemical composition, and relationship to partial resistance to *Phytophthora sojae*. *Plant Physiology, 144*(1), 299-311.

Tijet, N., & Brash, A. R. (2002). Allene oxide synthases and allene oxides. *Prostaglandins Other Lipid Mediat, 68-69*, 423-431.

Tyler, B. M. (2007). Phytophthora sojae: root rot pathogen of soybean and model oomycete. *Molecular Plant Pathology, 8*(1), 1-8.

Vincenti, S., Mariani, M., Alberti, J.-C., Jacopini, S., Brunini-Bronzini de Caraffa, V., Berti, L., & Maury, J. (2019). Biocatalytic Synthesis of Natural Green Leaf Volatiles Using the Lipoxygenase Metabolic Pathway. *Catalysts, 9*(10), 873.

Vollenweider, S., Weber, H., Stolz, S., Chételat, A., & Farmer, E. E. (2000). Fatty acid ketodienes and fatty acid ketotrienes: Michael addition acceptors that accumulate in wounded and diseased Arabidopsis leaves. *The Plant Journal, 24*(4), 467-476.

Wei, S., Bian, R., Andika, I. B., Niu, E., Liu, Q., Kondo, H., . . . Sun, L. (2019). Symptomatic plant viroid infections in phytopathogenic fungi. *Proceedings of the National Academy of Sciences, 116*(26), 13042-13050.

Wu, J., & Baldwin, I. T. (2010). New insights into plant responses to the attack from insect herbivores. *Annual Review of Genetics, 44*(1), 1-24. doi:10.1146/annurev-genet-102209-163500.

Zhao, J., Luo, Q., Deng, H., & Yan, Y. (2008). Opportunities and challenges of sustainable agricultural development in China. *Philosophical transactions of the Royal Society of London. Series B, Biological sciences, 363*(1492), 893-904.

Chapter five

Biochemical and histological changes in root of susceptible and tolerant soybean cultivars infected by *Phytophthora sojae*

Biochemical and histological changes in root of susceptible and tolerant soybean cultivars infected by *Phytophthora sojae*

5.1. Abstract

Root rot is a common infection of soybean caused by the oomycete *Phytophthora sojae* resulting in 40-50% annual crop losses globally at a value of $1-2B USD. However, we have limited understanding of the morphological and biochemical changes occurring during the infection process in soybean roots governing tolerance. We employed scanning electron microscopy and histochemical techniques to examine the infection process in soybean root following *P. sojae* infection to observe lipid mediated changes in soybean roots morphology associated with tolerance. We studied one susceptible and one tolerant soybean cultivar following inoculation with *P. sojae*. We hypothesized that the tissue damage would be more pronounced in the susceptible cultivar compared to the tolerant cultivar, and that the morphological or histochemical properties of the tolerant cultivar would suggest a mechanism for disease tolerance when compared to the morphological response in the susceptible cultivar following infection with *P. sojae*. Relative to mock inoculated controls, the epidermal and vascular bundles of the roots of both soybean cultivars were damaged when challenged with *P. sojae*. The results revealed more severe tissue damage in the root of the infected susceptible soybean cultivar compared to the infected tolerant soybean cultivar, and the epidermal cells and vascular cylinder cell wall of tolerant soybean cultivar appeared to be thicker in comparison to that of the susceptible soybean cultivar and the presence of biogenic crystals appeared to be reduced in the tolerant compared to the susceptible cultivar following infection. In addition, the quantity of the poly-aliphatic compounds in the root cell walls increased in the infected tolerant cultivar compared to the root of the infected susceptible cultivar. Therefore, reinforced chemical,

structural, and morphological barriers in soybean roots seems to be associated with the successful mechanisms used by tolerant soybeans to mitigate pathogen colonization and infection. This could ultimately help to reduce crop losses and improve food safety and food security through sustainable agricultural practices.

***Keywords*:** Soybean cultivars, *Phytophthora sojae*, pathogen invasion, scanning electron microscopy, histochemistry.

5.2. Introduction

Soybean (*Glycine max*) is one of the important crops cultivated across the globe. It is a staple food in many cultures and plays a critical role in global food security (Thomas et al., 2007). However, soybean production is significantly affected by *Phytophthora* root and stem rot caused by the waterborne pathogen *Phytophthora sojae* accounting for global annual crop yield losses of $1-2B USD (Bandara, Weerasooriya, Bradley, Allen, & Esker, 2020; Dorrance, McClure, & St. Martin, 2003; Thomas et al., 2007; Tyler, 2007). In the soybean-*P. sojae* interaction, the root is the first point of contact and infection site, following which infection can later spread to the stem of the plant. Zoospores produced from the sporangia swim to the root which they identify using recognition factors. The *P. sojae* zoospores are chemotactic to soybean root exudates (Zhang et al., 2019). The isoflavones secreted by soybean roots induce zoospore encystment on the root surface. Encysted zoospores germinate 2 h post-infection, and germ tubes then grow on the soybean root surface (Mideros, Nita, & Dorrance, 2007; Moy, Qutob, Chapman, Atkinson, & Gijzen, 2004). *P. sojae* infects soybean at any stage of growth from seedling to maturity

(Dorrance, 2018). Early-season symptoms of the infection include seed rot and pre-emergence and post-emergence damping off. The main symptom of Phytophthora root rot is a dark brown lesion on the lower stem that spreads to the taproot of the crop (Tyler, 2007). The dark lesion frequently extends to several nodes and will strap soybean stems, preventing flow of water, minerals, and nutrients, and later stunts or kills the plant. The oomycete *P. sojae* survives as oospores on the residue of the plant or in the soil when conditions are unfavorable. At soil temperatures of 16 °C and with saturated soil, germination of oospores occurs, producing zoospores and the disease develops at optimum temperatures of 25 °C to 30 °C (Tyler, 2007). Warm weather and saturated soil are conducive to disease immediately after planting. The pathogen can initially infect the roots and may later colonize the roots and stems when soil conditions favor pathogen development. The germ tube penetrates beside the root epidermal cells at 2.5 h post-inoculation. In susceptible plants, within 4 h post infection, hyphae can penetrate the fourth layer of the cell of the root cortex and an abundance of haustoria may form, which serves as the main sites to transfer nutrients from the plant to the pathogen. This is important for the growth, development, and reproduction of pathogens (Szabo & Bushnell, 2001). In contrast, hyphae may be found even up to the sixth cell layer in tolerant host by 4 h post inoculation, but haustoria would be rare and necrosis would occur in many cells of the cortex. The hyphae would have extended to the endodermis in both susceptible and tolerant soybean cultivars within 10 h post-inoculation. In the susceptible cultivar, the number of haustoria will continue to increase but in the tolerant cultivar, haustoria are very few, and necrotic cells are common (Ranathunge et al., 2008). At 15 h post-infection, the susceptible cultivar may reveal a sudden change as the hyphae colonized the root cells at initial point of infection and cell death initiation can be observed.

Furthermore, the vascular tissue would be extensively colonized. The pathogen colonizes the root and stem tissues where oospores are produced (Dorrance, 2018). Contrarily, in the tolerant cultivar, the cortex may be extensively colonized, but only some cells may be dead. In addition, hyphae spread within the endodermal cells are limited (Tyler, 2007).

The plant cell wall is known to play multiple physiological roles during plant-pathogen interactions (Thomas et al., 2007). The cell wall structurally consists of non-polysaccharides such as wax, lignin and carbohydrate-based polymers such as hemicellulose, cellulose in form of biogenic crystals, pectin, and chitin (Pauly & Keegstra, 2008; Thomas et al., 2007). Both hemicellulose and pectin are mixtures of highly branched polysaccharides in the cell wall of plants that spatially interact with each other (Wang, Zabotina, & Hong, 2012). The cellulose crystalline are bounded by hemicellulose and lignin (Wang et al., 2012). These crystalline are crosslinked into a tough network of fibrous molecules that are responsible for mechanical and structural strength of the cell walls and play active role during plant response to environmental stimuli (Caffall & Mohnen, 2009; Ling et al., 2018). Pectins are cell wall structural polysaccharides made up of abundant negatively charged residues like galacturonic acids mainly function in intercellular adhesion (Shin, Chane, Jung, & Lee, 2021). Pectins are also important during some cellular functions such as intercellular communication, morphogenesis, cell fate specification, and environmental recognition and signaling during interactions between plants and pathogens (Lara-Espinoza, Carvajal-Millán, Balandrán-Quintana, López-Franco, & Rascón-Chu, 2018; Parre & Geitmann, 2005; Shin et al., 2021). Pectins are mainly produced during the early stages of primary plant cell wall growth and development (Harholt, Suttangkakul, & Vibe Scheller, 2010; Wang et al., 2012). These multiple negative charges allow pectin to bind to positively charged ionic compounds and entrap water to produce a gel-like network that is

interconnected with the crosslinked cellulose crystalline to generate a single cohesive network (Ajdary, Tardy, Mattos, Bai, & Rojas, 2021; Caffall & Mohnen, 2009). Biogenic and biological crystals such as calcium oxalate are biosynthesized in various plant tissues, and they are mainly appeared during physiological and pathological processes (Cuéllar-Cruz, Pérez, Mendoza, & Moreno, 2020; Ilarslan, Palmer, & Horner, 2001). These crystals serve as support, protection or defense in plants (Cuéllar-Cruz et al., 2020; Ilarslan et al., 2001). In addition, plant cell walls contain different glycoproteins that are integrated into the matrix that are likely to provide more structural support to cell walls (Amos & Mohnen, 2019). Plant glycoproteins also involve in some biological functions during plant development and plant innate immunity (Nguema-Ona et al., 2014; Strasser, 2014).

In addition, the cell wall structure is also influenced by biotic environmental stressors including plant pathogens and undergoes physical and chemical changes as part of the successful response to limit or control exposure to these stressors (Kesten, Menna, & Sánchez-Rodríguez, 2017). For instance, during plant-pathogen interaction, plants depend on both constitutive and inducible defensive barriers to resist pathogen invasion (Adigun et al., 2021). These include wax and callose deposition to reinforce the cell wall (Kesten et al., 2017). The epidermis, which consists of diffuse suberin, is directly in contact with the physical environment and is always the site of initial penetration by infectious pathogens; as a result, it acts as the first line of defense against pathogenic invasion. In contrast, suberized endodermis provides the last line of defense before pathogens enter the vascular cylinder and then colonize the entire plant (Thomas et al., 2007). The plant vascular bundles have two major functions: delivery of water, sugar, essential mineral nutrients, and amino acids to the plant, and providing mechanical support (Lucas et al., 2013). Furthermore, the vascular system of higher plants also acts a conduit for effective long-

distance communication, using the phloem and the xylem to communicate information about biotic stressors within the environment (Lough & Lucas, 2006). In addition, studies have shown that pathogenic microorganisms are capable of penetrating root tissue mainly through natural openings or wounds and cause cell and tissue damages (Nash, Dalziel, & Fitzgerald, 2015). For instance, after penetration, hyphae of *Fusarium oxysporum* proceeded to inter- and intracellular components and then invaded the vascular cylinder of green beans (Pereira et al., 2013). The fungus extensively colonized the vascular cylinder, and this occur concomitant with disease development, although there may be some invasion of other tissues in the susceptible cultivar. Furthermore hyphal growth and movement of microconidia in the vascular cylinder were also observed (Pereira et al., 2013). Conversely, in the resistant cultivar, the colonization between adjacent xylem tubes was not possible, probably due to structural and chemical changes such as vascular occlusion, production of tyloses, gel plugs, and accumulation of addition wall layers (Pereira et al., 2013; Thomas et al., 2007). Chemical, structural, and morphological barriers play an important role in plant defense against pathogen invasion and could serve as mechanisms to improve resistance in certain plant-pathogen interactions (Adigun et al., 2021; Thomas et al., 2007). The most efficient preventive measure to control Phytophthora root rot disease of soybean is by pyramiding resistance-conferring gene in soybean with partial resistance (otherwise called quantitative resistance) or race-specific resistance (also known as qualitative resistance) against the pathogen (Burnham, Dorrance, Francis, Fioritto, & St. Martin, 2003; Burnham, Dorrance, VanToai, & St. Martin, 2003; Thomas et al., 2007). However, there is limited information on the histochemical defense response of soybean roots to infection by *P. sojae* resulting in a tolerant or susceptible phenotype or interaction. Therefore, this study aimed to better understand the

histochemical response or processes governing infection in both susceptible and tolerant soybean cultivars infected with *P. sojae*.

5.3. Materials and methods

5.3.1. Soybean growth and method of inoculation

A virulent strain of *P. sojae* race 2 (strain P6497) used as inoculum was acquired from the London Research and Development Center, Agriculture and Agri-Food Canada (AAFC-LRDC; London, ON, Canada). The oomycete *P. sojae* was cultured and aseptically maintained on 26 % V8-juice agar (8400 mg agar, 1600 mg $CaCO_3$, 156 mL V8-juice [Campbell Soup Company, Toronto, ON, Canada], and 440 mL of distilled water) for 8 days. Soybean seeds for both cultivars, Conrad (tolerant cultivar) and OX760-6 (susceptible cultivar), were acquired from AAFC-LRDC (London, ON, Canada). The seeds were surface decontaminated utilizing 0.5 % sodium hypochlorite (Commercial Javex Bleach; Clorox Co., Brampton, Ontario, Canada) for 5 min and rinsed 2 to 3 times with distilled water. The seeds were then submerged in distilled water for 12 h and then seeded. The bottom of a disinfected empty wax-paper cup was utilized to cut agar disks containing cultures of *P. sojae* P6497 which were later fitted into the bottom of wax-paper cups that were 15.0 cm deep with a diameter of 8.5 cm at the top (Merchants Paper Company, Windsor, ON, Canada), and the agar was then overlaid with medium-grade vermiculite. Five to six holes were produced in the wax-paper cups for drainage. The soaked seeds were seeded in medium-grade vermiculite containing six seeds per cup for each cultivar, and they were inoculated with *P. sojae* while other sets were mock-inoculated as the control using sterile V8-juice agar disks without a *P. sojae* culture. The soybeans were then allowed to grow for 10 days under controlled growth conditions in a growth chamber (Biochambers MB, Canada) at Grenfell Campus, Memorial

University of Newfoundland, under conditions of 8 h dark at 20 °C, 16 h light at 25 °C, and 60 % relative humidity. Seedlings were watered everyday, beginning 4 days after seeding using one-quarter-strength Knop's solution (Thomas et al., 2007). The entire seedlings were harvested after 10 days of growth and kept until further analysis at -80 °C. The plant samples were divided into three groups. The first group were used for membrane and storage lipid analysis, the second group were used for oxidized GL analysis, and the third group were used for histochemical analysis.

5.3.2. Preparation of samples for scanning electron microscopy

Soybean roots were collected from both non-inoculated (control) and inoculated plants of susceptible and tolerant soybean cultivars. The samples were rinsed with distilled water before further processing. Free-hand cross sections of the root were cut using a razor blade to a length of approximately 5 mm. Thin sections were mounted to aluminum stubs using colloidal graphite adhesive (Permatex, Canada, Incorporated). The samples were exposed to a temperature of -4.9 °C on a Peltier cooling stage to minimize differences in structure, while in the vacuum chamber. The images of the samples were collected using an environmental scanning electron microscope (ThermoFisher Quattro S with ESEM), to study the morphological properties of roots infected with *P. sojae*. High-resolution images were collected from 9-10 mm to 5-100 µm (magnification 788-8000X with the pressure 50-428 Pa).

5.3.3. Sample preparation for histochemical analysis

Free-hand cross sections of soybean root prepared as above were stained with 0.01 % (w/v) fluoro-yellow (FY) in polyethylene glycol-glycerol: distilled water (90:10 v/v) for 1 h to visualize aliphatic lipids in different regions of the root structure. After staining, the root sections were removed from the dye, washed 2-3 times with distilled water, mounted on a glass slide with 75 % glycerol, and viewed with the green fluorescent protein (GFP) filter with excitation peak at wavelength of 469 nm and emission peak at wavelength of 525 nm using a Synergy HT Image reader (Biotek, Fisher Scientific, Mississauga, ON, Canada). High-resolution images were collected from 30-200 μm.

5.4. Results

5.4.1. Histological changes in the root of both soybean cultivars infected with *Phytophthora sojae*.

To understand the morphological structure of soybean root and how changes occur in the morphology of the root during interaction with pathogens governing tolerance, scanning electron microscopy (SEM) was used to provide detailed images of soybean root morphology. Scanning electron microscopic images demonstrated opening in the cortex of the roots (Fig. 5.1a-c), the intact epidermis and cortical cell (Fig. 5.1d, e), degradation and crack in the cortical cells during interaction between soybean and *P. sojae* (Fig. 5.1f, g), and closing up of degradation and crack in the inner cortical side of epidermis and cortex.

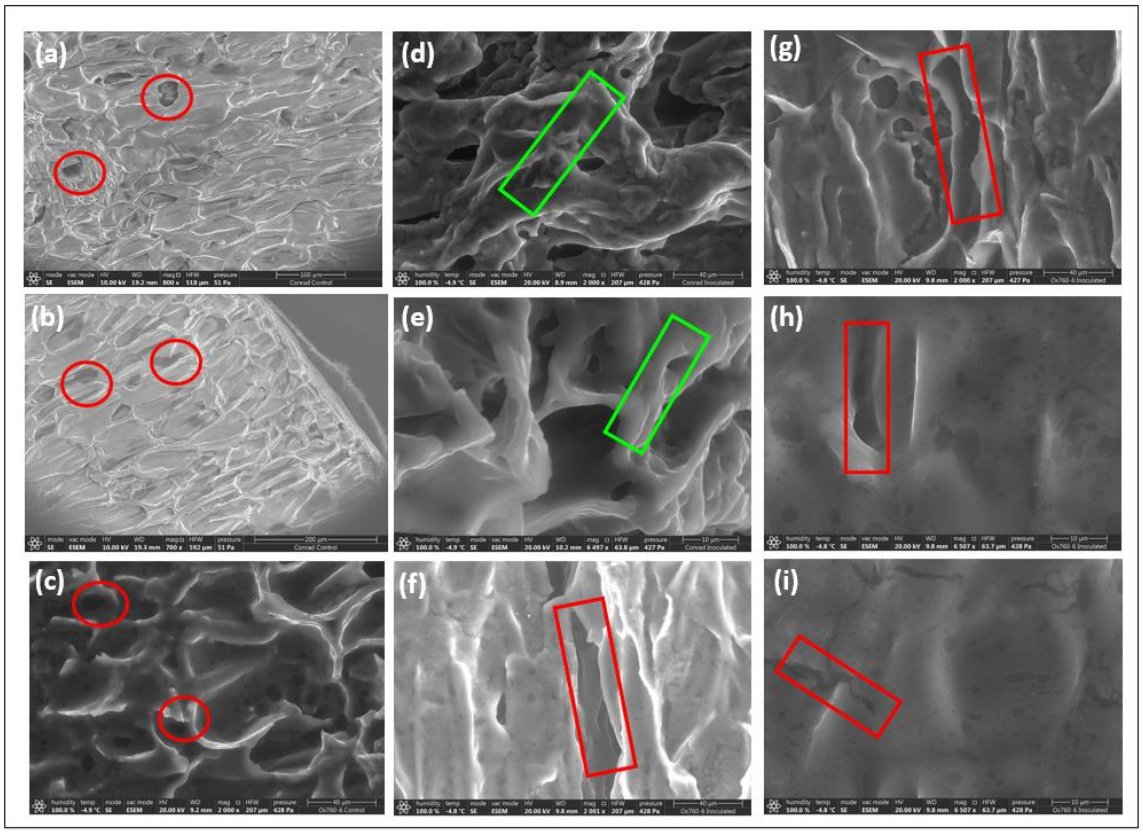

Fig. 5.1. Scanning electron microscopy (SEM) images demonstrating morphology of soybean root segments. Tiny opening in the cortical cells indicated by red circle (a-c; 40-200 µm), intact inner cortical side of epidermis and cortex denoted by green rectangle (d, e; 10, 40 µm), degradation and crack in the inner cortical side of epidermis and cortex indicated by red rectangle (f, g; 40 µm), closing up of degradation and crack in the inner cortical side of epidermis and cortex denoted by red rectangle (h, i; 10 µm).

Furthermore, the morphology of soybean roots reveals some features like epidermis, cortex and vascular cylinder of the root at lower magnification (Fig. 5.2a, b), demonstrate higher magnification of root tissues with different contraction (Fig. 5.2c, d), and identify certain elements, particularly the presence of occluding materials in the root cortex (Fig. 5.2e) and the presence and distribution of biogenic crystals of various morphologies and different sizes within vascular cylinder of soybean root (Fig. 5.2f-i).

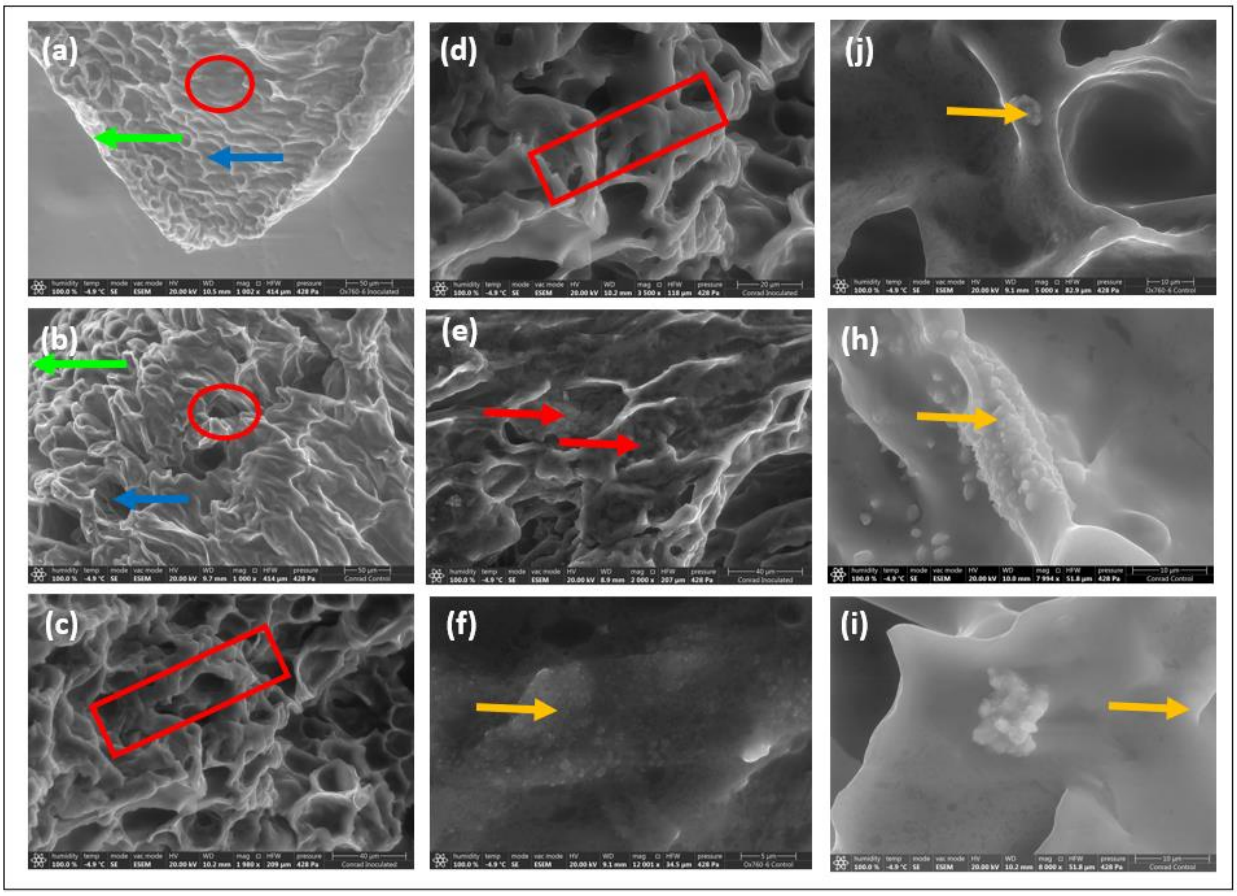

Fig. 5.2. Scanning electron microscopy images demonstrating unique features in soybean root morphology. The root epidermis, cortex and vascular cylinder with low magnification indicated by green arrow, blue arrow and red circle respectively (a, b; 50 µm). High magnification of root tissues showing contraction of root (c, d; 40 & 20 µm), the presence of occluding materials in the root cortex (e; 40 µm), and the presence and distribution of biogenic crystals within the vascular cylinder of soybean root (f-i; 5-10 µm).

Further examination on roots of both susceptible and tolerant soybean cultivars was done to better understand the morphological and histological basis for disease susceptibility or tolerance in soybean to pathogen invasion and associate it with the observed infection and colonization patterns. We observed few differences in the root epidermal walls of both soybean cultivars infected with *P. sojae* relative to their non-inoculated controls (Fig. 5.3a-d). The epidermal walls of the inoculated tolerant cultivar were visibly infected whereas in the inoculated susceptible cultivar, the cortex was highly infected, and the cortex appeared to be damaged (Fig. 5.3b, d). In the non-inoculated roots of both soybean cultivars, the cortical cells were observed to be closely packed without any damage (Fig. 5.3a, c).

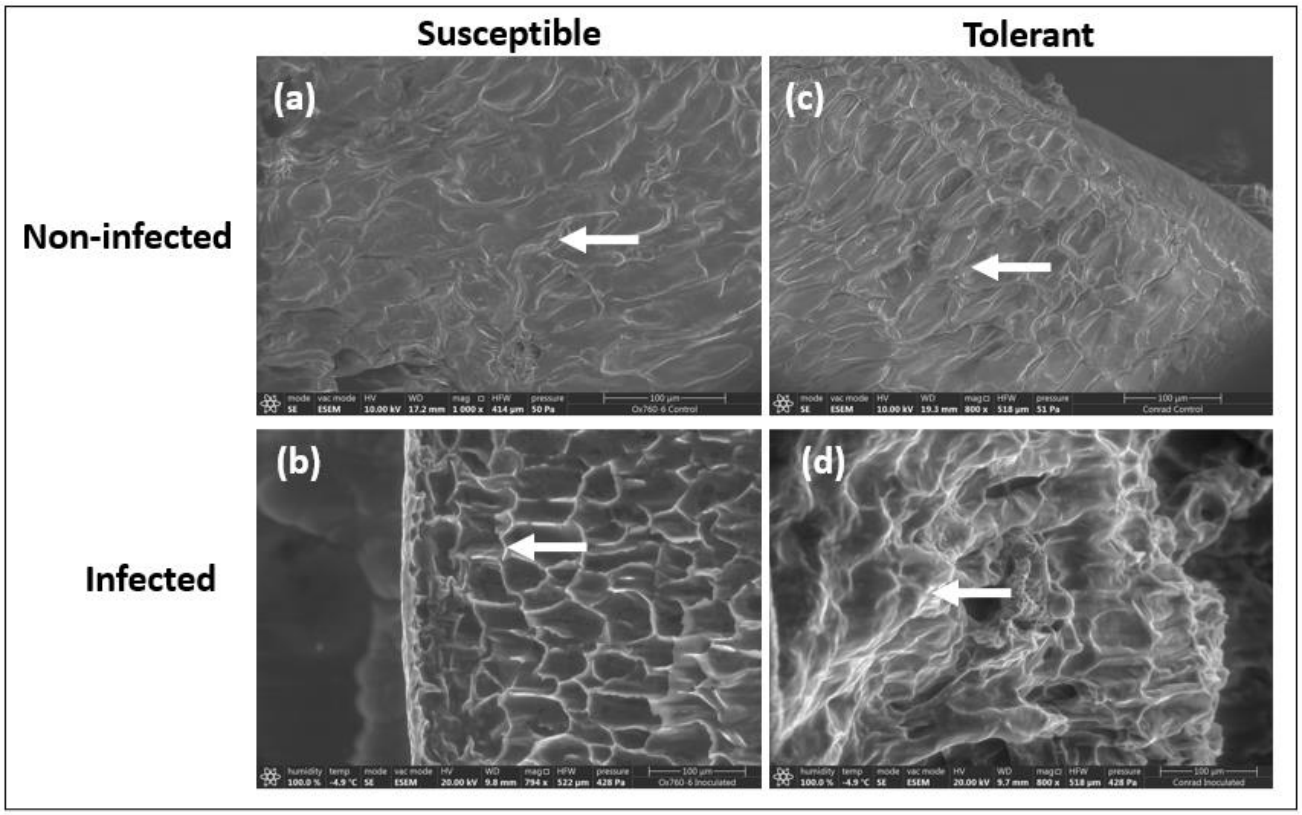

Fig. 5.3. Scanning electron microscopy images showing the root epidermal walls in susceptible (OX760-6) and tolerant (Conrad) soybean cultivars when inoculated with *P. sojae*. (a) The epidermal walls of the non-infected susceptible soybean cultivar, (b) Epidermal walls of the infected susceptible soybean cultivar, (c) Epidermal walls of the non-infected tolerant soybean cultivar, (d) Epidermal walls of the infected tolerant soybean cultivar. White arrows denote epidermal walls of the roots. The epidermal cells appear to be more regular in shape and clearly visible in the tolerant cultivar than in the susceptible cultivar. Bars: (a-d) 100 µm.

Tiny openings in the cortical cells were revealed in the non-infected and infected of both susceptible and tolerant soybean cultivars. Meanwhile, there were more opening in the infected susceptible cultivar than in the infected tolerant cultivar (Fig. 5.4 a-d).

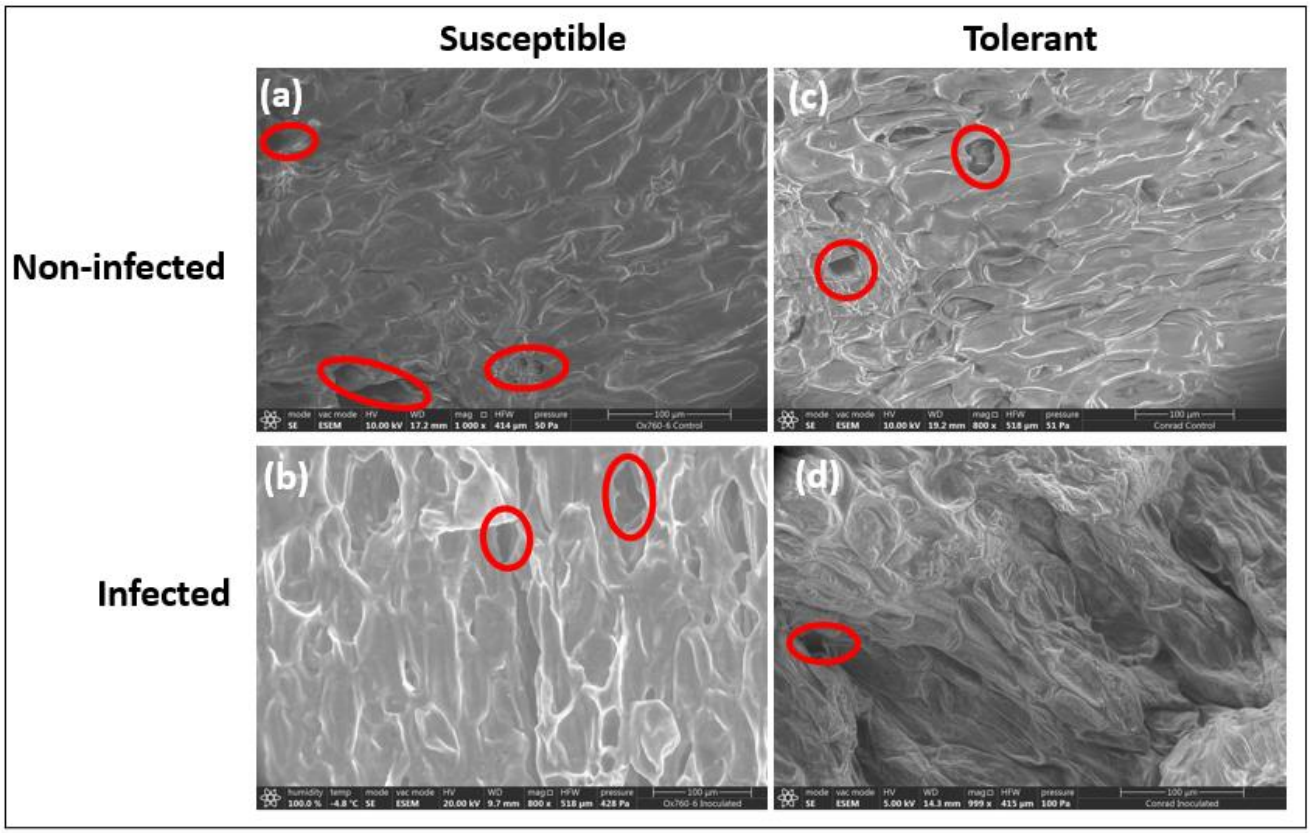

Fig. 5.4. Scanning electron microscopy images showing the tiny opening of root cortical cells of susceptible and tolerant soybean cultivars when inoculated with *P. sojae*. Tiny opening of cortical cells of the non-infected susceptible soybean cultivar (a), infected susceptible soybean cultivar (b), non-infected tolerant soybean cultivar (c), infected tolerant soybean cultivar (d). Red circles denote the tiny opening of epidermal cells of the roots. The tiny opening of epidermal cells appears to be larger in the susceptible cultivar compared to tolerant cultivar after infection. Bars: (a-d) 100 µm.

Similarly, hyphae were found in the vascular parenchyma of both the susceptible and tolerant cultivars after inoculation, but hyphae were not found in the non-inoculated root of either cultivar (Fig. 5.5a-d). Hyphae were found in vascular parenchyma of the root of the susceptible cultivar (Fig. 5.5b) but not found in the root of the tolerant cultivar (Fig. 5.5d) when both were inoculated by *P. sojae*.

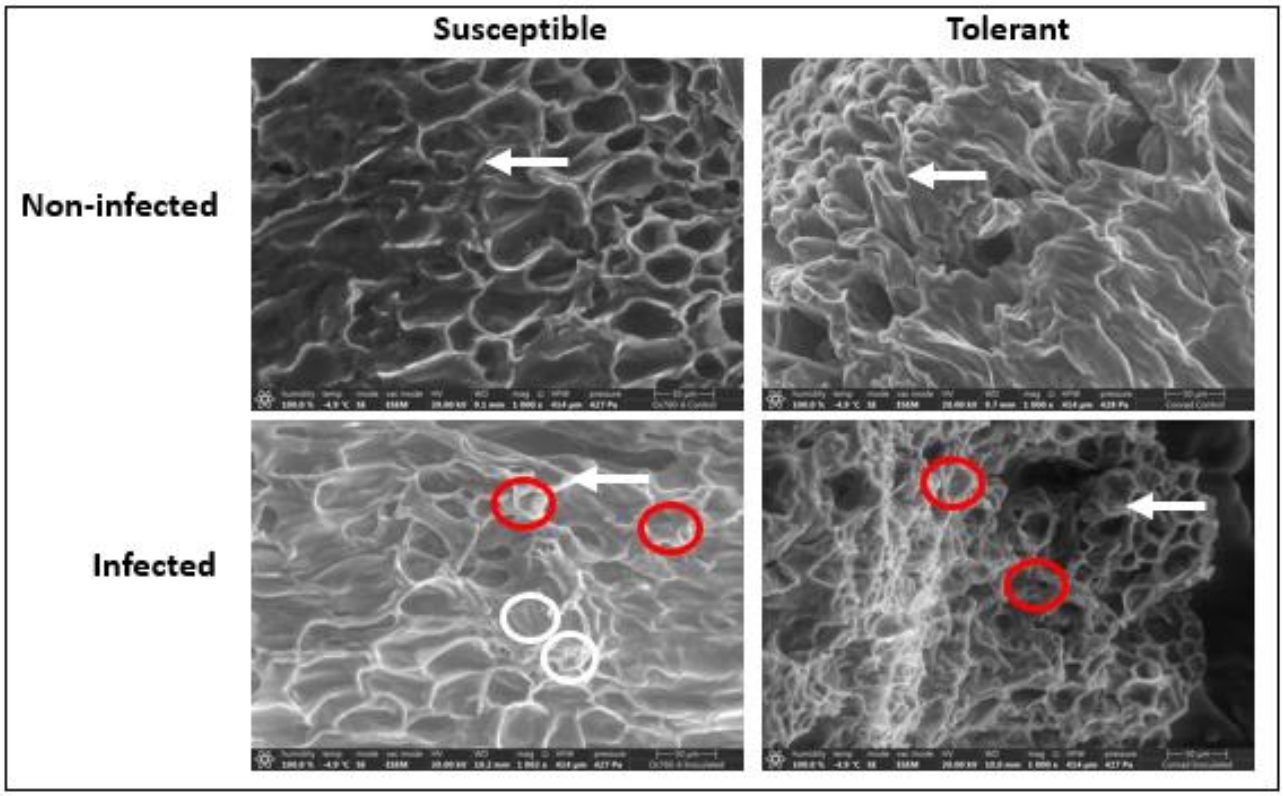

Fig. 5.5. Scanning electron microscopy images showing the root vascular parenchyma of susceptible and tolerant soybean cultivars when inoculated with *P. sojae*. (a) Vascular parenchyma of the non-infected susceptible soybean cultivar, (b) Vascular parenchyma of the infected susceptible soybean cultivar, (c) Vascular parenchyma of the non-infected tolerant soybean cultivar, (d) Vascular parenchyma of the infected tolerant soybean cultivar. Vascular parenchyma is denoted by white arrows, and hyphae in vascular parenchyma are denoted with a white circle. Bars: (a-d) 50 µm.

In addition, the root of the susceptible soybean cultivar contained small vascular cylinder while the root of the tolerant soybean cultivar had large vascular cylinder (Fig. 5.6a-d). The walls of these root cells were intact indicating that these cells were living when inoculated (Fig. 5. 6a, c). After 10 days of seedling growth, hyphae had generally penetrated the epidermis and the outer layers of cortical cells of both soybean cultivars. The hyphae were able to colonize the vascular cylinder of the susceptible cultivar only.

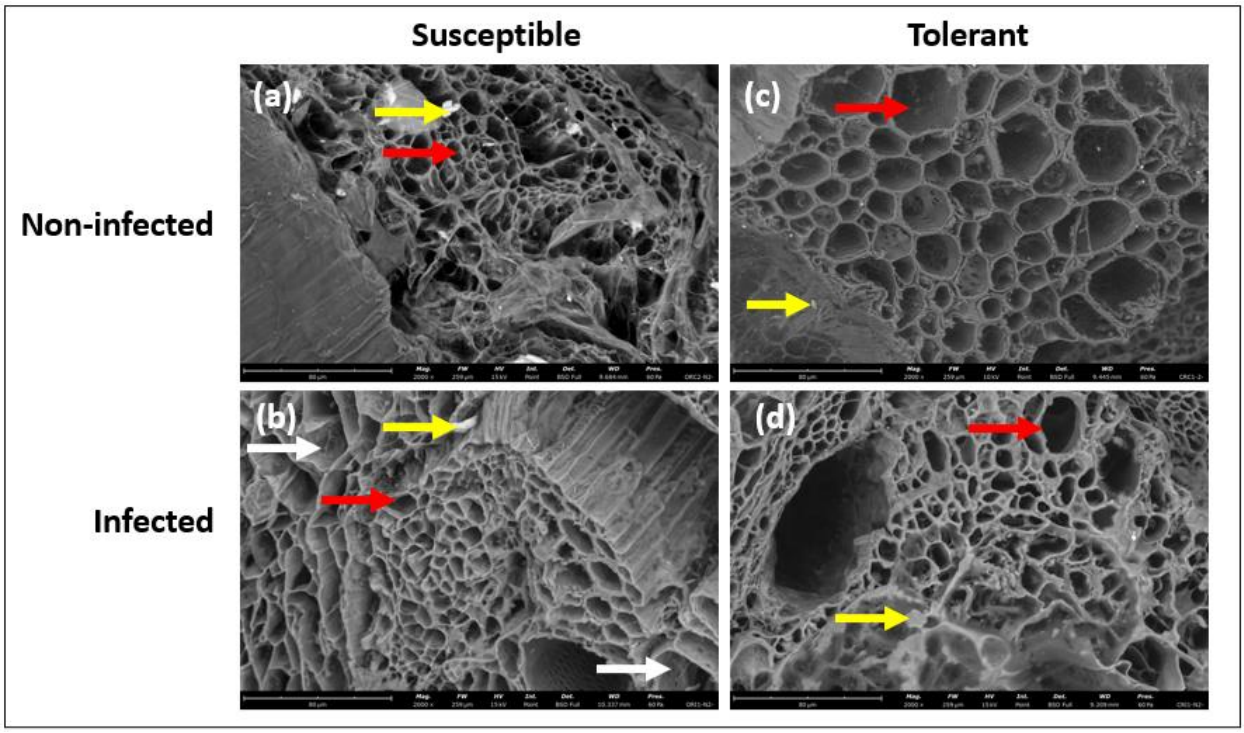

Fig. 5.6. Scanning electron microscopy images showing the root xylem vessels of susceptible and tolerant soybean cultivars when inoculated with *P. sojae.* (a) Vascular cylinder of the non-infected susceptible soybean cultivar, (b) Vascular cylinder of the infected susceptible soybean cultivar, (c) Vascular cylinder of the non-infected tolerant soybean cultivar, (d) Vascular cylinder of the infected tolerant soybean cultivar. The root of susceptible cultivar contains small vascular cylinder while the root of tolerant cultivar contains large vascular cylinder, denoted by red arrows. White arrows denote the presence of hyphae within the vascular cylinder and yellow arrows denote the presence of vermiculite. Bars: (a-d) 80 µm.

The presence of *P. sojae* hyphae was more pronounced in the vascular cylinder of the susceptible cultivar than in the vascular cylinder of the tolerant cultivar, which is denoted with green arrow (Fig. 5.7b, d). In addition, occluding materials were observed in the vascular cylinder of the tolerant cultivar but not observed in the vascular cylinder of the susceptible cultivar, which is denoted with red arrow (Fig. 5.7b, d), and the presence of unknown debris in cortical cell was more pronounced in the infected susceptible cultivar than in the infected tolerant cultivar (Fig. 5.7b, d). The presence of the vermiculite medium was observed in the roots of both non-infected and infected soybean cultivars (Fig. 5.6a-d; 5.7a-d).

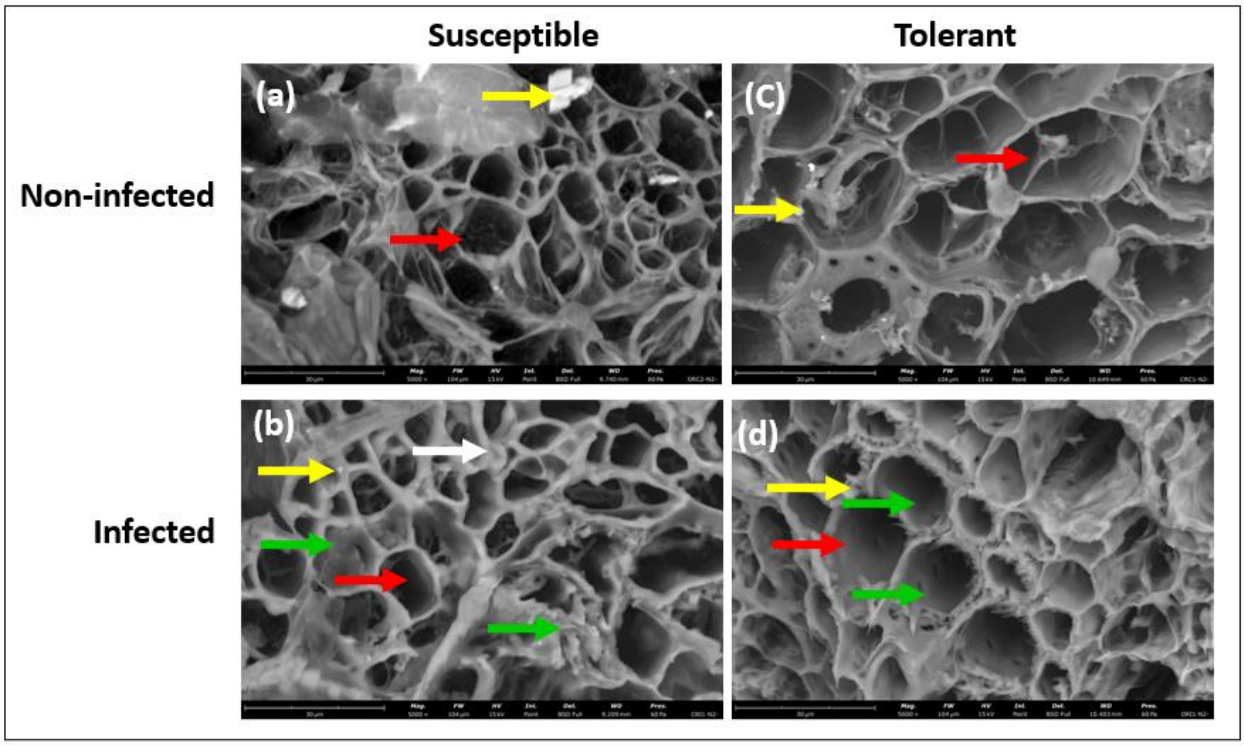

Fig. 5.7. Scanning electron microscopy images showing the large view of root vascular cylinder of susceptible and tolerant soybean cultivars when inoculated with *P. sojae.* (a) Cross section of the non-infected susceptible soybean cultivar, (b) Cross section of the infected susceptible soybean cultivar, (c) Cross section of the non-infected tolerant soybean cultivar, (d) Cross section of the infected tolerant soybean cultivar. The vascular cylinder of the susceptible cultivar contained hyphae while the vascular cylinder of tolerant cultivar shows the presence of occluding materials. Green arrows denote hyphae, white arrows denote the presence of unknown debris in cortical cells, red arrows denote the presence of occluding materials and yellow arrows denote the presence of vermiculite. Bars: (a-d) 30 µm.

The SEM micrographs show biogenic crystals of different morphologies in various locations in the soybean roots of both susceptible and tolerant cultivars. Biogenic crystals of various morphologies are present in the xylem in copious amounts in the non-infected and infected susceptible cultivar and these crystals were varies in sizes (Fig 5.8a, b). However, the amounts of the biogenic crystals observed in non-infected susceptible root remained unchanged in the infected susceptible root. (Fig 5.8a, b). In contrast, the crystals were observed to be present in copious amounts in the root of non-infected tolerant cultivar relative to the root of infected tolerant cultivar (Fig. 5.8c, d). Therefore, it was observed that biogenic crystals found in the roots of the infected susceptible cultivar were present in more copious amounts than in the infected tolerant cultivar (Fig. 5.8b, d) and vise-visa to their non-infected counterparts (Fig. 5.8a, c).

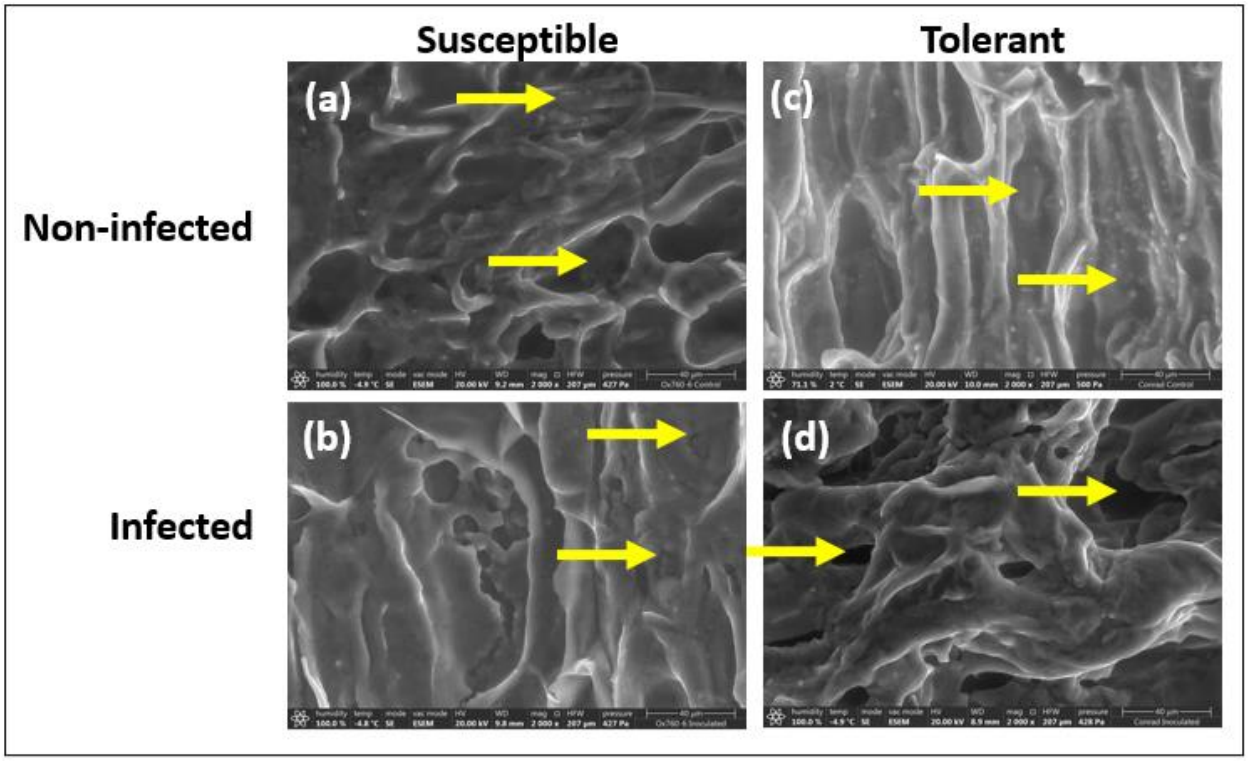

Fig. 5.8. Scanning electron microscopy images showing the presence of biogenic crystals in the root tissues of susceptible and tolerant soybean cultivars when inoculated with *P. sojae.* (a) Cross section of the non-infected susceptible soybean cultivar, (b) Cross section of the infected susceptible soybean cultivar, (c) Cross section of the non-infected tolerant soybean cultivar, (d) Cross section of the infected tolerant soybean cultivar. Yellow arrows denote the presence of biogenic crystals in the vascular cylinder in copious amounts in both non-infected susceptible and tolerant cultivars. Biogenic crystals were present in the vascular cylinder in copious amounts in the non-infected and infected susceptible cultivar, and in non-infected tolerant cultivar but their quantity was reduced in infected tolerant cultivar. Bars: (a-d) 40 µm.

Alteration in the morphology of the root tissues in both susceptible and tolerant cultivars was revealed by SEM images. It was observed that the tolerant cultivar contained larger vascular cylinder than the susceptible cultivar (Fig. 5.9a-d). In addition, the vascular cylinder of the tolerant cultivar was more compact and the level of *P. sojae* colonization was lower in comparison to the susceptible cultivar (Fig. 5. 9b, d). The root of non-infected control for both soybean cultivars demonstrated well-preserved cells with turgid tissue geometry relative to the infected roots of both susceptible and tolerant cultivars (Fig. 5.9b, d).

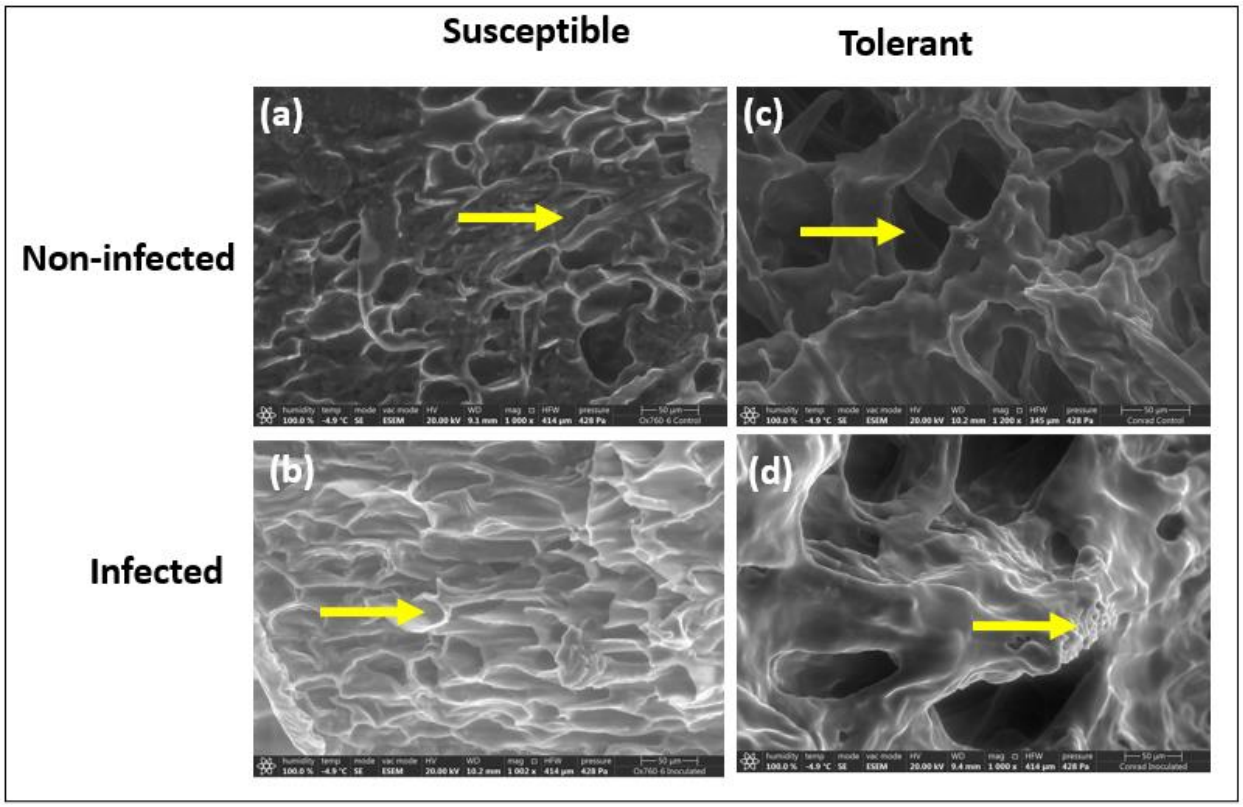

Fig. 5.9. Scanning electron microscopy images showing anatomical changes in the root vascular cylinder of susceptible and tolerant soybean cultivars when inoculated with *P. sojae.* (a) Vascular cylinder of the non-infected susceptible soybean cultivar, (b) Vascular cylinder of the infected susceptible soybean cultivar, (c) Vascular cylinder of the non-infected tolerant soybean cultivar, (d) Vascular cylinder of the infected tolerant soybean cultivar. The tolerant cultivar had larger vascular cylinder than susceptible cultivar, but the vascular cylinder of the infected tolerant cultivar was more compacted as compared to that of infected susceptible cultivar. Bars: (a-d) 50 µm.

The SEM also revealed alterations of xylem walls. The cell walls of vascular cylinder of the susceptible cultivar were observed to be degraded after infection compared to the tolerant cultivar (Fig. 5.10a-d). It was seen that the vascular cylinder of tolerant cultivar made up of thick cell walls capable as a physical response to confine or halt the pathogens from spreading further into the vascular cylinder compared to that of susceptible cultivar following infection with *P. sojae* (Fig. 5.10b, d).

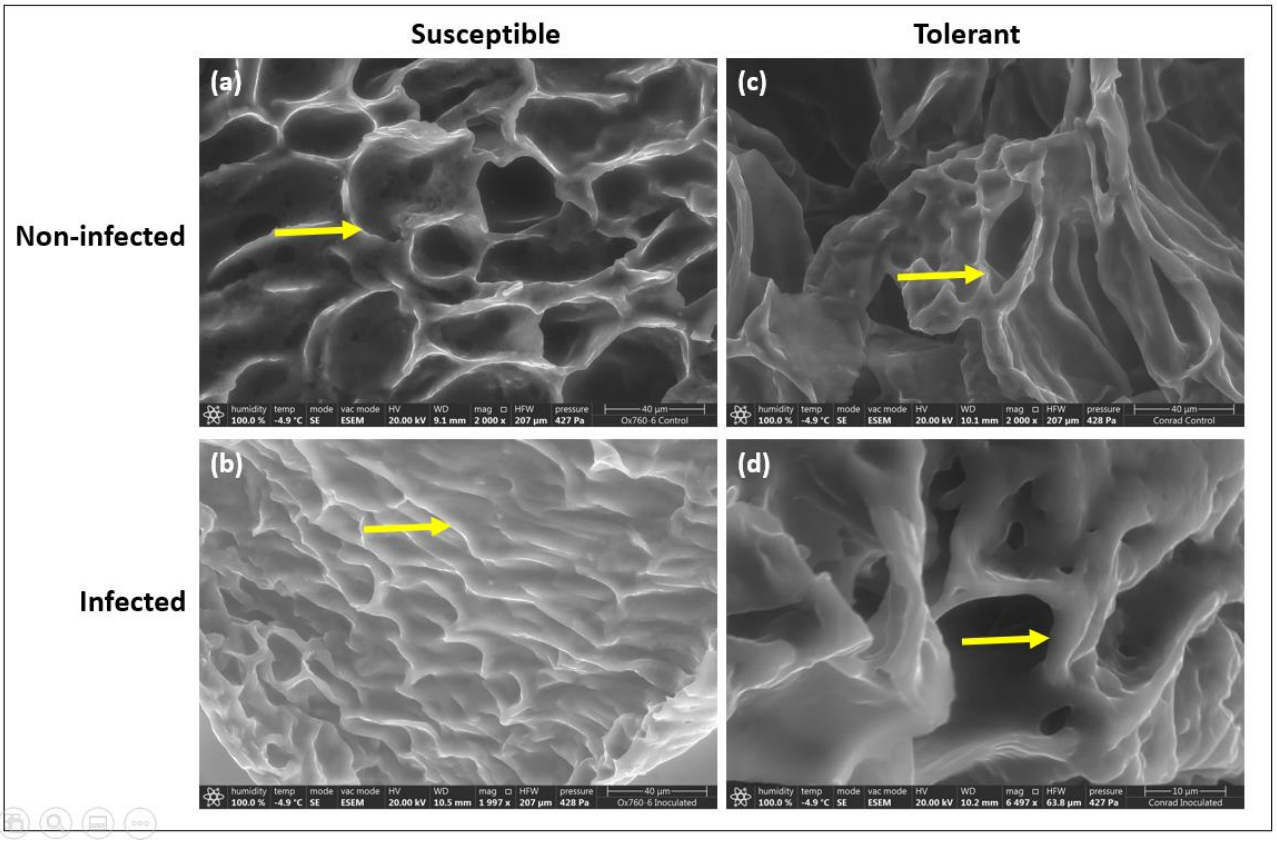

Fig. 5. 10. Scanning electron microscopy images showing the cell walls of vascular cylinder of the susceptible and the tolerant soybean cultivars when inoculated with *P. sojae*. (a) Cell wall of vascular cylinder of the non-infected susceptible soybean cultivar, (b) Cell wall of vascular cylinder of the infected susceptible soybean cultivar, (c) Cell wall of vascular cylinder of the non-infected tolerant soybean cultivar, (d) Cell wall of vascular cylinder of the infected tolerant soybean cultivar. The cell wall of vascular cylinder of the infected tolerant cultivar observed to be thicker compared to the cell wall of vascular cylinder of the susceptible cultivar. Bars: (a-d) 40 µm.

5.4.2. Histochemical changes in the root of susceptible and tolerant soybean cultivars challenged with *Phytophthora sojae* infection

In order to understand the histochemical changes in both soybean cultivars in response to pathogen invasion by *P. sojae*; roots of susceptible and tolerant cultivars of soybean were examined for histochemical responses. Thin sections of the roots were stained with the lipophilic fluorochrome fluorol yellow (FY) and viewed with the GFP filter and yellowish-green fluorescence was observed in all epidermal walls (Fig. 5.11). The histochemical study indicates that the aliphatic compounds in the epidermal walls were brighter in the infected roots of both cultivars (Fig. 5.11b, d,) compared to the non-infected roots of both cultivars (Fig. 5.11a, c). However, the results revealed that the aliphatic depositions in the epidermal walls of the infected tolerant cultivar were brighter than that of infected susceptible cultivar (Fig. 5.11b, d).

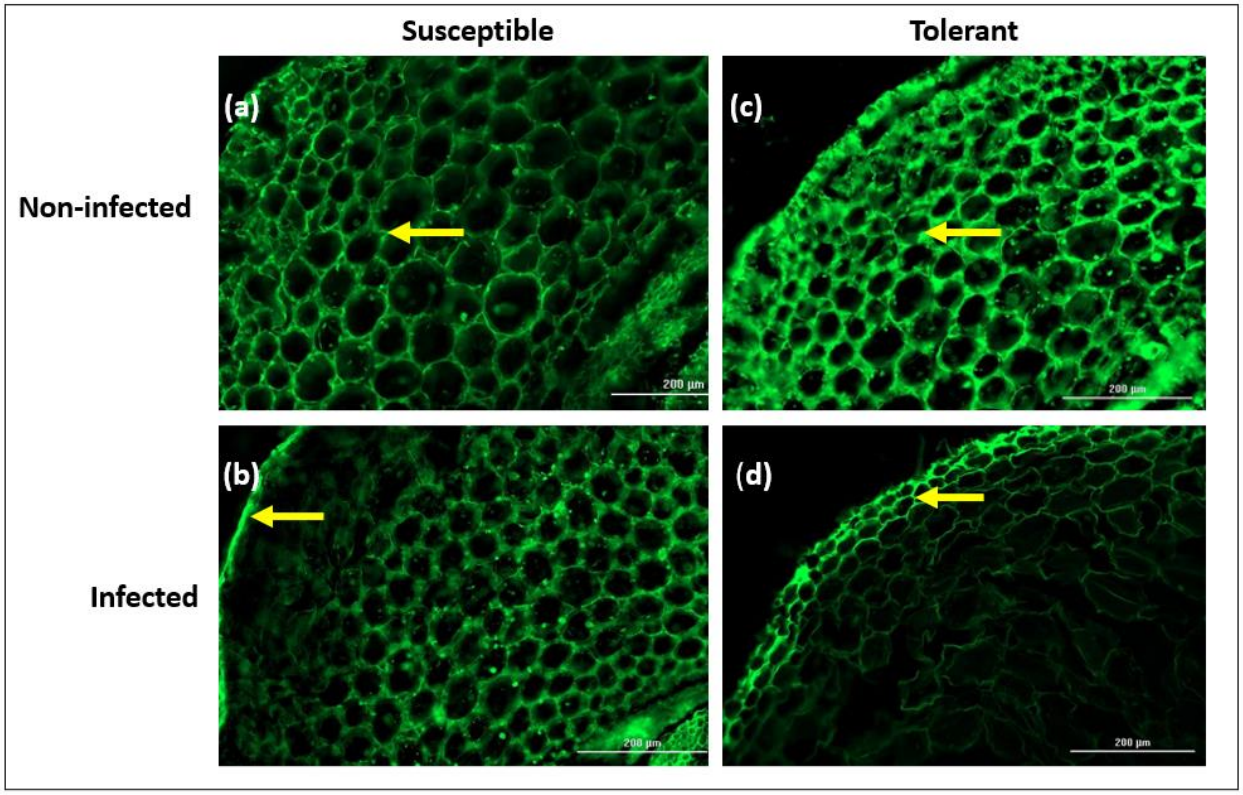

Fig. 5.11. Histochemical changes showing the aliphatic lipids in the root epidermal walls of susceptible and tolerant soybean cultivars when inoculated with *P. sojae*. Cross-sectioned roots were stained with Fluoro-yellow 088 to determine aliphatic content. (a) Preformed aliphatic deposition in the root epidermal and cortical cell walls of non-infected susceptible cultivar, (b) infected susceptible cultivar, (c) induced aliphatic deposition in the root epidermal walls of non-infected tolerant cultivar, (d) induced aliphatic deposition in the root epidermal walls of infected tolerant cultivar. The induced aliphatic lipid deposition appeared brighter in the root epidermal walls of the infected tolerant cultivar than in the root epidermal walls of infected susceptible cultivar and their non-infected counterparts. Yellow arrows denote the fluorescence of epidermal walls. Bars: (a-d) 200 µm.

In the same vein, the aliphatic components in root cortical cells were more pronounced in the infected roots of susceptible and tolerant cultivars than their non-infected counterparts (Fig. 5.12a-d). Meanwhile, the aliphatic deposition in root cortical cells of the infected tolerant cultivar appeared brighter than root cortical cells of the infected susceptible cultivar (Fig. 5.12b, d).

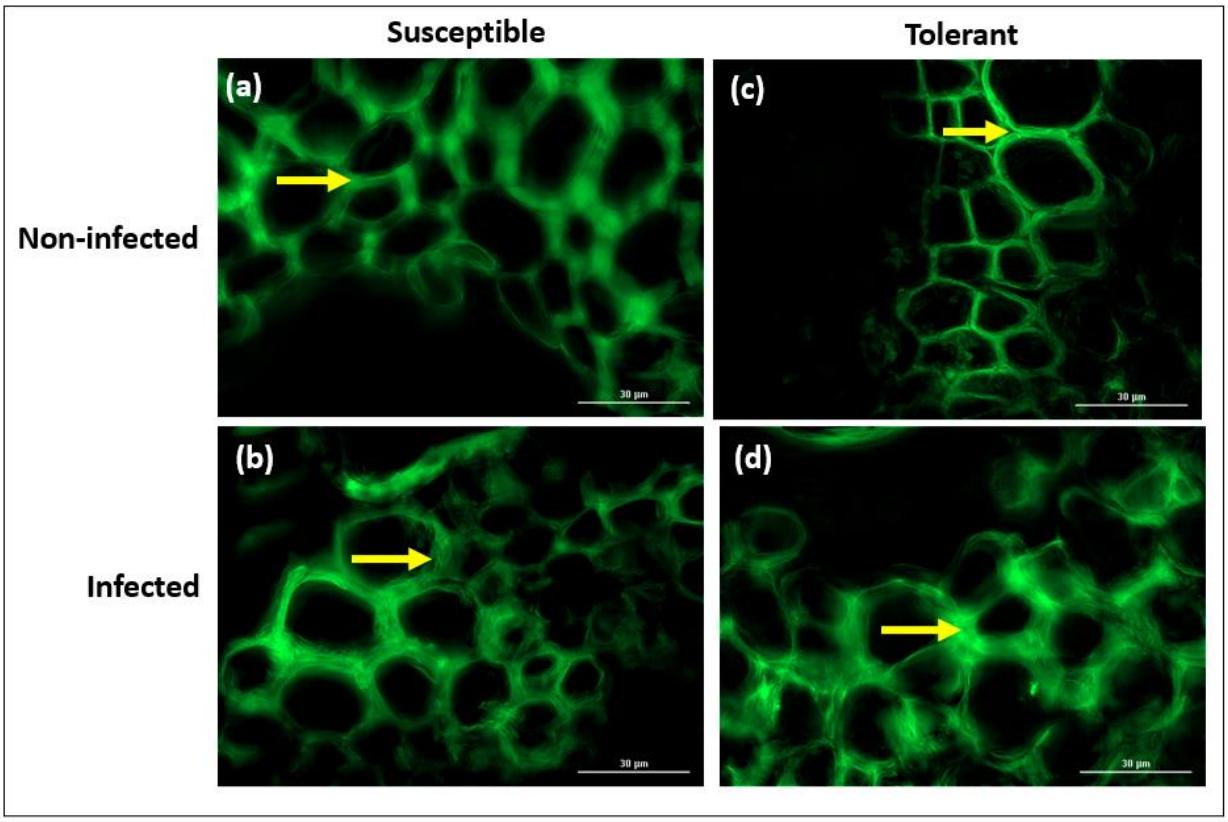

Fig. 5.12. Histochemical change showing the aliphatic lipids in the root cortical cells of susceptible and tolerant soybean cultivars when inoculated with *P. sojae*. Cross-sectioned roots stained with Fluoro-yellow 088 to determine aliphatic content. (a) Preformed aliphatic deposition in the root cortical cells of non-infected susceptible cultivar, (b) preformed aliphatic deposition in the root cortical cells of infected susceptible cultivar, (c) induced aliphatic deposition in the root cortical cells of non-infected tolerant cultivar, (d) induced aliphatic deposition in the root cortical cells of infected tolerant cultivar. The induced aliphatic deposition in the root cortical cells of the infected tolerant cultivar appears brighter than in the root cortical cells of the infected susceptible cultivar and their non-infected counterparts. Yellow arrows denote the fluorescence of cortical cells. Bars: (a-d) 30 µm.

5.5. Discussion

In this work, we used SEM to characterize the histological alterations in the roots of susceptible and tolerant soybean cultivars infected or mock-infected by *P. sojae*, to understand how chemical, physical and morphological changes could play an important role in disease tolerance during host-pathogen interaction.

Infectious pathogens usually colonize plant host to obtain nutrients for their own survival and frequently infect plant tissue such as leaves, stems or roots, facilitating likely spread within the entire plant (Turner et al., 2009; Xue, Lozano-Durán, & Macho, 2020). In addition, pathogen can particularly colonize cell types like the root epidermis, phloem or cortical cells and spread to vascular cylinder (Vailleau et al., 2007). Although pathogen invasion is normally specific to particular organs, and gain entry at a distant site (Turner et al., 2009; Xue et al., 2020). For instance, *R. solanacearum* enters plant roots through root surface or root tips, wounds, and secondary emerging points of roots as penetration sites. It then progresses through the cortex, then spread to the vascular cylinder and finally colonized and infected the entire plant (Digonnet et al., 2012; Turner et al., 2009; Xue et al., 2020). It seems that, upon contact with the soybean roots, *P. sojae* is recognized by the tolerant cultivar and activates defence responses against pathogen. It is normally accepted that the activation of a defence response by the host plant can have a major effect on plant growth and development, although the precise underlying strategies are yet not fully understood. Besides, the observation that infection of root by *P. sojae* involves morphological changes in certain cell types (Figs. 5.1, 5.2), This makes it possible that the overall root development could be changed by the *P. sojae* colonization and infection, either as a result of the activation of anti-fungi responses by tolerant plant or following active control by the pathogen.

Specifically, SEM images that show hyphae within the vascular bundle and vascular parenchyma cells in the root of the infected susceptible cultivar, whereas they appear only in the vascular parenchyma cells in the root of infected tolerant soybean cultivar (Fig. 5.5). Additionally, the components of the infected root of susceptible soybean cultivar were severely damaged compared with infected root of tolerant cultivar. Hyphae present in the xylem of the susceptible soybean cultivar can degrade the cell wall and cell content, including organelles. Proteolysis plays important function during the process of virulence in the infection cycle of the pathogen. Secreted enzymes such as proteases promote penetration and efficient spreading within the host plant by their involvement in degrading host plant's physical barriers (Figaj, Ambroziak, Przepiora, & Skorko-Glonek, 2019). Additionally, proteolytic enzymes allow the colonization of the plant host by attacking the host's defense response mechanisms (Figaj et al., 2019). These enzymes are expected to take part in the degradation of the components of the plant cell wall and/or participate in attacking the plant immune defenses (Feng et al., 2014; Figaj et al., 2019; Pel et al., 2014). Some of these enzymes play regulatory functions that permits pathogen's response to environmental clues and induce infection at the most proper time for pathogens (Figaj et al., 2019). The presence of intercellular hyphae in the susceptible soybean cultivar was higher than that in the tolerant soybean cultivar. The compositional role of the walls of the tolerant soybean cultivar appears to be resistant to the activity of these proteolytic enzymes in the infection of *P. sojae* and seems to play a vital role in limiting infection into the vascular cylinder, and this could be as a result of a defense mechanism that inhibits the expansion of the hyphae and ensures protection of the integrity of root cells and organelles. These findings were supported by work presented in the literature to better understand plant biotic stress response (Okubara & Paulitz, 2005). For instance, it was previously demonstrated that pathogens are

capable of penetrating intact roots, and can move up to the xylem tissue, can also penetrate through wounds or natural apertures to older parts of root and hypocotyl tissue (Okubara & Paulitz, 2005) . Likewise in plants, crystals may be present and distributed within a single or multiple tissues and varies among plant species though there are no generalities about where crystals can be found in plants (Franceschi & Nakata, 2005). It has been generally predicted that the morphology and the distribution of crystals are strictly regulated by plant genes and a specific species will generate a particular type of crystal (Franceschi & Nakata, 2005). For instance, calcium sulfate crystal and calcium oxalate were found in almost all plant tissues including sclerenchyma, parenchyma and mesophyll, and locations of types of crystals may not or may be tissue-specific (He, Bleby, Veneklaas, Lambers, & Kuo, 2012). Also, certain functions have been proposed for crystal formation in plants. For instance, in *Acacia* species, crystals consisting of magnesium, calcium, barium, and strontium ions are used to regulate the levels of these micronutrients in metabolic partitions in the plants and to avert toxicity (Hudgins, Krekling, & Franceschi, 2003). Likewise, biogenic and biological crystals are generally accepted to play some physiological and pathological roles such as support, protection and defense in plants (Cuéllar-Cruz et al., 2020; Ilarslan et al., 2001). Studies have demonstrated that anatomy and physiological functions of vascular cylinder is critically important to plant defense against pathogens (Morris, Brodersen, Schwarze, & Jansen, 2016). This study demonstrated interesting information about the system of compartmentalization of *P. sojae* in the root of soybean cultivars and recognizes the anatomy of xylem as a major factor of disease resistance. In the root of tolerant cultivar, compartmentalization may be contributory to wall-off *P. sojae* and ensure that the physiological functions and integrity of cellular structures are maintained.

Furthermore, occlusion materials are common structural changes made by many higher plants in defense response to pathogen infection (Sun, Sun, Walker, & Labavitch, 2013). Studies have demonstrated that the emergence and development of disease symptoms is attributed to the spread of pathogens through the vessel system. Because occlusion materials in the vascular cylinder often produce soon after plant infection through vascular system-localized pathogens and it is common for gel plugs and/or tyloses to block vessel lumens completely. However, it was hypothesized that occlusion may be involved in host plant resistance (Sun et al., 2013). For instance, it was demonstrated that the vascular cylinder of bean (*Manteigao Fosco II*) resistant cultivar generated occluding materials in response to *Fusarium oxysporum* infection , whereas occluding materials were not produced by bean (Meia Noite) susceptible cultivar as well as their non-infected counterparts (Pereira et al., 2013). This suggested that the occluding materials may be playing critical role in the resistance against this pathogen invasion (Pereira et al., 2013). However, the type of occluding materials observed in this study were not identified.

In addition, production of physical and chemical barriers in the xylem tissue is an effective defense response in disease resistant plants (Kashyap, Planas-Marquès, Capellades, Valls, & Coll, 2020). Plant resistance to pathogen invasion via colonizing the xylem may be correlated to the thickening of the xylem cell walls (Hall, Heath, & Guest, 2011). This is accordance with the result obtained in this study which demonstrated that the tolerant soybean cultivar possessed thicker xylem cell walls than the susceptible cultivar. Therefore, this may be one of the defense mechanisms used by tolerant soybean cultivar against *P. sojae* infection. In addition, suberin in plants is a deposition of a lipid-phenolic biopolyester in the cell walls of specific boundary layers of plants like root peridermis and endodermis. They serve as a protective physical barrier in the plant tissue layers, induce anti-microbial compounds against

pathogens, and regulate ions and water transport in plants (Vishwanath, Delude, Domergue, & Rowland, 2015).

Polymers such as poly-aliphatic components in plant contain C_{16}-C_{24} (medium chain) and C_{20}-C_{30} (long chain) FAs and they are lipid monomers that are found in suberin (Vishwanath et al., 2015). The aliphatic (monomeric composition) suberin in soybean roots is made up of high proportion of ω-hydroxy acids (C_{16}–C_{24}), predominantly $C_{18\text{-}1}$ and C_{24} FAs (Thomas et al., 2007). The quantity of the poly-aliphatic suberin components observed in infected roots were more than non-infected roots. The presence of aliphatic components in infected roots could be involved in the disease resistance mechanism used by tolerant soybean in response to pathogen invasion. There is information about differences in the histopathology of plant tissues infected by various pathogens. However, there is need for further study on the infection processes in plant tissues caused by different pathogens, especially comparing the defense mechanisms in susceptible and tolerant cultivars. This work has demonstrated how morphological changes could play important role in disease resistance by tolerant soybean cultivar when challenged by *P. sojae.*

5.6. Conclusion

In conclusion, we used scanning electron microscopy and histochemical analysis to demonstrate distinct differences in morphology and histochemistry in specific anatomical regions of soybean roots possibly contributing to disease tolerance or susceptibility in the soybean *P sojae* pathosystem. This study reported the chemical, physical and morphological changes in the roots of both susceptible and tolerant soybean cultivars challenged with *P. sojae* and to further

improve our understanding of the mechanism of infection in soybean-*P. sojae* interaction. Tissue damage was found to be less pronounced in the xylem tissue of tolerant cultivar compared to susceptible cultivar, and the xylem cell walls of tolerant soybean cultivar appears to be thicker in comparison to the susceptible soybean cultivar. The xylem walls of the tolerant cultivars appear to be more reinforced and resistant to the hydrolytic enzymes produce by the pathogens. More importantly, biogenic crystals are predicted to be present and distributed in the plant tissues and they varied among plant species. However, synthesis of biogenic and biological crystals in plants play active role during physiological and pathological processes such as physical support, protection and defense against any environmental clues. Additionally, it seems that the quantity of the poly-aliphatic components was higher in tolerant cultivar than susceptible cultivar especially at the edge of epidermis in response to pathogen invasion, which could further limit pathogen ingress into the cortex and vascular cylinder. Therefore, morphological changes could be claimed to play a critical role in disease resistance by tolerant plants, and they could be used to develop a novel strategy to engineer soybean crop cultivars for wide-ranging disease tolerance against *P.sojae* in this pathosystem. This could ultimately help to reduce crop losses and improve food safety and food security through sustainable agricultural practices aimed at using the plant natural defense to improve broad spectrum soybean disease tolerance to *P. sojae* infection.

5.7. References

Adigun, O. A., Nadeem, M., Pham, T. H., Jewell, L. E., Cheema, M., & Thomas, R. (2021). Recent advances in bio-chemical, molecular and physiological aspects of membrane lipid derivatives in plant pathology. *Plant, Cell & Environment, 44*(1), 1-16.

Ajdary, R., Tardy, B. L., Mattos, B. D., Bai, L., & Rojas, O. J. (2021). Plant nanomaterials and inspiration from nature: water interactions and hierarchically structured hydrogels. *Advanced Materials, 33*(28), 2001085.

Amos, R. A., & Mohnen, D. (2019). Critical review of plant cell wall matrix polysaccharide glycosyltransferase activities verified by heterologous protein expression. *Frontiers in Plant Science, 10*(915).

Bandara, A. Y., Weerasooriya, D. K., Bradley, C. A., Allen, T. W., & Esker, P. D. (2020). Dissecting the economic impact of soybean diseases in the United States over two decades. *PloS one, 15*(4), e0231141.

Burnham, K. D., Dorrance, A. E., Francis, D. M., Fioritto, R. J., & St. Martin, S. K. (2003). Rps8, a new locus in soybean for resistance to *Phytophthora sojae*. *Crop Science, 43*(1), 101-105.

Burnham, K. D., Dorrance, A. E., VanToai, T. T., & St. Martin, S. K. (2003). Quantitative trait loci for partial resistance to *Phytophthora sojae* in soybean. *Crop Science, 43*(5), 1610-1617.

Caffall, K. H., & Mohnen, D. (2009). The structure, function, and biosynthesis of plant cell wall pectic polysaccharides. *Carbohydrate Research, 344*(14), 1879-1900.

Cuéllar-Cruz, M., Pérez, K. S., Mendoza, M. E., & Moreno, A. (2020). Biocrystals in plants: A short review on biomineralization processes and the role of phototropins into the uptake of calcium. *Crystals, 10*(7).

Digonnet, C., Martinez, Y., Denancé, N., Chasseray, M., Dabos, P., Ranocha, P., . . . Goffner, D. (2012). Deciphering the route of *Ralstonia solanacearum* colonization in *Arabidopsis thaliana* roots during a compatible interaction: focus at the plant cell wall. *Planta, 236*(5), 1419-1431.

Dorrance, A. E. (2018). Management of Phytophthora sojae of soybean: a review and future perspectives. *Canadian Journal of Plant Pathology, 40*(2), 210-219.

Dorrance, A. E., McClure, S. A., & St. Martin, S. K. (2003). Effect of partial resistance on Phytophthora stem rot incidence and yield of soybean in Ohio. *Plant Disease, 87*(3), 308-312.

Feng, T., Nyffenegger, C., Højrup, P., Vidal-Melgosa, S., Yan, K. P., Fangel, J. U., . . . Mikkelsen, J. D. (2014). Characterization of an extensin-modifying metalloprotease: N-terminal processing and substrate cleavage pattern of *Pectobacterium carotovorum Prt1*. *Appl Microbiol Biotechnol, 98*(24), 10077-10089.

Figaj, D., Ambroziak, P., Przepiora, T., & Skorko-Glonek, J. (2019). The role of proteases in the virulence of plant pathogenic bacteria. *International Journal of Molecular Sciences, 20*(3), 672.

Franceschi, V. R., & Nakata, P. A. (2005). Calcium oxalate in plants: formation and function. *Annu Rev Plant Biol, 56*, 41-71.

Hall, C., Heath, R., & Guest, D. (2011). Rapid and intense accumulation of terpenoid phytoalexins in infected xylem tissues of cotton (*Gossypium hirsutum*) resistant to

Fusarium oxysporum f.sp. vasinfectum. *Physiological and Molecular Plant Pathology, 76*, 182-188.

Harholt, J., Suttangkakul, A., & Vibe Scheller, H. (2010). Biosynthesis of pectin. *Plant physiology, 153*(2), 384-395.

He, H., Bleby, T. M., Veneklaas, E. J., Lambers, H., & Kuo, J. (2012). Morphologies and elemental compositions of calcium crystals in phyllodes and branchlets of *Acacia robeorum* (*Leguminosae: Mimosoideae*). *Annals of Botany, 109*(5), 887-896.

Hudgins, J. W., Krekling, T., & Franceschi, V. R. (2003). Distribution of calcium oxalate crystals in the secondary phloem of conifers: a constitutive defense mechanism? *New Phytologist, 159*(3), 677-690.

Ilarslan, H., Palmer, R. G., & Horner, H. T. (2001). Calcium oxalate crystals in developing seeds of soybean. *Annals of Botany, 88*(2), 243-257.

Kashyap, A., Planas-Marquès, M., Capellades, M., Valls, M., & Coll, N. S. (2020). Blocking intruders: inducible physico-chemical barriers against plant vascular wilt pathogens. *Journal of Experimental Botany, 72*(2), 184-198.

Kesten, C., Menna, A., & Sánchez-Rodríguez, C. (2017). Regulation of cellulose synthesis in response to stress. *Curr Opin Plant Biol, 40*, 106-113.

Lara-Espinoza, C., Carvajal-Millán, E., Balandrán-Quintana, R., López-Franco, Y., & Rascón-Chu, A. (2018). Pectin and pectin-based composite materials: beyond food texture. *Molecules (Basel, Switzerland), 23*(4), 942.

Ling, S., Chen, W., Fan, Y., Zheng, K., Jin, K., Yu, H., . . . Kaplan, D. L. (2018). Biopolymer nanofibrils: structure, modeling, preparation, and applications. *Progress in polymer science, 85*, 1-56.

Lough, T. J., & Lucas, W. J. (2006). Integrative plant biology: role of phloem long-distance macromolecular trafficking. *Annu Rev Plant Biol, 57*, 203-232.

Lucas, W. J., Groover, A., Lichtenberger, R., Furuta, K., Yadav, S.-R., Helariutta, Y., . . . Kachroo, P. (2013). The plant vascular system: Evolution, development and functions. *Journal of Integrative Plant Biology, 55*(4), 294-388.

Mideros, S., Nita, M., & Dorrance, A. E. (2007). Characterization of components of partial resistance, Rps2, and root resistance to *Phytophthora sojae* in soybean. *The American Phytopathological Society, 97*(5), 655.

Morris, H., Brodersen, C., Schwarze, F. W. M. R., & Jansen, S. (2016). The parenchyma of secondary xylem and its critical role in tree defense against fungal decay in relation to the CODIT model. *Frontiers in Plant Science, 7*(1665).

Moy, P., Qutob, D., Chapman, B. P., Atkinson, I., & Gijzen, M. (2004). Patterns of gene expression upon infection of soybean plants by *Phytophthora sojae*. *Mol Plant Microbe Interact, 17*(10), 1051-1062.

Nash, A. A., Dalziel, R. G., & Fitzgerald, J. R. (2015). Mechanisms of cell and tissue damage. *Mims' Pathogenesis of Infectious Disease*, 171-231.

Nguema-Ona, E., Vicré-Gibouin, M., Gotté, M., Plancot, B., Lerouge, P., Bardor, M., & Driouich, A. (2014). Cell wall O-glycoproteins and N-glycoproteins: aspects of biosynthesis and function. *Frontiers in Plant Science, 5*, 499-499.

Okubara, P. A., & Paulitz, T. C. (2005). Root defense responses to fungal pathogens: A molecular perspective. In H. Lambers & T. D. Colmer (Eds.), *Root Physiology: from Gene to Function* (pp. 215-226). Dordrecht: Springer Netherlands.

Parre, E., & Geitmann, A. (2005). Pectin and the role of the physical properties of the cell wall in pollen tube growth of Solanum chacoense. *Planta, 220*(4), 582-592.

Pauly, M., & Keegstra, K. (2008). Cell-wall carbohydrates and their modification as a resource for biofuels. *The Plant Journal, 54*(4), 559-568.

Pel, M. J., van Dijken, A. J., Bardoel, B. W., Seidl, M. F., van der Ent, S., van Strijp, J. A., & Pieterse, C. M. (2014). *Pseudomonas syringae* evades host immunity by degrading flagellin monomers with alkaline protease *AprA*. *Mol Plant Microbe Interact, 27*(7), 603-610.

Pereira, A. C., Cruz, M. F. A., Júnior, T. J. P., Rodrigues, F. A., Carneiro, J. E. S., Vieira, R. F., & Carneiro, P. C. S. (2013). Infection process of *Fusarium oxysporum* f. sp. *phaseoli* on resistant, intermediate and susceptible bean cultivars. *Tropical Plant Pathology, 38*(4), 323-328.

Ranathunge, K., Thomas, R. H., Fang, X., Peterson, C. A., Gijzen, M., & Bernards, M. A. (2008). Soybean root suberin and partial resistance to root rot caused by Phytophthora sojae. *Phytopathology, 98*(11), 1179-1189. doi:10.1094/PHYTO-98-11-1179

Shin, Y., Chane, A., Jung, M., & Lee, Y. (2021). Recent advances in understanding the roles of pectin as an active participant in plant signaling networks. *Plants (Basel, Switzerland), 10*(8), 1712.

Strasser, R. (2014). Biological significance of complex N-glycans in plants and their impact on plant physiology. *Front Plant Sci, 5*, 363.

Sun, Q., Sun, Y., Walker, M. A., & Labavitch, J. M. (2013). Vascular occlusions in grapevines with Pierce's disease make disease symptom development worse. *Plant Physiology, 161*(3), 1529-1541.

Szabo, L. J., & Bushnell, W. R. (2001). Hidden robbers: The role of fungal haustoria in parasitism of plants. *Proceedings of the National Academy of Sciences, 98*(14), 7654-7655.

Thomas, R., Fang, X., Ranathunge, K., Anderson, T. R., Peterson, C. A., & Bernards, M. A. (2007). Soybean root suberin: Anatomical distribution, chemical composition, and relationship to partial resistance to *Phytophthora sojae Plant Physiology, 144*(1), 299-311.

Turner, M., Jauneau, A., Genin, S. p., Tavella, M.-J., Vailleau, F., Gentzbittel, L., & Jardinaud, M.-F. o. (2009). Dissection of bacterial wilt on *Medicago truncatula* revealed two type III secretion system effectors acting on root infection process and disease development *Plant physiology, 150*(4), 1713-1722.

Tyler, B. M. (2007). Phytophthora sojae: root rot pathogen of soybean and model oomycete. *Molecular Plant Pathology, 8*(1), 1-8.

Vailleau, F., Sartorel, E., Jardinaud, M.-F., Chardon, F., Genin, S., Huguet, T., . . . Petitprez, M. (2007). Characterization of the interaction between the bacterial wilt pathogen *Ralstonia solanacearum* and the model legume plant *Medicago truncatula*. *Molecular Plant-Microbe Interactions®, 20*(2), 159-167.

Vishwanath, S. J., Delude, C., Domergue, F., & Rowland, O. (2015). Suberin: biosynthesis, regulation, and polymer assembly of a protective extracellular barrier. *Plant Cell Reports, 34*(4), 573-586.

Wang, T., Zabotina, O., & Hong, M. (2012). Pectin-cellulose interactions in Arabidopsis primary cell wall from two-dimensional magic-angle-spinning solid-state NMR. *Biochemistry, 51*.

Xue, H., Lozano-Durán, R., & Macho, A. P. (2020). Insights into the root invasion by the plant pathogenic bacterium *Ralstonia solanacearum*. *Plants, 9*(4), 516.

Zhang, Z., Xu, Y., Song, G., Gao, X., Zhao, Y., Jia, M., . . . Wen, J. (2019). *Phytophthora sojae* zoospores differ in chemotaxis to the root and root exudates of host soybean and nonhost common bean. *Journal of General Plant Pathology, 85*(3), 201-210.

Chapter six

Summary, conclusions, and future studies

Summary, conclusions, and future studies

6.1. Summary of results and conclusion

The aims of the studies performed in this thesis were:

i. To better understand how tolerant soybean cultivar alter their lipid metabolism to successfully limit colonization and infection by *Phytophthora sojae.*

ii. To better understand how oxylipin induction in tolerant soybean cultivar successfully limit colonization and infection by *Phytophthora sojae.*

iii. To better understand how unique morphological and biochemical structures in tolerant soybean root successfully mitigate colonization and infection by *Phytophthora sojae.*

In this study, untargeted lipidomics analysis demonstrated both qualitative and quantitative alterations in membrane lipid metabolism involving GPLs, PSTs, as well as storage lipids (DGs and TGs) associated with tolerance to *P. sojae*. Additionally, lipid network analysis revealed some unique lipid biomarkers in the soybean roots and stems appear to be potentially discriminate between tolerant soybean cultivar and susceptible soybean cultivar following infection by *P. sojae*, which include TG(20:1/18:1/18:2), TG(18:1/18:1/18:1), TG(8:0/8:0/8:0), TG(18:0/16:0/18:1), TG(16:0/18:3/18:3), TG(16:0/16:0/18:3), TG(18:4/11:3/12:4), DG18:0/18:0, DG22:0/18:2, TG(12:0/12:0/12:0), TG(16:0/16:0/18:2), TG(10:0/10:0/14:0), DG20:0/22:0, TG(18:3/18:2/23:0, TG(10:0/10:0/10:0), DG(18:3/18:3), DG(16:0/18:3), TG(10:0/10:0/14:0), and DG(24:0/18:2. Furthermore, targeted lipidomics analysis also revealed qualitative and quantitative oxylipin inductions, which include 12-OPDA, and 12(S)-HpETE, 9-KOTrE, 13-HOTrE, 9-HpODE, and 13-KODE, 12, 13-DiHOME, 9, 10-DiHODE, and 16,17-

EpDPE in the soybean roots and stems of the susceptible (OX760-6) and the tolerant (Conrad) soybean cultivars used in this study. Meanwhile, these lipid molecular species, metabolites and oxylipins varied in the amounts of preformed and induced components in both cultivars, and these accounted for quantitative differences observed in the components of lipid metabolites and oxylipins between the susceptible and the tolerant soybean cultivars. Induced accumulation and overall increase in GPLs such as PA and PG, and GLs were observed in tolerant soybean cultivar compared to susceptible cultivar. In contrast, accumulation of stigmasterol, and total increase in the ratio of stigmasterol to β-sitosterol were observed in the susceptible cultivar compared to tolerant cultivar. These classes of lipids varied in a similar manner in the root and stem of each cultivar in response to *P. sojae* colonization and infection. These data are consistent with reports in the literature. For instance, the roles of plant lipid metabolism in the susceptibility or tolerance mechanism of eggplant cultivars against Fusarium wilt infection showing the significant difference in the lipid profiles of tolerant and susceptible eggplants to Fusarium infection, and this ensured the functions of the plant lipids in resistance mechanism against infection (Naguib, 2019). Similarly, phyto-oxylipins and oxidized GLs (Table 6.1) were induced in the roots and stems of both soybean cultivars following inoculation with *P. sojae.* A time course of induced phyto-oxylipins revealed various classes of oxylipins (Table 6.1) that were accumulated in the roots and stems of both soybean cultivars in response to pathogen infection. However, the level of accumulation was rapid and higher in the infected-tolerant plant compared to the infected-susceptible plant after four days post-inoculation. These classes of lipids varied in a similar manner in the root and stem of each cultivar in response to *P. sojae* colonization and infection. The differences between the susceptible and tolerant host plant, are related to rapid accumulation, or the rate at which these phyto-oxylipins are chemically express as a defense

response to pathogen invasion (Song, Li, Xie, Jian, & Yang, 2020). Overall, there seemed to be a relationship between the accumulation of certain classes of oxylipin induction, which are 9-HpODE, 13-HOTrE, 12(S)-HpETE, 9-KOTrE, 13-KODE, 12-OPDA, 9, 10-DiHODE, 12, 13-DiHOME and 16,17-EpDPE acid with associated role in soybean tolerance to *P. sojae* colonization and infection (Schuck, Kallenbach, Baldwin, & Bonaventure, 2014). Interestingly, this study has demonstrated that resistance in *Nicotiana attenuata* to *Phytophthora parasitica* can be achieved as result of accumulation of induced oxylipins (Schuck et al., 2014).

The root anatomical and histochemical studies of host plant-pathogen interaction revealed novel changes in root morphology as unique features observed in the roots of both susceptible and tolerant cultivars in response to pathogen invasion. This was carryout in order to better understand biochemical and morphological changes governing disease tolerance in the *P. sojae* soybean pathosystem. Results of SEM revealed that the tissue damage was found to be less pronounced in the xylem tissue of tolerant cultivar compared to susceptible cultivar, and the xylem cell walls of tolerant cultivar appears to be thicker in comparison to the susceptible cultivar. These were in accordance with the anatomical and biochemical properties in infected xylem tissues of cotton, and inducible physicochemical barriers against plant vascular wilt pathogens previously studied in the literature (Hall, Heath, & Guest, 2011; Kashyap, Planas-Marquès, Capellades, Valls, & Coll, 2020). Similarly, the xylem walls of the tolerant cultivars appear to be more reinforced and resistant to the hydrolytic enzymes produced by the pathogens, thereby limiting infection, and presence of biogenic crystals in soybean roots is also important factor in disease resistance due to the physiological and pathological roles in plant. For instance, the generation of biogenic crystals by plants has been suggested as a defense mechanism used by plants against environmental stressors (Cuéllar-Cruz, Pérez, Mendoza, & Moreno, 2020; Ilarslan,

Palmer, & Horner, 2001).The quantity of the aliphatic components observed in infected root of tolerant cultivar were more than the aliphatic component observed in infected root of susceptible cultivar. The results showed the root epidermis and cortical cell walls have more aliphatic depositions in the *P. sojae*-tolerant soybean cultivar than in the *P. sojae*-susceptible soybean cultivar, and the deposition of aliphatic components in root cortical cells of the *P. sojae*-tolerant soybean cultivar appeared brighter than root cortical cells of the *P. sojae*-susceptible soybean cultivar. The presence of aliphatic components could be involved in the disease resistance mechanism used by tolerant soybean in response to pathogen invasion. For instance, aliphatic components serve as a protective barrier in the tissue layers of the plants, trigger anti-microbial compounds against pathogens, and control ions and water transport in plants.

6.2. Limitations of the studies

The limitations observed during the studies were:

i. Lack of sufficient time due to COVID-19 pandemic.

ii. Reconstruction and renovation of pathological laboratory during the studies.

iii. Lack of proximity to certain facilities, materials, and services due the location of the campus and the laboratory.

6.3 Future studies

Although the pathogen signalling pathways in various plants have been studied in the past (Mogensen, 2009), we also need to better understand the molecular mechanism underlying pathogen signal transduction in the soybean *P. sojae* pathosystem. Meanwhile, it was observed that there are differences in the preformed and induced oxylipins, as well as unique lipid

biomarkers between susceptible and tolerant soybean cultivars. Therefore, we suggested that following soybean infection by *P. sojae*, PUFAs (C18:2 and C18:3) from lipid membrane were hydrolyzed via PLA resulting to oxidation that involve one, two or four oxygen atoms to biosynthesize oxidized GLs. Oxidized phospholipids and oxidized TG were biosynthesized by acyltransferases and DG acyltransferases respectively. These oxidized phospholipids and oxidized TG appear to serve as potential precursor for synthesis of the primary oxylipins forming the hydroperoxides as a result of strong correlations observed between these oxidized GLs and primary oxylipins. These hydroperoxides are further metabolized by enzymatic activities to generate various classes of oxylipins catalyzed by allene oxide synthase, LOX and CYP450 (Table 6.1). These could suggest that the lipid metabolites and induced oxylipins could be novel sources of disease tolerance in soybean to *P. sojae*. Studies have revealed that phyto-oxylipins are capable to regulate defense response and developmental pathways in tolerant host plants and several defense related genes have been demonstrated to co-localized with disease tolerance and may involved in partial resistance phenotypes expressed by host plants (Blée, 2002; Gao et al., 2008; García-Marcos, Pacheco, Manzano, Aguilar, & Tenllado, 2013). However, the molecular strategies and the defense response associated with partial disease resistance in tolerant soybean cultivars needs to be untangled by correlating the defense gene expression with partial resistance (Song et al., 2020; Vega-Sánchez, Redinbaugh, Costanzo, & Dorrance, 2005). The proposed pathways and genes biosynthesizing oxylipins and oxidized glycerolipids (Table 6.1) could be expressed in similar pattern and may be involved in the level of partial disease resistance phenotype of soybean during host-*P. sojae* interaction. Therefore, different aspects of the oxidized glycrolipids, oxylipins and proposed unique lipid biomarkers such as DG(18:0/18:0), DG(16:0/18:3), DG(24:0/18:2), TG(18:3/18:2/23:0), TG(10:0/10:0/10:0) and TG(10:0/10:0/14:0)

observed in this study needs to be further explored as possible targets for the development of future plant protection solutions in this pathosystem. Plants could be selected based on gene expression therefore, the proposed genes to target based on the altered lipid metabolites observed in this study are demonstrated in Table 6.1. To determine the presence of ribonucleic acid (RNA), transcription level and differential gene expression in the infected soybean cultivars, the application of quantitative real time polymerase chain reaction (qRT-PCR) or next generation sequencing (NGS) such as RNA-sequencing (RNA-seq) could be used to profile related defense genes (Conesa et al., 2016; Song et al., 2020). Similarly, advances in genomics analysis by profiling gene expressions in various plant-pathogen pathosystems have demonstrated that a group of defense-related genes are upregulated during the infection of tolerant plants with various pathogenic organisms (Fitoussi et al., 2021; Song et al., 2020). This suggests that unlike susceptible plants, tolerant plants, are capable of recognizing infectious pathogens as well induce successful defense responses (Lapin & Van den Ackerveken, 2013) to control infection. Thus, further detail transcriptomic analysis and enzyme assays associated with phyto-oxylipin biosynthesis pathways may reveal a class of genes or enzymes distinctly upregulated the changes in the lipid metabolites during pathogen infection. This may identify targeted biomarkers or oxylipin accumulation that are correlated with upregulated genes; therefore, the targeted genes could be used by breeders in pyramiding resistant soybean genotypes that could enhance resistance or higher tolerance to *P. sojae*, and consequently improve sustainable agriculture.

Table 6.1. Genes of interest for future gene expression analysis in soybean cultivars following *P. sojae* colonization and infection based on results of targeted and untargeted lipidomics and lipid network evaluation performed in this study.

S/N	Oxylipin	Pathway
1	12-OPDA	Allene oxide synthase
2	12 (S)-HpETE	Lipoxygenase
3	9-KOTrE	Lipoxygenase
4	13-HOTrE	Lipoxygenase
5	9-HpODE	Lipoxygenase
6	13-KODE	Lipoxygenase
7	12,13-DiHOME	Cytochrome P450
8	9,10-DiHODE	Cytochrome P450
9	16,17-EpDPE	Cytochrome P450
10	Ox-PA	Acyltransferase
11	Ox-TG	Acyltransferase
12	Ox-PC	Choline phosphotransferase
13	Ox-PE	Ethanolamine phosphotransferase
14	Ox-PI	Phosphatidylinositol synthase

Summary of primary oxylipins and oxidized GLs in the roots and stems of both soybean cultivars following infection with *P. sojae*, and the related genes and proposed pathways for biosynthesis of these oxidized lipids. 12-OPDA = 12-oxophytodienoic acid, 12(S)-HpETE = 12S-hydroperoxy-5(Z),8(Z),10(E),14(Z)-eicosatetraenoic acid, 9-KOTrE = 15(Z)-9-oxo-

octadecatrienoic acid, 13-HOTrE = 13S-hydroxy-9(Z),11(E),15(Z)-octadecatrienoic acid, 9-HpODE = 10(E*)*,12(E)-9-hydroperoxyoctadeca-10,12-dienoic acid, 10(E),12(Z), 13-KODE = (9Z,11E)-13-Oxo-9,11-octadecadienoic acid, 12,13-DiHOME = (*Z*)-12,13-dihydroxyoctadec-9-enoic acid, 9, 10-DiHODE = (12*Z*,15*Z*)-9,10-dihydroxyoctadeca-12,15-dienoic acid and 16,17-EpDPE = (4*Z*,7*Z*,10*Z*,13*Z*)-15-[3-[(*Z*)-pent-2-enyl]oxiran-2-yl]pentadeca-4,7,10,13-tetraenoic acid, oxidized phosphatidic acid (Ox-PA), oxidized triacylglycerol (Ox-TG), oxidized, phosphatidylcholine (Ox-PC), oxidized phosphatidylethanolamine (Ox-PE), and oxidized phosphatidylinositol (Ox-PI).

6.4. Reference

Blée, E. (2002). Impact of phyto-oxylipins in plant defense. *TRENDS in Plant Science, 7*(7), 315-321.

Conesa, A., Madrigal, P., Tarazona, S., Gomez-Cabrero, D., Cervera, A., McPherson, A., . . . Mortazavi, A. (2016). A survey of best practices for RNA-seq data analysis. *Genome Biology, 17*(1), 13.

Cuéllar-Cruz, M., Pérez, K. S., Mendoza, M. E., & Moreno, A. (2020). Biocrystals in plants: A short review on biomineralization processes and the role of phototropins into the uptake of calcium. *Crystals, 10*(7).

Fitoussi, N., Borrego, E., Kolomiets, M. V., Qing, X., Bucki, P., Sela, N., . . . Braun Miyara, S. (2021). Oxylipins are implicated as communication signals in tomato–root-knot nematode (*Meloidogyne javanica*) interaction. *Scientific Reports, 11*(1), 326.

Gao, X., Starr, J., Göbel, C., Engelberth, J., Feussner, I., Tumlinson, J., & Kolomiets, M. (2008). Maize 9-lipoxygenase ZmLOX3 controls development, root-specific expression of defense genes, and resistance to root-knot nematodes. *Molecular Plant-Microbe Interactions®, 21*(1), 98-109. doi:10.1094/mpmi-21-1-0098

García-Marcos, A., Pacheco, R., Manzano, A., Aguilar, E., & Tenllado, F. (2013). Oxylipin biosynthesis genes positively regulate programmed cell death during compatible infections with the synergistic pair potato virus X-potato virus Y and Tomato spotted wilt virus. *Journal of virology, 87*(10), 5769-5783.

Hall, C., Heath, R., & Guest, D. I. (2011). Rapid and intense accumulation of terpenoid phytoalexins in infected xylem tissues of cotton (*Gossypium hirsutum*) resistant to

Fusarium oxysporum f.sp. *vasinfectum*. *Physiological and Molecular Plant Pathology, 76*(3), 182-188.

Ilarslan, H., Palmer, R. G., & Horner, H. T. (2001). Calcium oxalate crystals in developing seeds of soybean. *Annals of Botany, 88*(2), 243-257.

Kashyap, A., Planas-Marquès, M., Capellades, M., Valls, M., & Coll, N. S. (2020). Blocking intruders: inducible physico-chemical barriers against plant vascular wilt pathogens. *Journal of Experimental Botany, 72*(2), 184-198.

Lapin, D., & Van den Ackerveken, G. (2013). Susceptibility to plant disease: more than a failure of host immunity. *Trends Plant Sci, 18*(10), 546-554.

Mogensen, T. H. (2009). Pathogen recognition and inflammatory signaling in innate immune defenses. *Clinical microbiology reviews, 22*(2), 240-273.

Naguib, D. M. (2019). Comparative lipid profiling for studying resistance mechanism against *Fusarium wilt*. *Physiological and Molecular Plant Pathology, 108*, 101421.

Schuck, S., Kallenbach, M., Baldwin, I., & Bonaventure, G. (2014). The *Nicotiana attenuata* GLA1 lipase controls the accumulation of *Phytophthora parasitica*-induced oxylipins and defensive secondary metabolites. *Plant, Cell & Environment, 37*.

Song, R., Li, J., Xie, C., Jian, W., & Yang, X. (2020). An overview of the molecular genetics of plant resistance to the verticillium wilt pathogen *Verticillium dahliae*. *International journal of molecular sciences, 21*(3), 1120.

Vega-Sánchez, M. E., Redinbaugh, M. G., Costanzo, S., & Dorrance, A. E. (2005). Spatial and temporal expression analysis of defense-related genes in soybean cultivars with different levels of partial resistance to *Phytophthora sojae*. *Physiological and Molecular Plant Pathology, 66*(5), 175-182.

APPENDICES

Supplementary data

Appendix I

Table S3.1 Uniquely changed lipids for each comparison.

Tissue	Contrast	Lipid
Root	ORC_ORI	TG(20:1/18:1/18:2)
	ORC_ORI	TG(18:1/18:1/18:1)
	ORC_ORI	TG(8:0/8:0/8:0)
	ORC_ORI	TG(18:0/16:0/18:1)
	ORC_ORI	TG(16:0/18:3/18:3)
	ORC_ORI	TG(16:0/16:0/18:3)
	CRC_CRI	TG(18:4/11:3/12:4)
	CRC_CRI	DG(18:0/18:0)
	ORI_CRI	TG(18:3/18:2/23:0)
	ORI_CRI	TG(10:0/10:0/10:0)
	ORI_CRI	DG(18:3/18:3)
	ORI_CRI	DG(16:0/18:3)
	OSC_OSI	DG(22:0/18:2)
Stem	CSC_CSI	TG(12:0/12:0/12:0)
	CSC_CSI	TG(16:0/16:0/18:2

CSC_CSI	TG(10:0/10:0/14:1)
CSC_CSI	DG(20:0/22:0)
OSI_CSI	TG(10:0/10:0/14:0)
OSI_CSI	DG(24:0/18:2)

This table lists lipids which are only significantly altered in the specified contrast when considering all root and stem treatment comparisons combined. All other lipids are not uniquely changed i.e., are significantly altered in more than 1 comparison. ORC = root of control susceptible soybean cultivar, ORI = root of inoculated susceptible soybean cultivar, CRC= root of control tolerant soybean cultivar, CRI = root of inoculated tolerant soybean cultivar, OSC = stem of control susceptible soybean cultivar, OSI = stem of inoculated susceptible soybean cultivar, CSC= stem of control tolerant soybean cultivar, CSI = stem of inoculated tolerant soybean cultivar.

Appendix II

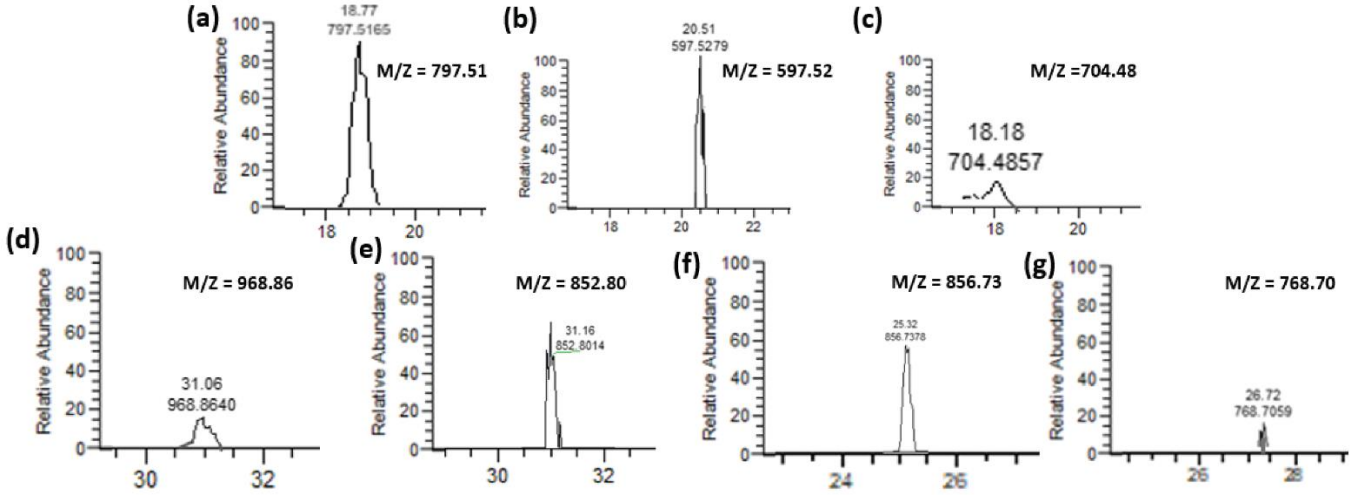

Fig. S3.1 Extracted ion chromatogram (XIC) of odd chain FAs (a) *m/z* 7971.51 for PI18:/13:0 $[M+H]^+$, (b) *m/z* 597.52 for DG15:0/16:0 $[M+NH_4]^+$, (c) *m/z* 704.48 for TG18:4/11:3/12:4 $[M+NH_4]^+$, (d) *m/z* 968.86 for TG18:3/18:2/23:0 [M+NH4]4, (e) *m/z* 852.80 for TG16:0/17:0/17:0 [M+NH4]+, (f) *m/z* 856.73 for TG15:0/18:2/18:3 [M+NH4]+ and (g) *m/z* 768.70 for TG15:0/14:0/15:0 precursor ions of the one phospholipid and six neutral lipids, identified in the positive ion mode; PI = phosphatidylinositol, DG = diacylglycerol, TG = triacylglycerol.

Appendix III

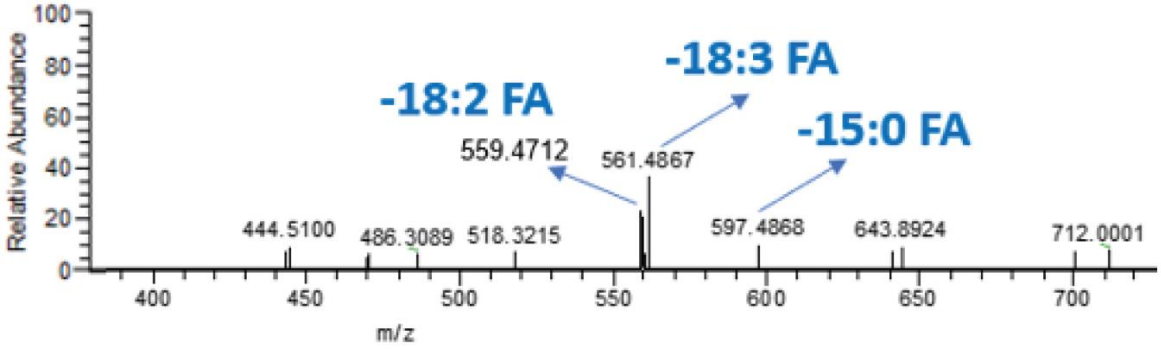

Fig. S3.2 MS^2 spectrum of *m/z* 856.73 representing TG 15:0/18:2/18:3 $[M+NH_4]^+$ identified in the positive ion mode.

Appendix IV

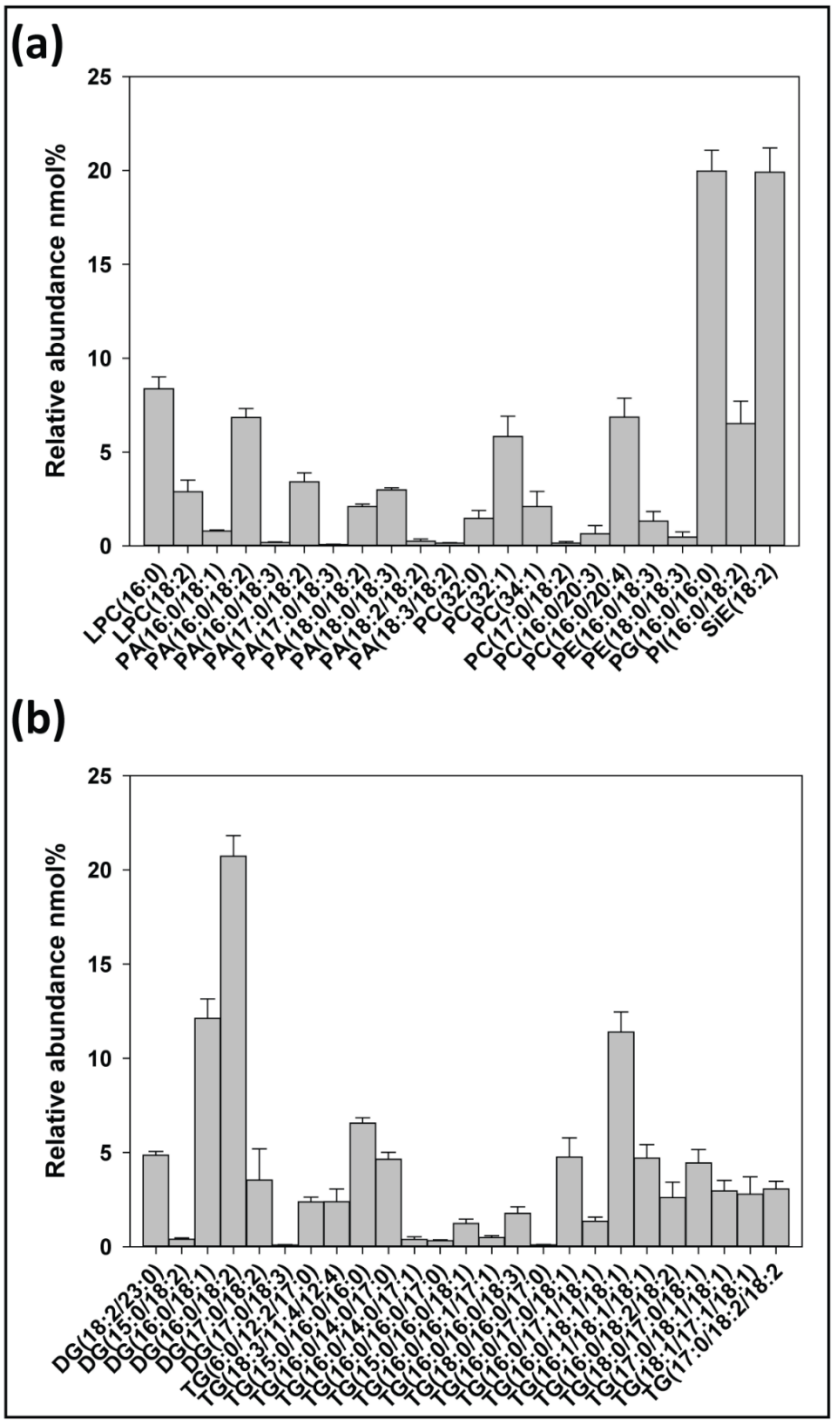
(a)
Relative abundance nmol%
25
20
15
10
5
0
LPC(16:0)
LPC(18:2)
PA(16:0/18:1)
PA(16:0/18:2)
PA(16:0/18:3)
PA(17:0/18:2)
PA(17:0/18:3)
PA(18:0/18:2)
PA(18:0/18:3)
PA(18:2/18:2)
PA(18:3/18:2)
PC(32:0)
PC(32:1)
PC(34:1)
PC(17:0/18:2)
PC(16:0/20:3)
PC(16:0/20:4)
PE(16:0/18:3)
PE(18:0/18:3)
PG(16:0/16:0)
PI(16:0/18:2)
SiE(18:2)
(b)
Relative abundance nmol%
25
20
15
10
5
0
DG(18:2/23:0)
DG(15:0/18:2)
DG(16:0/18:1)
DG(16:0/18:2)
DG(17:0/18:2)
TG(16:0/12:2/17:0)
TG(18:3/11:4/12:4)
TG(15:0/16:0/16:0)
TG(16:0/14:0/16:0)
TG(16:0/14:0/17:0)
TG(15:0/16:0/17:1)
TG(16:0/16:0/17:0)
TG(16:0/16:0/18:1)
TG(16:0/16:1/17:1)
TG(18:0/16:0/18:3)
TG(16:0/16:0/17:0)
TG(16:0/17:0/18:1)
TG(16:0/17:1/18:1)
TG(16:0/18:1/18:1)
TG(16:0/18:2/18:2)
TG(18:0/17:0/18:1)
TG(17:0/18:1/18:1)
TG(18:1/17:1/18:1)
TG(17:0/18:2/18:2

Fig. S3.3 Membrane lipid and neutral lipid molecular species identified in mycelium of *P. sojae*. (a) Membrane lipid molecular species identified in mycelium of *P. sojae* and (b) Neutral lipid molecular species identified in mycelium of *P. sojae*.